

DESIGN & DEVELOPMENT PI-CONJUGATED SYSTEMS WITH FLUXIONAL ELECTRONIC PROPERTIES

by

Garvin M. Peters

A dissertation submitted to Johns Hopkins University in conformity with the requirements for the
Degree of Doctor of Philosophy

Baltimore, Maryland
October 2019

© 2019 Garvin M. Peters
All Rights Reserved

Abstract

The ability to externally modulate conjugated polymer optoelectronic properties is an important challenge for modern organic electronics. One attractive approach entails the incorporation of stimuli-responsive molecular systems, such as photochromic diarylethenes, into polymeric materials. This dissertation details the design of polymers possessing photochromic moieties pendant to the main conjugated chain to allow for electronic influence along the polymer backbone while avoiding substantial conformational demands that may affect solid-state performance. Chapter I first describes the origins of diarylethene design as well as physical organic insights into the mechanism and structural prerequisites for effective switching. Modern devices based on structural variations of diarylethenes are provided to illustrate the scope of applications of these photochromes. The concept of pendant photochromic switching polymers is then introduced, with a brief historical overview of the great strides made by former graduate students.

Chapters II and III are concerned with the development of thieno[3,4-*b*]thiophene (**TT**) based photochromic switches. Chapter II describes a new design theory involving selective functionalization of thiophene-fused heteroacenes. Both failed and successful synthetic attempts are presented that exemplify how deceptively difficult selective functionalization of pendant switchable monomers can be. Photophysical data on the first three thieno[3,4-*b*]thiophene switches are reported, possessing strong on-off photochromic response. Chapter III presents a story of translating **TT** switch cores to oligomeric and polymeric systems. The presence of an alternative conjugated system on the molecule led to inactivation of some switches. Computational modelling theories were developed to not only identify key transitions associated with the switching event, but also to predict the most promising targets for incorporation into polymeric materials.

Chapter IV is dedicated to alternative switch cores explored both computationally and experimentally. Several switch cores were envisioned before and after the development of **TT**, ranging from double switch cores with two diarylethene motifs to those that may require oxidation before cyclization can occur. Many unusual switch cores are reported that may not produce the strong photochromic response seen in **TT**, but present opportunities to learn more about the photophysics of these systems. Other switch cores, like those based on benzo[*b*]thiophene (**BT**), may prove to be as responsive as the **TT** switch cores and have completed synthetic paths towards early photochromic models.

Finally, Chapter V details the incorporation of cycloparaphenylenes (CPPs), which possess a curved π surface, into linear conjugated polymer systems. In collaboration with Dr. Ramesh Jasti and Dr. Miklos Kertesz, [6]- and [8]CPPs featuring a di-alkyne functionalized subunit that allows for π extension primarily through Sonogashira cross couplings. The interplay of linear and curved conjugated systems is investigated in both small molecule and polymeric systems, with the goal of imparting effective electronic communication between the two π surfaces.

Thesis Advisor:

Professor John D. Tovar

Thesis Readers:

Dr. Rebekka Klausen, Dr. Arthur Bragg

Acknowledgements

I would like to express my deepest appreciation for all who supported me in this journey, many of which played an important role before I arrived at Johns Hopkins. I would first like to thank Dr. Steven Fleming, who taught my first two semesters of organic chemistry. Over my undergraduate years, Doc entertained my curiosity for the subject and encouraged me to pursue both research opportunities and higher-level chemistry courses. I consider myself extremely lucky to have learned under him, as he opened my eyes to an area of science I'm genuinely passionate about. I would also like to thank Dr. Jacqueline Tanaka and Dr. Elizabeth Russell-Mckenzie, former leaders of the Temple University MARC Research Program, for providing beginning-to-end training and guidance on my path towards my PhD career. It was through their recommendation that I joined the lab of my undergraduate mentor, Dr. Michael J. Zdilla. Dr. Z provided me with the first taste of scientific independence by allowing me to design my own experiments and act on my original ideas.

There were several people during my time at Hopkins that have strongly contributed to my growth in addition to keeping me sane during rough patches. Firstly, I would like to thank J.D. for being an incredible mentor in several aspects. His pedagogical approach instilled in me a strong sense of independence, allowing me to not only have confidence in my own ideas and technical skills, but also develop my problem solving and troubleshooting ability. I am incredibly grateful for his mentorship and the lab culture that stems from it, where scientific development is encouraged regardless of successes or failures. In addition, my committee members Dr. Rebekka Klausen and Dr. Art Bragg have been excellent sources of advice over the years.

I've seen many different graduate students, undergraduates, and post-docs come through the Tovar lab over the past 5 years, many of whom have provided both research-related and social support. In particular, I would like to thank Dr. Reid Messersmith and Dr. Herdeline Ann Mallari Ardoña, who quickly became my graduate student role models and remained so after they left.

Although they were both on completely different projects, I learned from them the amount of discipline and conscientiousness required to be successful in graduate school. I believe these qualities are crucial to the development of young scientists, especially in light of very challenging research, and I will always be grateful for the both the active and passive lessons they passed to me. In addition, I would also like to thank Boris Steinberg for not only holding the department together, but for also being a good friend throughout my time at Hopkins.

I am also deeply indebted to my family and friends outside of Hopkins who have, at times, tolerated my severe lack of presence in light of difficulties throughout my research. Contrary to their claims, I do not consider myself particularly intelligent and often found this dissertation work incredibly mentally taxing. This often meant doubling down and, in turn, less time spent with those close to me. I thank all of them for cheering for my successes and helping me rebound from failures. Finally, I would like to thank the love of my life, Joanna Lu, for always being a permanent source of positivity and joy. Even during the worst defeats, Jo has always managed to give me the strength to persevere and stay focused on the bigger picture. She means the world to me, and I'm excited to start the next chapter of our lives together.

*Dedicated to my loving parents,
Joyce & Godfrey Peters*

Table of Contents

	Abstract	ii
	Acknowledgements.....	iv
	List of Tables.....	ix
	List of Figures.....	x
	List of Schemes	xiii
Chapter I	Evolution of Photochromic Switches and Their Application to Pendant Switchable Polymers	
	Introduction	2
	Structure & Mechanism	7
	Applications.....	11
	Previous Work	16
	Conclusion.....	18
	References	20
Chapter II	Design and Synthesis of Photochromic Switch Monomers Based on Thieno[3,4-<i>b</i>]thiophene	
	Introduction	22
	Results & Discussion	26
	Conclusion.....	41
	Experimental	43
	References	53
Chapter III	Theory and Development of Pendant Photochromic Polymers Based on Thieno[3,4-<i>b</i>]thiophene	
	Introduction	55
	Results & Discussion	56
	Conclusion.....	92
	Experimental	93
	References	120
Chapter IV	Alternative Switch Cores and Future Directions for Pendant Photochromic Polymers	
	Introduction	122
	Results & Discussion	123
	Conclusion.....	142

	Experimental	144
	References	152
Chapter V	Synthesis and Characterization of Conjugated Copolymers involving Cycloparaphenylenes	
	Introduction	154
	Results & Discussion	158
	Conclusion.....	170
	Experimental	172
	References	182
Appendix	Supporting information	183
Curriculum Vitae.....		295

List of Tables

Table 3.1	Frontier molecular orbitals (B3LYP / 6-31G*) for the small molecules investigated to determine surface distribution across the switching motif.....	60
Table 3.2	Frontier molecular orbitals (B3LYP / 6-31G*) for the two energy minimized anti-periplanar isomers.....	62
Table 3.3	Frontier molecular orbitals (B3LYP / 6-31G*) for conformationally locked TT1Ph2 and the sterically hindered derivative.....	63
Table 3.4	Frontier molecular orbitals (B3LYP / 6-31G*) for DTT3 switch core and small-molecule derivatives.	64
Table 3.5	Donor screening with the initial acceptor TT3 (B3LYP / 6-31G*). Potentials are bolded and underlined.	66
Table 3.6	Acceptor screening with poor donors from the TT3 screening. TT5 shows desirable surfaces in all cases examined.	69
Table 3.7	Comparison of the frontier molecular orbitals (B3LYP / 6-31G*) of DTT2 and DTT5	70

List of Figures

Figure 1.1	Simplified two-dimensional ground- and excited state potential energy surfaces illustrating cyclization and cycloreversion paths around the conical intersection. [Adapted from reference 1.1]	8
Figure 1.2	Representative example of a perfluorocyclopentene-based diarylethene switch (a) and the corresponding UV-Vis profile (b). In isolation, there is a small conformational change between the open and the closed form (c). [Adapted from reference 1.1]	10
Figure 1.3	Demonstration of reversible bending of a single diarylethene crystal (a), photoacid generation upon cyclization (b), and switchable fluorescence (c). [Adapted from references 1.10 to 1.13]	13
Figure 1.4	Representative polymers featuring non-conjugated pendant (a) and conjugated main-chain (b,c) photochromic moieties.	14
Figure 1.5	Spatial effect of photoisomerization along polymers featuring a main-chain (a) or pendant (b) diarylethene motif.	16
Figure 2.1	X-Ray crystal structure of TT1 , depicting the anti-parallel conformation of the diarylethene switching arms. TT1 was recrystallized from hot acetonitrile.	35
Figure 2.2	UV-Vis absorption profile of open and closed TT1 . Cyclization and cycloreversion can be visualized in both in the dissolved and crystalline form. .	36
Figure 2.3	UV-Vis absorption spectrum of TT-BT for both the open and closed state. Orange coloration of the closed state is due to the extended conjugation from benzene to benzene.	38
Figure 2.4	(Left) Depiction of the steric clash of interest. (Right) Alkyl region of the NMR of TT-BT collected at several temperatures.	39
Figure 2.5	UV-Vis absorption spectra for the open and closed form of TT2 with intense blue coloration upon cyclization.	41
Figure 3.1.	UV Vis spectra for TT1-Th2 (left) and TT1-TDPP EH (right), each line representing 10 second irradiation intervals at 254 nm.	57
Figure 3.2	CV and spectroelectrochemistry for TT1-Th2 (top) and TT1-EDOT (bottom). Spectroelectrochemistry scans were separated by 0.1 V.	59
Figure 3.3	UV-Vis spectra for the open and closed form of TT2-Ph , demonstrating a relatively mild change in absorption profile upon reaching the photostationary state.	61
Figure 3.4	UV-Vis absorption spectrum of the open and closed switch TT5 and the corresponding coloration.	74
Figure 3.5	Photophysical response of the donor-acceptor polymer based on TT5 , where the same reduction and blue shift of the λ_{max} in previous pendant diarylethene polymers was observed.	77

Figure 3.6	Comparison between calculated and experimental UV-Vis absorption of the two functional photochromic oligomers TT3-Ph and TT3-Th , using DFT B3LYP / 6-31G*.	78
Figure 3.7	Frontier molecular orbital topologies for TT1 , TT1-Ph , and TT-Ph , with the magnitudes of the energy of their corresponding transitions.....	80
Figure 3.8	Frontier molecular orbital topologies for TT2 , TT2-Ph , and TT-Ph , with the magnitudes of the energy of their corresponding transitions.....	82
Figure 3.9	Frontier molecular orbital topologies for TT3 , TT3-Ph , and TT-Ph , with the magnitudes of the energy of their corresponding transitions.....	84
Figure 3.10	UV-Vis absorption spectra of the open and closed form of TT3 , with the extended conjugation resulting in a deep green compound upon cyclization.	87
Figure 3.11	UV-Vis absorption of the open and closed π -extended switch TT3-Ph , where photochromic activity is restored compared to TT1-Ph and TT2-Ph	89
Figure 3.12	UV-Vis absorption spectra for the three sterically hindered pendant photochromic polymers P-TT1 , P-TT2 , and P-TT3	91
Figure 4.1	Early low level calculations demonstrating LUMO (top) and HOMO (bottom) MO's of open (left) and closed (right) benzodithiophenes, in which a simple alkyne is used as a model for the conjugated backbone.	124
Figure 4.2	Photophysical response of BT-CF₃ in acetonitrile solution, where photoirradiation occurred with a handheld UV lamp and cycloreversion with a white LED.	134
Figure 4.3	Top: Frontier orbitals for the stabilized Q core. Bottom: HOMO-1 surface topology and its side-view. B3LYP 6-31G*.	135
Figure 4.4	UV-Vis spectra of the quinoxaline (Q) switch core featuring benzo[b]thiophene switching motif.	137
Figure 5.1	UV-Vis absorptions of model terphenyl species with π -extensions, and photoluminescence spectra for polymers.	162
Figure 5.2	UV-Vis spectra for oligomeric [6]- and [8]CPP units in comparison with the respective core ring structure.....	163
Figure 5.3	UV-Vis spectral comparison for both the di-phenylated and di-thienylated models and core CPPs.....	164
Figure 5.4	Absorption and emission spectra for both the phenylated and thienylated [6]- and [8]CPP cores, where [6]CPP species demonstrate very minimal fluorescence.	165
Figure 5.5	Absorption spectra bare and functionalized [6]CPP cores illustrating the impact of gradually extending the orthogonal conjugated system.	166
Figure 5.6	Absorption spectra bare and functionalized [8]CPP cores illustrating the impact of gradually extending the orthogonal conjugated system.	167
Figure 5.7	UV-Vis absorption and emission spectra for phenylated [8]CPPs compared to that of the linear analogue.	168

Figure 5.8	UV-Vis absorption and emission spectra for phenylated [8]CPPs compared to that of the linear analogue.	169
Figure 5.9	UV-Vis absorption, emission, and excitation of P[8]-Th to determine the source of photoluminescence.	170

List of Schemes

Scheme 1.1	An example of the reversible isomerization in (indeno)naphthopyrans, a common organic photochrome used in transition lenses	2
Scheme 1.2	Some common classes of photochromes: Thermally reversible azobenzenes (1a-b) and spiropyrans (2a-b), and thermally irreversible furylfulgides (3a-b) and diarylethenes (4a-b). [Adapted from reference 1.1]	3
Scheme 1.3	Isomerizations of Stilbene (a) and 2,3-dimesityl-2-butene (b) emphasizing differences in reversibility due to the presence of methyl substitutions.....	4
Scheme 1.4	Selected dithienylethene species reported by Kellogg <i>et. al.</i> demonstrated the irreversibly cyclized benzothiophene molecules in the presence of an oxidant. [Adapted from reference 1.6]	5
Scheme 1.5	Switches reported by Irie <i>et. al.</i> demonstrating incorporation of methyl groups and heteroatom substitution leading to thermal stability and resistance to oxidation. [Adapted from reference 1.7]	6
Scheme 1.6	Switches based on maleic anhydride removed the opportunity for the undesirable cis-trans isomerization. [Adapted from reference 1.7]	7
Scheme 1.7	Diarylethenes all feature a core cyclohexadiene system (a). Favorable orbital overlap for cyclization occurs during conrotatory motion	7
Scheme 1.8	For both steric and electronic reasons, diarylethenes that occupy a parallel conformation do not typically proceed through the electrocyclization reaction. [Adapted from reference 1.1]	9
Scheme 1.9	Upon further irradiation, the closed isomer of some diarylethenes can proceed through an irreversible 1,2-diatropic shift. [Adapted from reference 1.9]	11
Scheme 1.10	Selected photochromic cores developed by former group members towards pendant switchable conjugated polymers.....	18
Scheme 2.1	Two promising photochromic switch monomers based on thiophene-fused heteroacenes benzo[b]thiophene and thieno[3,4- <i>b</i>]thiophene.	22
Scheme 2.2	Theoretical depiction of a four-state pendant photochromic polymer controlled both photochemically and electrochemically.	24
Scheme 2.3	Numbering scheme for thieno[3,4- <i>b</i>]thiophene and depiction of desirable functionalization, where the diarylethene switching motif is built from the 2- and 3- positions and π -extension is to occur from the 4- and 6- positions.....	24
Scheme 2.4	First reported synthesis of the third thiophene: thieno[3,4- <i>b</i>]thiophene reported by Wynberg and Zwanenburg. [Adapted from reference 2.4]	26
Scheme 2.5	The second reported synthesis of thieno[3,4- <i>b</i>]thiophene reported by Brandsma and Verkruijsse. [Adapted from reference 2.5]	27

Scheme 2.6	Attempted synthetic routes towards (pre)functionalized TT switch cores utilizing modified literature syntheses.	28
Scheme 2.7	An example of a Larock-type ring closure, a subset of iodine-mediated electrophilic ring closures. Benzene is depicted here, but there is great variance in the (hetero)acene from which the reaction can occur.	31
Scheme 2.8	Retrosynthetic pathway for a novel TT synthesis utilizing the Larock-type ring closure as a means to both form the desired core and halogenate the 3- position.	31
Scheme 2.9	General synthetic pathway towards TT switch cores, with yields shown for the three key switches eventually developed (TT3 and derivatives discussed later).	33
Scheme 2.10	Synthesis of the TT switch derivative TT-BT , featuring benzo[b]thiophene switching arms initially developed for fatigue resistance.	37
Scheme 2.11	Synthesis of the TT2 switch core following the general procedure for the synthesis of TT switches. The switching arm arm was also initially chosen due to high fatigue resistance.	40
Scheme 3.1.	Structures of the first six polymeric species investigated, ranging from donor-acceptor polymers to alkyne-containing polymers.	56
Scheme 3.2	Alternative conjugation path for P-TT1-Th2 polymer, where the cyclized structure has forced planarity which may favor shorter conjugation paths along the switching arm.....	56
Scheme 3.3.	Molecular structures of the two acceptor species studied computationally.	68
Scheme 3.4	Attempted synthesis of the thiazole boronate ester utilizing both Negishi and Suzuki cross-coupling reactions.	71
Scheme 3.5	Assembly of the thiazole-based TT intermediates utilizing the Larock-type ring closure to obtain the iodinated core.	71
Scheme 3.6	Assembly of TT5 switch core using a stannylated switch arm for the final cross-coupling reaction.	72
Scheme 3.7	Attempted borylative cyclization that would result in boronate ester functionalization at the 3-position of TT	73
Scheme 3.8	Stepwise borylation of the the 3-position of thiophene by first performing the iodine-mediated electrophilic cyclization followed by lithium-halogen exchange to produce the desired boronate ester.....	73
Scheme 3.9	Dibromination of the TT5 switch core prior to π -extension at the 4- and 6-positions of thieno[3,4- <i>b</i>]thiophene.	75
Scheme 3.10	Stille polycondensation between di-brominated TT5 monomer and a benzodithiophene co-monomer to generate a donor-acceptor polymer.	76
Scheme 3.11	Synthetic pathway towards the TT3 photochromic switch core, constructed using a similar methodology to TT1 and TT2	86

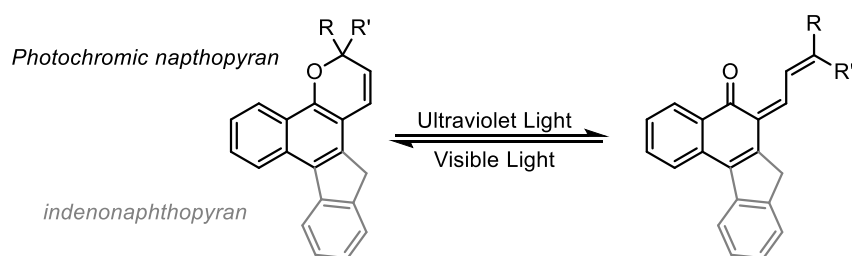
Scheme 3.12	General Suzuki polycondensation used in producing the sterically hindered pendant photochromic polymers P-TT(1-3) 90
Scheme 4.1	Benzo[1,2-b:4,5-b']dithiophene numbering scheme and locations for switch functionalization and π -extension for the double switch core. 123
Scheme 4.2	First synthetic design of the double switch monomer. i) (COCl) ₂ , DCM, r.t. ii) diethylamine, DCM, r.t. iii) n-BuLi, THF, 0°C. iv) Zn, NaOH, butyl p-toluenesulfonate, EtOH, 105°C. v) Br ₂ , CHCl ₃ , r.t. vi) 2,5-dimethylthien-3-yl boronic acid, Pd ₂ (dba) ₃ , SPhos, K ₃ PO ₄ , toluene, 100°C. vii) 4-iodophenoxyacetic acid, oxone viii) Ar, SnCl ₂ , H ₂ O..... 125
Scheme 4.3	Second synthetic pathway towards the double switch core. i) NaBH ₄ , EtOH, 85°C ii) Tf ₂ O, pyridine, DCM, 0°C iii) phenylboronic acid, Pd(PPh ₃) ₄ , 85°C iv) Br ₂ , CHCl ₃ , r.t. v) 2,5-dimethylthien-3-yl boronic acid, Pd ₂ (dba) ₃ , SPhos, K ₃ PO ₄ , toluene, 100°C. 127
Scheme 4.4	Selected C-H arylation conditions used for various thiophene substrates applied to two BDT cores, aimed at selectively functionalizing the β -positions. 128
Scheme 4.5	C-H arylation of thiophenes and benzo[b]thiophenes with high regioselectivity proposed by Colletto <i>et. al.</i> [Adapted from reference 4.2] 129
Scheme 4.6	Benzo[b]thiophene numbering and target photochromic cores, where polymerization occurs from the 4- and 7-positions while the switch is built from the 2- and 3-positions. 129
Scheme 4.7	Synthetic route reported by Morita <i>et. al.</i> on the synthesis of a 4- 7-dihalogenated BT core. Reagents and conditions: (i) t-BuSNa, N,N-dimethylformamide (DMF), -30 °C, 7 h; (ii) K ₂ CO ₃ , MeOH, 0 °C to r.t.; (iii) AuCl (5mol%), 1,4-dioxane, H ₂ O, r.t., 10 min..... 131
Scheme 4.8	Synthetic path towards the di-chlorinated BT switch core, featuring a modified Larock-type ring closure with a t-butyl group (as opposed to a methyl group) as the leaving group. 132
Scheme 4.9	Synthesis of the Quinoxaline core, containing a benzo[b]thiophene switching motif..... 136
Scheme 4.10	Bis(trifluoromethyl)phenyl switching component derivatives. 138
Scheme 4.11	Proposed synthesis of switch core DTBDT , where the diarylethene is built from the center of the long conjugated fused acene dithienobenzodithiophene. 139
Scheme 4.12	Potential switch borepin, where a fatigue-resistant diarylethene switching motif is fused to a dithienoborepin. 140
Scheme 4.13	“Open” and “closed” structures for the diarylethene functionalized dithienoborepin, demonstrating the interruption of the aromaticity in the borepin core..... 141
Scheme 4.14	Other potential pendant photochromic molecules that may prove valuable in the development of switchable polymers..... 142

Scheme 5.1	Structures of [5]-[10] cycloparaphenylenes (CPPs), depicting para-linked benzenes in a hoop-like structure.....	154
Scheme 5.2	Attempted synthesis of [2]CPP via two routes of desulfurization, proposed by Parekh and Guha in 1934.	155
Scheme 5.3	Synthesis of [9], [10], and [11]CPP reported by Jasti and Bertozzi in 2008. Reagents and conditions: (a) (i) <i>n</i> -BuLi, THF, -78 °C, (ii) benzoquinone; (b) (i) NaH, THF, 0 °C, (ii) MeI, 0 °C to rt; (c) (i) <i>n</i> -BuLi, THF, -78 °C, (ii) isopropyl pinacol borate (Bpin), -78 °C; (d) Pd(PPh ₃) ₄ , Cs ₂ CO ₃ , toluene/methanol (10:1), 80 °C. [Adapted from reference 5.3]......	156
Scheme 5.4	Synthesis of [8]CPP from a square-shaped platinum complex a) [PtCl ₂ (cod)] (1 equiv), THF, reflux, 35 h, 57%. b) dppf (4.0 equiv), CH ₂ Cl ₂ , RT, 20 h, 91%. c) Br ₂ (7 equiv), toluene, 95 °C, 17 h, 49%. [Adapted from reference 5.5]	157
Scheme 5.5	Representative synthesis of m[8] designed by the Jasti lab, featuring macrocyclization with a dialkyne-functionalized benzene prior to deprotection and aromatization.....	158
Scheme 5.6	Linear and curved oligomeric and polymeric species investigated in this study, involving π extension through the incorporation of alkynes and either thiophene or benzene rings.....	160

CHAPTER I

Evolution of Photochromic Switches and Their Application to Pendant Switchable Polymers

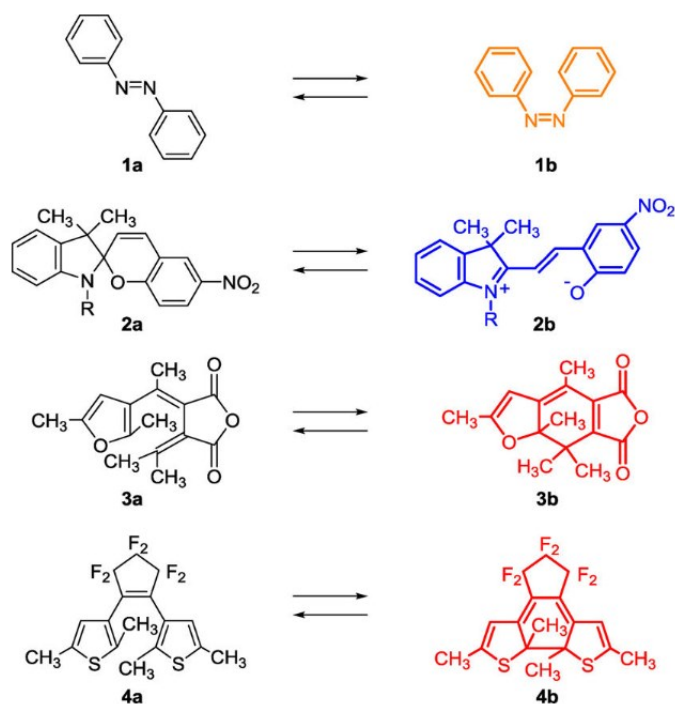
Stimuli-responsive molecules and materials represent a broad and beautiful area of chemistry that allows for one to obtain desirable mechanical or electronic effects via external input. Of the many stimuli-responsive compounds in existence, photochromic molecules represent a particularly interesting group due to the strong change in electronic structure, often coupled with substantial structural change. A photochrome (from latin roots *photo* meaning “light” and *chrom* meaning “color”) can be described as a molecule that can reversibly isomerize between two states based on the wavelength of light it is irradiated with. Possibly the most pervasive application of photochromic molecules in everyday life comes in the form of photochromic (or transition) lenses for eyeglasses, which darken in sunlight to produce a shading effect similar to sunglasses, and return to a colorless state in the dark or under artificial lighting. Modern transition lenses use a thin film of the organic photochrome as one of the layers on the glass, common ones being naphthopyrans and indenonaphthopyrans, shown below. The UV light present in sunlight triggers an isomerization, which causes an increase in conjugation and allows the compound to absorb at longer wavelengths. This new absorption often lands in the visible region, resulting in some form of coloration and thus allowing for the glass to be tinted. Once exposed to UV-free light, the molecule can isomerize back to its original uncolored state.



Scheme 1.1 An example of the reversible isomerization in (indeno)naphthopyrans, a common organic photochrome used in transition lenses.

Chemists and materials scientists are always looking for novel and exciting photochromes, and this has spurred the creations of several different classes, some of the most common are shown below.¹ Azobenzenes (**Scheme 1.2, 1a-b**) and spiropyrans (**Scheme 1.2, 2a-**

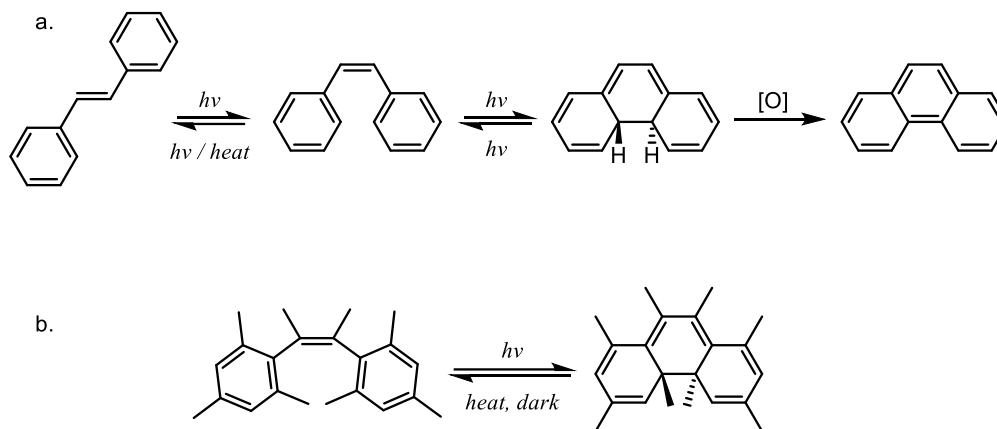
b) represent a subset of photochromes called T type, meaning that their reverse isomerization can be accomplished thermally at room temperature. While these compounds have found several applications,²⁻³ most use-cases would require more rigorous preservation of each isomeric form would be more desirable. Furylfulgides (**Scheme 1.2, 3a-b**) and diarylethenes (**Scheme 1.2, 3a-b**) are two classes of photochromes that were subsequently developed and are thermally irreversible at room temperature in both isomeric forms. These are P-type switches, in which both isomers require photoirradiation to interconvert.



Scheme 1.2 Some common classes of photochromes: Thermally reversible azobenzenes (**1a-b**) and spiropyrans (**2a-b**), and thermally irreversible furylfulgides (**3a-b**) and diarylethenes (**4a-b**). [Adapted from reference 1.1]

Of particular interest are diarylethenes (**Scheme 1.2, 4a-b**) which, through structural modifications, can lead to high thermal stability of both isomers and very high coloration/decoloration cycles (fatigue resistance). The earliest investigations into diarylethene began with the well-studied isomerizations of stilbene.⁴ Stilbene, shown below, can proceed through cis-trans isomerization of the central double bond. *Trans*-stilbene, a white crystalline

solid, could be converted to the clear colorless liquid *cis*-stilbene photochemically, while the reverse reaction can occur with heat or light (**Scheme 1.3a**). *Cis*-stilbene can also be irradiated to generate a cyclized product through a well-known 6- π electrocyclization.⁵ In the presence of oxygen, this species can lose two hydrogens to obtain phenanthrene, with global aromaticity as the driving force.

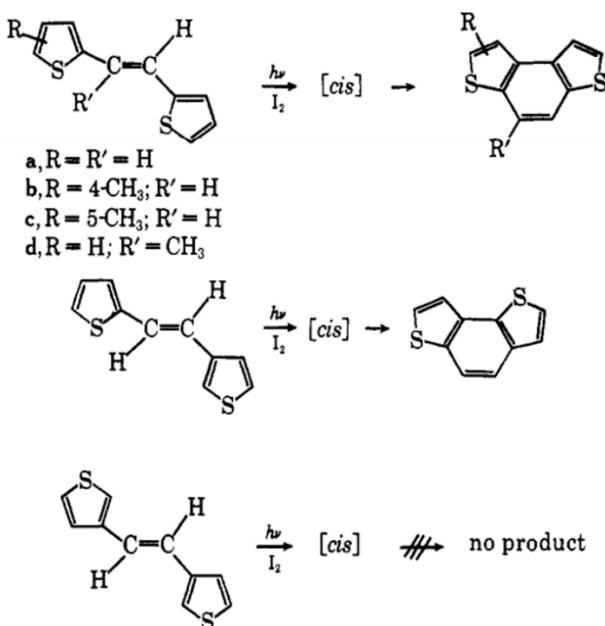


Scheme 1.3 Isomerizations of Stilbene (a) and 2,3-dimesityl-2-butene (b) emphasizing differences in reversibility due to the presence of methyl substitutions.

When 2,3-dimesityl-2-butene (**Scheme 1.3b**) was irradiated at 289 nm, a yellow color appeared that was found to be the cyclized product. When left in the dark at 30° C for 3 minutes, the yellow coloration disappeared as the cyclized form reverted to the open molecule again. The methyl groups at the interior position were found not to be labile in the presence of oxygen as in the case with cyclized stilbene, proving that this functionalization was effective at preventing the irreversible oxidation of the cyclized species. The cyclized form, however, was still thermally unstable and thus quickly reverted to the open-ring form after a short period.

Kellogg *et. al.* also explored these hexatriene to cyclohexadiene type cyclizations using heteroarene systems in thiophene and furan (as opposed to benzene used in the stilbene systems) with the intent of providing further mechanistic clarification, some of which are shown below for thiophene derivatives.⁶ Similar to the simplified *cis*-stilbene cyclization, photoirradiation of

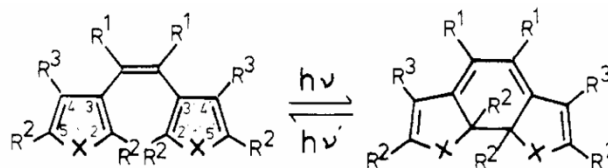
difuryl- or dithienylethene resulted in the cyclized dihydro species that loses two hydrogen atoms in the presence of oxygen to generate the irreversible products benzodifuran and benzodithiophene.



Scheme 1.4 Selected dithienylethene species reported by Kellogg *et. al.* demonstrated the irreversibly cyclized benzothiophene molecules in the presence of an oxidant. [Adapted from reference 1.6]

In the absence of air, however, some of the cyclized thiophene derivatives demonstrated prolonged lifetimes (upwards of 15 hours) in the dark at room temperature without cycloreversion. This indicates that substitution of the diarylethenes with heteroacenes as opposed to benzene may lead to more stable cyclized species, at least for the dihydro- forms.

In 1988, Irie and Mohri reported the reversible cyclization of diarylethene derivatives.⁷ It was found that, for diarylethenes that contained both heteroatoms and methyl substitutions at interior positions led to photoswitches that both thermally irreversible and resistant to oxidation (Scheme 1.5).

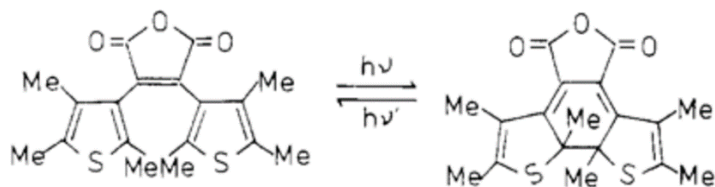


a, X = S; R¹ = R² =
 R³ = H
b, X = S; R¹ = R² =
 CH₃; R³ = H
c, X = O; R¹ = R² =
 CH₃; R³ = H
d, X = S; R¹ = CN; R² =
 R³ = CH₃

a, X = S; R¹ = R² =
 R³ = H
b, X = S; R¹ = R² =
 CH₃; R³ = H
c, X = O; R¹ = R² =
 CH₃; R³ = H
d, X = S; R¹ = CN; R² =
 R³ = CH₃

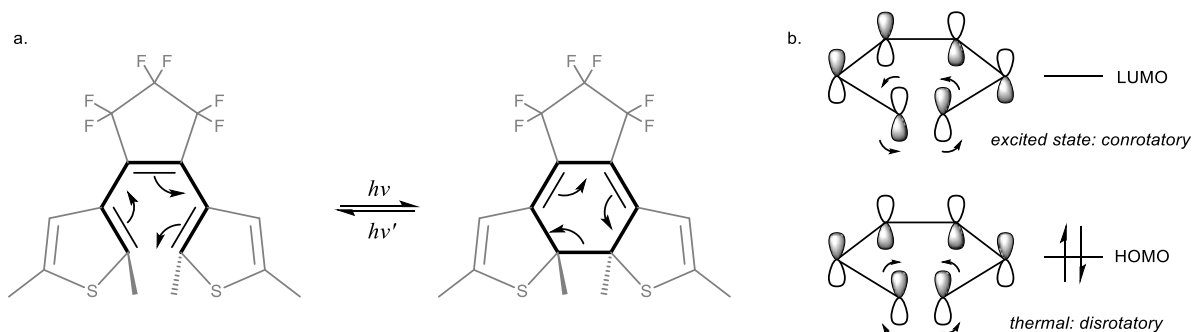
Scheme 1.5 Switches reported by Irie *et. al.* demonstrating incorporation of methyl groups and heteroatom substitution leading to thermal stability and resistance to oxidation. [Adapted from reference 1.7]

For compounds **3b** and **3c**, photoirradiation at 313 nm transformed clear colorless solutions to yellow, where a new absorption maxima was observed at 431 nm (**4b**) and 391 nm (**4c**). When these solutions were exposed to visible light irradiation (>390 nm), the coloration rapidly disappeared. It was found for these species that exposure to air caused no decrease in coloration, indicating that oxygen did not cause the condensed irreversible product to form. These compounds were also found to be very thermally stable, maintaining the same absorbance spectrum for 12 hours at 80° C. One of the only downsides of this reaction, however, was the ultraviolet irradiation would also generate the *trans*- byproduct, which competed with the formation of the desirable cyclized product. This at the time was circumvented by either replacing the methyl groups along the bridging ethene with cyano groups to shift the absorbance to longer wavelengths, or by having the bridging ethene be a part of a ring system where cis-trans isomerization is impossible, as in maleic anhydride. Both of these methods proved extremely successful, and the maleic anhydride even demonstrated thermal stability of both isomers up to 300° C (**Scheme 1.6**). This work represents the first of many reported by both Irie and other scientists on thermally stable diarylethenes.



Scheme 1.6 Switches based on maleic anhydride removed the opportunity for the undesirable cis-trans isomerization. [Adapted from reference 1.7]

Structure and Mechanism. Although the (hetero)acenes and substitutions can vary, all photochromic diarylethenes share a central hexatriene core (**Scheme 1.7a**). Once photoirradiated with the appropriate wavelength, the photochrome proceeds through the well-known^{5, 8} 6- π electrocyclization reaction to yield a cyclohexadiene moiety. The thermal version of this reaction requires disrotatory motion (**Scheme 1.7b**), which is often impossible due to steric reasons. The excited state species, however, requires conrotatory motion which often has good orbital overlap and has ample space for the substitutions on the terminal position of the hexatriene unit.



Scheme 1.7 Diarylethenes all feature a core cyclohexadiene system (a). Favorable orbital overlap for cyclization occurs during conrotatory motion.

Higher mechanistic insight involves considerations as to what occurs in the excited state of these species. **Figure 1** illustrates a simplified two-dimensional version of the ground state and excited state surfaces involved with the photoisomerization processes, which generally involves an excited species relaxing to a conical intersection, a point at which transition between potential

energy surfaces is highly efficient. Inspection of the two major potential energy surfaces (**1A** and **2A**) reveals that both possess a transition state. Once excited, the open-ring isomer occupies the Frank-Condon state **1BFC(o)**. Since this state is very close in energy to the **2A** state, rapid internal conversion occurs, and the species moves down to the conical intersection **2A/1A CI**. Ground state decay from this point results in highly efficient conversion to the closed ring isomer. For the reverse reaction, a similar excitation happens to the Frank-Condon state that also converts to the **2A** surface, though now there is the presence of the transition state that needs to be energetically overcome before reaching the conical intersection. Because of this, the ring-opening process for these species not only depends on the wavelength of irradiation, but also the temperature.

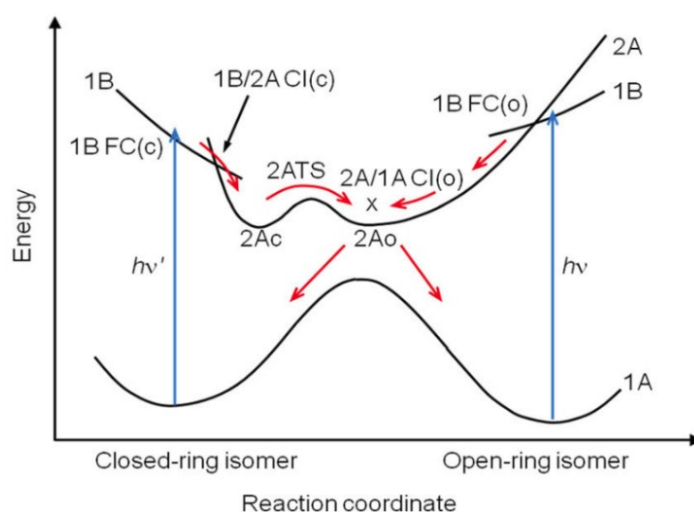
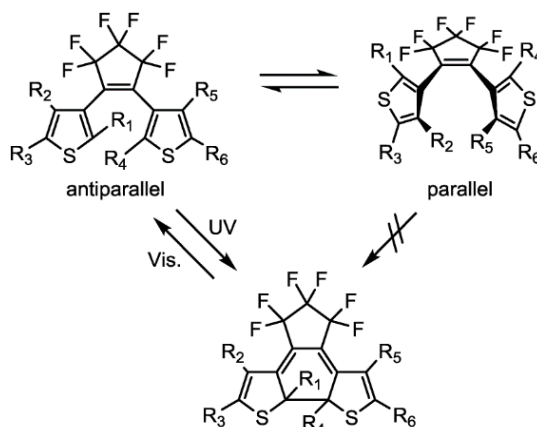


Figure 1.1 Simplified two-dimensional ground- and excited state potential energy surfaces illustrating cyclization and cycloreversion paths around the conical intersection. [Adapted from reference 1.1]

When considering the whole system (including the heteroacenes fused to the hexatriene core), we see that diarylethenes can occupy two primary conformations, so-called parallel and anti-parallel conformers (**Scheme 1.8**). In many species, there is a substantial amount of rotation that would allow for these two conformers to interconvert in solution, but often time one conformation in the crystalline phase. Because the key isomerization occurs photochemically

through conrotatory motion, the orbitals only have *favorable* overlap in the anti-parallel conformation, and hence the vast majority of photochromic activity stems from this conformer.



Scheme 1.8 For both steric and electronic reasons, diarylethenes that occupy a parallel conformation do not typically proceed through the electrocyclization reaction. [Adapted from reference 1.1]

Upon isomerization, there are notable electronic and structural changes observed (**Figure 1.2**). A signature feature of diarylethenes is the drastic coloration seen upon cyclization. This is due to the increase in conjugation from the hexatriene moiety to systems containing four or more conjugated double bonds. The extended conjugation results in a smaller highest occupied molecular orbital – lowest unoccupied molecular orbital (HOMO-LUMO) gap, allowing the compound to absorb light at lower wavelengths. The diarylethene in solution goes from clear to red after irradiation with UV light. This stark color change can be seen in the UV-Vis spectrum as well (**Figure 1.2b**), where the “closed” switch has two new red-shifted peaks. Geometrically, a surprisingly small conformational change during ring formation (**Figure 1.2c**), amounting to 10% or less in any direction. The small conformational change allows many photochromic species to be switched not only in solution, but also in the crystalline form, as long as it is in the anti-parallel conformation.

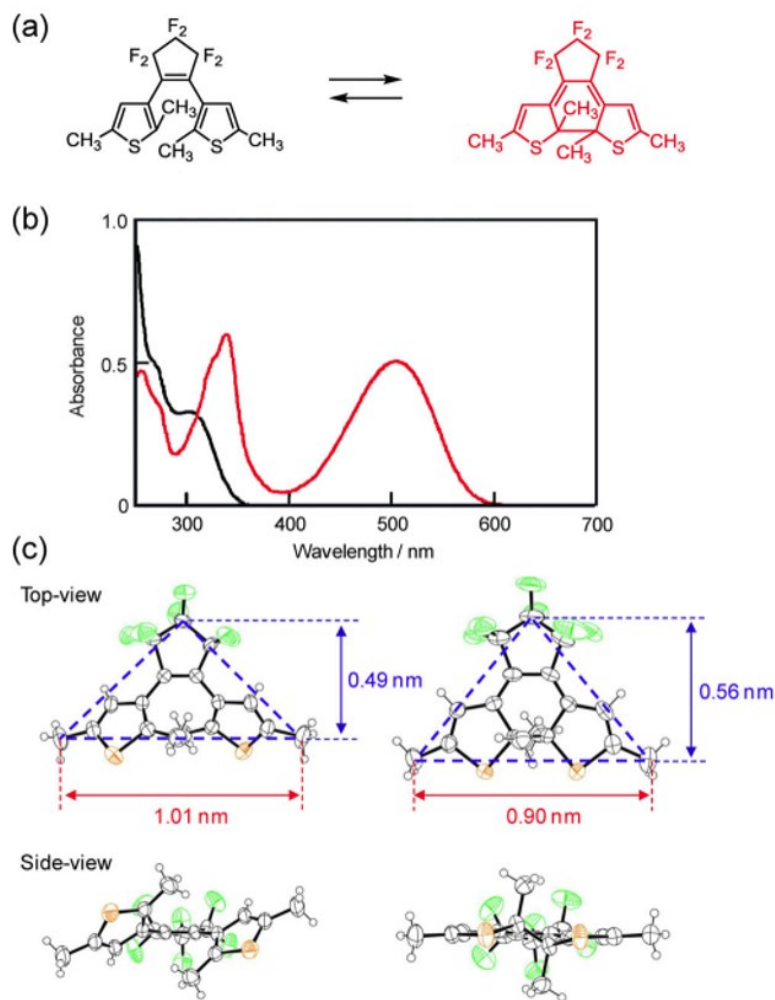
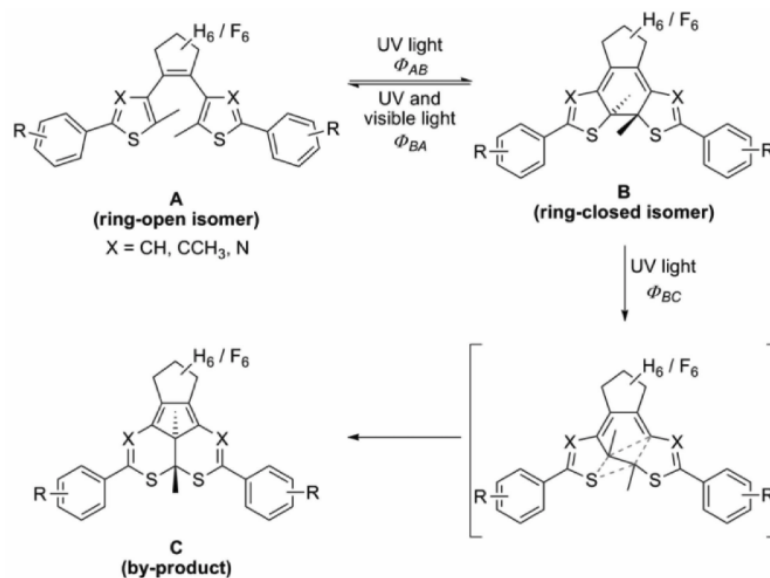


Figure 1.2 Representative example of a perfluorocyclopentene-based diarylethene switch (a) and the corresponding UV-Vis profile (b). In isolation, there is a small conformational change between the open and the closed form (c). [Adapted from reference 1.1]

While imparting methyl substituents on the aryl group in place of hydrogens results in protection from oxidation due to the loss of two hydrogen atoms, diarylethenes are still susceptible to conversion to an irreversible product (**Scheme 1.9**). Presented here is an example of the photoisomerization discussed thus far, the interconversion between the ring-open isomer **A** and the ring-closed isomer **B** with UV and/or visible light. It has been observed that, upon further irradiation of the closed switch with UV light, the molecule proceeds through a 1,2-dyotropic shift to produce the photochemically irreversible byproduct **C**.⁹ This product has been confirmed for several switch derivatives as the main by-product for diarylethene switches, where more

fatigue-resistant compounds are less likely to have their ring-closed isomer irreversibly converted. Imparting electron deficient groups to the system appears to be the most effective way to increase the fatigue resistance of the compound (a topic to be visited with more depth later), though the exact reason for this increased robustness is still not yet known. Nevertheless, incorporation of electron-accepting groups such as the CF₃- moiety.



Scheme 1.9 Upon further irradiation, the closed isomer of some diarylethenes can proceed through an irreversible 1,2-dyotropic shift. [Adapted from reference 1.9]

Applications. The structural diversity and ease of synthesis has led to the development of hundreds of diarylethene-based photochromes with various applications, with the most prominent being applications involving memory and data writing.¹ A few examples, however, can illustrate the diversity of applications (**Figure 1.3**). For example, Terao *et. al.*¹⁰ developed a crystalline diarylethene that can reversibly curl and straighten upon successive irradiation cycles. The small conformational change in diarylethene photoisomerizations allows the event to occur in the solid state. Often times, this effect goes unnoticed, but in some species (**Figure 1.3a**) can severely contort, resulting in a hairpin shaped-crystal, which can completely regain its original linear form.

Some of these crystals have actuation properties,¹¹ capable of moving nanoparticles 50 times the mass of the crystal several micrometers without breakage.

Another dramatic example is the use of diarylethenes as photoacid generators, developed first by the Kawai group.¹² As discussed earlier, methyl groups tend to replace hydrogen atoms at the internal position of the diarylethene, as these groups are oxidation-resistant. Nakashima and coworkers, however, decided to capitalize on the lability of the protons and other substituents at this internal position, that results in the irreversible but controlled generation of a proton, with mesityl alcohol as the other leaving group. They went on to demonstrate that this system can be used as a photoacid catalyst in the controlled polymerization of cyclohexene oxide.

Yet another example comes in the form of a photoswitchable biomarker. Zou *et. al.* synthesized a biocompatible diarylethene switch that could be inserted into human nasopharyngeal epidermal carcinoma cells (KB cells)¹³ (**Figure 1.3c**). In the open state, the switch is fluorescent green, and can be detected in the cytoplasm with a 50:1 contrast ratio. Upon irradiation with 405 nm light (avoiding the ultraviolet region), the switch ring-closes, and the fluorescence is diminished by 98%. To their surprise, the photoisomerization process could be repeated several times without any apparent fatigue of this photochrome, and also possessed low cytotoxicity, marking its potential use as a cellular label in living systems.

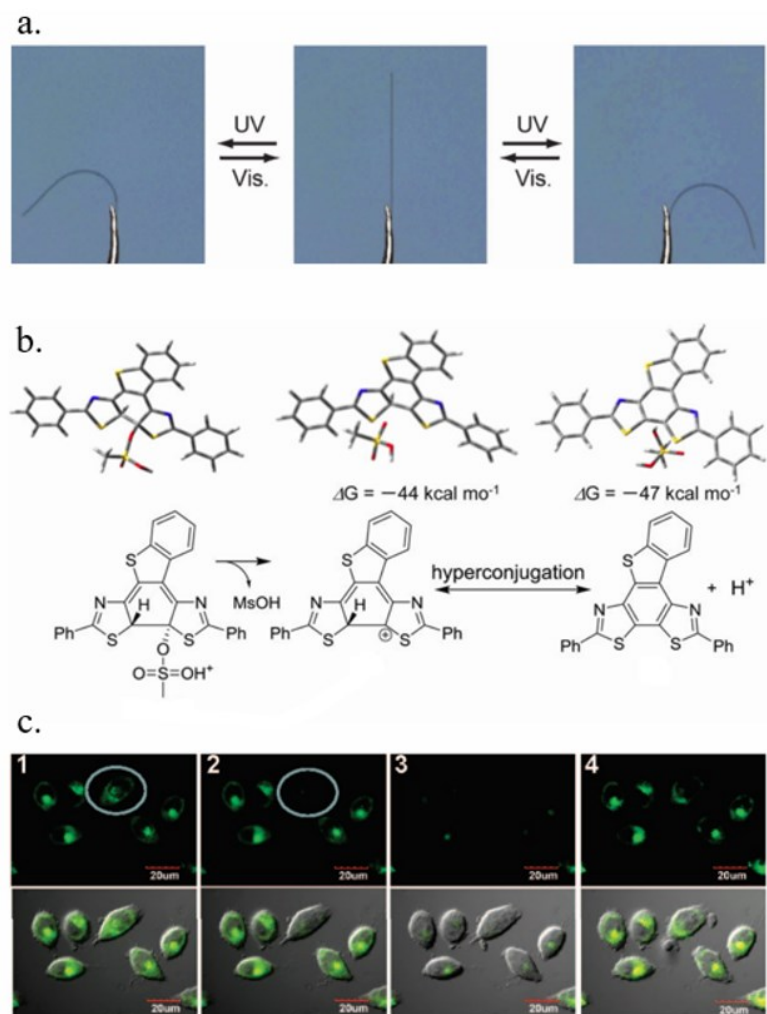


Figure 1.3 Demonstration of reversible bending of a single diarylethene crystal (a), photoacid generation upon cyclization (b), and switchable fluorescence (c). [Adapted from references 1.10 to 1.13]

Diarylethenes can also be incorporated into polymeric structures, either embedded directly into the polymeric backbone or as a side-chain unit. If the switching motif is not conjugated to the polymer backbone, the photophysical properties of the switch are relatively unchanged, and as a consequence there is little impact on the polymer itself. For example, Myles and Branda used ring-opening metathesis polymerization (ROMP) to produce a pendant photochromic polymer (**Figure 1.4a**). In this case, the isolated switch possessed spectral features that were nearly identical to the polymeric version. However, relatively little work has been

devoted to diarylethene-based photochromes as part of π -conjugated systems. In this situation, reversible isomerization of these embedded photochromes would be expected to drastically change the electronic properties of the polymer. The first diarylethene-based main-chain conjugated polymer was reported by Stelacci *et. al.*, where the open and closed switch displayed substantially different optical properties.¹⁴ Following this report, electrically conductive conjugated polymers featuring the diarylethene switching motif were reported (**Figure 1.4b-c**). In these cases, the open switch is actually cross-conjugated before it gets to the hexafluorocyclopentene unit. Upon ring-closing of the switching motif, the system becomes directly conjugated with the main polymer backbone. Indeed, increased conductivity of the closed switch relative to the open switch was observed, a beautiful and promising result that diarylethene can potentially be used in stimuli-responsive materials.

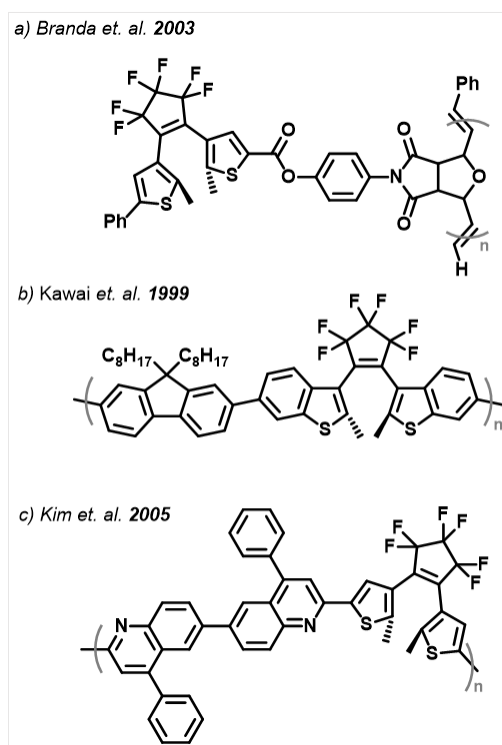


Figure 1.4 Representative polymers featuring non-conjugated pendant (a) and conjugated main-chain (b,c) photochromic moieties.

The main-chain photochromes represent the more common polymer design, in which the entire π -conjugated pathway is directly connected to that of the comonomer, thus playing an integral part in the conjugated backbone of the material. This certainly seems like the most likely design to have the strongest impact on the electronic nature of the polymer overall, though perhaps it possesses one major drawback. It was discussed earlier that there is a small conformational change upon isomerization for diarylethenes, which is a major reason that photoswitching can still occur in the crystalline state. One can imagine all diarylethenes in a lattice cyclizing and slightly sliding past each other to adopt the new conformation, without building up any strain in the material. This is different in a polymeric system however (**Figure 1.5**). While there is a small conformation demand in main-chain diarylethene-based polymers *per switch*, one would expect several switching isomerizing along a polymer strand to impart some torsional demand on the material, which may not be possible in the solid state. This idea is defended by experiments performed by Kawai *et. al.*, where the irradiated and bleached polymer showed significantly different weights when characterized by gel permeation chromatography.¹⁵

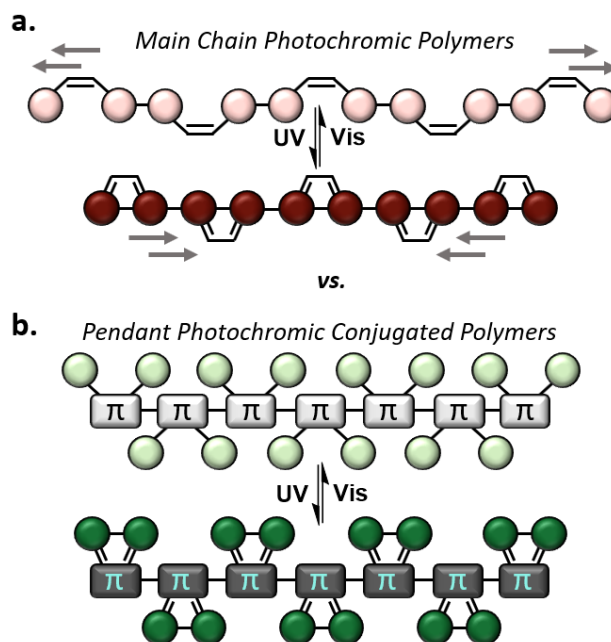


Figure 1.5 Spatial effect of photoisomerization along polymers featuring a main-chain (a) or pendant (b) diarylethene motif.

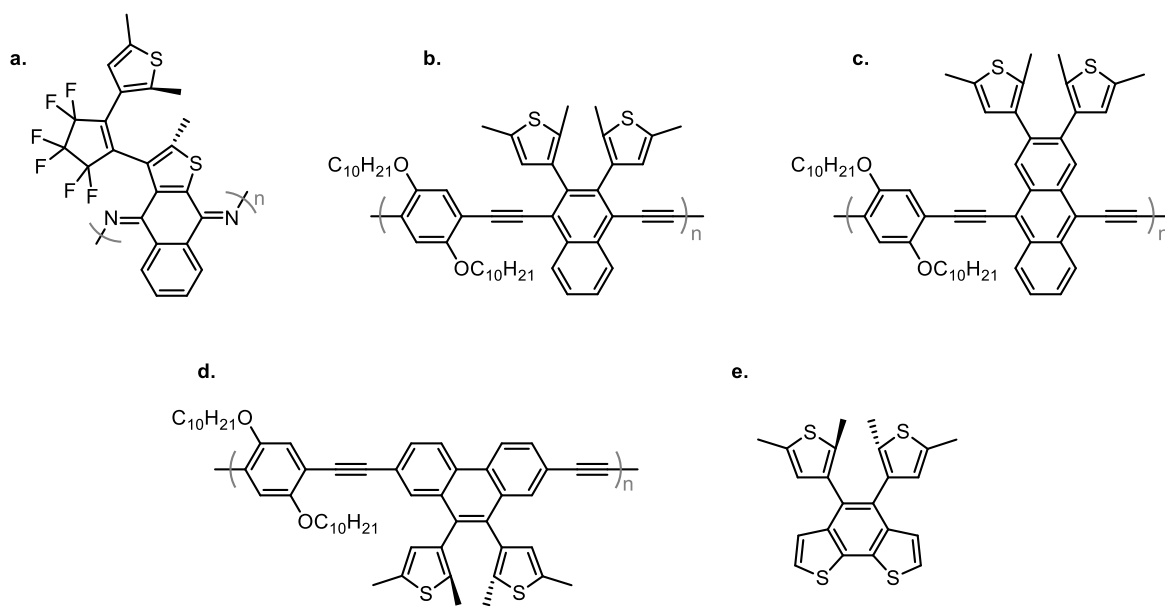
An alternative polymer design involves having the photochromic switch be pendant to, but still conjugated with, the polymer backbone. Due to this conjugation, one would still expect there to be an electronic impact on the conjugated polymer, albeit possibly less so since it is not directly embedded into the main-chain. However, one would expect less main-chain polymer reorganization upon photoisomerization, since the conformational demand per diarylethene cyclization is off-chain (**Figure 1.5b**).

Wonderful work has been done in the past by previous members of the Tovar lab, some notable examples are shown in **Scheme 1.10**. One of the earliest targets proposed was that of Dr. Alicia Fraind, which featured an anthracene-like core (**Scheme 1.9a**). It is well-known that anthracene and related cores have localized aromaticity on the terminal ring systems so as to maintain two Clar-sextets, resulting in limited charge mobility in polymers where the conjugated system involves transfer through the central ring of the anthracene-like core. The key idea behind this compound is to have one of the fused aromatic cores also be an aryl group of the switching

motif. As discussed previously, this will result in breaking aromaticity in the aryl groups upon ring-closure. Thus, one can expect that the electrons in the double-bond at the fused position to no longer be localized due to aromaticity, and thus free to participate in charge transfer. The overall polymer wire would then possibly behave as an “off” switch when open, and an “on” switch upon cyclization. Unfortunately, this molecule proved very synthetically challenging and was not realized. Dr. Fraind also worked on anthracene- and naphthalene-based switch cores (**Scheme 1.9b-c**). These molecules proved to be much more synthetically tractable, and were made with the intention of investigating the effect of extending the fused arene from which the switch was built. While several compounds were synthesized to probe this effect, in almost all cases it was not possible to confirm that the closed switch was obtained by either chemical or photochemical methods.

Dr. Christopher Harvey also synthesized a series of phenanthrene-based switch cores for oligomeric models and polymeric species, one of which is shown in **Scheme 1.9d**. Here again, Dr. Harvey found great success in synthesizing these complex targets, though none of the species showed the desirable response upon photoirradiation, i.e. the substantial red-shift in the absorbance spectrum indicating the closed switch. In the polymeric species, almost no response was seen.

Dr. Justin DeFrancisco successfully synthesized a core in which a dithienylethene was built off of a benzodithiophene unit (**Scheme 1.9e**). This compound was found to be photochromic, where a new absorbance grew in the visible region that was almost completely reversible. In this system, if one thinks of each thiophene possessing a Clar sextet, then the remaining double bond can be treated as bridging ethylene that can more easily participate in the switching event, as opposed to having to break the aromaticity of benzene. Difficulty arose when attempting to functionalize the material for inclusion in to polymeric material. Multiple methods of bromination, boronation, and C-H activation were attempted, though none were successful.



Scheme 1.10 Selected photochromic cores developed by former group members towards pendant switchable conjugated polymers.

All three scientists made many more attempts to synthesize more photochromes or make structural modifications to existing photochromes than reported here, which speaks to the great difficulty in achieving the end goal of a pendant photochromic polymeric material. The switch core necessitates having locations on the molecule where very specific substitutions must be made. Two adjacent atoms bridged by a double bond must be available from which the switching motif can be built, and yet another two atoms on the core must be susceptible to functionalization for polymerizations. The synthetic demand for functionalizing these (hetero)acenes is thus very high, prevailing as a major barrier to the development. In addition, there is underlying theory that still needs to be understood about the photochromes developed in the Tovar lab thus far to better explain the weak or absent response to UV irradiation.

Conclusion

Diarylethenes and other photochromes are feature-rich molecules that exhibit desirable properties outside of their visual transformations. One of the most attractive features of some

diarylethene-based switches is the drastic electronic change with minimal conformational change upon isomerization of individual molecules. An interesting application is in conjugated photochromic polymers, where conductivity differences can be seen for the “open” and “closed” states. Unfortunately, while conformational demands for individual switches along the chain are relatively minute, the collective cyclizations have strong reorganizational demands. An alternative involves having the switching motif pendant, but still conjugated to, the π -extended polymer backbone. Work by several remarkable scientists has laid the foundation for future development of this concept.

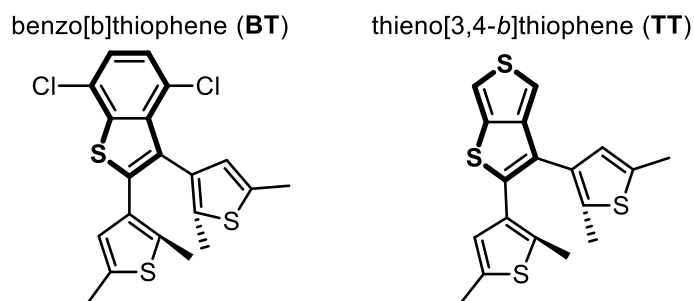
References

1. Irie, M.; Fukaminato, T.; Matsuda, K.; Kobatake, S. Photochromism of Diarylethene Molecules and Crystals: Memories, Switches, and Actuators. *Chemical Reviews* **2014**, *114* (24), 12174-12277.
2. Klajn, R. Spiropyran-based dynamic materials. *Chemical Society Reviews* **2014**, *43* (1), 148-184.
3. Beharry, A. A.; Woolley, G. A. Azobenzene photoswitches for biomolecules. *Chemical Society Reviews* **2011**, *40* (8), 4422-4437.
4. Waldeck, D. H. Photoisomerization dynamics of stilbenes. *Chemical Reviews* **1991**, *91* (3), 415-436.
5. Houk, K. N.; Li, Y.; Evanseck, J. D. Transition Structures of Hydrocarbon Pericyclic Reactions. *Angewandte Chemie International Edition in English* **1992**, *31* (6), 682-708.
6. Kellogg, R. M.; Groen, M. B.; Wynberg, H. Photochemically induced cyclization of some furyl- and thienylethenes. *The Journal of Organic Chemistry* **1967**, *32* (10), 3093-3100.
7. Irie, M.; Mohri, M. Thermally irreversible photochromic systems. Reversible photocyclization of diarylethene derivatives. *The Journal of Organic Chemistry* **1988**, *53* (4), 803-808.
8. Hoffmann, R.; Woodward, R. B. Conservation of orbital symmetry. *Accounts of Chemical Research* **1968**, *1* (1), 17-22.
9. Herder, M.; Schmidt, B. M.; Grubert, L.; Patzel, M.; Schwarz, J.; Hecht, S. Improving the Fatigue Resistance of Diarylethene Switches. *Journal of the American Chemical Society* **2015**, *137* (7), 2738-2747.
10. Terao, F.; Morimoto, M.; Irie, M. Light-Driven Molecular-Crystal Actuators: Rapid and Reversible Bending of Rodlike Mixed Crystals of Diarylethene Derivatives. *Angewandte Chemie International Edition* **2012**, *51* (4), 901-904.
11. Kobatake, S.; Takami, S.; Muto, H.; Ishikawa, T.; Irie, M. Rapid and reversible shape changes of molecular crystals on photoirradiation. *Nature* **2007**, *446* (7137), 778-781.
12. Nakashima, T.; Tsuchie, K.; Kanazawa, R.; Li, R.; Iijima, S.; Galangau, O.; Nakagawa, H.; Mutoh, K.; Kobayashi, Y.; Abe, J.; Kawai, T. Self-Contained Photoacid Generator Triggered by Photocyclization of Triangle Terarylene Backbone. *Journal of the American Chemical Society* **2015**, *137* (22), 7023-7026.
13. Zou, Y.; Yi, T.; Xiao, S.; Li, F.; Li, C.; Gao, X.; Wu, J.; Yu, M.; Huang, C. Amphiphilic Diarylethene as a Photoswitchable Probe for Imaging Living Cells. *Journal of the American Chemical Society* **2008**, *130* (47), 15750-15751.
14. Stellacci, F.; Toscano, F.; Gallazzi, M. C.; Zerbi, G. From a photochromic diarylethene monomer to a dopable photochromic polymer: optical properties. *Synthetic Metals* **1999**, *102* (1), 979-980.
15. Kawai, T.; Nakashima, Y.; Irie, M. A Novel Photoresponsive π -Conjugated Polymer Based on Diarylethene and its Photoswitching Effect in Electrical Conductivity. *Advanced Materials* **2005**, *17* (3), 309-314.

CHAPTER II

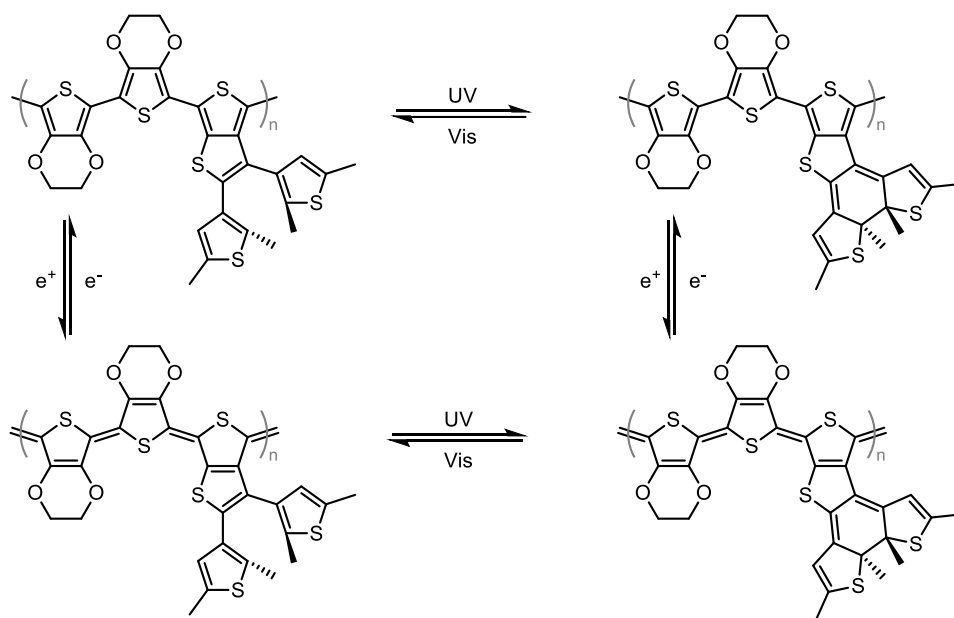
Design and Synthesis of Photochromic Switch Monomers Based on Thieno[3,4-*b*]thiophene

Work done by previous group members demonstrates the difficulty not only in synthesizing these switch cores, but also predicting their photophysical behavior. I started my investigation into value-added cores by considering (hetero)acenes that are frequently encountered in conjugated materials. Several structures are revisited from the literature for their OFET or OPV performances, including thiophenes, benzodithiophenes, diketopyrrolopyrroles. Ideally, one would like to retain the desirable properties observed in these polymers, with the added feature of being able to “switch” the properties via external stimuli. Synthetic tractability is of utmost importance, so the list of potential heteroacenes was narrowed to those targets with reasonable synthetic paths that accomplished two major structural goals: 1) There must be two contiguous locations across an ethene-like bridge that can be functionalized to build the diarylethene switching motif and 2) there must be two locations that can be functionalized for pi-extension, either via single acene extension or polymerization. The synthetic caveat is accomplishing both goals without having one objective interfere with the other. For example, the site-selectivity for building the switch may be difficult to accomplish in the presence of more reactive sites. From the narrowed list of desirable cores, two prevailed as the most reasonable both in terms of properties and synthetic tractability, benzo[b]thiophene and thieno[3,4-*b*]thiophene (**Scheme 2.1**), the latter of which will be discussed in detail.



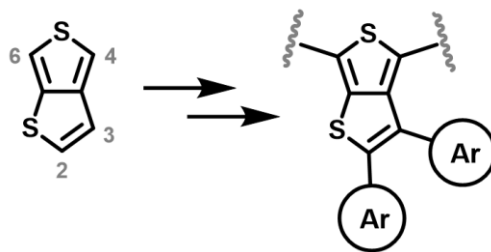
Scheme 2.1 Two promising photochromic switch monomers based on thiophene-fused heteroacenes benzo[b]thiophene and thieno[3,4-*b*]thiophene.

TT represents a relatively recent thioacene that possesses several attractive properties, with arguably the most well-known being the performance of **TT** containing polymers in organic photovoltaics, in which a copolymer containing benzodithiophene demonstrated cutting-edge OPV performance for organic materials at the time.¹ Several other works, especially those by Sotzing *et. al.*, demonstrate that the inclusion of **TT** into polymeric species results in a low bandgap material, and those with a high **TT** content demonstrate high optical transparency.²⁻³ These and several other features illustrate that **TT** is a highly desirable core in polymeric materials. Early in the investigation, **TT** seemed particularly attractive due to the potential for multi-state switching, in which the polymer backbone can be made optically transparent based on the applied voltage, while the switch acted as a photoresponsive unit that further changes the electronic properties. In the example below, a co-polymer between ethylenedioxythiophene (EDOT) and a switch-functionalized **TT** would have four potential states, two via electrochemical control, and two through photochemical control (**Scheme 2.2**). Because switches tend to be colorless (optically transparent in the visible region), it was theorized that the colored polymer can be made optically transparent upon application of the appropriate voltage, and then colorized through irradiation of the pendant switches. Due to the lack of experience with pendant photochromic compounds, picking the ideal core from which to start a thorough investigation is based on both underlying theory as to why an individual core may be found desirable, and also whether it is synthetically tractable. These reasons led to the choice of **TT**.



Scheme 2.2 Conceptual depiction of a four-state pendant photochromic polymer controlled both photochemically and electrochemically.

The synthetic demands for the pendant photochromic polymer, however, are starkly different than those of reported polymers. One can start by describing the addressable carbons on the **TT** core (**Scheme 2.3**).

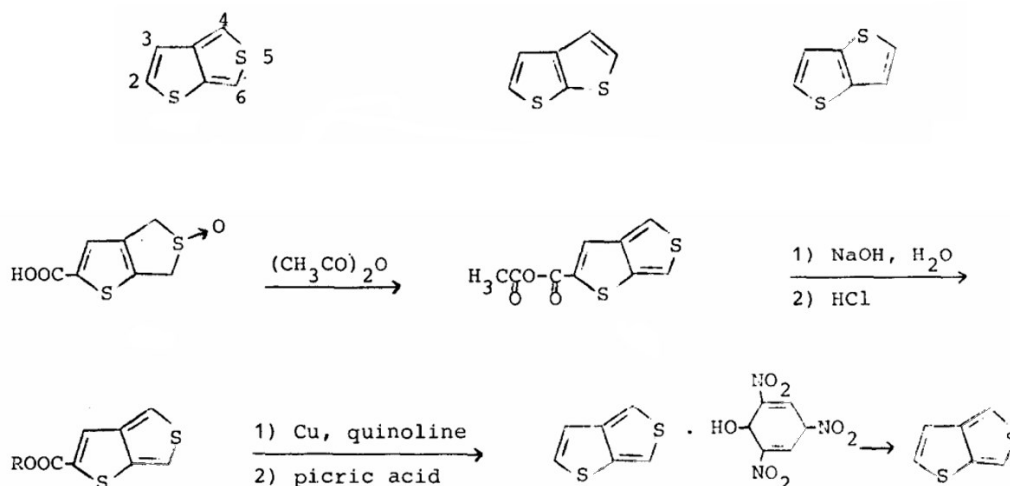


Scheme 2.3 Numbering scheme for thieno[3,4-*b*]thiophene and depiction of desirable functionalization, where the diarylethene switching motif is built from the 2- and 3- positions and π -extension is to occur from the 4- and 6- positions.

Polymerizations on **TT** typically occur from the 4- and 6- positions, which are also conveniently the positions that are easiest to halogenate. Reactivity is relative to the reaction

under investigation, but here we are discussing the ability to halogenate a particular location, which in turn can be subjected to cross coupling procedures to obtain the pi-extended species. The reactivity of the 4- and 6- positions of thieno[3,4-*b*]thiophene track well with track well with that of thiophene. However, the asymmetric electronic structure of **TT** results in a preference for initial bromination at the 6- position. This is inconsequential for polymerizations, as the species would ideally be di-halogenated without concern of which carbon is functionalized first, but a wonderful result for regioselective functionalizations. The “bottom” ring of **TT** also has similar reactivity to thiophene in that the *pseudo* α - position (the 2- position) is more reactive than the *pseudo* β - position (the 3- position), with the latter also being the least reactive position of the four.

With carbon reactivities in mind, an appropriate synthetic strategy must be employed not only to build the molecular switch core, but also impart functionalities that allow for pi-extension. Ideally, one would preferentially install the switching motif. At the time the concepts and ideas for this switch were developed, two synthetic routes towards thieno[3,4-*b*]thiophene were reported in the literature. In an attempt to avoid reinventing the wheel on **TT** synthesis, synthetic procedures toward **TT**-based photoswitches first involved modified literature procedures. At the time of this writing, three syntheses of **TT** were reported in the literature. Wynberg and Zawanenburg were the first to report the synthesis of the third “thiophthene” **TT**, which was found to be the most stable of the three thiophthenes (**Scheme 2.4**).⁴

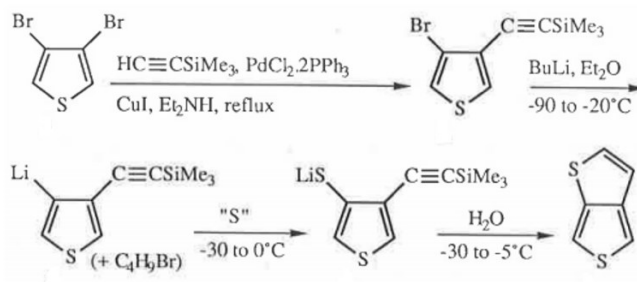


Scheme 2.4 First reported synthesis of the third thiophene: thieno[3,4-*b*]thiophene reported by Wynberg and Zawaneburg. [Adapted from reference 2.4]

Their synthesis begins from dihydrothiophene sulfoxide which has proven useful in the synthesis of other thiophene derivatives. Simply refluxing in acetic anhydride resulted in both anhydride formation from the carboxylic acid at the 2- position, and aromatization of the fused thiophene ring. This anhydride was then reconverted back to the acid over two steps, and subsequently decarboxylated under reflux with copper powder in quinoline. After concentration, the oil was treated with picric acid to generate the picrate. It was found that the free thiophene generated by decomposition of the picrate in ammonia solution rapidly turned yellow, but was stable for a few days. While this seminal work allowed for access to **TT**, a simplified route from more common starting materials was desirable.

In 1990, Brandsma and Verkruijsse published an alternative synthesis, in which **TT** could be prepared on much larger scales due to the readily available starting materials 3,4-dibromothiophene and trimethylsilylacetylene (**Scheme 2.5**).⁵ Unlike the starting material in the Wynberg synthesis that already contained a fused ring system, here one of the fused thiophenes are built onto the ring. The synthesis begins with a single Sonogashira cross coupling reaction to substitute one of the β -position bromine atoms to a TMS-protected alkyne. Very careful lithiation

and thiolation resulted in the thiolithiate, which then ring-closes using the alkyne as an electrophile to generate **TT**.

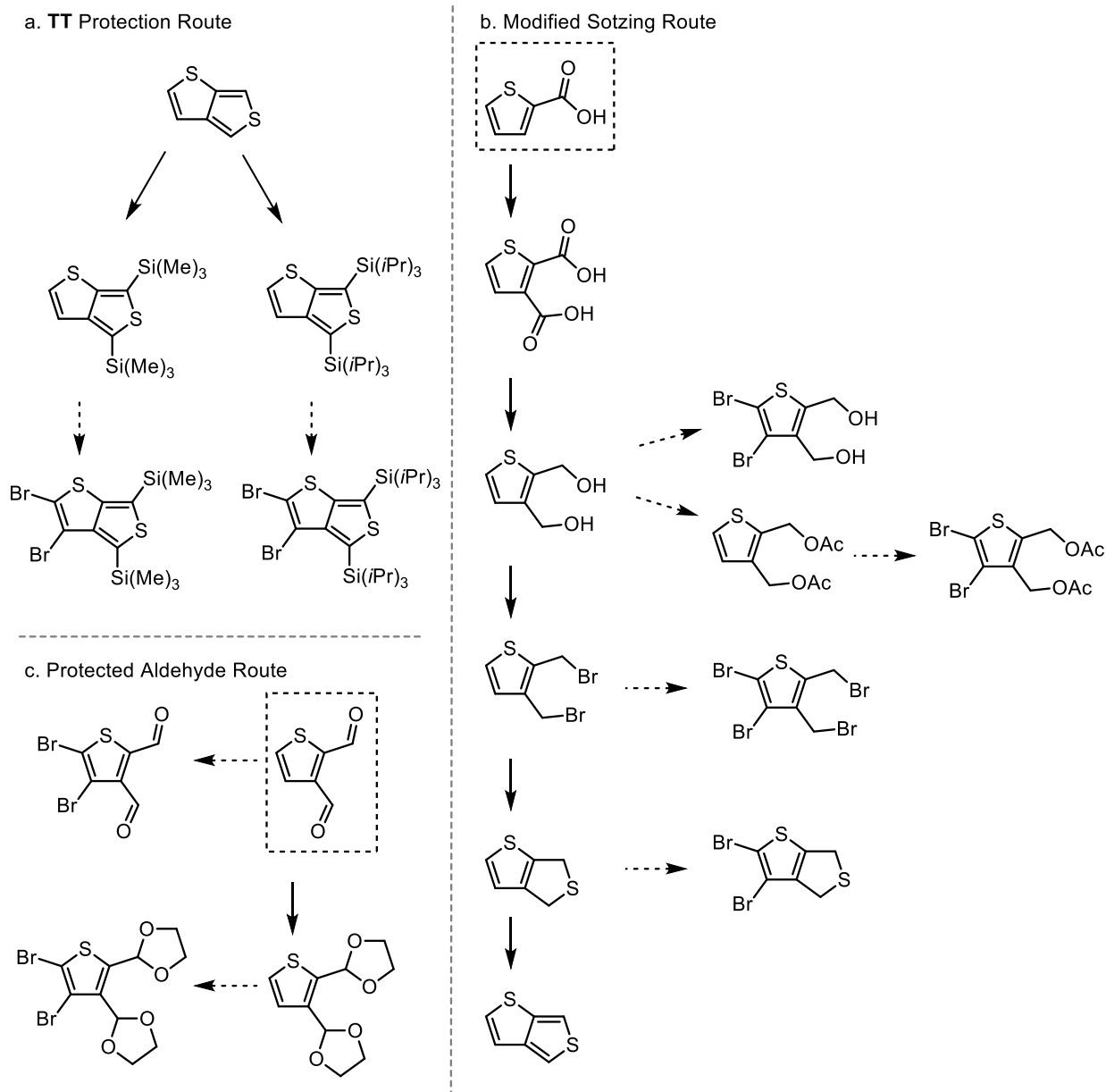


Scheme 2.5 The second reported synthesis of thieno[3,4-*b*]thiophene reported by Brandsma and Verkuijsse. [Adapted from reference 2.5]

While this synthetic route allows for easier access for starting reagents, the synthetic protocol is rather tricky, requiring careful temperature control as well as several intermediate distillations. In addition, other labs have reported difficulty in matching to the reported yield of 77%.⁶ In 2002, Sotzing and Lee published a modified synthetic procedure that slightly simplified the process while increasing yields, and was the procedure followed to generate the first batch of **TT** for switch studies.²

Due to the versatility in transition-metal catalyzed cross coupling reactions, it would be ideal if both the switching substituents at the 2- and 3- positions and the pi-extended (hetero)acenes at the 4- and 6- positions were attached in this fashion. Since the reactivity of the four functionalizable carbon atoms on **TT** vary, a synthetic strategy must be employed that accomplishes both the goal of installing a pendant switching motif and di-halogenation for pi-extension, without either structural modifications interfering with each other. For example, one may want to brominate the 2- and 3- positions of **TT** from which the switch arms can be installed through standard cross coupling reactions. To the best of my knowledge, these locations cannot be *selectively* brominated in the presence of the more reactive and “free” 4- and 6- positions. Likewise, it may be unreasonable to functionalize the 4- and 6- positions prior to installing the

switch; Halogen atoms at these positions will also react in the cross-coupling reactions necessary to build the switching motif. It therefore seemed reasonable to protect the 4- and 6- positions before halogenation.



Scheme 2.6 Attempted synthetic routes towards (pre)functionalized **TT** switch cores utilizing modified literature syntheses.

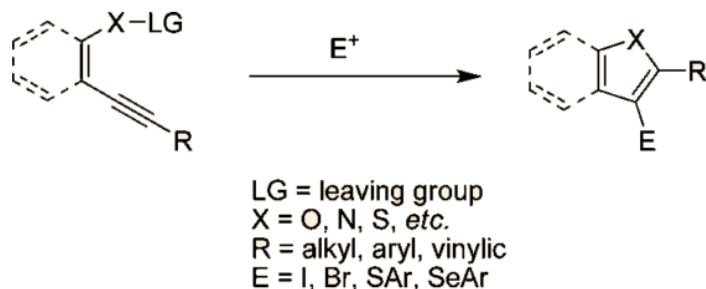
The first step towards a switch-functionalized TT involved silyl protection of the 4- and 6- positions (**Scheme 2.6**), which was already accomplished in the literature for both trimethylsilyl (TMS) and triisopropylsilyl (TiPS) protecting groups.⁷ Both compounds were synthesized due to uncertainty in which is more likely to result in the dibrominated species. For example, TMS protecting groups provide less steric hindrance than TiPS groups, but are susceptible to desilylation and subsequent bromination. TiPS groups are more resilient, though the large bulky nature of this substituent may hinder bromination of the 3-position, which is in close proximity. Preliminary bromination tests on the TMS protected TT with molecular bromine confirmed fears, as there was indeed loss of protecting groups. Running the reaction at colder temperatures resulted in the same result, possibly indicating that the HBr generated as a byproduct may result in partial/complete deprotection. Bromination via *N*-bromosuccinimide (NBS) resulted in only mono-bromination of the substrate, most likely at the 2- position. NBS may not be aggressive enough, or the TMS group is a large enough protecting group that it also hinders clear approaches to the 3-position. The reasons for not using a lithiation approach is two-fold. In some cases, a TMS protected thiophene proved to be labile in the presence of organolithiates. In addition, dilithiation of many aromatic compounds are possible but can be quite tricky in some cases, especially in situations similar to this where the two anions would be adjacent to each other.

The TiPS-protected substrate never lost its protecting groups under any conditions, but saw only mono-halogenation in any of the bromination trials with Br₂ or NBS even at temperatures up to 60° C, after which resulted in decomposed material. Fears were effectively confirmed here as well, as it seems the protecting group proved to be too bulky.

With limited knowledge of brominating reagents at the time, working with protected TT seemed fruitless. I then decided to explore functionalizations of intermediates on the way towards TT. The route proposed by Brandsma and Verkruijsse leaves no room for switch

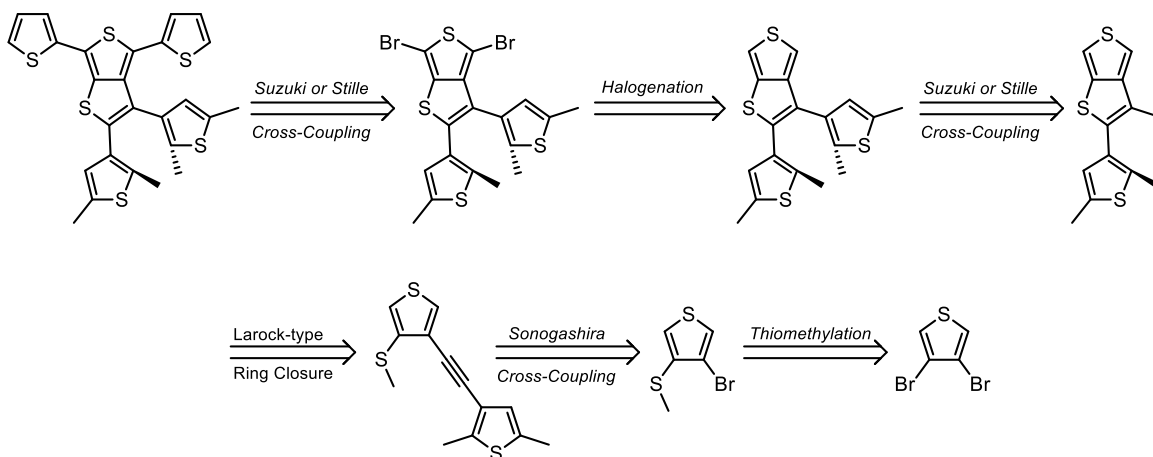
functionalization, because the ring from which it is built is not assembled until the final step, and the 3- position remains invariable. The last route towards **TT** was that proposed by Sotzing *et. al.*, where this time the thiophene containing the 4- and 6- positions is being built, whereas in the previous cases, this ring was preformed.⁶ Theoretically, the switch could be built from the 2- and 3- positions from an intermediate in this pathway prior to final aromatization. Functionalization of the dicarboxylic acids was avoided, as there are very few examples in the literature of effective bromination of these compounds. Bromination thus began at the di-hydroxymethane intermediate. Bromination of each intermediate from the dihydroxymethane intermediate up until the penultimate step resulted in decomposed material, or material that rapidly degraded upon halogenation attempt. The most promising intermediate was the dihydro **TT** species, which appeared relatively stable compared to the previous intermediates.

In the midst of several trial reactions with plans of revisiting halogenation trials for various Sotzing intermediates, an alternative route that is not reliant on intermediate functionalization was developed. This was primarily concerned with Larock type ring closures (**Scheme 2.7**), which are class of iodine-mediated ring closures used to generate substituted thiophene-containing heterocycles.⁸ An example of this is shown below, in which a (hetero)acene with the prerequisite functionalities on contiguous carbons (such as a thiomethyl next to an adjacent alkyne) is exposed to an electrophile (such as molecular iodine). While the mechanism for this reaction is not completely understood, it is believed that that atom “X” acts as the nucleophile that attacks the antibonding orbital of the alkyne (which is conveniently pointed towards this atom), whose generated anion then acts as a nucleophile for the electrophile, which is in most cases a halogen.



Scheme 2.7 An example of a Larock-type ring closure, a subset of iodine-mediated electrophilic ring closures. Benzene is depicted here, but there is great variance in the (hetero)acene from which the reaction can occur.

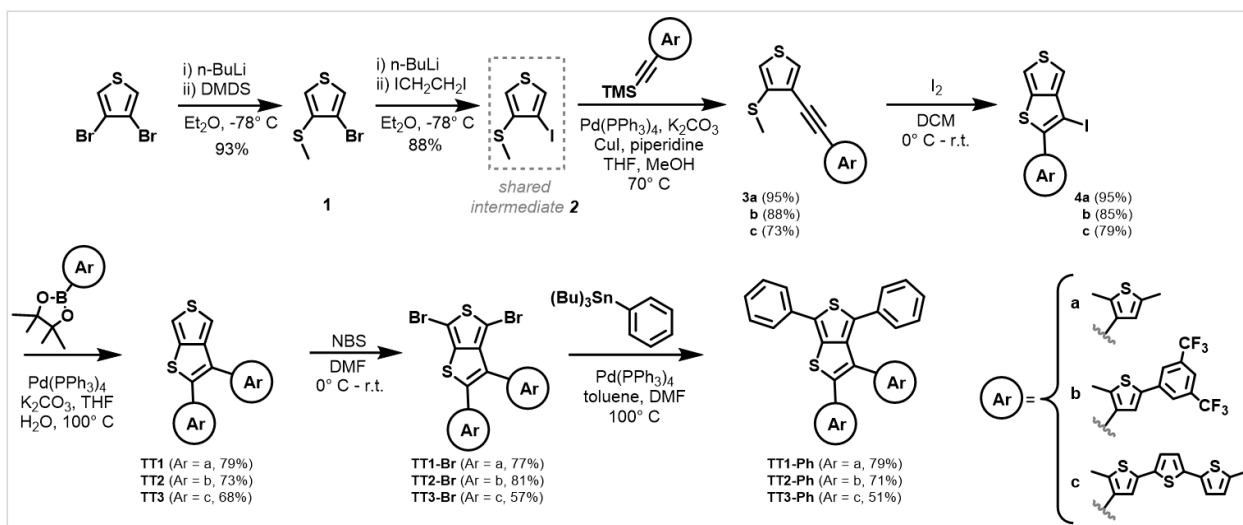
This chemistry has been used to generate several fused heteroacenes such as benzo[b]thiophene and benzo[b]furan, but this work has never been applied to the synthesis of **TT**. In theory, one could have the prerequisite functionalities at the 3- and 4- positions of thiophene, and Larock-type ring-closure would result in some form substituted **TT** based on the substituents present prior to electrophile addition. Arguably the most beautiful aspect of this idea is that if iodine is the electrophile of choice, an iodine substituent will be present at the 3- position on **TT**, effectively placing the most desirable and reactive halogen at the least reactive position. Thus, a retrosynthetic route was designed as shown in **Scheme 2.8**.



Scheme 2.8 Retrosynthetic pathway for a novel **TT** synthesis utilizing the Larock-type ring closure as a means to both form the desired core and halogenate the 3- position.

Working backwards from the pi-extended desirable product, one would have a **TT** core with a switch built at the 2- and 3- positions, while the 4- and 6- positions are halogenated to allow for cross coupling. These bromines could be installed through traditional bromination techniques, which have already been demonstrated on **TT** molecules in the past. The second switching arm (at the 3- position) can be coupled on via Suzuki or Stille cross coupling. The **TT** formation step and the functionalization of the 2- position occurs simultaneously from the Larock-type ring-closure, as the substituent on the opposite end of the alkyne (often times a TMS group) ends up being the substituent at the 2- position. Occasionally, this is not true if the alkyne is substituted with a labile group. A Sonogashira cross coupling reaction of a switch-arm substituted alkyne with a β -halogen on the core starting thiophene accomplishes the necessary functionalities for the ring-closure to take place. The thiomethyl-substituted thiophene can be synthesized from the 3,4-dihalogenated species using dimethyl-disulfide.

Preliminary low-level Spartan 04 calculations revealed that the thiomethyl group and the adjacent alkyne at the β positions are in closer proximity to than in other substrates where iodine-mediated ring-closures have been successful in, such as benzene. With several aspects of this photochrome's design being rather attractive from a synthetic perspective, it was pursued, culminating in the synthetic route shown in **Scheme 2.9**.



Scheme 2.9 General synthetic pathway towards **TT** switch cores, with yields shown for the three key switches eventually developed (**TT3** and derivatives discussed later).

The initial portion of the synthesis is concerned with functionalizing the 3- and 4-positions of thiophene for the switching motif, which involves thiomethylation and alkylation. While there was an option as to which step would be performed first, thiomethylation seemed like the logical path as the Sonogashira cross coupling reaction to introduce the alkyne could result in a byproduct that coupled to both bromine atoms. Thiomethylation, however, first requires a lithium-halogen exchange that effectively guarantees reaction with just one of the halogens present. Several Sonogashira cross coupling reactions were performed on **1**, but the yields remained fairly low (below 50%). Typically, it is more difficult to couple to halogenated β positions on thiophene as opposed to those at α positions. It is also possible that the thiomethyl substitution could be interfering with the reaction as well. Because Iodine atoms are often better coupling partners than bromine atoms, an intermediate reaction was introduced to convert the bromine atom to the more reactive halogen. Coupling reactions at the β position with the aryl iodide as the halogenated partner resulted in yields greater than 80%. While this did introduce an additional step in the synthetic scheme, it resulted in higher overall yields and more material moving forward. Often times, the alkyne for iodine-mediated electrophilic ring closures is TMS

protected at one end. If we were to proceed through this route, the TMS group would end up at the 2- position, and one would then have to perform 2-3 additional synthetic steps to arrive at switch functionalization at this position (deprotection, bromination, and coupling, or simultaneous bromination/deprotection and coupling). Having a switch arm pre-installed on the alkyne greatly simplifies this, so various switching arms were prepared for different functions (to be discussed later). To generate **TT** through Larock-type ring closure, solutions of iodine in DCM were added to cooled solutions of **3**. It was found that temperature control was particularly important for these reactions, as higher temperatures resulted in a byproduct in which iodine added twice across the triple bond. This was easily circumvented by adding iodine in dilute solutions at 0° C, which exclusively generated the iodinated intermediate **4**. Standard Suzuki cross coupling with a suitable aryl boronate ester generated the switch cores **TT1-TT3**, which are the three switches that were heavily investigated throughout this study. While these switches were not made in chronological order, we will reserve the first three shorthand notations of **TTX** for these photochromes. It is worth noting that because the switch arms are introduced at different steps, there is an opportunity present to introduce a different switching arm than the first. Many potential asymmetric switches are thus possible, but at this time only “symmetric” switches with identical switching arms were investigated.

For both tradition and simplicity, the first photochrome (**TT1**) features a 2,5-dimethylthiophene switching arm. The open form is an air stable white crystalline solid. The chemical structure was fully confirmed by the x-ray crystal structure (**Figure 2.1**), obtained by vapor-diffusion recrystallization from acetonitrile to produce white needles. The switch arms can be seen in anti-parallel conformation in the solid state. As with other reported crystalline DTEs in the literature, those that crystallize in the anti-parallel conformation tend to favor solid-state switching. This is also seen with **TT1**, which upon irradiation with a 254 nm handheld lamp (or more slowly via sunlight) causes the silvery-white needles to transition to vibrant pink as some

molecules are excited and proceed through the 6π electrocyclization (**Figure 2.2**). The ring-opening reverse reaction, or “bleaching”, can be accomplished by irradiation with a white LED (or more slowly via ambient room lighting), recovering the white needles.

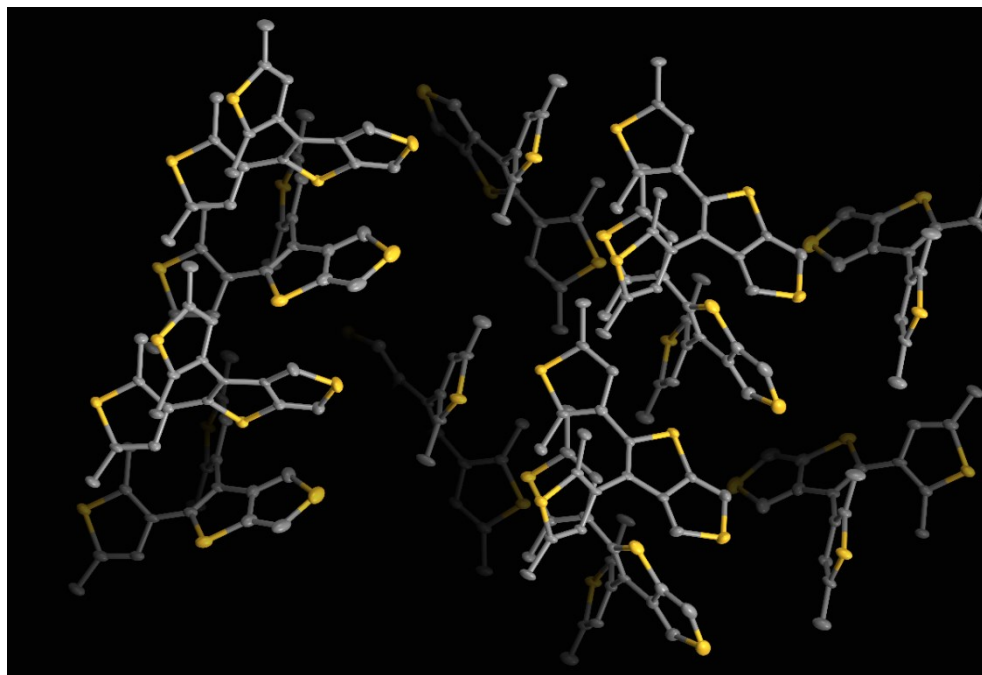


Figure 2.1 X-Ray crystal structure of **TT1**, depicting the anti-parallel conformation of the diarylethene switching arms. **TT1** was recrystallized from hot acetonitrile.

In acetonitrile solution, the open switch appears clear and colorless (**Figure 2.2**). Upon irradiation with a UV light source, the solution turns deep red. The colorless open form can be recovered by irradiation with a white light source. The UV-Vis spectra for the open and closed **TT1** in acetonitrile are also shown below. The key transition can be seen at $\lambda_{\text{max}} = 245$ nm, and the lowest energy absorbance remains in the UV region (below $\lambda_{\text{abs}} = 360$ nm), explaining the lack of coloration. Irradiation with a standard shortwave handheld UV lamp (254 nm) proved sufficient for obtaining the photostationary state, which has two major absorbances at $\lambda_{\text{abs}} = 344$ nm and $\lambda_{\text{abs}} = 524$ nm, with the latter being the source of the intense red color. This is due to the “octatetraene” portion of the closed switch, whose extended conjugate relative to the open form

results in a drastic red-shift upon irradiation. Photobleaching was accomplished with a 530 nm LED to regenerate the open isomer. This switching cycle goes to completion at least ten times in deaerated solutions, though it is unclear how fatigue resistant the compound truly is.

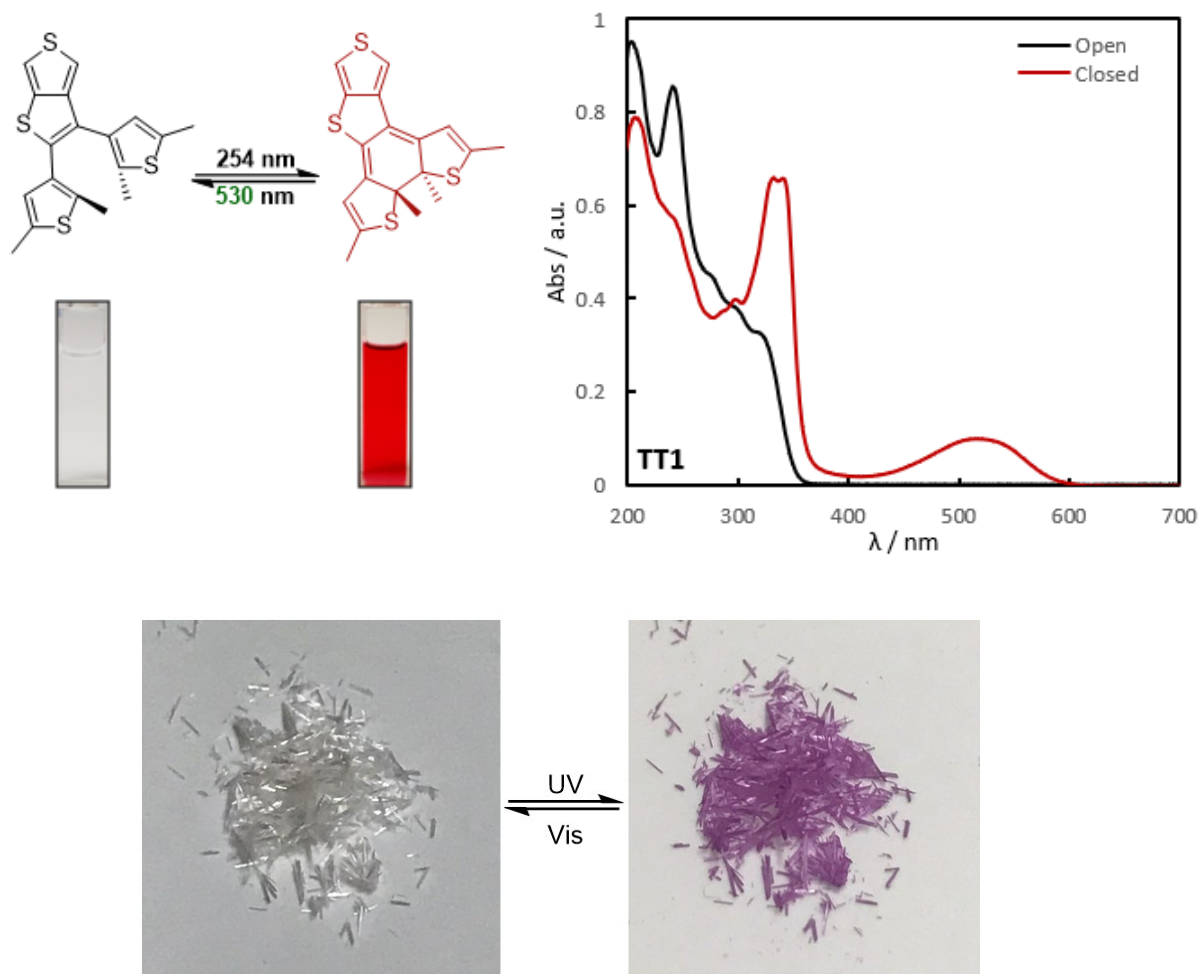
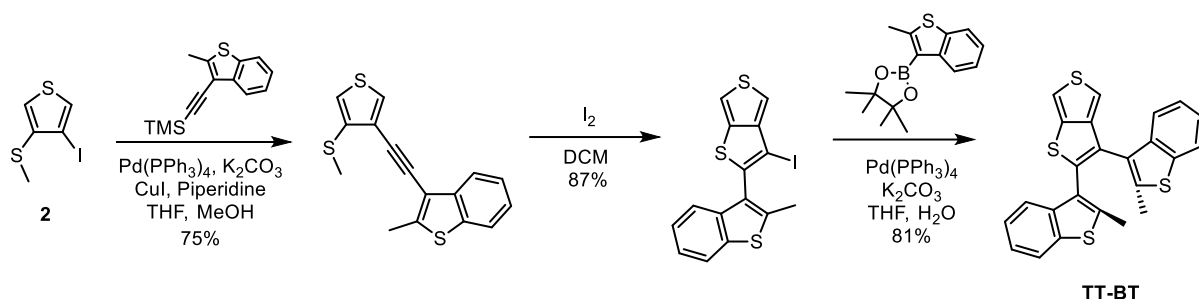


Figure 2.2 UV-Vis absorption profile of open and closed **TT1**. Cyclization and cycloreversion can be visualized in both in the dissolved and crystalline form.

With an efficient synthetic route towards **TT** established, three switch cores with variances in switching arms were synthesized for various reasons, as discussed below. **TT1** was made as the standard model and served as the starting point for other derivations. Several switch studies on substituted perfluorocyclopentenes in the literature are concerned with the “fatigue resistance” of a compound, or how many open and close cycles the switch can proceed through

without significant degradation or byproduct formation. This property is extremely important in the context of our goal of making switchable polymers for materials applications, since it is directly related to the long-term performance of the material. One of the earliest motifs that demonstrated high fatigue resistance involved benzo[b]thiophene (**BT**), which can proceed through over ten thousand cycles with minimal byproduct formation in inert atmosphere. This was incorporated into our **TT** synthesis through the route in **Scheme 2.10** to generate **TT-BT**, starting from the common intermediate **2**.



Scheme 2.10 Synthesis of the **TT** switch derivative **TT-BT**, featuring benzo[b]thiophene switching arms initially developed for fatigue resistance.

This photochrome was reddish orange in color, not drastically different from **TT1** (**Figure 2.3**). This can be sourced from the degree of extended conjugation in the closed form, which is comparable to that of the standard model. Although completely qualitative, it was observed that **TT-BT** took considerably longer to reach its photostationary state compared to **TT1**, under the same irradiation conditions of a handheld UV lamp.

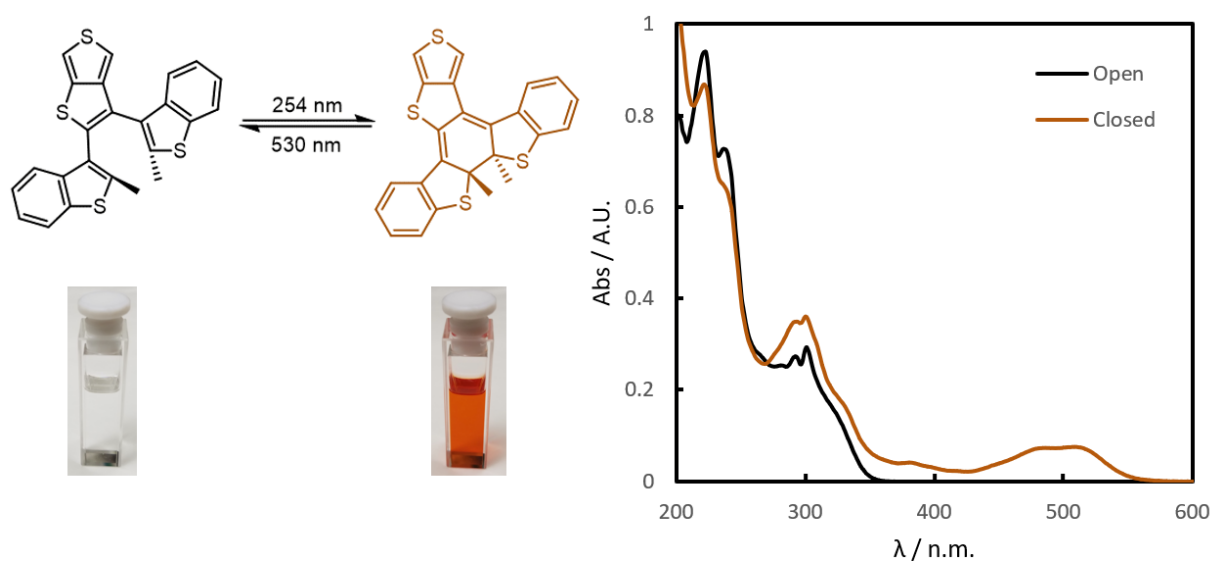


Figure 2.3 UV-Vis absorption spectrum of **TT-BT** for both the open and closed state. Orange coloration of the closed state is due to the extended conjugation from benzene to benzene.

NMR data potentially provides an explanation for this (below). Due to the asymmetry in **TT1**, there should be four different methyl peaks in the alkyl region as different conformers (parallel vs. antiparallel) rapidly exchange faster than the NMR timescale. If the same logic is applied to **TT-BT**, we should only see two methyl peaks in the alkyl region (one for each switching arm). The NMR for **TT-BT** at room temperature features double the number of alkyl peaks that expected. This can be explained by the presence of both the parallel and anti-parallel conformations in solution, which are interconverting slower than the NMR timescale. To confirm this, temperature-dependent NMR was used, in which the temperature was increased in 25° increments (**Figure 2.4**). As the temperature is increased, merging of methyl peaks is observed, indicating that higher temperature is facilitating interconversion between parallel and anti-parallel conformers. In general, DTEs will only proceed through the 6 π electrocyclization in the anti-parallel conformation. Slow conversion of parallel-conformation **TT-BT** to antiparallel conformation during the irradiation process provides a rationale for its slow approach to the photostationary state. This typically is not a problem for switches in the literature that feature **BT** switching motifs and might be inherent to **TT** switches. A reasonable source for the lack of

interconversion may be due to hydrogen-hydrogen clash seen between the 4-position and a hydrogen atom on the benzene portion of the 3-position switch arm (shown below). Indeed, rotation of this switching arm in a DFT geometry optimized structure shows direct clashing of these two hydrogen atoms. While this switch may in fact be highly fatigue resistant, it is undesirable to have unfavorable steric interactions between pendant substitutions and what would be the location of pi extended substitutions.

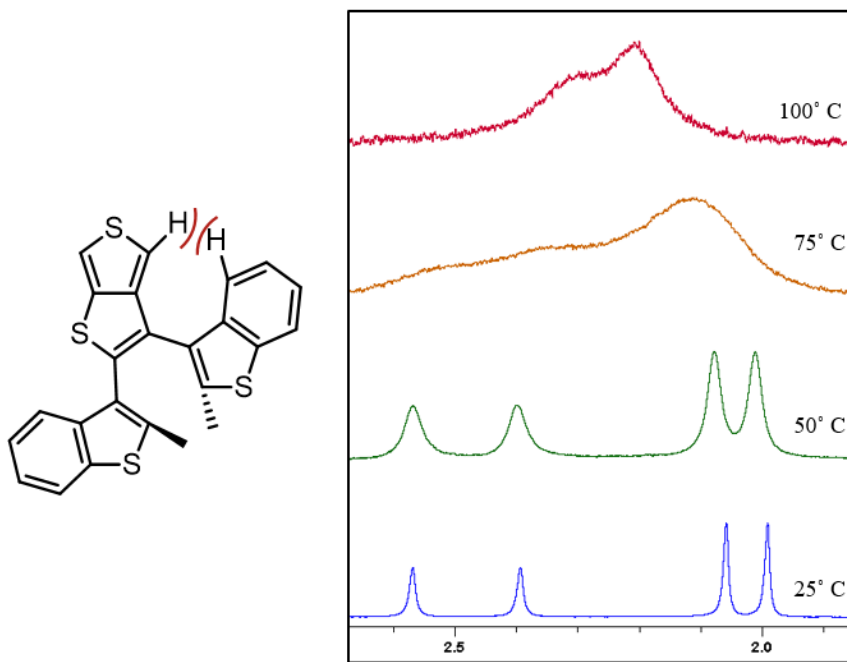
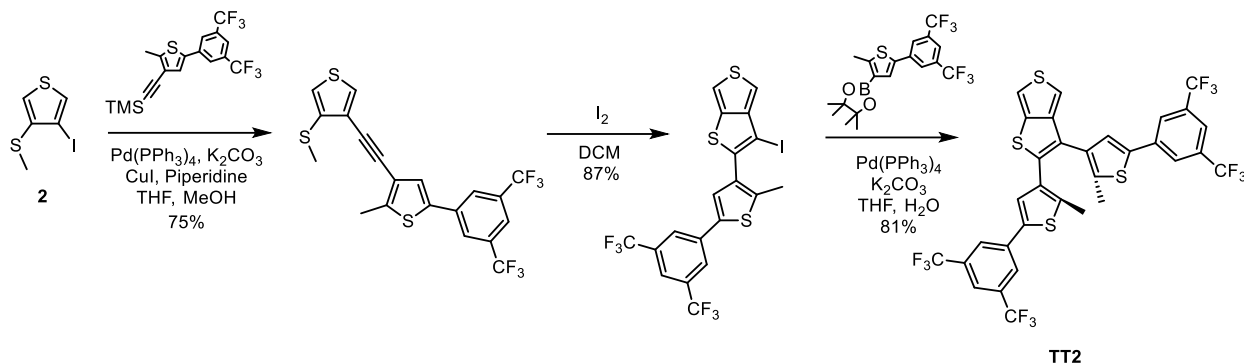


Figure 2.4 (Left) Depiction of the steric clash of interest. (Right) Alkyl region of the NMR of **TT-BT** collected at several temperatures.

Although **TT-BT** may be a robust switch core, other switching arms that avoid steric clash may prove more valuable. More recently, Hecht *et. al.* demonstrated that switching motifs featuring certain electron withdrawing groups provided greater fatigue resistance in the species under investigation. Of particular interest is the switch arm which features a thiophene substituted with a (bis)trifluoromethylbenzene, which was utilized in the construction of **TT2**, shown below.



Scheme 2.11 Synthesis of the **TT2** switch core following the general procedure for the synthesis of **TT** switches. The switching arm arm was also initially chosen due to high fatigue resistance.

Synthesis of the **TT2** switch core is proceeded smoothly following the general procedure for **TT1**, with the only major difference being in the purification where both crude and purified material needed to be adequately shielded from trace sunlight to prevent cyclization. Columns were run wrapped in aluminum foil, concentration via rotovap needed to be covered, and the purified solid needed to be kept in the dark. Simply leaving the compound on the bench for a few minutes results in a pale blue coloration, a feature of the cyclized switch. Photophysical characterization for this photochromic core is shown in **Figure 2.5**. Much like **TT1** and **TT-BT**, the open form of **TT2** is completely contained within the UV region, reflected by the white color in the solid state or the clear colorless solution when dissolved. The solid quickly turns pale blue when exposed to trace amounts of sunlight, and thus needs to be kept shielded from any form of UV light. Photoirradiation with 254 nm rapidly brings **TT2** the photostationary state, featuring two major absorptions ($\lambda_{\text{abs}} = 395 \text{ nm}$ and $\lambda_{\text{abs}} = 630 \text{ nm}$), with the lower energy transition being very broad. The NMR data showed no conformational issues that prevented interconversion between the parallel and anti-parallel conformation. In addition, the molecular design indicates no steric clash between the substituent at the 3-position and that at the 4-position. **TT2** thus represents a fatigue resistant alternative to **TT-BT** that may be more fitting for incorporation into polymeric species as it may provide fewer steric issues.

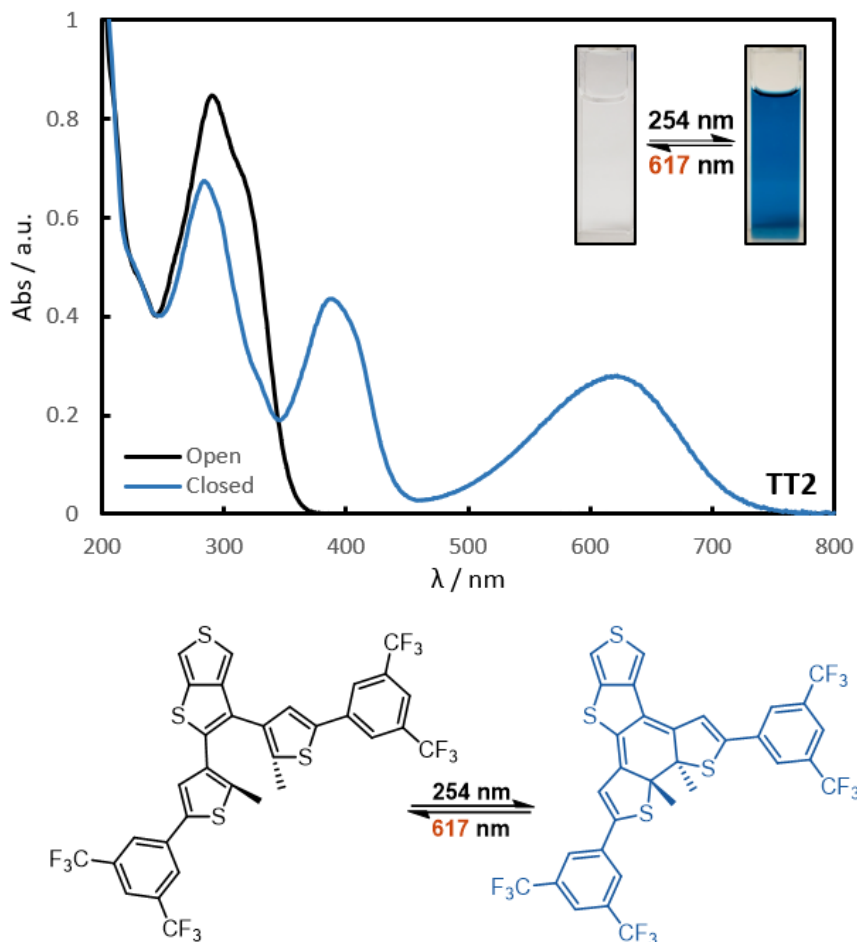


Figure 2.5 UV-Vis absorption spectra for the open and closed form of **TT2** with intense blue coloration upon cyclization.

Conclusion

The design of pendant photochromic polymers is deceptively tricky in that the monomer requires highly selective functionalization to both install the diarylethene switching motif at what would be a pendant location, and halogenation at two positions from which the monomer can be (co)polymerized. Thieno[3,4-*b*]thiophene was chosen as an ideal core for the development for the photochromic monomer due to attractive photophysical properties. Several attempts were made to adapt literature preparations of **TT** in the design of these photochromes, though none were realized synthetically. A novel approach to the synthesis of pre-functionalized **TT** involving an iodine-mediated electrophilic cyclization was used, allowing for selective functionalization of all

locations on **TT**, resulting in the synthesis of the first target photochromes **TT1**, **TT-BT**, and **TT2**. These switch cores proved crucial in the development of future pendant photochromic polymers.

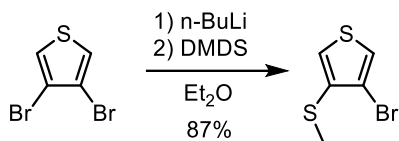
Experimental

General Information

5-(3,5-bis(trifluoromethyl)phenyl)-3-bromo-2-methylthiophene (**5**) was prepared according to the literature procedure.¹ Diethyl ether, toluene, and THF were purified using Innovative Technologies SPS-400-6 Solvent Purification System and further dried over Acros Organics 4Å molecular sieves prior to use. Dichloromethane was distilled prior to use. All other solvents and reagents were purchased from Sigma-Aldrich, Fisher Scientific, Alfa Aesar, or Oakwood Chemicals and used without further purification.

¹H NMR spectra were obtained on either a Bruker Avance 400 MHz Spectrometer or a Bruker Avance III 400 MHz Spectrometer, with residual protio-solvent resonances used as the internal standard (CHCl₃: 7.26 ppm, CHDCl₂: 5.32 ppm). Data are reported as: Chemical shift (multiplicity, integration, coupling constant). ¹³C NMR spectra were obtained on either a Bruker Avance 400 MHz Spectrometer (100 MHz) or a Bruker Avance III 400 MHz Spectrometer (100 MHz), with solvent resonances used as the internal standard (CDCl₃: 77.2 ppm). Data are reported as chemical shifts (ppm). High resolution mass spectrometry (HRMS) was performed on a VG-70SE Magnetic Sector Mass Spectrometer. UV-Vis data were collected on a Cary 50 Bio UV-Vis Spectrophotometer. Gel permeation chromatography was performed on an Agilent 1260 Infinity Series (degasser, iso pump, TCC, DAD) using unstabilized THF at 40° C vs. Agilent EasiVial PS-M polystyrene standards. Ultraviolet light source for switching experiments was an Analytikjena UVP UVGL-25 254/365 nm 4 Watt handheld lamp. Visible light sources are Luxeon Rebel LEDs on SinkPAD-II 20mm. Flash Chromatography was performed under manual air pressure on silica (SiO₂, 40-63 μm, 230-400 mesh).

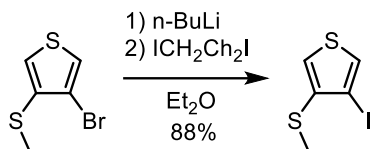
3-bromo-4-(methylthio)thiophene (**1**)



3,4-dibromothiophene (5.000 g, 20.70 mmol) was added to anhydrous diethyl ether (25 mL), and *n*-BuLi (12.7 mL, 1.63 M in hexanes) was added dropwise at -78° C. The solution was stirred at this temperature for 30 min. Then, dimethyl disulfide (1.950 g, 20.70 mmol) was added over 1 min., and the solution was allowed to slowly come to room temperature over 12 h. The reaction mixture was diluted with an additional 25 mL of diethyl ether, washed twice with 50 mL of DI H₂O, once with 50 mL brine, and dried over MgSO₄ before concentrating under reduced pressure. Purification by column chromatography (silica, 100% hexanes) afforded compound **1** (4.030 g, 19.30 mmol, 93%) as a clear colorless oil.

¹H NMR (400 MHz, CDCl₃): δ 7.33 (d, 1H, 3.4 Hz), 6.93 (d, 1H, 3.4 Hz), 2.47 (s, 3H). **¹³C (1H) NMR (100 MHz, CDCl₃):** δ 135.6, 124.1, 119.7, 112.4, 17.4. **HRMS (EI):** found *m/z*: 207.9012; calc. for C₅H₅BrS₂: 207.9016.

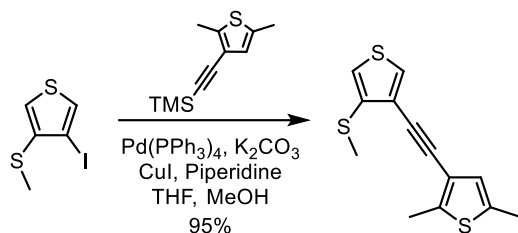
3-iodo-4-(methylthio)thiophene



3-bromo-4-(methylthio)thiophene (**1**) (1.000 g, 4.780 mmol) was added to anhydrous diethyl ether (10 mL), and *n*-BuLi (3.25 mL, 1.63 M in hexanes) was added dropwise at -78° C. Then, diiodoethane (1.480 g, 5.260 mmol) was added in over 1 min., and the solution was allowed to slowly come to room temperature over 10 h. The reaction mixture was then diluted with an additional 10 mL of diethyl ether, washed twice with 20 mL DI H₂O, once with 20 mL brine and dried over MgSO₄ before concentrating under reduced pressure. Purification by column chromatography (silica, 100% hexanes) afforded compound **2** (1.080 g, 4.210 mmol, 88%) as a clear colorless oil.

¹H NMR (400 MHz, CDCl₃): δ 7.49 (d, 1H, 3.3 Hz), 6.88 (d, 1H, 3.3 Hz), 2.47 (s, 3H). **¹³C (1H) NMR (100 MHz, CDCl₃):** δ 139.0, 130.0, 128.3, 126.6, 119.2, 83.4, 18.2. **HRMS (EI):** found *m/z*: 255.8879; calc. for C₅H₅IS₂: 255.8877.

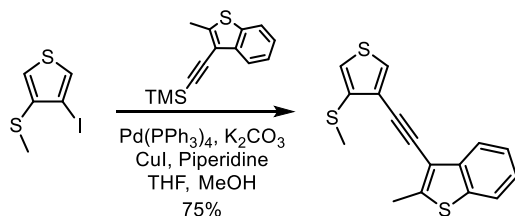
2,5-dimethyl-3-((4-(methylthio)thiophen-3-yl)ethynyl)thiophene



3-iodo-4-(methylthio)thiophene (**2**) (2.800 g, 10.90 mmol), ((2,5-dimethylthiophen-3-yl)ethynyl)trimethylsilane (2.270 g, 10.90 mmol), and potassium carbonate (3.310 g, 24.00 mmol) were added to THF (200 mL), and the solution was sparged with N₂ for 15 min. Then, copper(I) iodide (104 mg, 0.540 mmol) and Pd(PPh₃)₄ (630. mg, 0.540 mmol) were added under increased N₂ flow, followed by a degassed solution of piperidine (10.8 mL, 109 mmol) in methanol (100 mL). The reaction mixture was refluxed at 70° C for 18 h. The solution allowed to cool to room temperature and then washed twice with 50 mL sat. NH₄Cl, once with 50 mL brine, and dried over MgSO₄ before concentrating under reduced pressure. Purification of the orange oil by column chromatography (silica, 95:5 hexanes:DCM) afforded compound **3a** (2.740 g, 10.40 mmol, 95%) as a clear colorless oil.

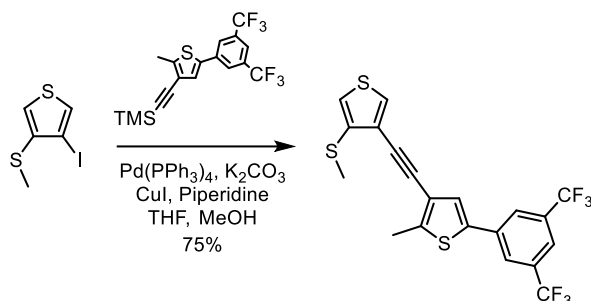
¹H NMR (400 MHz, CDCl₃): δ 7.40 (d, 1H, 3.2 Hz), 6.72 (d, 1H, 3.2 Hz), 6.62 (d, 1H, 1.2 Hz), 2.50 (s, 3H), 2.40 (s, 3H), 2.31 (d, 3H, 1.2 Hz). **¹³C (¹H) NMR (100 MHz, CDCl₃):** δ 141.8, 136.8, 136.0, 128.7, 127.2, 123.1, 119.1, 117.9, 87.9, 84.5, 16.7, 15.2, 14.6. **HRMS (EI):** found *m/z*: 264.0104; calc. for C₁₃H₁₂S₃: 264.0101.

2-methyl-3-((4-(methylthio)thiophen-3-yl)ethynyl)benzo[b]thiophene



A solution of 3-iodo-4-(methylthio)thiophene (1.00 g, 3.90 mmol), trimethyl((2-methylbenzo[b]thiophen-3-yl)ethynyl)silane (954 mg, 3.90 mmol), and potassium carbonate (1.19 g, 8.58 mmol) in THF (70 mL) was sparged with N₂ for 15 min. Under positive N₂ pressure, copper(I) iodide (37 mg, 0.54 mmol) and Pd(PPh₃)₄ (225 mg, 0.540 mmol) were added, followed by piperidine (3.85 mL, 39.0 mmol) and methanol (30 mL). The reaction mixture was refluxed for 18 h, after which it was washed twice with sat. NH₄Cl (25 mL) and once with brine (50 mL). The organic layer was dried over anhydrous MgSO₄, filtered, and concentrated under reduced pressure. The off-white solid was purified by column chromatography (silica, 80:20 hexanes:dichloromethane) to yield a white solid (819 mg, 2.73 mmol, 70%). ¹H NMR (400 MHz, CDCl₃): δ 7.96 (d, 1H), 7.73 (d, 1H), 7.59 (d, 1H), 7.41 (t, 1H), 7.32 (t, 1H), 6.91 (d, 1H), 2.75 (s, 3H), 2.55 (s, 1H). ¹³C (1H) NMR (100 MHz, CDCl₃): δ 145.4, 140.0, 137.6, 136.9, 129.1, 124.9, 124.6, 123.2, 122.7, 122.1, 118.4, 115.8, 87.7, 86.0, 17.0, 15.6. HRMS (EI) found m/z = 300.0091 (M⁺), calculated for C₁₆H₁₂S₃: 300.0101.

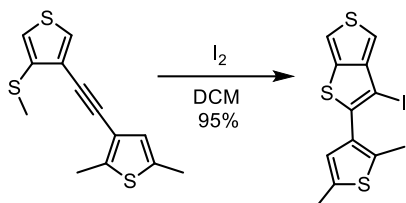
5-(3,5-bis(trifluoromethyl)phenyl)-2-methyl-3-((4-(methylthio)thiophen-3-yl)ethynyl)thiophene



3-iodo-4-(methylthio)thiophene (**2**) (636 mg, 2.48 mmol), ((5-(3,5-bis(trifluoromethyl)phenyl)-2-methylthiophen-3-yl)ethynyl)trimethylsilane (1.010 g, 2.480 mmol), and potassium carbonate (685 mg, 4.96 mmol) were added to THF (50 mL), and the solution was sparged with N₂ for 15 min. Then, copper(I) iodide (104 mg, 0.540 mmol) and Pd(PPh₃)₄ (630. mg, 0.540 mmol) were added under increased N₂ flow, followed by a degassed solution of piperidine (2.45 mL, 24.8 mmol) in methanol (25 mL). The reaction mixture was refluxed at 70° C for 18 h. The solution allowed to cool to room temperature and then washed twice with 25 mL sat. NH₄Cl, once with 25 mL brine, and dried over MgSO₄ before concentrating under reduced pressure. Purification of the orange oil by column chromatography (silica, 95:5 hexanes:DCM) afforded compound **3b** (1.01 g, 2.19 mmol, 88%) as a clear colorless oil which was used without further purification.

¹H NMR (400 MHz, CDCl₃): δ 7.93 (s, 2H), 7.75 (s, 1H), 7.54 (d, 1H, 3.2 Hz), 7.40 (s, 1H), 6.89 (d, 1H, 3.2 Hz), 2.67 (s, 3H), 2.54 (s, 3H). **¹³C (¹H) NMR (100 MHz, CDCl₃):** δ 145.6, 137.0, 136.9, 136.1, 132.6 (q, 2C, ²J_{C-F} = 33.3 Hz), 129.5, 127.5, 125.4, 125.3, 123.4 (q, 2C, ¹J_{C-F} = 272.2 Hz), 122.7, 121.5, 120.8, 118.3, 86.6, 85.8, 16.9, 15.0. **HRMS (EI):** found *m/z*: 462.0006; calc. for C₂₀H₁₂F₆S₃: 462.0005.

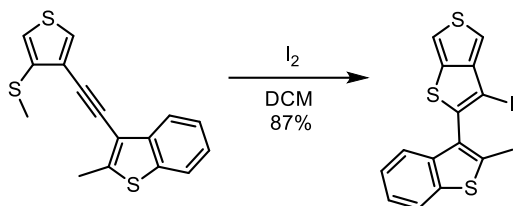
2-(2,5-dimethylthiophen-3-yl)-3-iodothieno[3,4-b]thiophene



2,5-dimethyl-3-((4-(methylthio)thiophen-3-yl)ethynyl)thiophene (**3a**) (2.83 g, 10.7 mmol) was added to 100 mL DCM, and cooled to 0° C. A solution of iodine (2.72 g, 10.7 mmol) in DCM (100 mL) was then added dropwise and stirred until the starting material was consumed, as monitored by TLC. The solution was then washed once with 50 mL sat. Na₂S₂O₃, once with 50 mL brine, and dried over MgSO₄ before concentrating under reduced pressure. Purification by column chromatography (90:10 hexanes:DCM) afforded compound **4a** (3.820 g, 10.15 mmol, 95%) as a white solid which was used without further purification.

¹H NMR (400 MHz, CDCl₃): δ 7.37 (d, 1H, 2.9 Hz), 7.32 (d, 1H, 2.9 Hz), 6.68 (s, 1H), 2.45 (s, 3H), 2.41 (s, 3H). **¹³C (¹H) NMR (100 MHz, CDCl₃):** δ 150.6, 143.6, 137.0, 136.6, 136.5, 131.3, 127.0, 114.7, 112.1, 71.7, 15.4, 14.9. **HRMS (EI):** found m/z : 375.8903; calc. for C₁₂H₉IS₃: 375.8911.

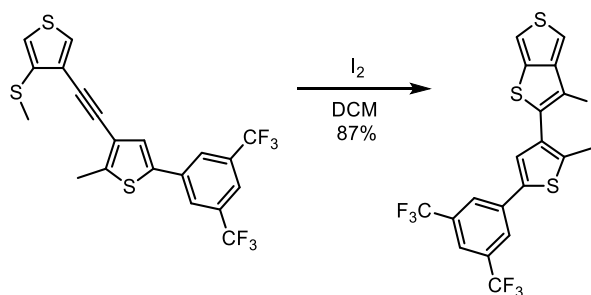
3-(3-iodothieno[3,4-b]thiophen-2-yl)-2-methylbenzo[b]thiophene



A Solution of 2-methyl-3-((4-(methylthio)thiophen-3-yl)ethynyl)benzo[b]thiophene (665 mg, 2.21 mmol) in dichloromethane (50 mL) was titrated with an iodine solution (674 mg, 2.66 mmol in 100 mL DCM) at room temperature until the starting material was consumed, as monitored by

TLC. The reaction mixture was then washed once with sat. $\text{Na}_2\text{S}_2\text{O}_3$ (10 mL), twice with DI H_2O (10 mL), and once with brine (10 mL). The organic layer was dried over anhydrous MgSO_4 , filtered, and concentrated under reduced pressure. The yellow solid was purified by column chromatography (silica, 80:20 hexanes:dichloromethane) to yield a white solid (794 mg, 1.92 mmol, 87%). ^1H NMR (400 MHz, CDCl_3): δ 7.80 (m, 1H), 7.52 (m, 1H), 7.44 (d, 1H), 7.40 (d, 1H), 7.32 (m, 2H), 2.54 (s, 3H). ^{13}C (^1H) NMR (100 MHz, CDCl_3): δ 150.4, 141.8, 141.6, 139.3, 138.1, 137.1, 127.1, 124.6, 124.4, 122.8, 122.2, 115.1, 112.4, 74.0, 15.4. HRMS (EI) found m/z = 411.8901 (M^+), calculated for $\text{C}_{15}\text{H}_9\text{IS}_3$: 411.8911.

2-(5-(3,5-bis(trifluoromethyl)phenyl)-2-methylthiophen-3-yl)-3-iodothieno[3,4-b]thiophene

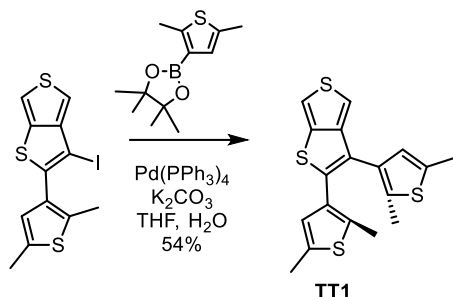


5-(3,5-bis(trifluoromethyl)phenyl)-2-methyl-3-((4-(methylthio)thiophen-3-yl)ethynyl)thiophene (**3b**) (792 mg, 1.71 mmol) was added to 50 mL DCM, and cooled to 0°C . A solution of iodine (522 mg, 1.71 mmol) in DCM (50 mL) was then added dropwise and then stirred until the starting material was consumed, as monitored by TLC. The solution was then washed once with 30 mL sat. $\text{Na}_2\text{S}_2\text{O}_3$, once with 30 mL brine, and dried over MgSO_4 before concentrating under reduced pressure. Purification by column chromatography (90:10 hexanes:DCM) afforded compound **4b** (790. mg, 1.38 mmol, 80%) as a white solid.

^1H NMR (400 MHz, CDCl_3): δ 7.96 (s, 2H), 7.76 (s, 1H), 7.42 (d, 1H, 3.0 Hz), 7.38 (m, 2H, 3.0 Hz), 2.53 (s, 3H) ^{13}C (^1H) NMR (100 MHz, CDCl_3): δ 150.3, 142.0, 141.2, 137.3, 136.4, 136.2,

133.5, 132.7, 132.3, 130.5, 127.1, 125.5, 124.7, 120.8, 115.3, 112.5, 72.8, 15.2. **MS (EI):** found m/z : 573.9; calc. for $C_{19}H_9F_6IS_3$: 573.8815.

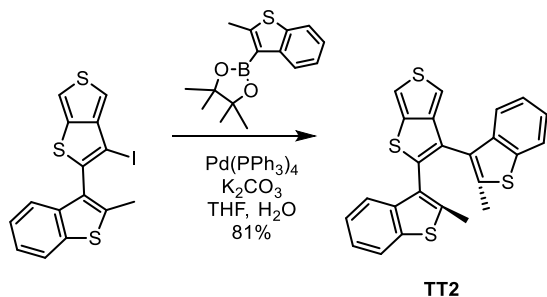
2,3-bis(2,5-dimethylthiophen-3-yl)thieno[3,4-b]thiophene (TT1)



2-(2,5-dimethylthiophen-3-yl)-3-iodothiophene (**4a**) (2.000 g, 5.320 mmol) and 2-(2,5-dimethylthiophen-3-yl)-4,4,5,5-tetramethyl-1,3,2-dioxaborolane (**11**) (1.390 g, 5.840 mmol) were added to THF (20 mL) and sat. K_2CO_3 solution (10 mL), and the solution was subjected to three freeze-pump-thaw cycles. $Pd(PPh_3)_4$ (307 mg, 0.27 mmol) was added under increased N_2 flow, and the solution was refluxed at $100^\circ C$ for 16 h. The reaction mixture was then cooled to room temperature and diluted with 20 mL of diethyl ether, washed twice with 40 mL of DI H_2O , once with 40 mL brine, and dried over $MgSO_4$ before concentrating under reduced pressure. Purification by column chromatography (silica, hexanes) afforded **TT1** (1.510 g, 4.200 mmol, 79%) as a white solid.

1H NMR (400 MHz, $CDCl_3$): δ 7.21 (d, 1H, 2.9 Hz), 7.17 (d, 1H, 2.9 Hz), 6.64 (s, 1H), 6.53 (s, 1H), 2.42 (s, 3H), 2.37 (s, 3H), 2.01 (s, 3H), 1.93 (s, 3H). **^{13}C (1H) NMR (100 MHz, $CDCl_3$):** δ 150.5, 143.6, 136.9, 136.6, 136.3, 131.4, 127.0, 114.8, 112.2, 71.9, 27.2, 15.5, 15.1. **HRMS (EI):** found m/z : 375.8903; calc. for $C_{12}H_9IS_3$: 375.8911.

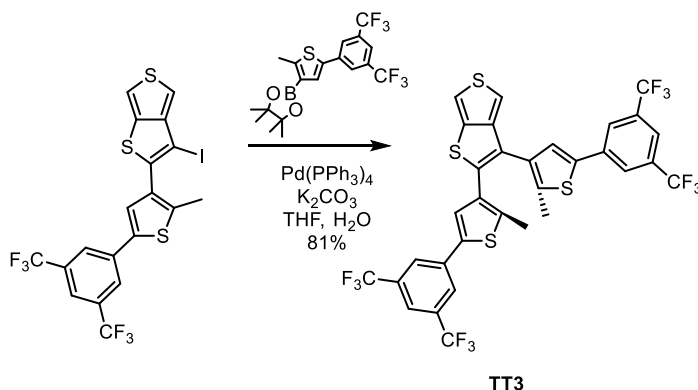
3,3'-(thieno[3,4-b]thiophene-2,3-diyl)bis(2-methylbenzo[b]thiophene) TT-BT



$\text{Pd(PPh}_3)_4$ (111 mg, 9.6×10^{-5} mol), 4,4,5,5-tetramethyl-2-(2-methylbenzo[b]thiophen-3-yl)-1,3,2-dioxaborolane (578 mg, 2.11 mmol), and 3-(3-iodothieno[3,4-b]thiophen-2-yl)-2-methylbenzo[b]thiophene (790 mg, 1.92 mmol) were added to a 25 mL Schlenk flask, which was evacuated and backfilled with N_2 three times. THF (10 mL), and saturated K_2CO_3 solution (5 mL) was added, and the reaction mixture was heated to reflux for 16 h. The mixture was then diluted with diethyl ether (20 mL) and washed twice with water (30 mL) and once with brine (30 mL). The organic layer was dried over anhydrous MgSO_4 , filtered, and concentrated under reduced pressure. The brown solid was purified by column chromatography (silica, 80:20 hexanes:DCM) to yield the product as a white solid (669 mg, 1.55 mmol, 81%). ^1H NMR (400 MHz, CDCl_3): δ 7.96 (d, 1H), 7.73 (m, 1H), 7.59 (m, 2H), 7.32 (m, 4H), 7.06 (m, 2H).

2,3-bis(5-(3,5-bis(trifluoromethyl)phenyl)-2-methylthiophen-3-yl)thieno[3,4-b]thiophene

(TT2)



2-(5-(3,5-bis(trifluoromethyl)phenyl)-2-methylthiophen-3-yl)-3-iodothieno[3,4-b]thiophene (**4b**) (700. mg, 1.22 mmol) and 2-(5-(3,5-bis(trifluoromethyl)phenyl)-2-methylthiophen-3-yl)-4,4,5,5-tetramethyl-1,3,2-dioxaborolane (585 mg, 1.34 mmol) were added to THF (10 mL) and sat.

K₂CO₃ solution (5 mL), and the solution was subjected to three freeze-pump-thaw cycles.

Pd(PPh₃)₄ (71 mg, 61 μmol) was added under increased N₂ flow, and the solution was refluxed at 100° C for 22 h. The reaction mixture was then cooled to room temperature and diluted with 10 mL of diethyl ether, washed twice with 20 mL of DI H₂O, once with 20 mL brine, and dried over MgSO₄ before concentrating under reduced pressure. Purification by column chromatography (silica, hexanes) afforded **TT2** (674 mg, 0.890 mmol, 73%) as a white solid.

¹H NMR (400 MHz, CDCl₃): δ 7.92 (s, 2H), 7.86 (s, 2H), 7.76 (s, 1H), 7.74 (s, 1H), 7.41 (s, 1H), 7.35 (d, 1H, 2.7 Hz), 7.30 (d, 1H, 2.7 Hz), 7.23 (s, 1H). 2.27 (s, 3H), 2.15 (s, 3H). **¹³C (¹H) NMR (100 MHz, CDCl₃):** δ 148.2, 139.8, 139.7, 139.6, 139.0, 137.7, 137.4, 137.1, 136.3, 136.0, 133.7, 133.2, 132.53 (q, 4C, ²J_{C-F} = 33.2 Hz), 127.0, 126.5, 125.3, 125.2, 124.7, 124.6, 123.2, 122.0, 121.9, 120.9, 113.0, 111.5, 14.8, 14.6 **HRMS (EI):** found *m/z*: 755.9939; calc. for C₃₂H₁₆F₁₂S₄: 755.9943.

References

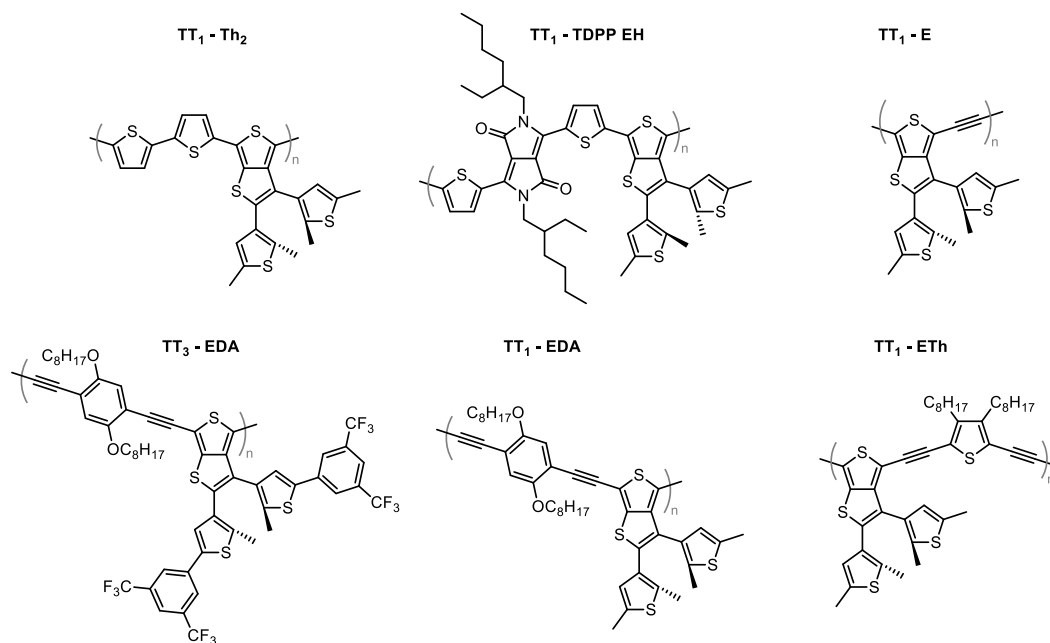
1. Liang, Y.; Feng, D.; Wu, Y.; Tsai, S.-T.; Li, G.; Ray, C.; Yu, L. Highly Efficient Solar Cell Polymers Developed via Fine-Tuning of Structural and Electronic Properties. *Journal of the American Chemical Society* **2009**, *131* (22), 7792-7799.
2. Sotzing, G. A.; Lee, K. Poly(thieno[3,4-b]thiophene): A p- and n-Dopable Polythiophene Exhibiting High Optical Transparency in the Semiconducting State. *Macromolecules* **2002**, *35* (19), 7281-7286.
3. Seshadri, V.; Wu, L.; Sotzing, G. A. Conjugated Polymers via Electrochemical Polymerization of Thieno[3,4-b]thiophene (T34bT) and 3,4-Ethylenedioxythiophene (EDOT). *Langmuir* **2003**, *19* (22), 9479-9485.
4. Wynberg, H.; Zwanenburg, D. J. Thieno[3,4-b]thiophene. The third thiophene. *Tetrahedron Letters* **1967**, *8* (9), 761-764.
5. Brandsma, L.; Verkruijsse, H. D. An Alternative Synthesis of Thieno[3,4-b]Thiophene. *Synthetic Communications* **1990**, *20* (15), 2275-2277.
6. Dey, T.; Navarathne, D.; Invernale, M. A.; Berghorn, I. D.; Sotzing, G. A. Versatile synthesis of 3,4-b diheteropentalenes. *Tetrahedron Letters* **2010**, *51* (16), 2089-2091.
7. Lee, B.; Yavuz, M. S.; Sotzing, G. A. Poly(thieno[3,4-b]thiophene)s from Three Symmetrical Thieno[3,4-b]thiophene Dimers. *Macromolecules* **2006**, *39* (9), 3118-3124.
8. Mehta, S.; Larock, R. C. Iodine/Palladium Approaches to the Synthesis of Polyheterocyclic Compounds. *The Journal of Organic Chemistry* **2010**, *75* (5), 1652-1658.

CHAPTER III

Theory and Development of Pendant Photochromic Polymers Based on Thieno[3,4-*b*]thiophene

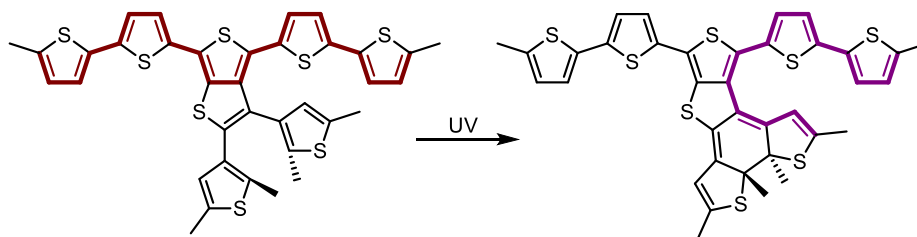
With the successful synthesis of three thieno[3,4-b]thiophene (TT) switch cores complete, attention was turned to π -extension from the 4- and 6- positions. Bromination proceeded efficiently for TT1 and TT3, but was neglected for TT2 because this species may be too sterically encumbered in the polymer as previously discussed. Other functionalizations of the 4- and 6- positions were attempted, such as di-stannylation and di-boronate ester formation, but lithium halogen exchange only seems to result in the mono-substituted byproduct. It appears that the dilithiated species does not form under the conditions attempted, so the dibrominated species was used for all coupling reactions discussed.

While small molecule π -extension (such as di-functionalization with benzene or thiophene) were planned, excitement led me to pursue polymeric species first. Initial polymer designs were based on simple and/or common conjugated backbones (bithiophene for a basic conjugated polymer, diketopyrrolopyrrole for a donor-acceptor (D-A) type polymer, etc., (**Scheme 3.1**) to observe how the switch behaves in the polymeric state. These polymerizations were carried out using either Stille or Sonogashira polycondensations. In the case of thiophene linkages, Stille copolymerizations were chosen since Suzuki couplings between thiophenes and TT were found to be more sluggish. Polymerizations seemed to struggle, as the yields were 40-50% and the molecular weights of the species ranged from 6-10 kDa. All polymers were soluble in chloroform except for TT₁-E, which was found to be completely insoluble in all available solvents. The physical appearance of these polymers varied; some were red or black powders, while others were metallic brown or gold flakes. All of the purified polymers appear to be stable when stored at 0-2° C based on UV Vis traces after a month.



Scheme 3.1. Structures of the first six polymeric species investigated, ranging from donor-acceptor polymers to alkyne-containing polymers.

Following synthesis, UV-Vis spectra were taken where the polymer solutions were irradiated with 254 or 365 nm. An unexpected result occurred in the thiophene-linked species (**Figure 3.1**). While a visible-region absorbance was expected to grow in upon irradiation, a decrease was observed, in addition to a slight blue shift in the λ_{max} . This was coupled with a NIR band increasing, though it is uncertain at this point if a peak grows in due to instrument limitations.



Scheme 3.2 Alternative conjugation path for **P-TT₁-Th₂** polymer, where the cyclized structure has forced planarity which may favor shorter conjugation paths along the switching arm.

There are currently two explanations for the observed phenomenon. If cyclization is occurring under UV irradiation, the increase in planarity of the closed switch may create an alternate delocalization pathway extending from a portion of the conjugated backbone to the switch, as opposed to completely along the backbone. The delocalization is thus “chopped up” into shorter segments (**Scheme 3.2**), potentially resulting in a decrease in visible region absorbance and a hypsochromic shift. This new conjugated pathway may interfere with the symmetry of the frontier molecular orbitals, preventing the switch from reopening. This theory doesn’t necessarily explain why the NIR absorbance grows in, however. The second theory is that the polymer is simply decomposing or going through a certain transformation that wouldn’t be easy to determine.

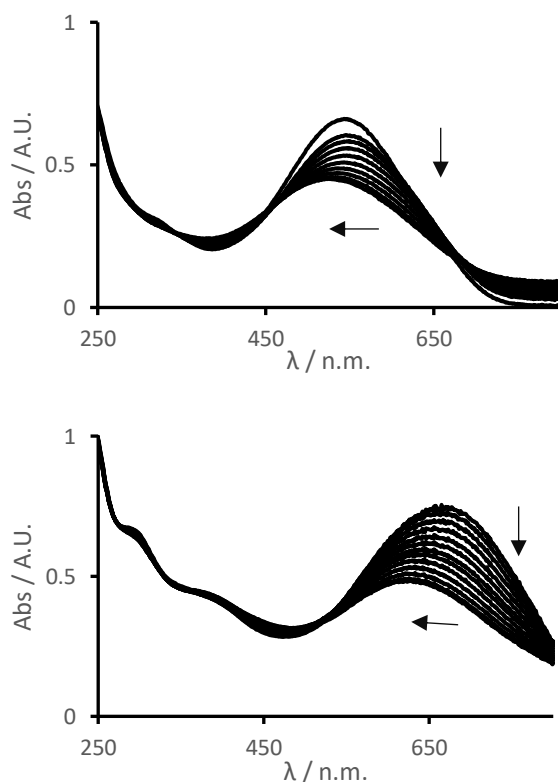


Figure 3.1. UV Vis spectra for **TT1-Th2** (left) and **TT1-TDPP EH** (right), each line representing 10 second irradiation intervals at 254 nm.

Electrochemistry was also employed, using bithiophene and EDOT as copolymers and TT1 as the photochrome (**Figure 3.2**). Bithiophene coelectropolymerizations were performed for comparison with the chemically polymerized analogue. While the general UV-Vis shape is similar to the chemically polymerized species, differences are possibly due to the effective chain length of the polymers (possibly shorter chains from electropolymerization onto ITO). The electropolymerized species did not respond to UV light, however.

EDOT coelectropolymerizations were performed to capitalize on the potential optical transparency of the resulting polymer in the oxidized state. PEDOT was first polymerized, subject to spectroelectrochemistry, and compared to the literature to verify the technique was correct before coelectropolymerization. The resulting polymer on ITO did not respond to UV light, but did respond to voltage changes (as did the bithiophene polymer). In the oxidized state, TT1-EDOT polymer still failed to respond to UV light.

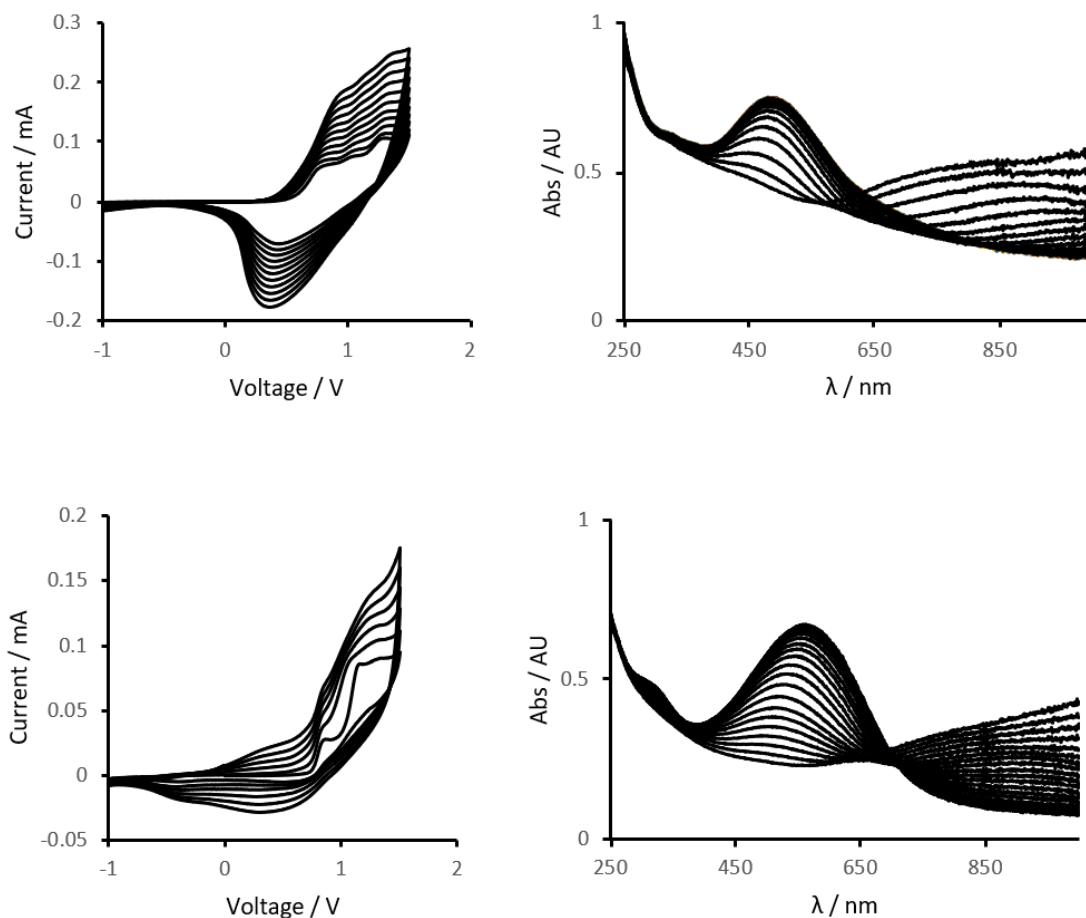


Figure 3.2 CV and spectroelectrochemistry for **TT1-Th2** (top) and **TT1-EDOT** (bottom). Spectroelectrochemistry scans were separated by 0.1 V. Collected on a platinum button working electrode with a Ag/Ag^+ reference electrode in MeCN.

With the lack of photochromic response from both the chemically and electrochemically polymerized species, attention was returned to small molecules. **TT1-Th** was synthesized early on before polymer work. This species at the time was observed to lack photochromism, but was found to be highly fluorescent compared to the core switch. DFT calculations (B3LYP / 6-31G*) were used to demonstrate that the frontier molecular orbitals were delocalized across what would be the conjugated backbone. It became clear that the switching component of the molecule was not far enough removed from the conjugated backbone to be treated as an isolated system. This led to the idea that there should be significant LUMO delocalization across the switching motif for the photochrome to cyclize, which is not seen in this case. Calculations were then performed

on three other derivatives, involving phenyl as a slightly bulkier backbone alternative and/or TT3 as a π -extended switching motif (**Table 3.1**). **TT2-Ph** was the only species of this group that demonstrated LUMO density across one of the switching arms, and only slightly along the conjugated backbone. Due to geometry optimization, the energy-minimized structure doesn't account for possible conformational rotations that would also favor switching (such as an angled aryl backbone and a more planar β switching arm, leading to delocalization along both switching arms). But as significant delocalization along one arm led to a photochromic compound, calculations which demonstrate this were treated as ideal target compounds.

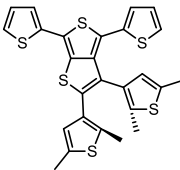
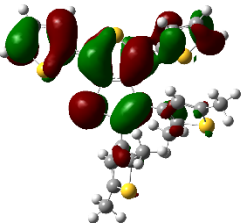
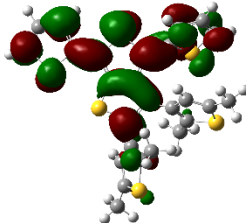
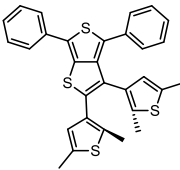
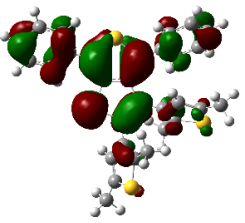
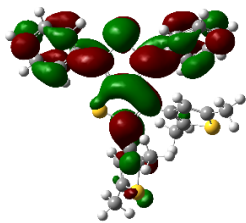
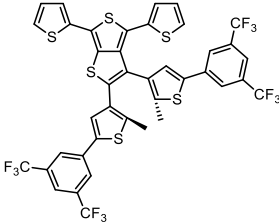
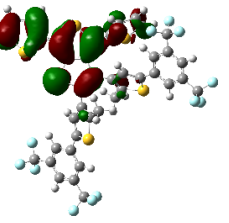
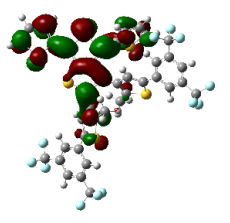
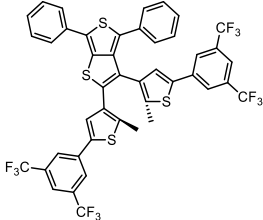
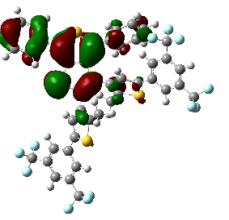
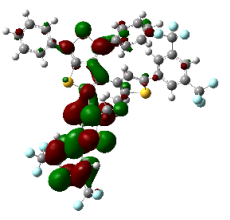
Name	Structure	HOMO	LUMO
TT1-Th			
TT1-Ph			
TT2-Th			
TT2-Ph			

Table 3.1 Frontier molecular orbitals (B3LYP / 6-31G*) for the small molecules investigated to determine surface distribution across the switching motif.

In an effort to see if these calculated structures translated to real-world properties, the three derivatives were synthesized. Stille coupling with the corresponding stannane resulted in mostly desirable product, but there was a small portion of photochromic mono-coupled species present in each reaction. NMR reveals a missing bromine (possibly lost due to the temperature of the reaction). Both **TT2-Ph** and **TT2-Th** were both found to be weakly photochromic, with the former demonstrating a larger change in the UV-Vis (**Figure 3.3**). These two compounds behave like other switch cores, though it was particularly difficult to photo-bleach, requiring irradiation with an intense white light for approximately 45 minutes (TT switches typically bleach in under 5 minutes). Both **TT1-Ph** and **TT1-Th** were fluorescent yellow compounds that showed no change upon UV irradiation.

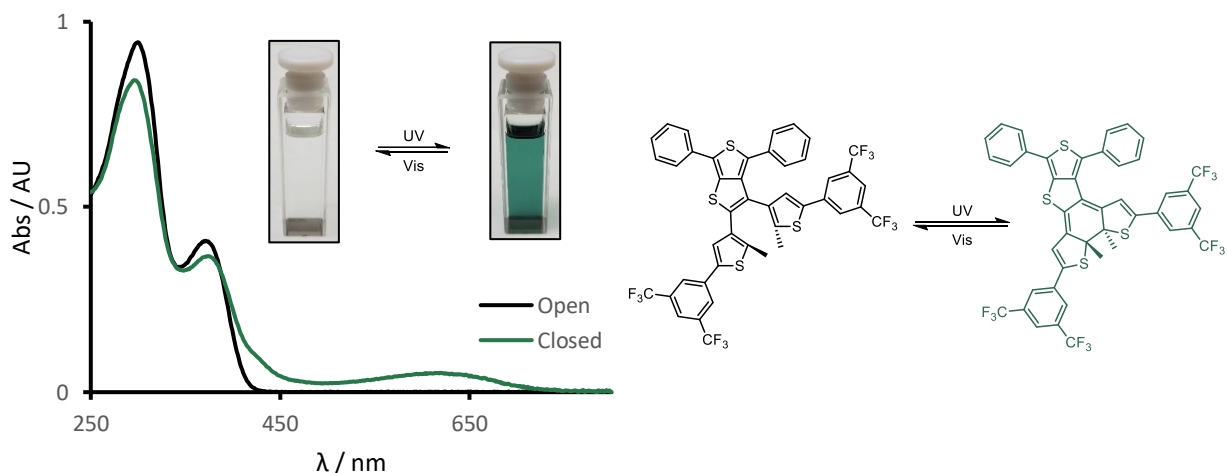


Figure 3.3 UV-Vis spectra for the open and closed form of **TT2-Ph**, demonstrating a relatively mild change in absorption profile upon reaching the photostationary state.

Returning attention to the DFT calculations, it was initially thought that incorporating **TT2** as a switching motif would re-seize the frontier molecular orbitals (due to its conjugated system being more extended than the backbone), but this wasn't the case in **TT2-Th**. Comparing **TT2-Th** to **TT2-Ph**, the size of benzene compared to thiophene doesn't appear to be a major influence, as the dihedral angles between the two calculated structures are very similar. In

solution, however, the backbone containing thiophene may in fact be more planar than the benzene analogue. It is also possible that delocalization is more effective across thiophene than benzene due to the lower aromaticity of the former. Regardless, it appears that a qualitative interpretation of the frontier molecular orbitals may reflect photochromic functionality in the target molecule. A series of calculations were run to test potential ideas to solve the polymeric species problem. There are two anti-periplanar conformations that can potentially cyclize (interconversion between the two isomers to find the lowest energy conformation does not occur). Both conformations were computationally tested (**Table 3.2**) to confirm both the HOMO and LUMO orbitals have similar distributions along the molecule. Even though both conformations are effectively equivalent, the conformation that was found in the crystal structure for **TT1** was used as the default conformation for consistency among calculations.

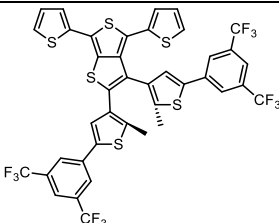
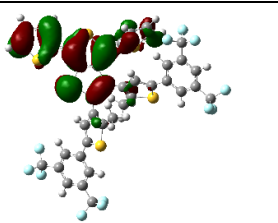
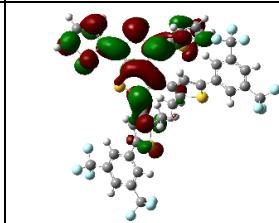
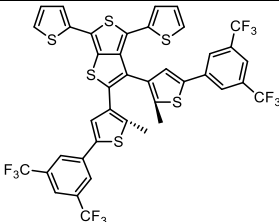
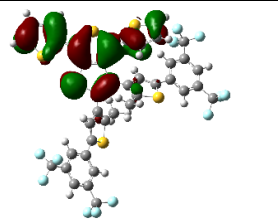
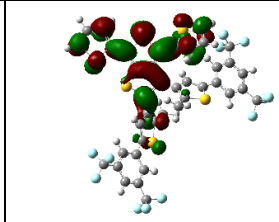
Name	Structure	HOMO	LUMO
TT3Th2			
TT3Th2Flip			

Table 3.2 Frontier molecular orbitals (B3LYP / 6-31G*) for the two energy minimized anti-periplanar isomers.

There are several plausible ideas that may be used as a guide towards building functional switches. The first involves backbone distortion; If the aryl groups attached at the conjugated backbone are tilted out of plane from that of TT, the main conjugated pathway may then be distributed across the switch. This can be visualized by locking the dihedral angle between **TT**

and the pi-extended aryl substituent (**Table 3.3**). As the dihedral angle is taken from 0° to 90°, the orbital densities gradually migrate from the conjugated backbone to the switching motif. DFT calculations 2,6-dimethylbenzene substituted TT were performed as a bulky representative of a 90° dihedral angle. These two out-of-plane examples show similar results. Synthesis of this substrate was attempted to provide empirical support, but the substrate proved to be sterically encumbered to couple effectively.

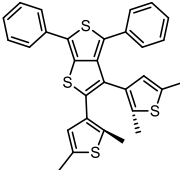
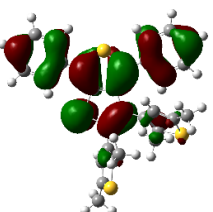
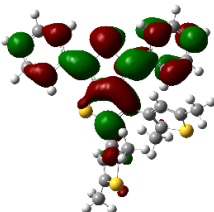
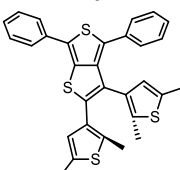
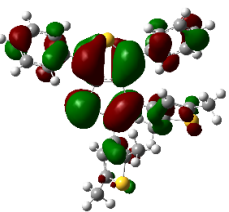
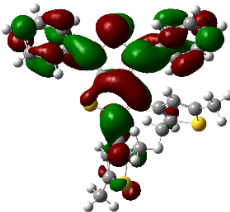
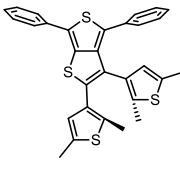
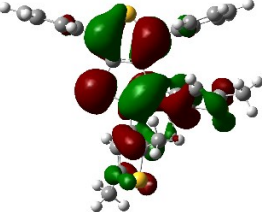
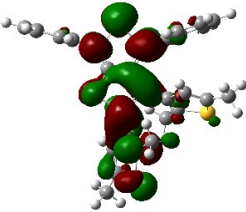
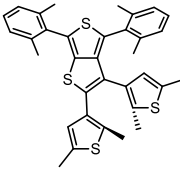
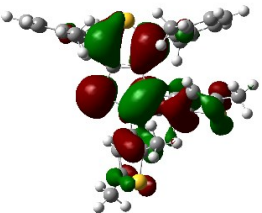
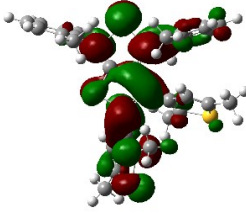
Name	Structure	HOMO	LUMO
TT1-Ph Lock0	dihedral angle = 0° 		
TT1-Ph Lock45	dihedral angle = 45° 		
TT1-Ph Lock90	dihedral angle = 90° 		
TT1-DMPH			

Table 3.3 Frontier molecular orbitals (B3LYP / 6-31G*) for conformationally locked **TT1Ph2** and the sterically hindered derivative.

A second theory involves further extending the switching motif away from the backbone. A synthetically tractable derivative of **TT** is **DTT** (Table 3.4), which involves the insertion of another fused thiophene ring (though it more resembles a bridging sulfur between thiophene rings to maintain two aromatic portions). The frontier molecular orbitals for **DTT2** and its substituted derivatives were found, but besides the lack of steric hindrance between the β switching arm and the aryl substituents, this model appears to be slightly worse than its **TT3** analogues. Pendant models past this point start having improbable synthetic pathways.

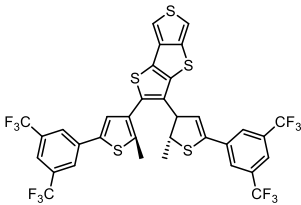
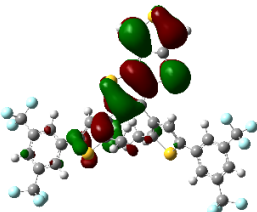
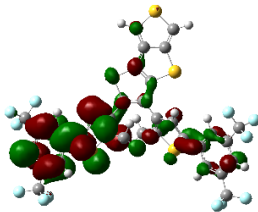
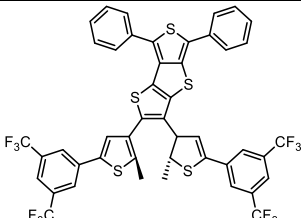
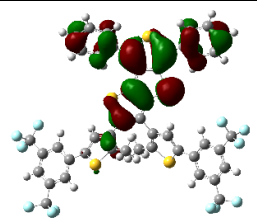
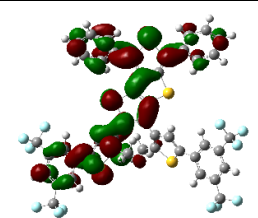
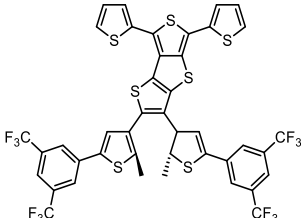
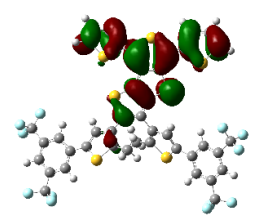
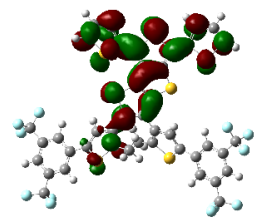
Name	Structure	HOMO	LUMO
DTT3			
DTT3Ph2			
DTT3Th2			

Table 3.4 Frontier molecular orbitals (B3LYP / 6-31G*) for **DTT3** switch core and small-molecule derivatives.

As backbone out-of-planarity is undesirable quality of future polymers, and a completely isolated switching system that still effects the main chain polymer may not be feasible, the third theory may prove to be the most reliable. In the case of donor-acceptor systems, it may be

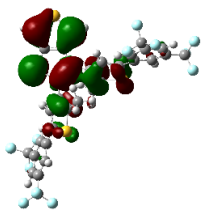
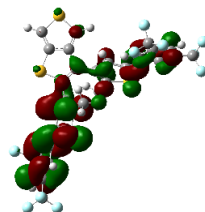
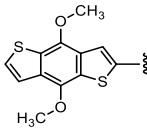
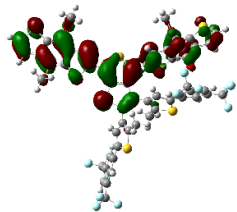
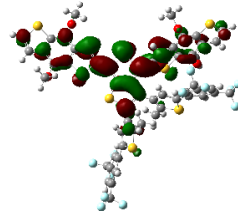
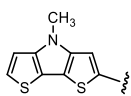
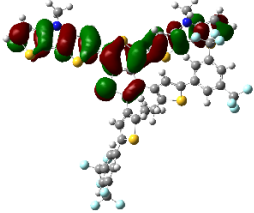
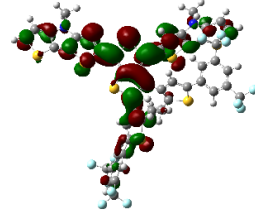
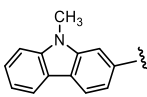
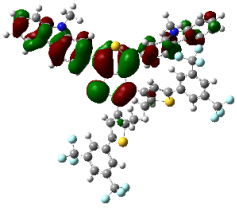
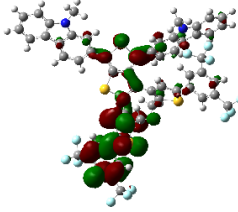
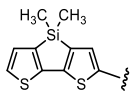

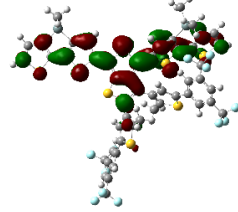
possible to localize the LUMO on the switching motif (should it be electron deficient enough) and have the HOMO remain on the conjugated backbone. Although **TT2** initially served as a π -extended and fatigue resistant switching motif, it also serves as an “acceptor” due to high fluorine substitution. **TT2** was thus screened against several donor molecules in the literature (**Table 3.5**), from popular to uncommon electron rich substrates. Substitutions were done on the 4- and 6-positions as in previous cases for extended backbone delocalization; should the donor-acceptor system not be strong enough, it is expected that the HOMO and LUMO will simply reside along the backbone as in cases with **TT1** (**Table 3.1**).

Several systems that were expected to show desirable HOMO / LUMO surfaces due to electron richness (such as **TT2D1**, **Table 5**) maintained orbital densities along the backbone. Some promising structures are **TT2D3**, **TT2DAPh2**, and **TT2EDOT2**, all of which show LUMO distribution on one switching arm as in the case with **TT2Ph2**. Attempts are being made to calculate extended repeat units of these species to see if the same properties are seen in oligomeric species, but such a large molecule might be outside computational limits.

Asymmetric systems like **TT2D6** were calculated in both “oxygen atoms in” and “oxygen atoms out” isomers, but would only be treated as a good donor if the poorer isomer had the proper orbitals. This donor was chosen since it is reported as being more electron rich, though in these systems both isomers are lackluster in switch arm delocalization.

A few donor systems showed rather unusual FMO surfaces, but only one is shown; the germanium species **TT2D5** had orbital surfaces effectively across the entire molecule. While delocalization across both switching arms would normally be desirable, the current qualitative criteria for switching based on DFT calculations involves the majority density on the switching arm. Nevertheless, this compound may be worth investigating in the future.

It is also worth noting here that the systems that are analogous to synthesized polymers (**TT1-Th** and **TT2-EDAPh2**, **Scheme 3.1**) do not have the ideal HOMO / LUMO surfaces according to DFT. Since the polymers did not switch, these findings further defend this DFT correlation.

Name	Donor (4- and 6- Positions)	HOMO	LUMO
TT2	None		
TT2D1			
TT2D2			
<u>TT2D3</u>			
TT2D4			

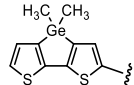
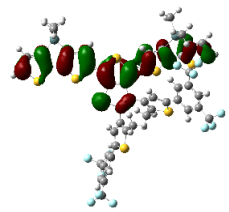
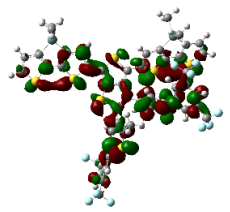
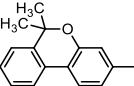
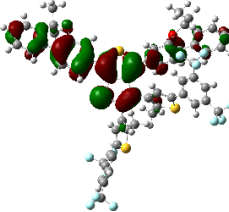
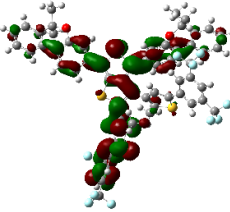
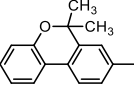
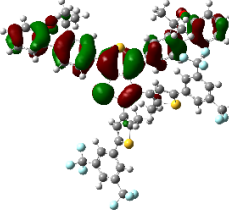
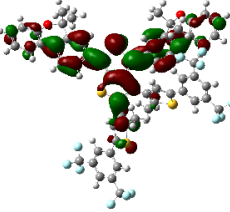
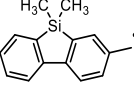
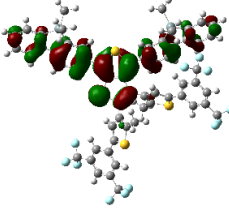
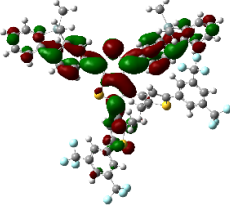
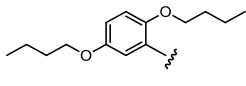
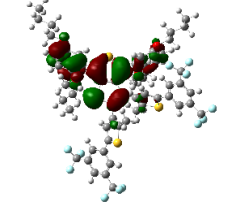
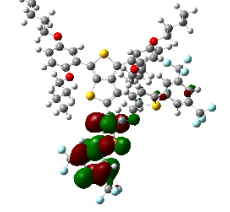
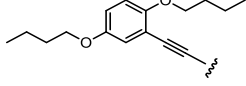
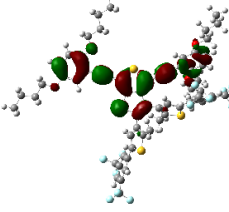
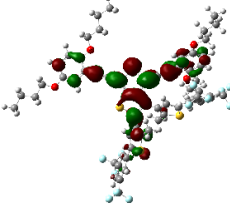
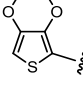
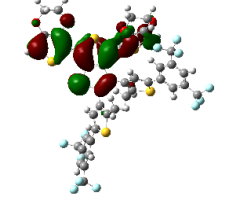
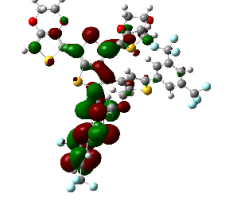
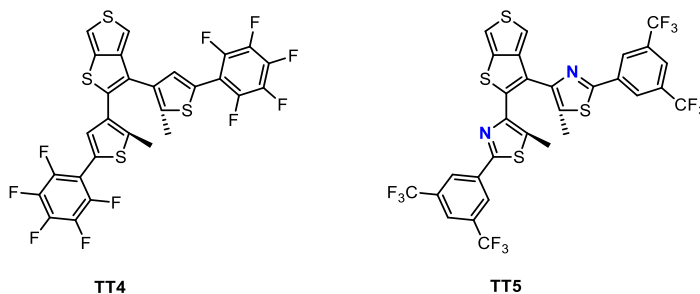
TT2D5			
TT2D6A			
TT2D6B			
TT2D7			
<u>TT2DAPh2</u>			
TT2EDAPh2			
<u>TT2EDOT2</u>			

Table 3.5 Donor screening with the initial acceptor **TT3** (B3LYP / 6-31G*). Potentials are bolded and underlined.

Optimizing the switch core itself to be a stronger acceptor unit was also computationally investigated. The two proposed derivatives are **TT4** and **TT5** (Scheme 3.3, Table 3.6).

Calculations were performed on both of these species using donors that showed poor LUMO surfaces from **TT3** trials (Table 5), as it is easier to see improvements between acceptors.



Scheme 3.3. Molecular structures of the two acceptor species studied computationally.

TT4 was chosen simply because it was believed that direct fluorine substitution onto phenyl would be more electron deficient than having the trifluoromethyl substituents as in **TT2**. Surprisingly, **TT4** appeared similar or worse to the analogous **TT2** structures. With no significant difference between the two, the trifluoromethyl groups will be kept, and future modifications are directed towards the thiophene portion of the switch arm. When the thiophene is replaced by a thiazole as in **TT5**, it was thought that the additional electron deficiency of including sp^2 hybridized nitrogen atoms will help struggling **TT2** based donor acceptor systems have favorable orbital densities. Again, **TT5** systems were calculated using electron-poor **TT3** analogues. Across the board, HOMO densities stayed on the conjugated backbone, while the LUMO surfaces resided almost exclusively on the switching arm of **TT5**.

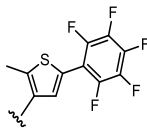
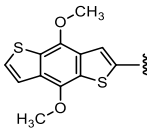
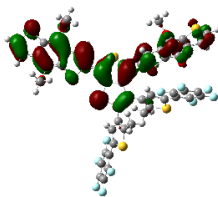
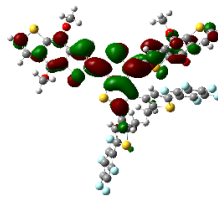
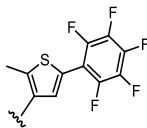
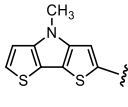
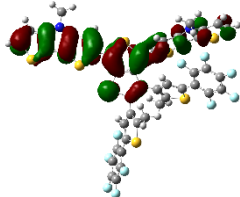
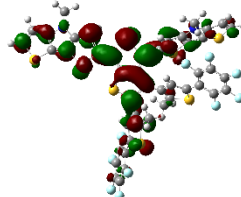
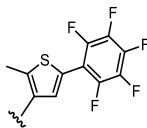
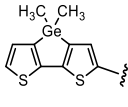
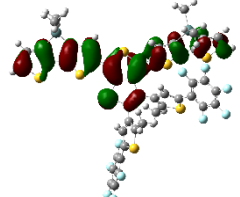
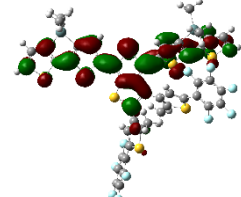
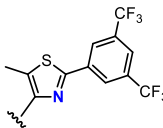
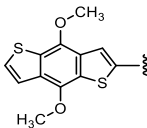
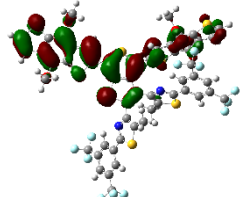
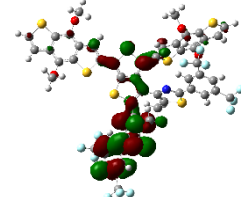
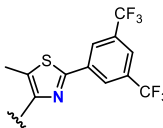
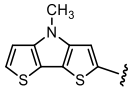
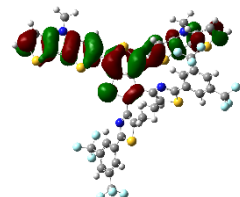
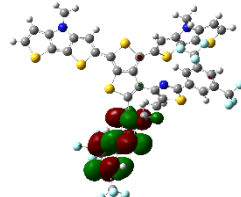
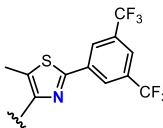
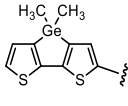
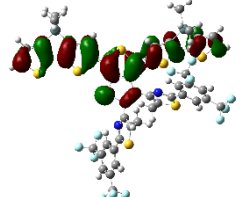
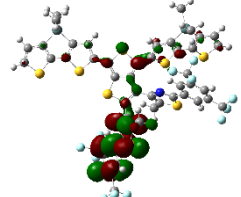
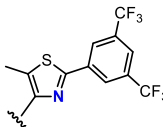
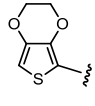
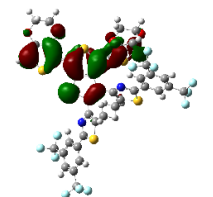
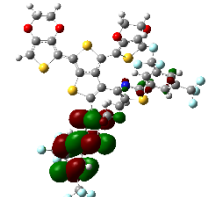
Name	Switch	Donor	HOMO	LUMO
TT4D1				
TT4D2				
TT4D5				
TT5D1				
TT5D2				
TT5D5				
TT5EDO T2				

Table 3.6 Acceptor screening with poor donors from the TT3 screening. TT5 shows desirable surfaces in all cases examined.

This acceptor unit can be further extended to the **DTT** motif mentioned earlier (**Table 3.7**), which also shows significant FMO surface improvement over the **DTT3** analogue. It is even more dramatic in this case, as the LUMO is distributed across both switching arms as opposed to one, and no density along the core itself.

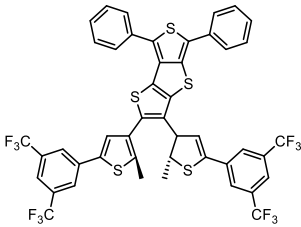
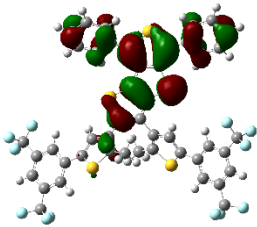
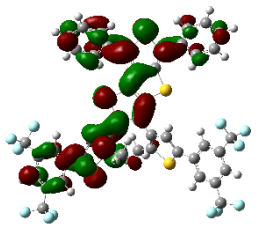
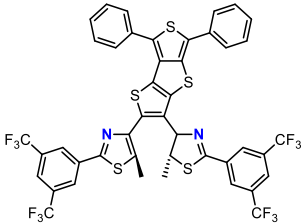
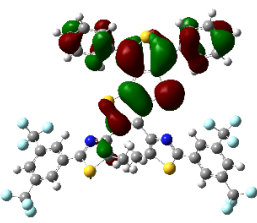
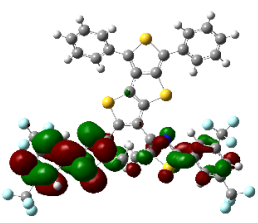
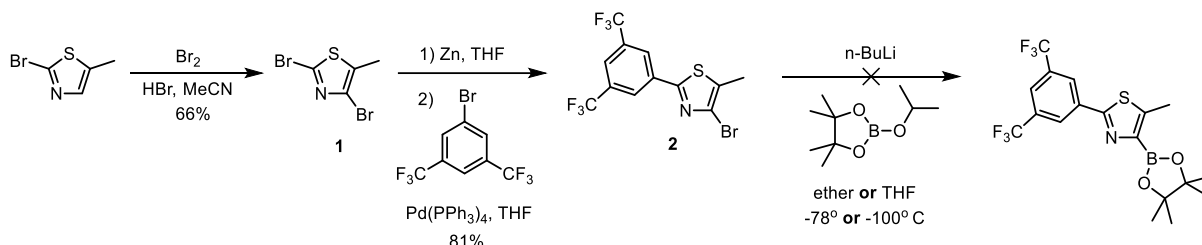
Name	Structure	HOMO	LUMO
DTT2Ph2			
DTT5Ph2			

Table 3.7 Comparison of the frontier molecular orbitals (B3LYP / 6-31G*) of **DTT2** and **DTT5**.

At the time of these calculations, the donor-acceptor systems appeared to be the most promising route towards a functional pendant photochromic polymer, with significant variety in the co-monomers **TT2** or **TT5** can be paired with. The sterically hindered pathway may have potential, though it is not ideal as the conjugated pathway is hampered and there is greater limitation on the co-monomer used. While these calculations do seem to act as a guide, they may not reflect how the polymer behaves at all. The extended conjugation in “linear” or steric hindrance-free polymeric species may have sufficient enough conjugation to represent the HOMO-LUMO gap, assuming the donor-acceptor strength is insufficient. Regardless, synthesis of **TT5** was pursued.

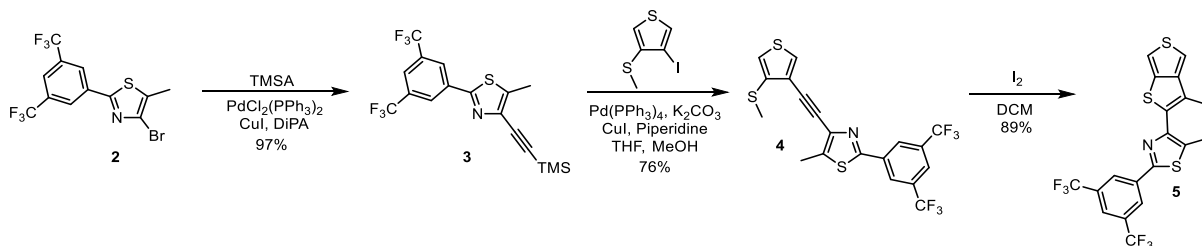
On paper, the synthesis was supposed to be very comparable to the other TT switches, but working with thiazole is relatively more difficult in terms of reactivity and purification. After

halogenation and a Negishi coupling, literature compound **2** (Scheme 3.4) was prepared in yields comparable or better than that reported. Several attempts were made to prepare the boronate ester of this species to have an analogous synthetic pathway to earlier **TT** switch arms, but the desirable product was never obtained. Hecht's group reported the synthesis of the stannane, which is not usually a first choice, so it was assumed that the boronate ester is unreasonable to make.



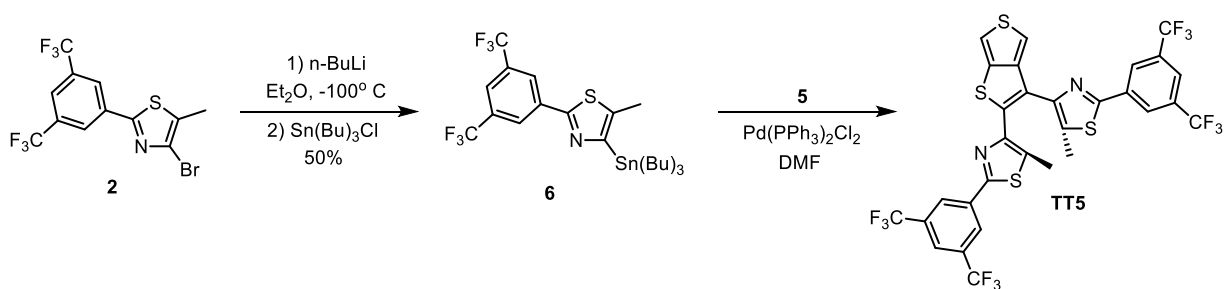
Scheme 3.4 Attempted synthesis of the thiazole boronate ester utilizing both Negishi and Suzuki cross-coupling reactions.

Thiazole intermediate **2** was also used in the assembly of the iodinated **TT** core (Scheme 3.5). Sonogashira cross coupling to install the protected alkyne proceeded in surprisingly high yields, a potential feature of halogenated thiazoles. Although the TMS-protected switch arm is not volatile, the simultaneous *in situ* deprotection and Sonogashira cross coupling was used to avoid adding an unnecessary purification step, yielding pre-Larock intermediate **4**. Larock-type ring closure to produce **5** worked very efficiently at room temperature with no detection of byproduct formation.



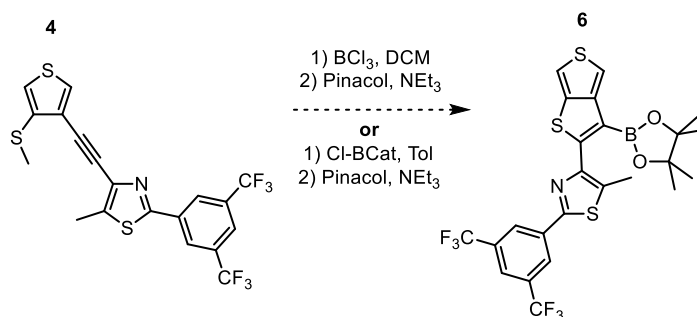
Scheme 3.5 Assembly of the thiazole-based **TT** intermediates utilizing the Larock-type ring closure to obtain the iodinated core.

The reported stannylation was followed for the generation of the intermediate **6** proceeded in 50% yield, allowing for the typical Suzuki coupling with the iodinated **TT** precursor **5** to be replaced with a Stille cross coupling (**Scheme 3.6**). It is believed that this reaction worked to a certain extent due to observed photochromic activity, but the obtained materials proved exceptionally difficult to purify due to the presence of tin byproducts and starting material which happen to coelute during chromatography.



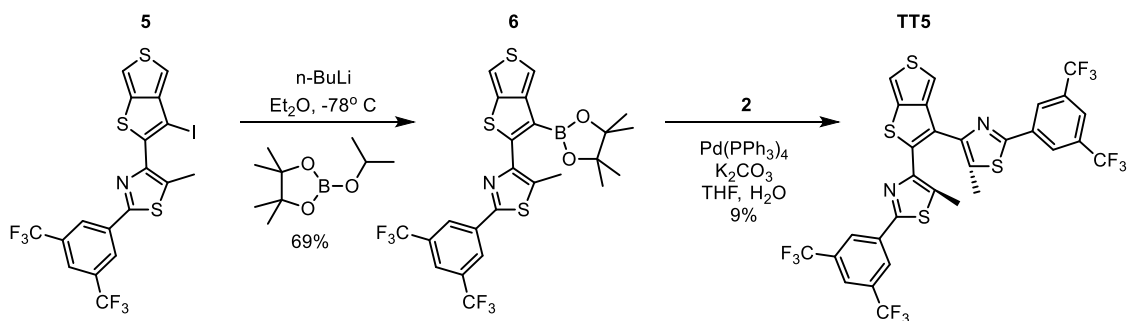
Scheme 3.6 Assembly of **TT5** switch core using a stannylated switch arm for the final cross-coupling reaction.

At the same time, other routes were explored to allow access to **TT5** that would result in easier purification. One alternative involves generating the boronate ester from the iodinated **TT** precursor. This would allow for a Suzuki cross coupling as with other switches, though this time the locations of the boronate ester and the halogen are flipped. This wasn't considered in the past as it seemed simpler to make the boronate ester on the entering switch arm than this more sterically hindered 3- position on **TT**. It is not unreasonable to expect this reaction to proceed efficiently, however. The first attempt at this substrate was a borylative cyclization (**Scheme 3.7**), for which there are two literature procedures that demonstrate its use on beno[*b*]thiophene derivatives. This is similar to the iodine-mediated electrophilic cyclizations, except now the electrophile is a substituted boron that gets converted to a pinacol boronate ester. Unfortunately, no conversion to the desirable product was observed by NMR.



Scheme 3.7 Attempted borylative cyclization that would result in boronate ester functionalization at the 3-position of **TT**.

One can argue that it was a little ambitious trying to directly obtain the boronate ester-substituted **TT** from the alkyne, effectively trying to “cut out the middle man” that would be the Larock-type ring closure with iodine followed by lithium-halogen exchange and subsequent quench with a boronate. This two-step method was then attempted and worked in low yields (**Scheme 3.8**). This may be due to the instability of the boronate ester at higher temperatures, which was found to decompose on its own in heated deaerated solution tests over a few hours. This alternative route was considerably easier to purify, however.



Scheme 3.8 Stepwise borylation of the 3-position of thiophene by first performing the iodine-mediated electrophilic cyclization followed by lithium-halogen exchange to produce the desired boronate ester.

Coincidentally, after completion of this alternative route, it was found that the switch product from the Stille route could be separated from both the tin byproducts and the starting

material by precipitation in acetonitrile, allowing access to **TT5** in greater amounts than the Suzuki method. Nevertheless, it may be useful in the future to know that the 3-position iodine can tolerate lithium-halogen exchange.

Photophysical data for **TT5** is shown in **Figure 3.4**. **TT5** in its open form features one major absorption peak ($\lambda_{\text{max}} = 298 \text{ nm}$) with the absorption cutoff occurring before the visible region ($\lambda_{\text{abs}} = 399 \text{ nm}$), confirmed by the colorless nature of the purified solid. Upon irradiation with a handheld lamp, two peaks emerge in the visible region ($\lambda_{\text{abs}} = 409 \text{ nm}$ and $\lambda_{\text{abs}} = 600 \text{ nm}$), while the λ_{max} of the open switch is both depleted and blue shifted. Like **TT2**, **TT5** reaches the photostationary state rapidly in under thirty seconds of irradiation, but takes over 4 min for cycloreversion to go to completion.

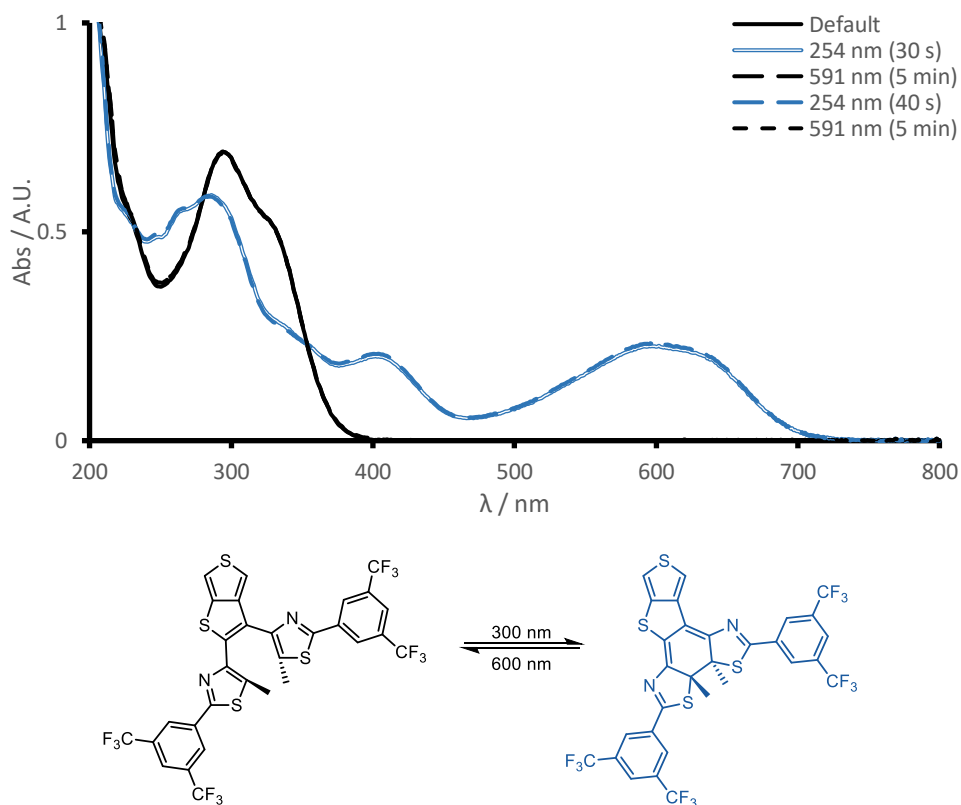
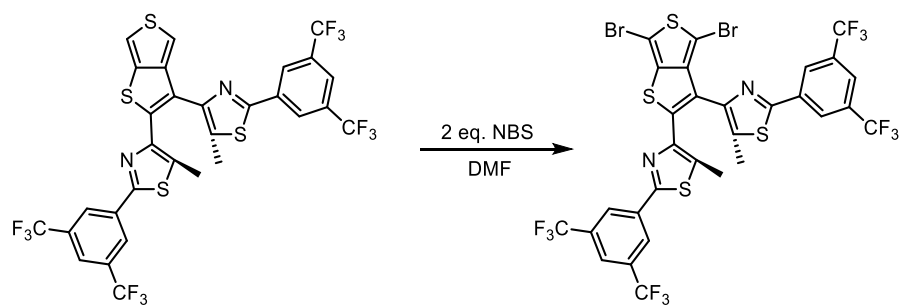


Figure 3.4 UV-Vis absorption spectrum of the open and closed switch **TT5** and the corresponding coloration.

Some minor issues appeared when attempting to brominate this compound (**Scheme 3.9**). Two equivalents of NBS does not result in full conversion of starting material to desired product. A substantial portion of the mono-brominated product was present, as judged by NMR analysis. It was considered reasonable to add excess NBS (2.5 eq) to drive the reaction to completion, since there are no other reasonable locations to halogenate on **TT5** other than the 4- and 6- positions. This is due to the presence of the thiazole nitrogen atoms, occupying the beta position of “thiophene” which could normally be halogenated under these conditions. Surprisingly, excess NBS simply destroys everything, so the low yield of 2 eq. NBS was tolerated.



Scheme 3.9 Dibromination of the **TT5** switch core prior to π -extension at the 4- and 6- positions of thieno[3,4-*b*]thiophene.

Bromination of **TT5** meant that this substrate can now be incorporated into polymeric species to test the current donor-acceptor theory (**Scheme 3.10**). A suitable electron-rich comonomer was chosen as shown below for the polymerization.

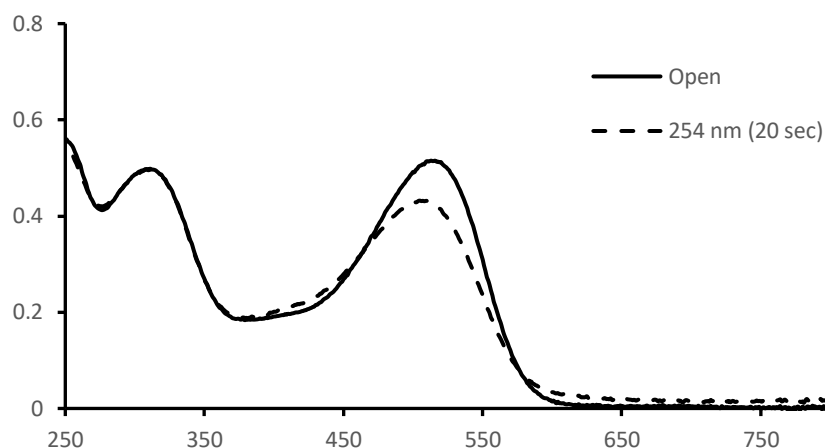


Figure 3.5 Photophysical response of the donor-acceptor polymer based on **TT5**, where the same reduction and blue shift of the λ_{max} in previous pendant diarylethene polymers was observed.

This single example is a demonstration that the donor-acceptor concept is inherently flawed. While it is still believed that the frontier-molecular orbital topology being distributed across the switching motif, it doesn't necessitate that the excited state decays down a photochromically-productive pathway. Due to the high fluorescence seen in these pendant photochromic polymers (and also the **TT1** small molecules), it seems as though the excited species would preferentially release a photon upon excitation as opposed to proceeding through the 6π electrocyclization. For example, in the polymeric materials, the absorption of the π -extended conjugated backbone appears in the visible region while the absorption of the switching component usually absorbs in the ultraviolet region. Although Kasha's rule indicates that the most likely radiative transition occurs from the lowest excited state (in this case, the energy gap corresponding to the "diphenylthiophene" backbone), we initially believed that the pendant diarylethene switching motif would be far enough removed from this system to act independently of this π -extended region, that is, proceed through cyclization similar to the parent photochromic cores. However, the lack of photochromic response for **TT1-Ph** suggests that the electronic structure of these systems should be treated globally, where the two photoresponsive regions effectively compete for the lowest energy transitions, one of which leads to cyclization through

the conical intersection while the other leads to emission of a photon. Time-dependent density functional theory (TD-DFT) calculations provided support for this idea. Several basis sets and levels of theory were tested to identify the appropriate method which best match current experimental data. As shown in **Figure 3.6**, B3LYP / 6-31G* matched experimental data quite well for all switches up to this point. Higher level computational methods showed minimal changes in terms of frontier molecular orbital topology and transition energies, so this simpler method was chosen to reduce computational time. It is worth noting that other groups have come to the same conclusion for diarylethene switches.

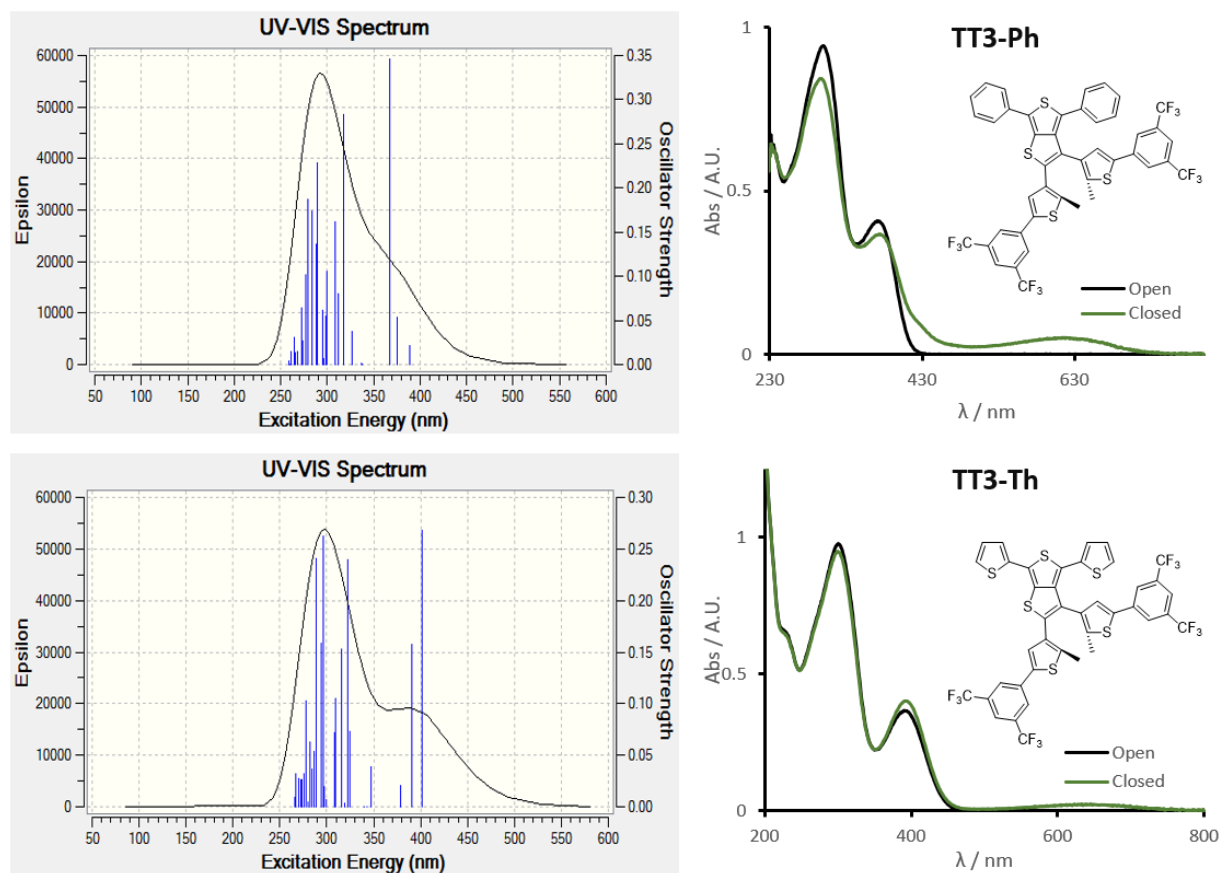


Figure 3.6 Comparison between calculated and experimental UV-Vis absorption of the two functional photochromic oligomers **TT3-Ph** and **TT3-Th**, using DFT B3LYP / 6-31G*.

Key transitions were then calculated for **TT1-Ph** and **TT2-Ph** as well as for their isolated competing chromophores: the 4-6-diphenylated thieno[3,4-*b*]thiophene (**TT-Ph**) and the 2-3-disubstituted switch cores **TT1** and **TT2** (**Figure 3.7**). Examining both the **TT** switch core and the competing “oligomeric” backbone independently would allow ready correlation of key transitions with the diarylated model compounds under investigation. As expected, the frontier molecular orbital (FMO) topologies for **TT1-Ph** more closely resemble that of **TT-Ph**, indicating that the highest occupied molecular orbital–lowest unoccupied molecular orbital (HOMO–LUMO) transition is associated with the α -diphenylated thiophene portion. It is not until the LUMO+1 of **TT1-Ph** that we see electronic distribution across the switching motif that resembles **TT1**’s LUMO. Interpretation of the energetics of these transitions is also very telling. The energy of the HOMO-LUMO transition for **TT1-Ph** is almost identical to that of **TT-Ph** (3.61 eV and 3.57 eV). This indicates that the photochromic motif does not drastically impact the energetics of transitions elsewhere in the molecule, possibly due to the lack of planarity of the switch arms. The HOMO-LUMO+1 transition energy, that is, the energy of the transition that would correspond to a productive photochromic reaction, is much higher in energy at 4.48 eV. Even though the two major transitions under investigation can be segregated and interpreted separately through computational methods, how the molecule behaves upon excitation must be treated *holistically*. Thus, upon excitation, the molecule most likely relaxes down to the lowest energy excited state which in this case is that of the “oligomeric” backbone. From here, the molecule releases a photon as opposed to proceeding through the conical intersection that results in switching. This reasoning explains why π -extended **TT1** molecules are fluorescent rather than photochromic.

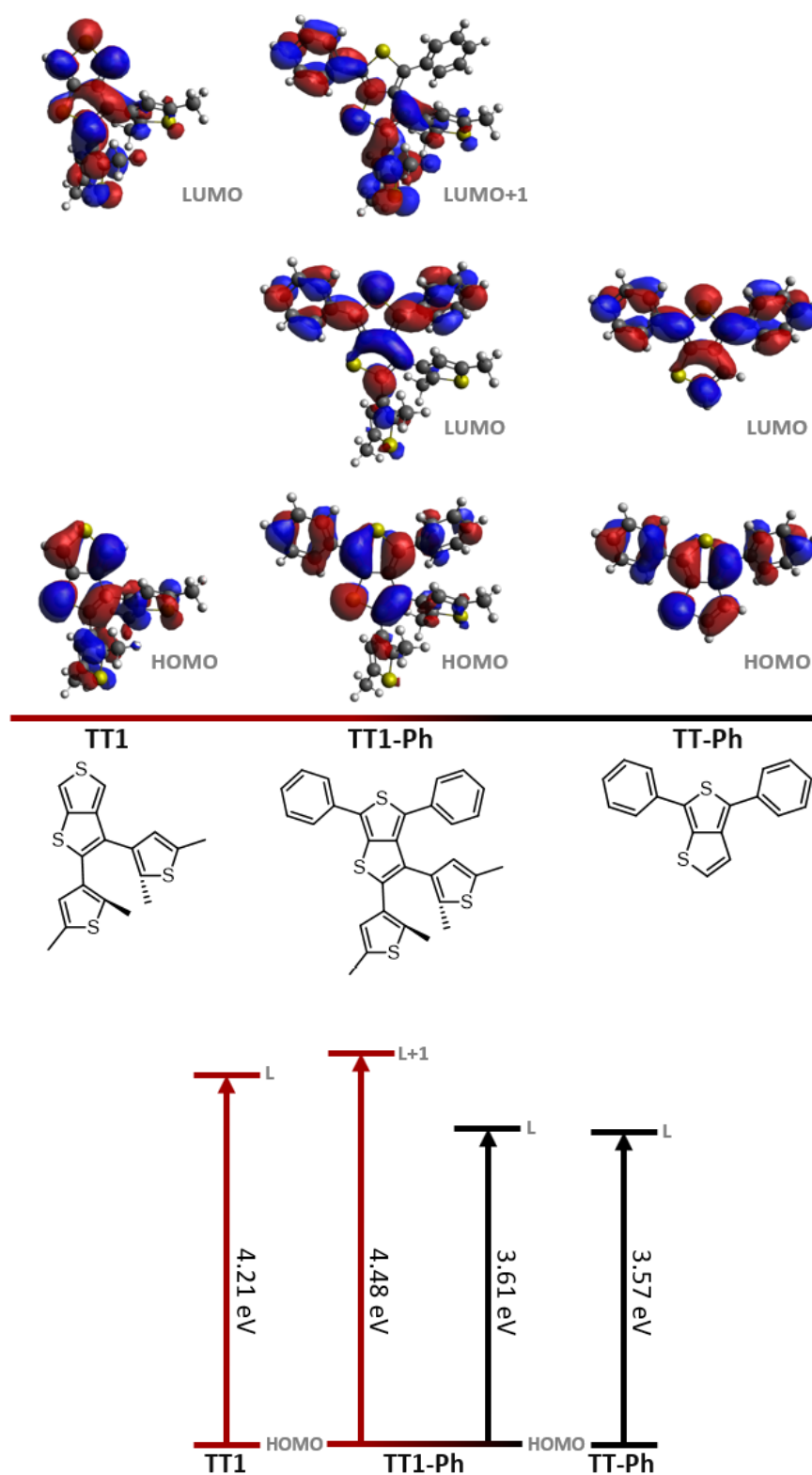


Figure 3.7 Frontier molecular orbital topologies for TT1, TT1-Ph, and TT-Ph, with the magnitudes of the energy of their corresponding transitions.

The same analysis was performed for π -extended **TT2** switches (**Figure 3.8**), which were again compared to the conjugated backbone **TT-Ph**. Here, the transitions are not that clear. When observing the frontier molecular orbitals, the HOMO-LUMO transition of **TT2-Ph** does indeed resemble that of **TT2**, where the LUMO has significant contributions from the switch arms. The situation is not completely reverse compared to **TT1** since the LUMO+1 doesn't necessarily resemble the LUMO of **TT-Ph**, but rather a combination of both species' LUMO. Interpretation of the transition energies indicate that all of the orbitals under investigation are all roughly the same energy with the HOMO-LUMO transition for **TT2-Ph** being *slightly* lower than the HOMO-LUMO+1 transition (3.61 eV versus 3.71 eV). The empirical manifestation of this is weak photochromic activity seen from **TT2-Ph** and **TT2-Th**. The closeness of the energies of the key transitions indicates that there might be directly competing relaxation pathways, where the cyclization event is sometimes favored. It is worth noting that these are gas-phase calculations, so the transition energies are not accounting for intermolecular interactions. In addition, the calculations are performed for one conformation, whereas the switch in reality can occupy a range of conformations in different solvent environments where switching may or may not be favored.

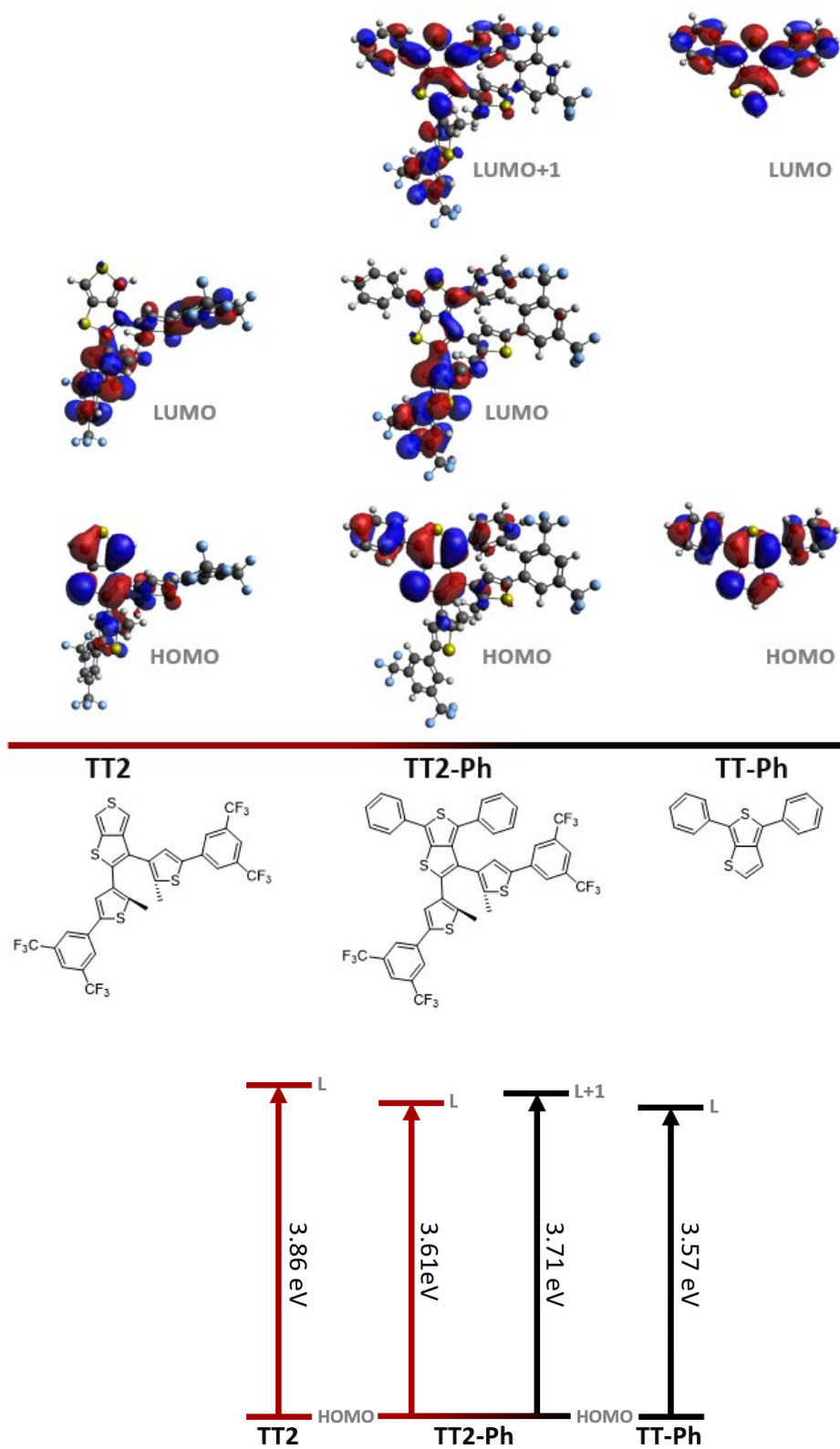


Figure 3.8 Frontier molecular orbital topologies for TT2, TT2-Ph, and TT-Ph, with the magnitudes of the energy of their corresponding transitions.

Following this new concept on switch behavior based on calculations, it appears that lowering the transition energy of the switching motif compared to the conjugated backbone should favor cyclization over fluorescence. For this, both the frontier molecular orbital topology *and* the transition energy of key transitions were interpreted. This removes the deception of having electron withdrawing substituents as in the case with **TT5**; while this switch had desirable orbital topologies, the key transition energies were unfavorable for switching. Several photochromes were screened, but the most ideal in terms of desirable energetics and synthetic tractability was found to be a terthiophene switching motif (**Figure 3.9**). The frontier molecular orbital topologies for this switch are completely ideal in that both the LUMO and the LUMO+1 are distributed exclusively over the diarylethene portion of the molecule. It is not until the LUMO+2 (not shown) that the surface topology begins to resemble the conjugated backbone portion of the molecule. Now the key transition energy corresponding to the switch is clearly favored over that of the phenyl-thiophene-phenyl portion of the molecule (3.31 eV versus 3.53 eV, respectively).

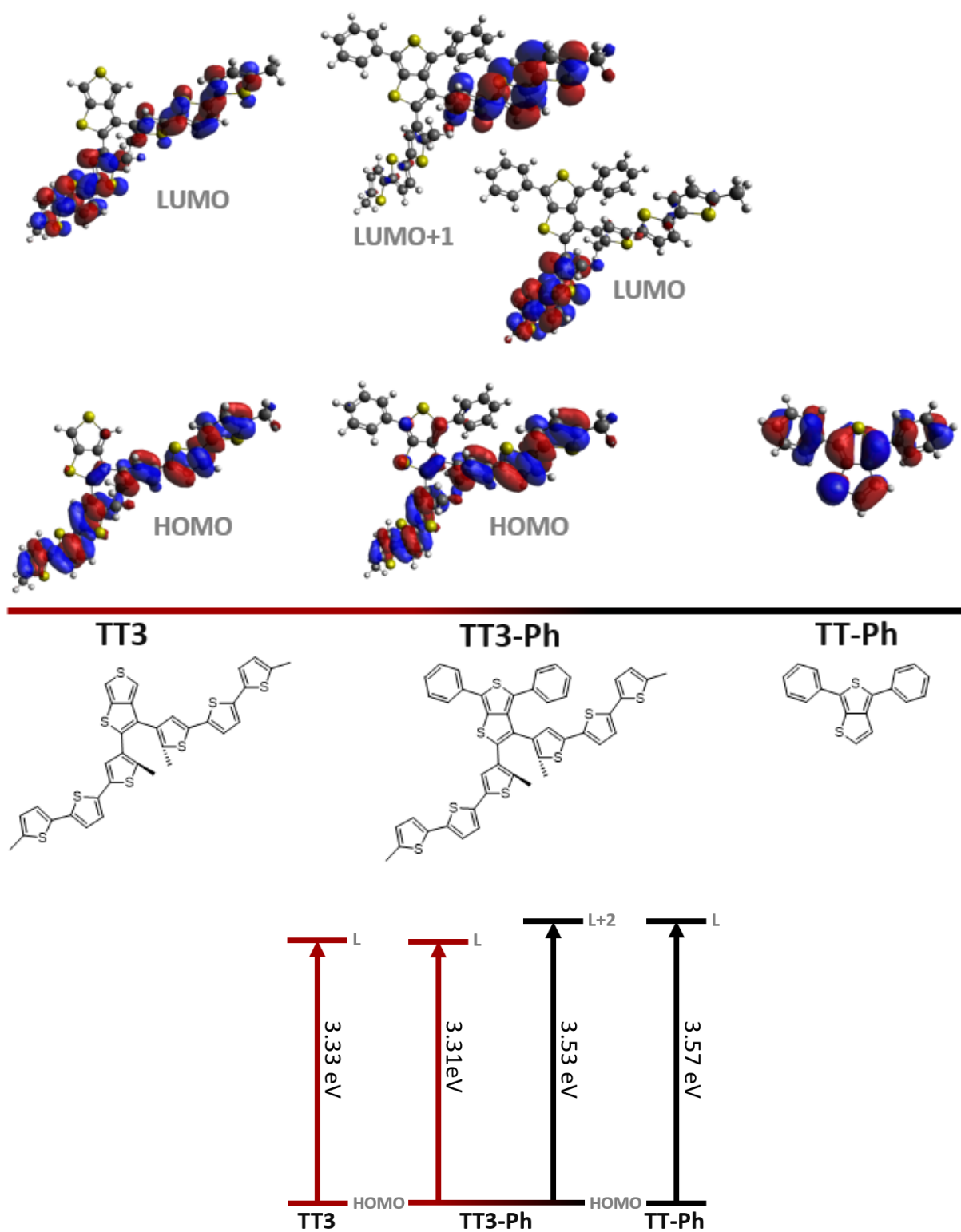
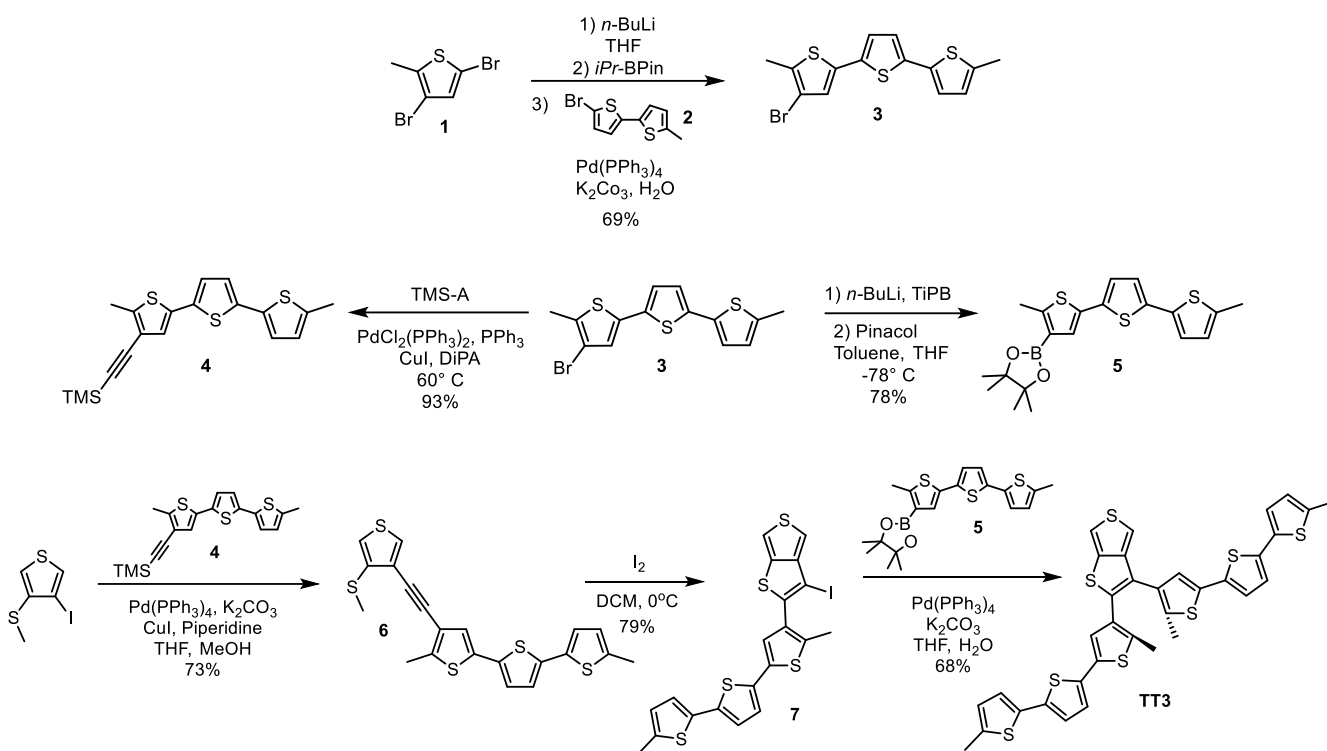


Figure 3.9 Frontier molecular orbital topologies for **TT3**, **TT3-Ph**, and **TT-Ph**, with the magnitudes of the energy of their corresponding transitions.

As with other switching components, the switching arm was synthesized first, starting with 2,4-dibromo-5-methylthiophene (**1**, **Scheme 3.11**). A one-pot transformation to **3** first involved lithium-halogen exchange of **1** at -78° C followed by quench with a borate to generate the 2-position boronate ester. The reaction was then warmed to room temperature, after which **2** was added in addition to standard Suzuki coupling reagents. Reflux resulted in the generation of **3** almost exclusively. Compound **3** was then split, where approximately half of the material was used for a sonogashira cross coupling to make **4**, whereas the other half was used to make another boronate ester. **4** was then coupled to the shared intermediate for **TT** switch synthesis via *in-situ* deprotected Sonogashira cross coupling. As with other **TT** intermediate featuring relatively electron-rich substrates, the cyclization upon addition of iodine was performed at 0° C to avoid double addition of the halogen across the triple bond. A final Suzuki coupling with boronate ester **5** to produce **TT3** in 68% yield. This switch was found to be fairly insoluble for purification via column chromatography. Fortunately, all impurities can be washed away with cold ether, leaving **TT3** as a pale green powder.



Scheme 3.11 Synthetic pathway towards the **TT3** photochromic switch core, constructed using a similar methodology to **TT1** and **TT2**.

The photochromic activity for **TT5** can be seen in **Figure 3.10**. It is particularly difficult to photobleach this compound in the solid state, so the compound must be dissolved first and bleached in solution. Major absorbance of the open form is still in the UV region ($\lambda_{\text{max}} = 363$ nm) but the absorption profile extends into the visible region ($\lambda_{\text{abs}} = 435$ nm), meaning that the cyclization between the open and closed form can be entirely controlled with visible light. The switch also reaches the photostationary state with a handheld UV lamp in under fifteen seconds with a 4 watt handheld UV lamp. Bleaching takes several minutes, however, though it is difficult to quantify due to variances in the intensity of the LED light source. Complete recovery of the open switch is accomplished with prolonged irradiation with no noticeable degradation in deaerated solutions for at least 10 cycles.

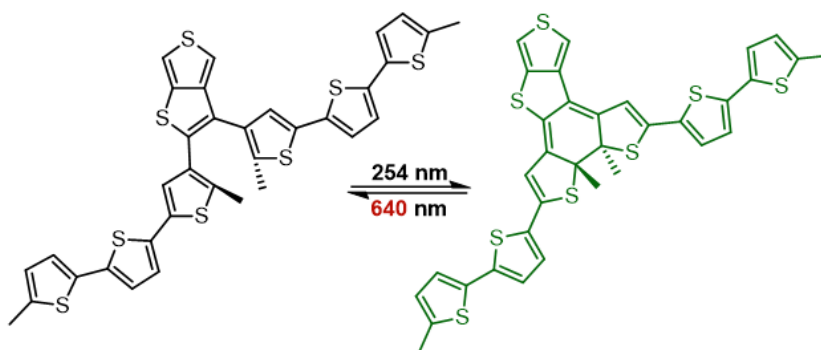
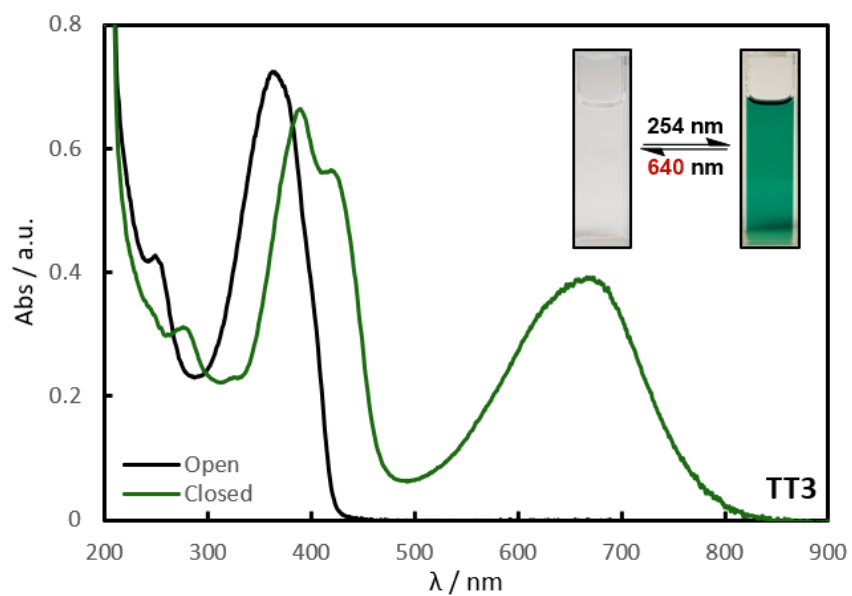


Figure 3.10 UV-Vis absorption spectra of the open and closed form of **TT3**, with the extended conjugation resulting in a deep green compound upon cyclization.

Bromination of **TT3** proved rather tricky, and did not result in full conversion to the di-halogenated species. Excess bromine could not be used, as the ten free β positions can also be halogenated. Similar solubility is seen for both the product, mono-halogenated, and di-halogenated species, meaning that flash chromatographic methods are fruitless for purification. In addition, the stability of the dibrominated species seems low. The crude material was thus pushed forward to the Stille cross coupling reactions with minimal purification beforehand. Luckily, the diphenylated and dithienylated product are substantially different in retention factor that the low solubility did not prevent isolation of the desirable species **TT3-Ph** and **TT3-Th**. The absorption profile for **TT3-Ph** features one major peak ($\lambda_{\text{abs}} = 365 \text{ nm}$). This differs from **TT1-Ph** and **TT2-Ph**, which both have two segregated peaks corresponding to the conjugated backbone and the switching motif. In the case of **TT3-Ph**, it appears that the absorption of these two regions are coincident, which is defended by the energetic similarities between the two competing regions. The switching activity for **TT3-Ph** is very strong compared to the analogous **TT1** and **TT2** switches, confirming this theoretical approach to switch design.

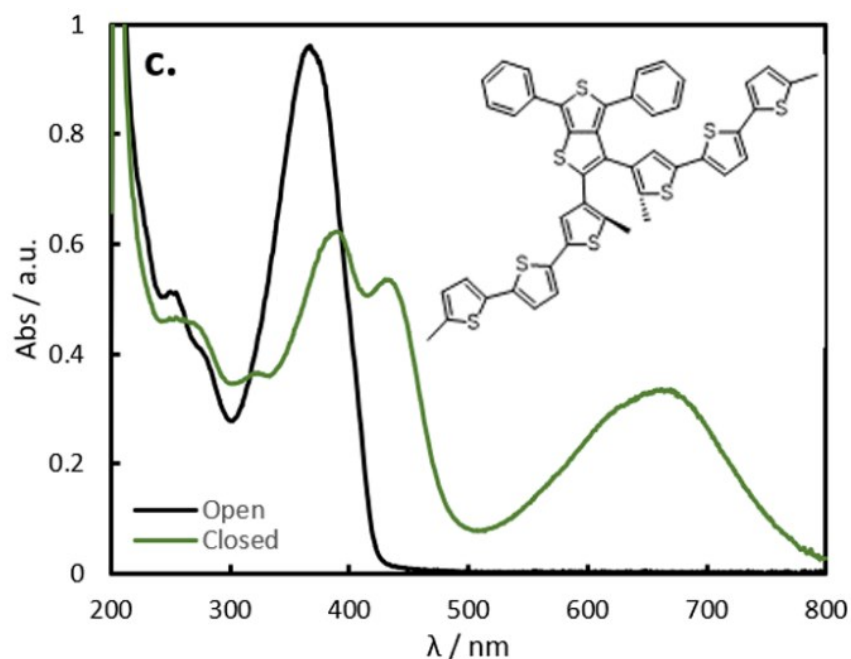
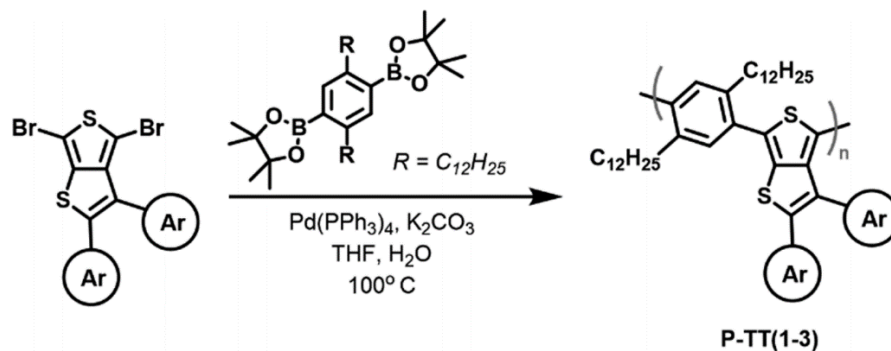


Figure 3.11 UV-Vis absorption of the open and closed π -extended switch **TT3-Ph**, where photochromic activity is restored compared to **TT1-Ph** and **TT2-Ph**.

While extended conjugation along the pendant aryl groups of the DAE restored photochromic function to **TT3-Ph**, this strategy likely cannot be generalized to the analogous polymers, where the longer effective conjugation pathway will typically have the lowest energy transition. Thus, we sought a different approach to distort the polymer backbone and interrupt this long-range conjugation, thus allowing in the pendant switch chromophore to remain the dominant lowest-energy transition. We prepared sterically congested polymers **P-TT1**, **P-TT2**, and **P-TT3** by way of Suzuki polycondensation with a dialkylated phenylene comonomer, where the alkyl groups were expected to provide enough backbone distortion to limit the effective conjugation length along the polymer (scheme **3.12**).



Scheme 3.12 General Suzuki polycondensation used in producing the sterically hindered pendant photochromic polymers **P-TT(1-3)**.

The absorption profiles (Figure 3.12) for these polymers are very similar to their analogous model compounds in which an absorbance band can be seen around ca. 375 nm, again attributed to the α -diphenylated thiophene (**TT-Ph**) segment. As in previous delocalized systems, **P-TT1** demonstrated no photoisomerization upon irradiation. The small degree of steric hindrance imposed on the polymer by the 2,5-dimethylthiophene units may not be enough to further interrupt extended conjugation along the polymer. Calculations also suggest that it only takes two planarized flanking benzenes around the **TT1** core to lead to inactivity. Both **P-TT2** and **P-TT3** were photochromic. The larger switching motifs in **P-TT2** and **P-TT3** lead to more congested systems that may not be able to accommodate a planarized backbone over multiple repeat units. While both experimental and computational results demonstrate that these two switch cores can tolerate local planarity of flanking benzene subunits and still respond productively to irradiation, the added steric congestion in **P-TT2** facilitated out-of-plane distortion, leading to a relatively stronger photochromic response. Analogous to an experiment performed by Kawai *et. al.*,¹ the GPC profiles for **P-TT2** and **P-TT3** were performed for both the bleached state and the irradiated photostationary state. There was no significant difference between the polymer molecular weights between the two isomeric forms, indicating no substantial polymer expansion or contraction following isomerization. Thus, we propose that

there is little to no conformational impact on the polymer backbone featuring pendant switching motifs compared to the more common main-chain counterparts.

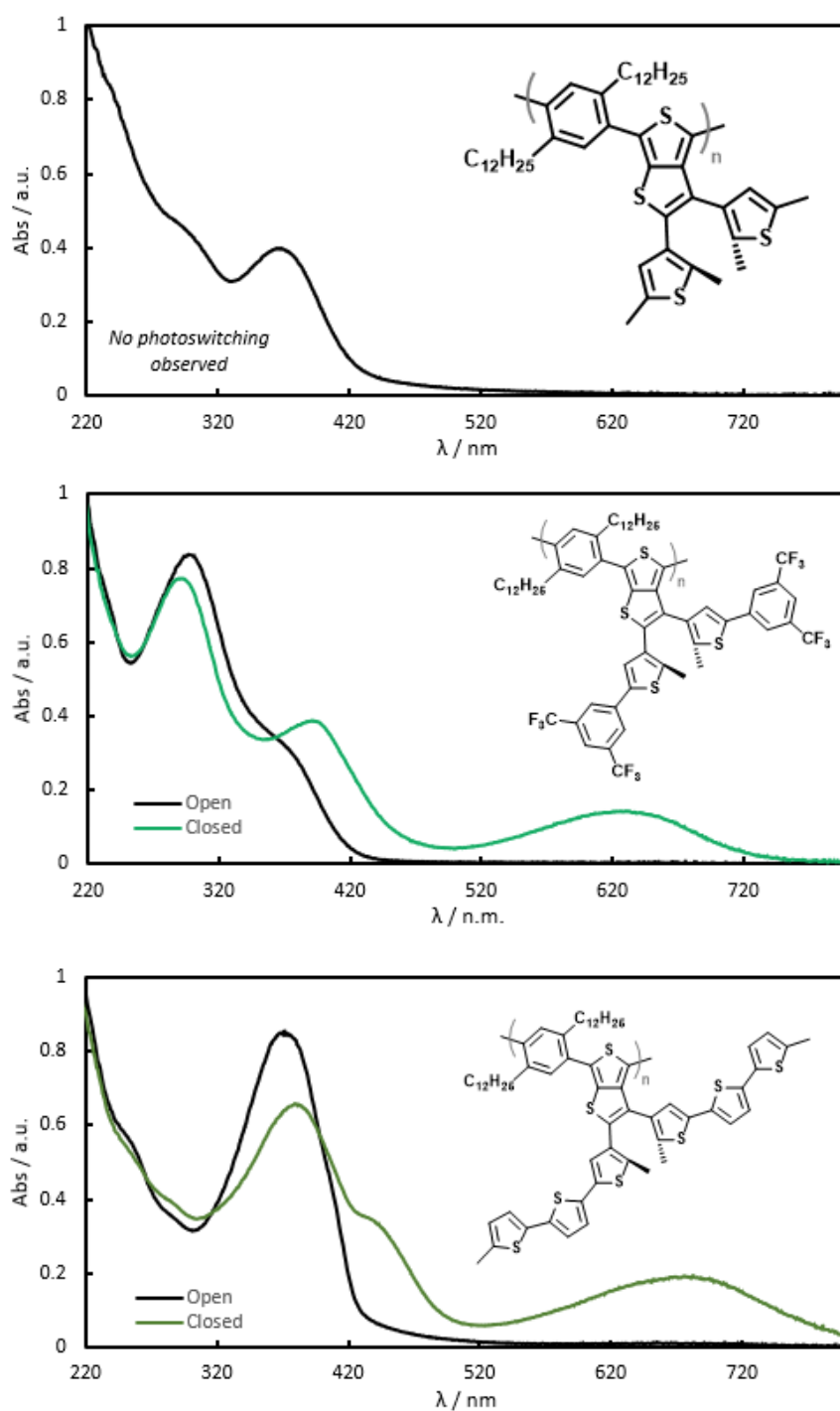


Figure 3.12 UV-Vis absorption spectra for the three sterically hindered pendant photochromic polymers **P-TT1**, **P-TT2**, and **P-TT3**.

Conclusion

Preliminary pendant photochromic polymers were photoresponsive, but not switchable in the traditional sense. The first conceptual insights based on density functional theory suggested that a donor-acceptor system demonstrated favorable frontier molecular orbital topologies in that there was significant surface distribution across the diarylethene portion. This led to the design and synthesis of **TT5**, a highly electron-deficient thiazole-based switch. Unfortunately, these polymers behaved similarly to the previous polymers developed. This simplistic idea was revised to account for favorable excited state transitions and their corresponding relaxation paths to the ground state. It was found that the switching event is in direct competition with fluorescence, but the substituents can be tuned to favor one or the other. Time-dependent density functional theory was utilized to analyze which switch architectures would favor an excited state that proceeded through the conical intersection associated with cyclization, leading to the development of **TT3**, which surpassed computational expectations. As extended conjugation on the diarylethene switching motif has limitations in length, this concept is not generally applicable to planar polymers where the conjugation length is extended over a relatively longer scale. Sterically hindered co-monomers were thus introduced to polymeric species to interrupt long-range conjugation along the polymer backbone, which restored photochromic activity and allowed for the realization of the first pendant photochromic conjugated polymers.

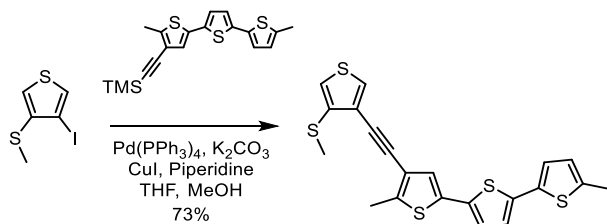
Experimental

General Information

5-(3,5-bis(trifluoromethyl)phenyl)-3-bromo-2-methylthiophene (**5**) was prepared according to the literature procedure.¹ Diethyl ether, toluene, and THF were purified using Innovative Technologies SPS-400-6 Solvent Purification System and further dried over Acros Organics 4Å molecular sieves prior to use. Dichloromethane was distilled prior to use. All other solvents and reagents were purchased from Sigma-Aldrich, Fisher Scientific, Alfa Aesar, or Oakwood Chemicals and used without further purification.

¹H NMR spectra were obtained on either a Bruker Avance 400 MHz Spectrometer or a Bruker Avance III 400 MHz Spectrometer, with residual protio-solvent resonances used as the internal standard (CHCl₃: 7.26 ppm, CHDCl₂: 5.32 ppm). Data are reported as: Chemical shift (multiplicity, integration, coupling constant). ¹³C NMR spectra were obtained on either a Bruker Avance 400 MHz Spectrometer (100 MHz) or a Bruker Avance III 400 MHz Spectrometer (100 MHz), with solvent resonances used as the internal standard (CDCl₃: 77.2 ppm). Data are reported as chemical shifts (ppm). High resolution mass spectrometry (HRMS) was performed on a VG-70SE Magnetic Sector Mass Spectrometer. UV-Vis data were collected on a Cary 50 Bio UV-Vis Spectrophotometer. Gel permeation chromatography was performed on an Agilent 1260 Infinity Series (degasser, iso pump, TCC, DAD) using unstabilized THF at 40° C vs. Agilent EasiVial PS-M polystyrene standards. Ultraviolet light source for switching experiments was an Analytikjena UVP UVGL-25 254/365 nm 4 Watt handheld lamp. Visible light sources are Luxeon Rebel LEDs on SinkPAD-II 20mm. Flash Chromatography was performed under manual air pressure on silica (SiO₂, 40-63 μm, 230-400 mesh).

5,5''-dimethyl-4-((4-(methylthio)thiophen-3-yl)ethynyl)-2,2':5',2''-terthiophene (3c)

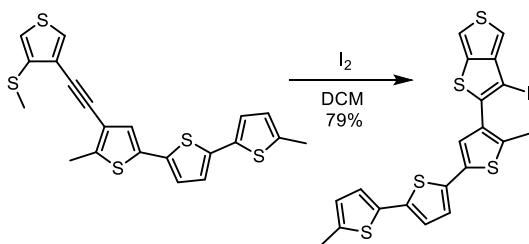


3-iodo-4-(methylthio)thiophene (**2**) (38 mg, 0.15 mmol), ((5,5''-dimethyl-[2,2':5',2''-terthiophen]-4-yl)ethynyl)trimethylsilane (**11**) (55 mg, 0.15 mmol), and potassium carbonate (46 mg, 0.33 mmol) were added to THF (12 mL), and the solution was sparged with N₂ for 15 min. Then, copper(I) iodide (1 mg, 4 μmol) and Pd(PPh₃)₄ (9 mg, 8 μmol) were added under increased N₂ flow, followed by a degassed solution of piperidine (0.15 mL, 1.5 mmol) in methanol (2 mL). The reaction mixture was refluxed at 70° C for 22 h. The solution allowed to cool to room temperature and then washed twice with 10 mL sat. NH₄Cl, once with 10 mL brine, and dried

over MgSO₄ before concentrating under reduced pressure. Purification of the orange oil by column chromatography (silica, 95:5 hexanes:DCM) afforded compound **3c** (47 mg, 0.11 mmol, 73%) as a clear colorless oil.

¹H NMR (400 MHz, CD₂Cl₂): δ 7.53 (s, 1H), 7.31 (s, 1H), 7.06 (s, 1H), 6.99 (s, 2H), 6.87 (s, 1H), 6.66 (s, 1H), 2.58 (s, 3H), 2.49 (s, 3H), 2.45 (s, 3H). **¹³C (¹H) NMR (100 MHz, CDCl₃):** δ 142.9, 139.4, 136.7, 134.9, 134.7, 133.4, 129.0, 126.0, 125.3, 124.1, 123.7, 123.5, 122.9, 120.3, 118.3, 86.9, 85, 16.8, 15.4, 14.7. **HRMS (EI):** found m/z : 427.9847; calc. for C₂₁H₁₆S₅: 427.9856.

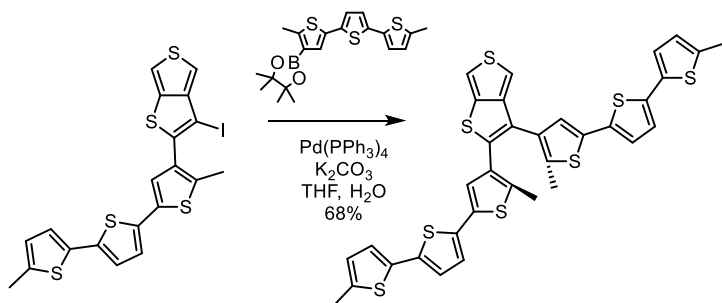
2-(5,5''-dimethyl-[2,2':5',2''-terthiophen]-4-yl)-3-iodothieno[3,4-b]thiophene (4c)



5,5''-dimethyl-4-((4-(methylthio)thiophen-3-yl)ethynyl)-2,2':5',2''-terthiophene (**3c**) (29 mg, 0.070 mmol) was added to 5 mL DCM, and cooled to 0° C. A solution of iodine (17 mg, 0.070 mmol) in DCM (5 mL) was then added dropwise and stirred until the starting material was consumed, as monitored by TLC. The solution was diluted with 10 mL diethyl ether, washed once with 15 mL sat. Na₂S₂O₃, once with 15 mL brine, and dried over MgSO₄ before concentrating under reduced pressure. Purification by column chromatography (90:10 hexanes:DCM) afforded compound **4c** (32 mg, 0.06 mmol, 85%) as a white solid.

¹H NMR (400 MHz, CD₂Cl₂): δ 7.44 (d, 1H, 2.8 Hz), 7.38 (d, 1H, 2.8 Hz), 7.11 (s, 1H), 7.05 (d, 1H, 3.8 Hz), 7.01 (d, 1H, 3.7 Hz), 6.98 (d, 1H, 3.7 Hz), 6.69 (d, 1H, 3.8 Hz), 2.48 (s, 3H), 2.47 (s, 3H). **¹³C (¹H) NMR (100 MHz, CDCl₃):** δ 150.3, 142.5, 139.4, 138.2, 136.8, 136.4, 135.0, 134.7, 133.8, 132.4, 126.0, 124.9, 124.2, 123.7, 123.5, 114.9, 112.1, 72.1, 15.4, 14.9. **HRMS (EI):** found m/z : 539.8669; calc. for C₂₀H₁₃IS₅: 539.8665.

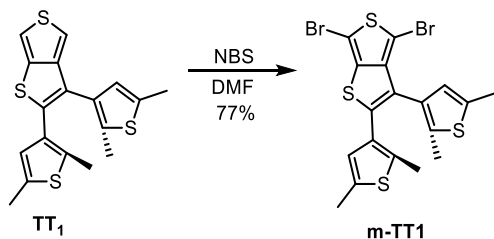
2,3-bis(5,5''-dimethyl-[2,2':5',2''-terthiophen]-4-yl)thieno[3,4-b]thiophene (TT3)



2-(5,5''-dimethyl-[2,2':5',2''-terthiophen]-4-yl)-3-iodothieno[3,4-b]thiophene (**4c**) (50. mg, 0.090 mmol) and 2-(5,5''-dimethyl-[2,2':5',2''-terthiophen]-4-yl)-4,4,5,5-tetramethyl-1,3,2-dioxaborolane (**12**) (38 mg, 0.094 mmol) were added to THF (6 mL) and sat. K₂CO₃ solution (2 mL), and the solution was subjected to three freeze-pump-thaw cycles. Pd(PPh₃)₄ (5 mg, 5 μmol) was added under increased N₂ flow, and the solution was refluxed at 100° C for 20 h. The reaction mixture was then cooled to room temperature and diluted with 10 mL of diethyl ether, washed twice with 20 mL of DI H₂O, once with 20 mL brine, and dried over MgSO₄ before concentrating under reduced pressure. Purification by column chromatography (silica, 90:10 hexanes:DCM) afforded **TT3** (42 mg, 0.060 mmol, 68%) as a pale green solid.

¹H NMR (400 MHz, CD₂Cl₂): δ 7.33 (d, 1H, 2.7 Hz), 7.29 (d, 1H, 2.7 Hz), 7.13 (s, 1H), 7.00 (m, 7H), 6.67 (m, 2H), 2.47 (s, 6H), 2.17 (s, 3H), 2.07 (s, 3H). **¹³C (¹H) NMR (100 MHz, CDCl₃):** δ 148.5, 139.6, 139.4, 139.3, 137.1, 136.8, 136.7, 136.5, 135.9, 135.6, 135.1, 134.8, 134.7, 133.9, 133.8, 132.6, 132.3, 126.0, 124.9, 124.5, 123.9, 123.8, 123.6, 123.6, 123.5, 123.0, 112.7, 110.9, 15.4, 14.4, 14.3 **HRMS (EI):** found *m/z*: 687.9637; calc. for C₃₄H₂₄S₈: 687.9644.

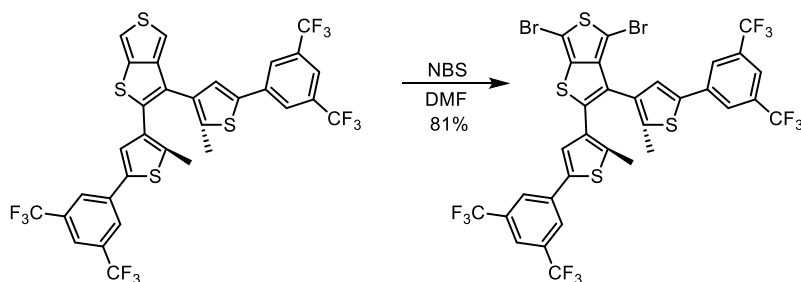
4,6-dibromo-2,3-bis(2,5-dimethylthiophen-3-yl)thieno[3,4-b]thiophene (TT1-Br)



2,3-bis(2,5-dimethylthiophen-3-yl)thieno[3,4-b]thiophene (**TT1**) (200. mg, 0.550 mmol) was added to 20 mL DMF, and the solution was cooled to 0° C. NBS (198 mg, 1.11 mmol) was added in one portion, and the reaction mixture was allowed to come to room temperature over 4 h in the dark. The solution was then diluted with 25 of diethyl ether, washed twice with 20 mL sat NH₄Cl, once with 20 mL brine and dried over MgSO₄ before concentrating under reduced pressure. Purification of the crude tacky solid by column chromatography (silica, 90:10 hexanes:DCM) afforded **TT1-Br** as a white powder (220 mg, 0.42 mmol, 77%).

¹H NMR (400 MHz, CDCl₃): δ 6.45 (s, 1H), 6.38 (s, 1H), 2.39 (s,3H), 2.33 (s, 3H), 2.18 (s, 3H), 2.02 (s,3H). **¹³C (¹H) NMR (100 MHz, CDCl₃):** δ 144.4, 142.4, 139.5, 136.1, 135.9, 135.6, 134.9, 130.4, 129.3, 128.1, 126.9, 124.6, 97.9, 96.2, 15.4, 15.2, 14.4, 14.1. **HRMS (EI):** found m/z : 515.8353; calc. for C₁₈H₁₄Br₂S₄: 515.8345.

2,3-bis(5-(3,5-bis(trifluoromethyl)phenyl)-2-methylthiophen-3-yl)-4,6-dibromothiopheno[3,4-b]thiophene (TT2-Br)

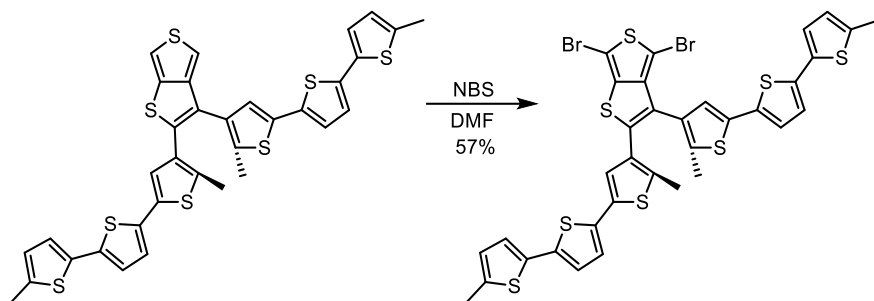


2,3-bis(5-(3,5-bis(trifluoromethyl)phenyl)-2-methylthiophen-3-yl)thieno[3,4-b]thiophene (**TT2**) (100. mg, 0.130 mmol) was added to 15 mL DMF, and the solution was cooled to 0° C. NBS (47 mg, 0.26 mmol) was added in one portion, and the reaction mixture was allowed to come to room temperature over 6 h in the dark. The solution was then diluted with 10 mL of diethyl ether, washed twice with 20 mL sat NH₄Cl, once with 20 mL brine and dried over MgSO₄ before concentrating under reduced pressure. Purification of the crude tacky solid by column chromatography (silica, 90:10 hexanes:DCM) afforded **TT2-Br** as a white powder (98 mg, 0.11 mmol, 81%).

¹H NMR (400 MHz, CDCl₃): δ 7.91 (s, 2H), 7.75 (s, 2H), 7.73 (s, 1H), 7.71 (s, 1H), 7.31 (s, 1H), 7.04 (s, 1H). **¹³C (¹H) NMR (100 MHz, CDCl₃):** δ 143.7, 141.7, 140.6, 140.5, 139.1, 137.3, 136.8, 136.2, 135.8, 132.7, 132.7, 132.4, 132.1, 131.5, 128.0, 126.8, 125.3, 125.1, 124.1, 98.7, 97.2, 14.9, 14.4. **HRMS (EI):** found m/z : 911.8131; calc. for C₃₂H₁₄Br₂F₁₂S₄: 911.8153.

4,6-dibromo-2,3-bis(5,5''-dimethyl-[2,2':5',2''-terthiophen]-4-yl)thieno[3,4-b]thiophene

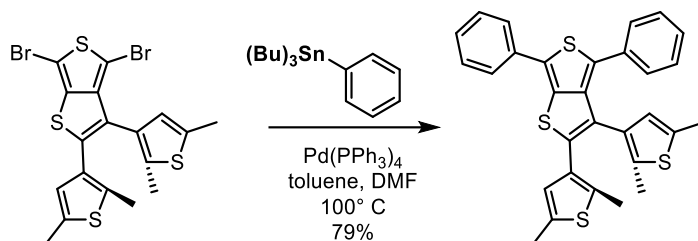
(TT3-Br)



2,3-bis(5,5''-dimethyl-[2,2':5',2''-terthiophen]-4-yl)thieno[3,4-b]thiophene (**TT3**) (20. mg, 29 μ mol) was added to 10 mL DMF, and the solution was cooled to 0° C. NBS (14 mg, 80. μ mol) was added dropwise until the starting material was consumed, as monitored by TLC. The solution was then diluted with 20 mL diethyl ether, washed twice with 20 mL sat NH_4Cl , once with 20 mL brine and dried over MgSO_4 before concentrating under reduced pressure. Purification by column chromatography (95:5 to 90:10 hexanes:DCM) afforded **TT3-Br** (14 g, 17 μ mol, 57%) as a white solid.

^1H NMR (400 MHz, CD_2Cl_2): δ 6.93-6.83 (m, 7H), 6.78 (s, 1H), 6.59 (d, 1H, 3.5 Hz), 6.56 (d, 1H, 3.5 Hz), 2.39 (s, 3H), 2.37 (s, 3H), 2.26 (s, 3H), 2.03 (s, 3H). **^{13}C (^1H) NMR (100 MHz, CDCl_3):** δ 143.9, 141.9, 139.4, 139.3, 139.2, 137.5, 137.4, 136.8, 136.4, 135.7, 134.9, 134.8, 134.7, 133.7, 132.9, 131.2, 130.24, 129.8, 126.3, 126.0, 124.9, 124.2, 124.0, 123.7, 123.6, 123.5, 123.5, 98.3, 96.6, 15.4, 15.4, 14.6, 14.1. **HRMS (EI):** found m/z : 843.7862; calc. for $\text{C}_{34}\text{H}_{22}\text{Br}_2\text{S}_8$: 843.7854.

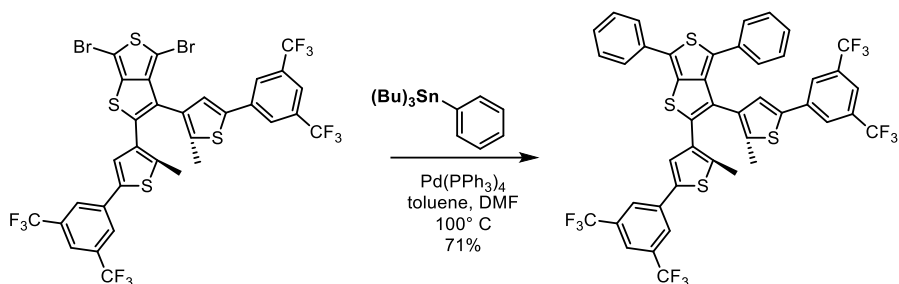
2,3-bis(2,5-dimethylthiophen-3-yl)-4,6-diphenylthieno[3,4-b]thiophene (TT1-Ph)



4,6-dibromo-2,3-bis(2,5-dimethylthiophen-3-yl)thieno[3,4-b]thiophene (**TT1-Br**) (30. mg, 0.060 mmol) and Pd(PPh₃)₄ (4 mg, 3 μmol) were added to a Schlenk flask, which was then evacuated and backfilled with N₂ three times. tributyl(phenyl)stannane (51 mg, 0.14 mmol), dry and degassed toluene (4 mL) and DMF (1 mL) were added, and the reaction mixture was stirred at 100° C for 16 h. The solution was then cooled to room temperature and diluted with 20 mL of diethyl ether, washed twice with 20 mL sat NH₄Cl, once with 20 mL brine and dried over MgSO₄ before concentrating under reduced pressure. Purification by column chromatography (silica, 90:10 hexanes:DCM) afforded **TT1-Ph** (23 mg, 0.050 mmol, 79%) as a yellow solid.

¹H NMR (400 MHz, CD₂Cl₂): δ 7.73 (d, 2H, 8.5 Hz), 7.48 (t, 2H, 7.5 Hz), 7.30 (t, 1H, 7.5 Hz), 7.13 (m, 6H), 6.51 (s, 1H), 6.3 (s, 1H), 2.35 (s, 3H), 2.13 (s, 3H), 2.11 (s, 3H), 1.80 (s, 3H). **¹³C**
(¹H) NMR (100 MHz, CDCl₃): δ 143.2, 140.1, 135.6, 135.4, 134.8, 134.2, 134.0, 133.7, 132.9, 131.6, 131.1, 131.0, 129.4, 129.1, 127.5, 127.4, 127.1, 127.0, 126.9, 125.7, 124.6, 77.2, 15.1, 14.8, 14.2, 13.6. **HRMS (EI):** found *m/z*: 512.0769; calc. for C₃₀H₂₄S₄: 512.0761.

2,3-bis(5-(3,5-bis(trifluoromethyl)phenyl)-2-methylthiophen-3-yl)-4,6-diphenylthieno[3,4-b]thiophene (TT2-Ph)

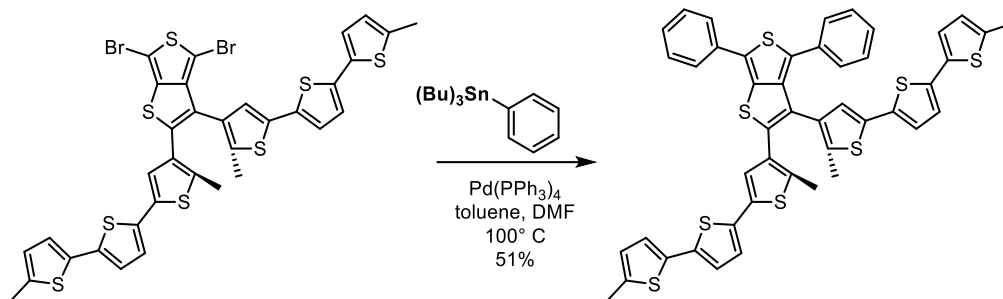


2,3-bis(5-(3,5-bis(trifluoromethyl)phenyl)-2-methylthiophen-3-yl)-4,6-dibromothiopheno[3,4-b]thiophene (**TT2-Br**) (30. mg, 0.030 mmol) and Pd(PPh₃)₄ (2 mg, 2 μmol) were added to a Schlenk flask, which was then evacuated and backfilled with N₂ three times. tributyl(phenyl)stannane (29 mg, 0.070 mmol), dry and degassed toluene (4 mL) and DMF (1 mL) were added, and the reaction mixture was stirred at 100° C for 20 h. The solution was then cooled to room temperature and diluted with 20 mL of diethyl ether, washed twice with 20 mL sat NH₄Cl, once with 20 mL brine and dried over MgSO₄ before concentrating under reduced pressure. Purification by column chromatography (silica, 90:10 hexanes:DCM) afforded **TT2-Ph** (21 mg, 0.02 mmol, 71%) as a yellow solid.

¹H NMR (400 MHz, CDCl₃): δ 7.80 (s, 2H), 7.76 (d, 2H, 8.6 Hz), 7.72 (s, 1H), 7.68 (s, 1H), 7.50 (t, 2H, 7.5 Hz), 7.44 (s, 2H), 7.34 (t, 1H, 7.5 Hz), 7.19 (d, 2H, 8.6 Hz), 7.13 (t, 2H, 7.3 Hz), 7.12 (s, 1H), 7.04 (t, 1H, 7.3 Hz), 6.67 (s, 1H), 2.33 (s, 3H), 2.02 (s, 3H). **¹³C (¹H) NMR (100 MHz, CDCl₃):** δ 142.8, 140.0, 139.6, 138.9, 137.2, 136.5, 136.3, 136.1, 133.9, 133.5, 133.1, 133.0, 132.9, 132.7, 132.4, 132.3, 132.2, 132.0, 129.7, 129.4, 128.5, 128.3, 127.9, 127.9, 127.4, 127.2, 126.0, 125.7, 125.6, 125.4, 124.7, 124.7, 124.1, 122.0, 120.9, 15.0, 14.22 **HRMS (EI):** found *m/z*: 908.0571; calc. for C₄₄H₂₄F₁₂S₄: 908.0569.

2,3-bis(5,5''-dimethyl-[2,2':5',2''-terthiophen]-4-yl)-4,6-diphenylthieno[3,4-b]thiophene

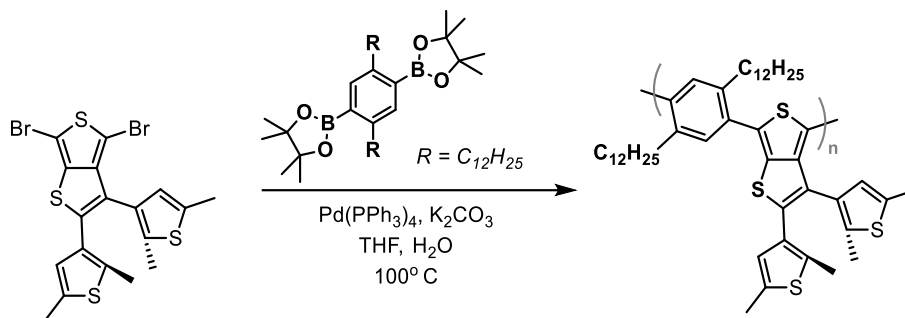
(TT3-Ph)



4,6-dibromo-2,3-bis(5,5''-dimethyl-[2,2':5',2''-terthiophen]-4-yl)thieno[3,4-b]thiophene (**TT3-Br**) (10. mg, 0.010 mmol) and Pd(PPh₃)₄ (1 mg, 1 μmol) were added to a Schlenk flask, which was then evacuated and backfilled with N₂ three times. tributyl(phenyl)stannane (12 mg, 0.030 mmol), dry and degassed toluene (4 mL) and DMF (1 mL) were added, and the reaction mixture was stirred at 100° C for 16 h. The solution was then diluted with 20 mL of diethyl ether, washed twice with 20 mL sat NH₄Cl, once with 20 mL brine and dried over MgSO₄ before concentrating under reduced pressure. Purification by column chromatography (silica, 90:10 hexanes:DCM) afforded **TT2-Ph** (5 mg, 6 mmol, 51%) as a yellow solid.

¹H NMR (400 MHz, CD₂Cl₂): δ 7.76 (d, 2H, 8.4 Hz), 7.50 (t, 2H, 7.5 Hz), 7.33 (t, 1H, 7.0 Hz), 7.15 (m, 5H), 6.94 (m, 6H), 6.76 (d, 1H, 3.8 Hz), 6.66 (m, 2H), 6.52 (s, 1H), 2.47 (s, 3H), 2.46 (s, 3H), 2.26 (s, 3H), 1.92 (s, 3H). **¹³C (¹H) NMR (100 MHz, CDCl₃):** δ 142.9, 139.9, 139.5, 139.3, 137.2, 136.8, 136.4, 136.3, 135.8, 135.4, 135.1, 134.9, 134.2, 133.7, 133.7, 133.6, 132.9, 132.8, 132.7, 132.4, 132.3, 132.2, 132.1, 129.5, 129.3, 127.9, 127.8, 127.7, 127.2, 126.2, 126.1, 125.9, 125.6, 125.4, 124.5, 124.1, 123.9, 123.8, 123.77, 123.73, 123.6, 123.57, 123.52. **HRMS (EI):** found *m/z*: 840.0281; calc. for C₄₀H₃₂S₈: 840.0270.

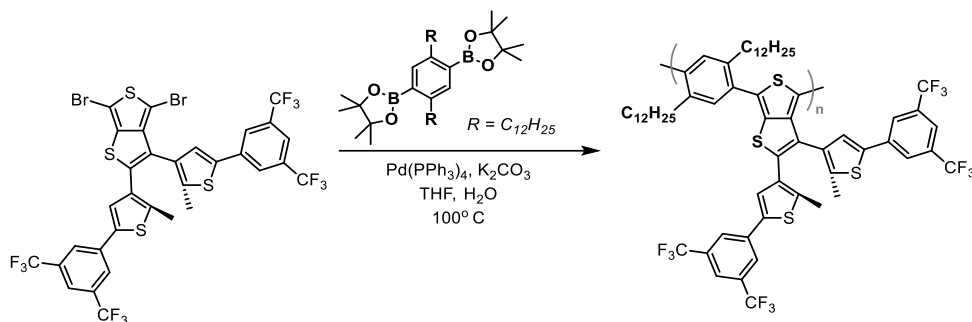
P-TT1



4,6-dibromo-2,3-bis(2,5-dimethylthiophen-3-yl)thieno[3,4-b]thiophene (**TT1-Br**) (16 mg, 0.030 mmol) and 2,2'-(2,5-didodecyl-1,4-phenylene)bis(4,4,5,5-tetramethyl-1,3,2-dioxaborolane) (**12**) (20. mg, 0.030 mmol) were added to THF (6 mL) and sat. K_2CO_3 solution (2.5 mL), and the solution was subjected to three freeze-pump-thaw cycles. $Pd(PPh_3)_4$ (2 mg, 2 μ mol) was added under increased N_2 flow, and the solution was refluxed at $100^\circ C$ for 72 h. The aqueous layer was removed, and the organic layer was concentrated to approximately 0.5 mL before being rapidly added to 50 mL MeOH. The precipitate was collected by filtration, and was purified by Soxhlet extraction: methanol (24 h), acetone (24 h), chloroform (2 h). The chloroform extract was concentrated and precipitated with 50 mL MeOH. Filtration yielded **P-TT1** as an off-white solid.

1H NMR (400 MHz, $CDCl_3$): δ 7.47-6.34 (m), 4.14-3.19 (m), 2.52-0.70 (m).

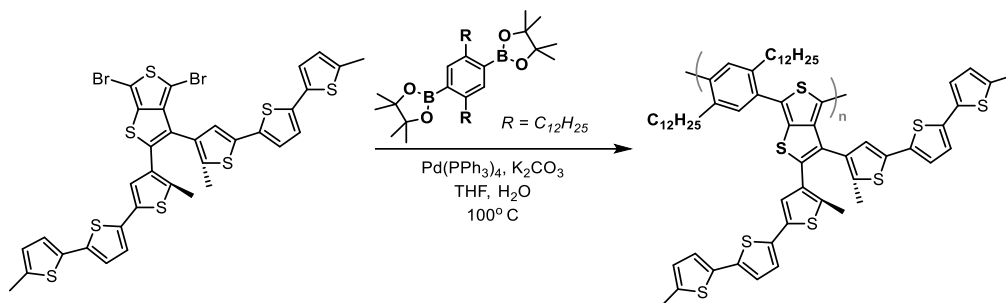
P-TT2



2,3-bis(5-(3,5-bis(trifluoromethyl)phenyl)-2-methylthiophen-3-yl)-4,6-dibromothiophene (**TT2-Br**) (60. mg, 0.070 mmol) and 2,2'-(2,5-didodecyl-1,4-phenylene)bis(4,4,5,5-tetramethyl-1,3,2-dioxaborolane) (**12**) (44 mg, 0.070 mmol) were added to THF (6 mL) and sat. K_2CO_3 solution (2.5 mL), and the solution was subjected to three freeze-pump-thaw cycles. $\text{Pd(PPh}_3)_4$ (4 mg, 3 μmol) was added under increased N_2 flow, and the solution was refluxed at 100°C for 72 h. The aqueous layer was removed, and the organic layer was concentrated to approximately 1.0 mL before being rapidly added to 100 mL MeOH. The precipitate was collected by filtration, and was purified by Soxhlet extraction: methanol (24 h) and acetone (24 h). The acetone extract was concentrated and precipitated with 50 mL MeOH. Filtration yielded **P-TT2** as an off-white solid.

$^1\text{H NMR}$ (400 MHz, CDCl_3): δ 7.97-6.85 (m), 4.19-3.36 (m), 2.52-0.70 (m).

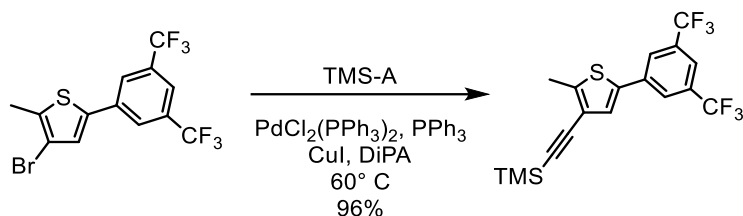
P-TT3



4,6-dibromo-2,3-bis(5,5''-dimethyl-[2,2':5',2'']-terthiophen)-4-ylthieno[3,4-b]thiophene (**TT3-Br**) (19 mg, 0.020 mmol) and 2,2'-(2,5-didodecyl-1,4-phenylene)bis(4,4,5,5-tetramethyl-1,3,2-dioxaborolane) (**12**) (15 mg, 0.020 mmol) were added to THF (6 mL) and sat. K_2CO_3 solution (2.5 mL), and the solution was subjected to three freeze-pump-thaw cycles. $\text{Pd}(\text{PPh}_3)_4$ (2 mg, 2 μmol) was added under increased N_2 flow, and the solution was refluxed at 100°C for 72 h. The aqueous layer was removed, and the organic layer was concentrated to approximately 0.5 mL before being rapidly added to 50 mL MeOH. The precipitate was collected by filtration, and was purified by Soxhlet extraction: methanol (24 h), acetone (24 h), chloroform (6 h). The chloroform extract was concentrated and precipitated with 50 mL MeOH. Filtration yielded **P-TT3** as an off-white solid.

^1H NMR (400 MHz, CDCl_3): δ 7.79-6.42 (m), 3.06-1.79 (m), 1.44-0.70 (m).

((5-(3,5-bis(trifluoromethyl)phenyl)-2-methylthiophen-3-yl)ethynyl)trimethylsilane



To a Schlenk tube were added 5-(3,5-bis(trifluoromethyl)phenyl)-3-bromo-2-methylthiophene (**5**) (1.0 g, 2.56 mmol), $\text{PdCl}_2(\text{PPh}_3)_2$ (90 mg, 0.13 mmol), triphenylphosphine (67 mg, 0.26 mmol), and copper (I) iodide (49 mg, 0.26 mmol), and the flask was evacuated and backfilled with N_2 three times. An anhydrous, degassed solution of trimethylsilyl acetylene (379 mg, 3.85 mmol) in diisopropylamine (50 mL) was added, and the solution was heated to 60°C for 12 h. The reaction mixture was then cooled to room temperature, filtered through a silica plug using diethyl ether as the eluent, and concentrated under reduced pressure. Purification of the crude oil by column chromatography (silica, 80:20 hexanes:DCM) afforded compound **6** (1.00 g, 2.47 mmol, 96%) as a white solid.

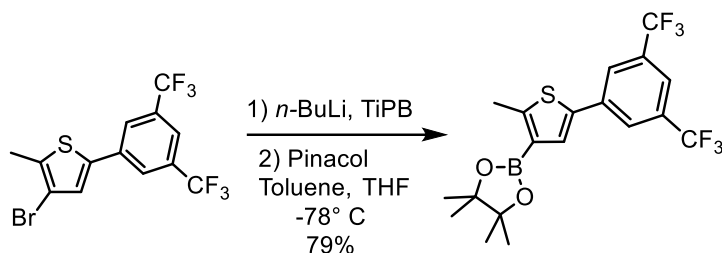
^1H NMR (400 MHz, CDCl_3): δ 7.90 (s, 2H), 7.74 (s, 1H), 7.34 (s, 1H), 2.57 (s, 3H), 0.26 (s, 9H).

^{13}C (^1H) NMR (100 MHz, CDCl_3): δ 150.8, 150.7, 146.3, 136.6, 136.1, 132.6, 132.3, 127.7,

125.3, 121.9, 98.7, 97.7, 14.0, 0.2. HRMS (EI): found m/z : 406.0640; calc. for $\text{C}_{18}\text{H}_{16}\text{F}_6\text{SSi}$:

406.0646.

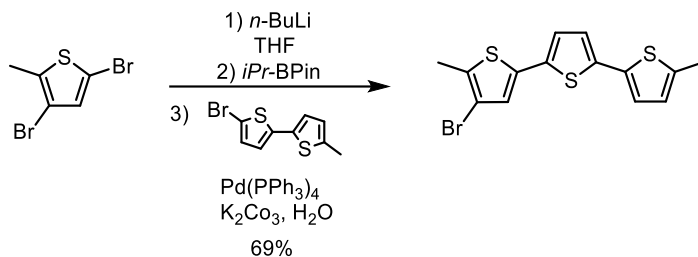
2-(5-(3,5-bis(trifluoromethyl)phenyl)-2-methylthiophen-3-yl)-4,4,5,5-tetramethyl-1,3,2-dioxaborolane



5-(3,5-bis(trifluoromethyl)phenyl)-3-bromo-2-methylthiophene (**5**) (2.00 g, 5.13 mmol) and triisopropyl borate (1.16 g, 6.17 mmol) were added to an anhydrous solution of toluene (5 mL) and THF (20 mL), and *n*-BuLi (3.70 mL, 1.67 M in hexanes) was added dropwise at -78° C. Then pinacol (729 mg, 6.17 mmol) was added in one portion, and the solution was allowed to slowly come to room temperature over 5 h. The reaction mixture was diluted with 25 mL of diethyl ether, washed twice with 30 mL of DI H₂O, once with 30 mL brine, and dried over MgSO₄ before concentrating under reduced pressure. Purification of the light brown solid by column chromatography (silica, 80:20 hexanes:DCM) afforded compound **7** as a white powder (1.76 g, 4.03 mmol, 79%).

¹H NMR (400 MHz, CDCl₃): δ 7.95 (s, 2H), 7.69 (s, 1H), 7.55 (s, 1H), 2.72 (s, 3H), 1.35 (s, 12H). **¹³C (¹H) NMR (100 MHz, CDCl₃):** δ 154.8, 137.5, 136.7, 132.3 (q, 2C, ²J_{C-F} = 33.5 Hz), 131.4, 125.4, 123.5 (q, 2C, ¹J_{C-F} = 272.3 Hz), 120.2, 83.8, 25.1, 16.2. **HRMS (EI):** found *m/z*: 436.1099; calc. for C₁₉H₁₉BF₆O₂S: 436.1103.

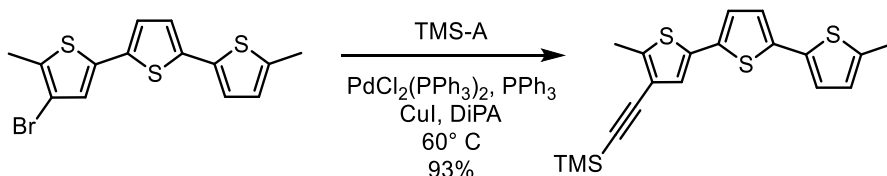
4-bromo-5,5''-dimethyl-2,2':5',2''-terthiophene



3,5-dibromo-2-methylthiophene (**8**) (494 mg, 1.93 mmol) was added to anhydrous THF (8 mL), and $n\text{-BuLi}$ (0.76 mL, 2.68 M in hexanes) was added dropwise at -78°C , and the solution was allowed to stir at this temperature for 1 h. 2-isopropoxy-4,4,5,5-tetramethyl-1,3,2-dioxaborolane (377 mg, 2.03 mmol) was added dropwise over 5 min, and the solution was allowed to slowly come to room temperature over 2 h. Then 5-bromo-5'-methyl-2,2'-bithiophene (**9**) (500. mg, 1.93 mmol), $\text{Pd(PPh}_3)_4$ (67 mg, 58 μmol), and degassed DI H_2O (2 mL) were added, and the solution was refluxed at 80°C for 12 h. The reaction mixture was diluted with 20 mL of diethyl ether, washed twice with 30 mL of DI H_2O , once with 30 mL brine, and dried over MgSO_4 before concentrating under reduced pressure. Purification of the off-white solid by column chromatography (silica, 80:20 hexanes:DCM) afforded compound **10** as a white solid (473 mg, 1.33 mmol, 69%). It is worth noting that the compound is photochromic on the column, and that it should be wrapped with aluminum foil since the open and closed form do not share the same retention factor values.

$^1\text{H NMR}$ (400 MHz, CD_2Cl_2): δ 7.95 (s, 2H), 7.69 (s, 1H), 7.55 (s, 1H), 2.72 (s, 3H), 1.35 (s, 12H). ^{13}C (^1H) NMR (100 MHz, CDCl_3): δ 139.7, 137.2, 134.7, 134.6, 134.5, 133.2, 126.2, 125.8, 124.3, 123.9, 123.7, 109.8, 15.5, 14.9. HRMS (EI): found m/z : 372.0496; calc. for $\text{C}_{19}\text{H}_{20}\text{S}_3$: 372.0493.

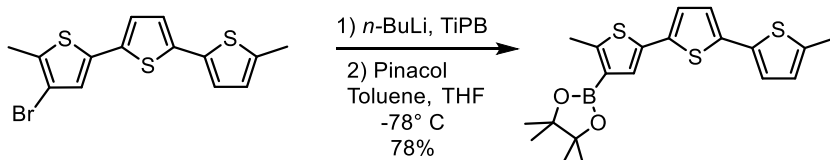
2-(5,5''-dimethyl-[2,2':5',2''-terthiophen]-4-yl)ethynyl)trimethylsilane



To a Schlenk tube were added 4-bromo-5,5''-dimethyl-2,2':5',2''-terthiophene (**10**) (150 mg, 0.420 mmol), PdCl₂(PPh₃)₂ (15 mg, 0.020 mmol), triphenylphosphine (11 mg, 0.040 mmol), and copper (I) iodide (4 mg, 0.02 mmol), and the flask was evacuated and backfilled with N₂ three times. An anhydrous, degassed solution of trimethylsilyl acetylene (83 mg, 0.84 mmol) in diisopropylamine (6 mL) was added, and the solution was heated to 60° C for 16 h. The reaction mixture was then cooled to room temperature, filtered through a silica plug using diethyl ether as the eluent, and concentrated under reduced pressure. Purification of the crude oil by column chromatography (silica, 80:20 hexanes:DCM) afforded compound **11** (146 mg, 0.393 mmol, 93%) as a yellow solid.

¹H NMR (400 MHz, CD₂Cl₂): δ 7.25 (s, 1H), 7.01 (s, 1H), 6.94 (m, 2H), 6.66 (s, 1H), 2.51 (s, 3H), 2.48 (s, 3H) 0.26 (s, 9H). **¹³C (¹H) NMR (100 MHz, CDCl₃):** δ 143.8, 139.6, 136.9, 135.2, 134.9, 133.3, 126.2, 125.6, 124.2, 123.8, 123.7, 120.9, 99.3, 97.0, 15.6, 14.6. **HRMS (EI):** found m/z : 372.0494; calc. for C₁₉H₂₀S₃Si: 372.0496.

2-(5,5''-dimethyl-[2,2':5',2''-terthiophen]-4-yl)-4,4,5,5-tetramethyl-1,3,2-dioxaborolane

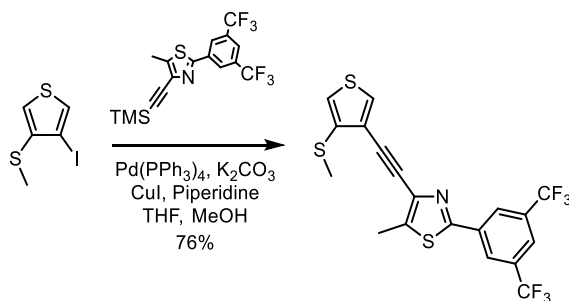


4-bromo-5,5''-dimethyl-2,2':5',2''-terthiophene (**10**) (100. mg, 0.280 mmol) and 2-Isopropoxy-4,4,5,5-tetramethyl-1,3,2-dioxaborolane (63 mg, 0.34 mmol) were added to an anhydrous solution

of toluene (1 mL) and THF (4 mL), and *n*-BuLi (0.13 mL, 2.68 M in hexanes) was added dropwise at -78° C. The solution was allowed to slowly come to room temperature over 4 h. The reaction mixture was diluted with 10 mL of diethyl ether, washed twice with 15 mL of DI H₂O, once with 15 mL brine, and dried over MgSO₄ before concentrating under reduced pressure. Purification of the orange solid by column chromatography (silica, 90:10 hexanes:DCM) afforded compound **12** as a yellow powder (88 mg, 0.22 mmol, 78%).

¹H NMR (400 MHz, CD₂Cl₂): δ 7.26 (bs, 1H), 7.00 (bs, 3H), 6.72 (bs, 1H). **¹³C (¹H) NMR (100 MHz, CDCl₃):** δ 152.2, 139.3, 136.2, 136.1, 135.2, 134.0, 129.5, 126.1, 123.8, 123.6, 123.5, 83.5, 25.1, 16.0, 15.6. **HRMS (EI):** found *m/z*: 402.0943; calc. for C₂₀H₂₃BO₂S₃: 402.0953.

2-(3,5-bis(trifluoromethyl)phenyl)-5-methyl-4-((4-(methylthio)thiophen-3-yl)ethynyl)thiazole

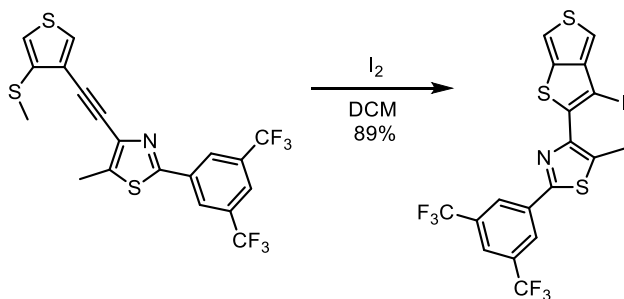


3-iodo-4-(methylthio)thiophene (**2**) (317 mg, 1.24 mmol), 2-(3,5-bis(trifluoromethyl)phenyl)-5-methyl-4-((trimethylsilyl)ethynyl)thiazole (505 mg, 1.24 mmol), and potassium carbonate (377 mg, 2.73 mmol) were added to THF (25 mL), and the solution was sparged with N₂ for 15 min. Then, copper(I) iodide (12 mg, 0.62 μ mol) and Pd(PPh₃)₄ (72 mg, 0.62 μ mol) were added under increased N₂ flow, followed by a degassed solution of piperidine (1.22 mL, 12 mmol) in methanol (10 mL). The reaction mixture was refluxed at 70° C for 20 h. The solution allowed to cool to room temperature and then washed twice with 25 mL sat. NH₄Cl, once with 25 mL brine, and dried over MgSO₄ before concentrating under reduced pressure. Purification of the orange oil by

column chromatography (silica, 95:5 hexanes:DCM) afforded compound **3c** (436 mg, 0.94 mmol, 76%) as a clear colorless oil.

¹H NMR (400 MHz, CD₂Cl₂): δ 8.37 (s, 2H), 7.90 (s, 1H), 7.66 (d, 1H), 6.91 (d, 1H), 2.73 (s, 3H), 2.55 (s, 3H).

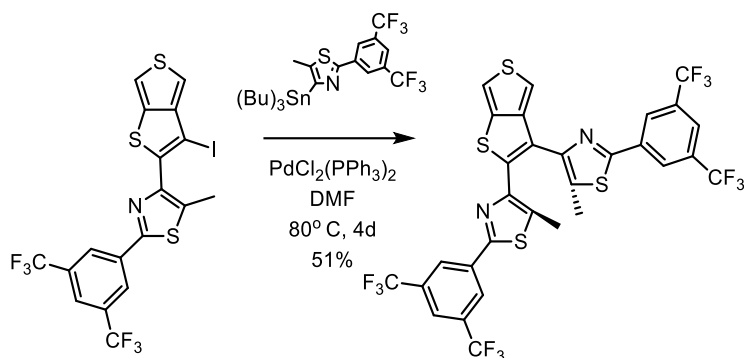
2-(3,5-bis(trifluoromethyl)phenyl)-4-(3-iodothiophen-2-yl)-5-methylthiazole



2-(3,5-bis(trifluoromethyl)phenyl)-5-methyl-4-((4-(methylthio)thiophen-3-yl)ethynyl)thiazole (366 mg, 0.79 mmol) was added to 30 mL DCM, and cooled to 0° C. A solution of iodine (220 mg, 0.87 mmol) in DCM (35 mL) was then added dropwise and stirred until the starting material was consumed, as monitored by TLC. The solution was diluted with 25 mL diethyl ether, washed once with 15 mL sat. Na₂S₂O₃, once with 25 mL brine, and dried over MgSO₄ before concentrating under reduced pressure. Purification by column chromatography (90:10 hexanes:DCM) afforded compound **4c** (408 mg, 0.70 mmol, 89%) as a white solid.

¹H NMR (400 MHz, CD₂Cl₂): δ 8.38 (s, 2H), 7.90 (s, 1H), 7.45 (m, 2H), 2.61 (s, 3H).

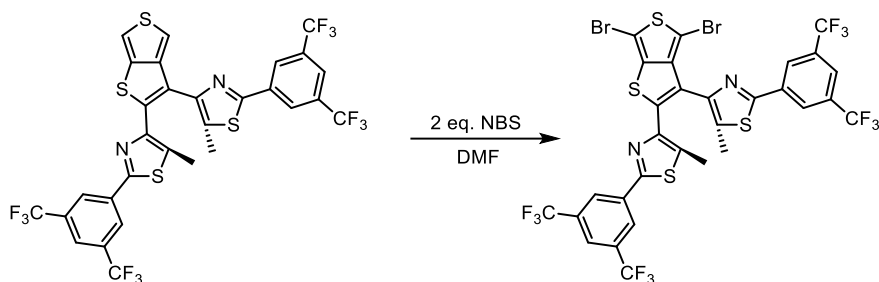
4,4'-(thieno[3,4-b]thiophene-2,3-diyl)bis(2-(3,5-bis(trifluoromethyl)phenyl)-5-methylthiazole) (TT5)



2-(3,5-bis(trifluoromethyl)phenyl)-4-(3-iodothieno[3,4-b]thiophen-2-yl)-5-methylthiazole (150. mg, 0.26 mmol) and 2-(3,5-bis(trifluoromethyl)phenyl)-5-methyl-4-(tributylstannyl)thiazole (**12**) (235 mg, 0.39 mmol) were added to DMF (5 mL), and the solution was subjected to three freeze-pump-thaw cycles. $\text{PdCl}_2(\text{PPh}_3)_2$ (5 mg, 5 μmol) was added under increased N_2 flow, and the solution was refluxed at 100°C for 24 h. The reaction mixture was then cooled to room temperature and diluted with 10 mL of diethyl ether, washed twice with 10 mL of NH_4Cl , twice with 10 mL KF , and dried over MgSO_4 before concentrating under reduced pressure. Purification by column chromatography (silica, 95:5 hexanes:EtOAc) afforded **TT5** (101 mg, 0.132 mmol, 51%) as a pale turquoise solid.

^1H NMR (400 MHz, CD_2Cl_2): δ 8.36 (s, 2H), 8.28 (s, 2H), 7.90 (s, 1H), 7.89 (s, 1H), 7.48 (d, 1H), 7.36 (d, 1H), 2.18 (s, 3H), 2.10 (s, 3H).

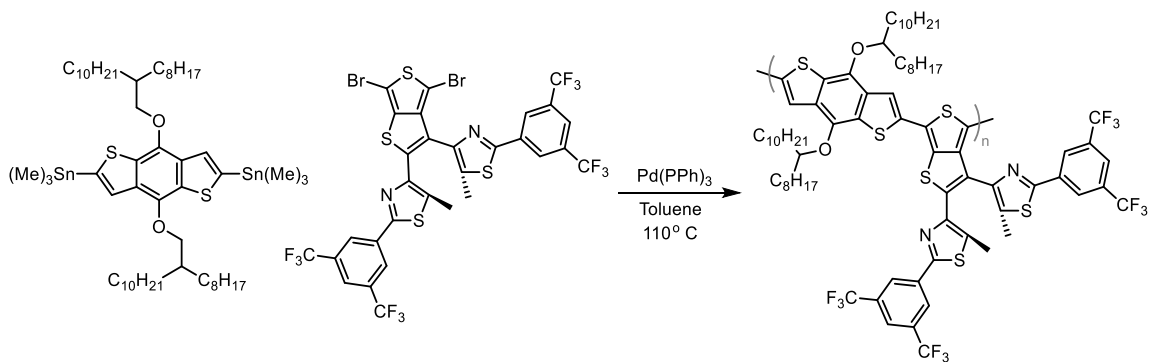
4,4'-(4,6-dibromothieno[3,4-b]thiophene-2,3-diyl)bis(2-(3,5-bis(trifluoromethyl)phenyl)-5-methylthiazole)



4,4'-(thieno[3,4-b]thiophene-2,3-diyl)bis(2-(3,5-bis(trifluoromethyl)phenyl)-5-methylthiazole) (**TT5**) (20. mg, 26 μ mol) was added to 5 mL DMF, and the solution was cooled to 0° C. NBS (9 mg, 50 μ mol) was added dropwise until the starting material was consumed, as monitored by TLC. The solution was then diluted with 20 mL diethyl ether, washed twice with 20 mL sat NH_4Cl , once with 20 mL brine and dried over MgSO_4 before concentrating under reduced pressure. Purification by column chromatography (95:5 to 90:10 hexanes:DCM) afforded **TT5-Br** (4 mg, 3.9 μ mol, 15%).

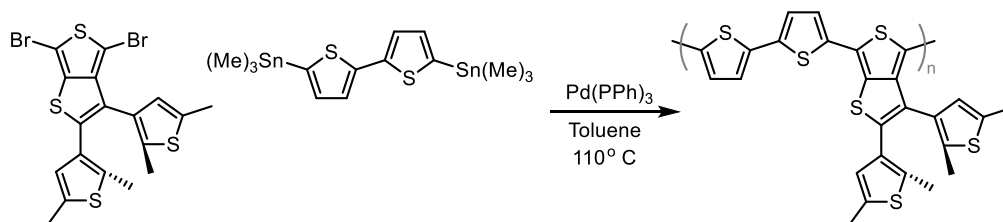
^1H NMR (400 MHz, CD_2Cl_2): δ 8.35 (s, 2H), 8.17 (s, 2H), 7.88 (s, 1H), 7.86 (s, 1H), 2.39 (s, 3H), 2.20 (s, 3H).

P-TT5



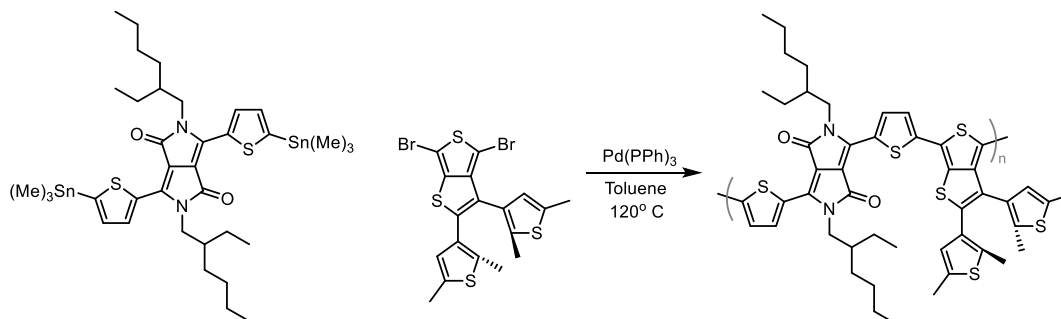
4,4'-(4,6-dibromothieno[3,4-b]thiophene-2,3-diyl)bis(2-(3,5-bis(trifluoromethyl)phenyl)-5-methylthiazole) (99 mg, 0.108 mmol), (4,8-bis((2-octyldodecyl)oxy)benzo[1,2-b:4,5-b']dithiophene-2,6-diyl)bis(trimethylstannane) (120 mg, 0.108 mmol) and toluene (4 mL) were added to a 25 mL pear-bottom Schlenk flask, and the solution was subjected to three freeze-pump-thaw cycles. Pd(PPh₃)₄ (5 mg, 4 μmol) was added under increased N₂ flow, and the solution was refluxed at 100° C for 72 h. The organic layer was concentrated to approximately 1.0 mL before being rapidly added to 100 mL MeOH. The precipitate was collected by filtration, and was purified by Soxhlet extraction: methanol (24 h) and acetone (24 h), and CHCl₃ (2 h). The chloroform extract was concentrated and precipitated with 50 mL MeOH. Filtration yielded **P-TT5** dark gold solid (100 mg).

TT1-Th2



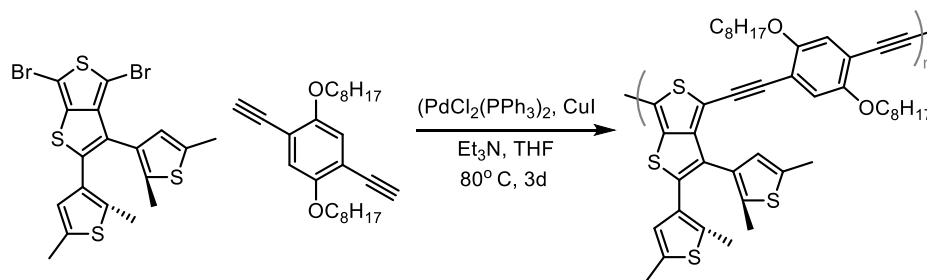
5,5'-bis(trimethylstannyl)-2,2'-bithiophene (194 mg, 0.39 mmol) and Pd(PPh₃)₄ (23 mg, 20 μmol), and **mTT1** (204 mg, 0.39 mmol) were added to a 25 mL Schlenk flask, which was evacuated and backfilled with N₂ three times. Toluene (10 mL) and DMF (2 mL) were added, and the solution was heated to 110° C. After stirring for 48 hr, the reaction mixture was concentrated to a purple oil and precipitated with MeOH (200 mL). The precipitate was subjected to Soxhlet extraction with MeOH (24 hr), acetone (24 hr), and CHCl₃ (24 hr). The chloroform layer was concentrated via rotovap, and precipitated with MeOH to yield a metallic dark brown solid (180 mg, 45%).

TT1-TDPP EH



Bis(trimethylstannyl) TDPP-EH (321 mg, 0.38 mmol), **mTT1** (195 mg, 0.38 mmol), and $\text{Pd(PPh}_3)_4$ (11 mg, 9.4 μmol) were added to a 50 mL 3-neck round bottom flask equipped with a reflux condenser, which was then evacuated and backfilled with N_2 three times. Toluene (20 mL) was added, and the solution was allowed to reflux at 120°C . After stirring for 72 hr, the reaction mixture was concentrated to a dark red oil and precipitated with MeOH (200 mL). The precipitate was subjected to Soxhlet extraction with MeOH (24 hr), acetone (24 hr), and CHCl_3 (24 hr). The chloroform layer was concentrated via rotovap, and precipitated with MeOH to yield a dark red powder (227 mg, 44%).

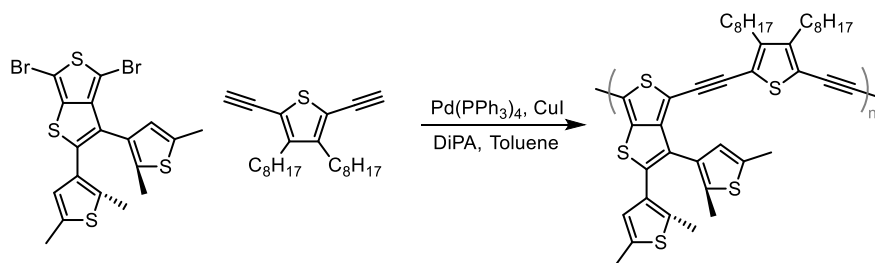
TT1-EDA



1,4-diethynyl-2,5-bis(octyloxy)benzene (258 mg, 0.67 mmol), **mTT1** (350 mg, 0.67 mmol), CuI (3 mg, 0.01 mmol), and $\text{PdCl}_2(\text{PPh}_3)_2$ (10 mg, 0.01 mmol) were added to a 100 mL 3-neck round bottom flask equipped with a reflux condenser, which was then evacuated and backfilled with N_2

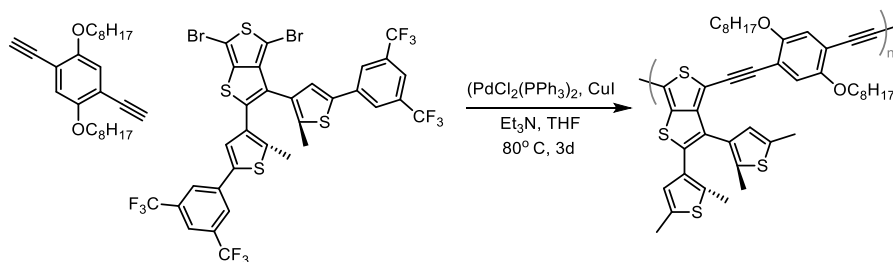
three times. Dry, degassed triethylamine (10 mL) and THF (10 mL) were added, and the reaction mixture was heated to 85° C. After refluxing for 72 hr, the solution was concentrated and precipitated with MeOH (200 mL). The precipitate was subjected to Soxhlet extraction with MeOH (24 hr), acetone (24 hr), and CHCl₃ (24 hr). The chloroform layer was concentrated via rotovap, and precipitated with MeOH to yield a dark red powder (238 mg, 39%).

TT1-Eth



2,5-diethynyl-3,4-dioctylthiophene (148 mg, 0.41 mmol), **mTT1** (215 mg, 0.41 mmol), CuI (50 mg, 0.30 mmol), and Pd(PPh₃)₄ (48 mg, 0.04 mmol) were added to a 100 mL 3-neck round bottom flask equipped with a reflux condenser, which was then evacuated and backfilled with N₂ three times. Dry, degassed diisopropylamine (10 mL) and toluene (15 mL) were added, and the reaction mixture was heated to 85° C. After refluxing for 72 hr, the solution was concentrated and precipitated with MeOH (200 mL). The precipitate was subjected to Soxhlet extraction with MeOH (24 hr), acetone (24 hr), and CHCl₃ (24 hr). The chloroform layer was concentrated via rotovap, and precipitated with MeOH to yield a golden flaky solid (154 mg, 42% yield).

TT3-EDA



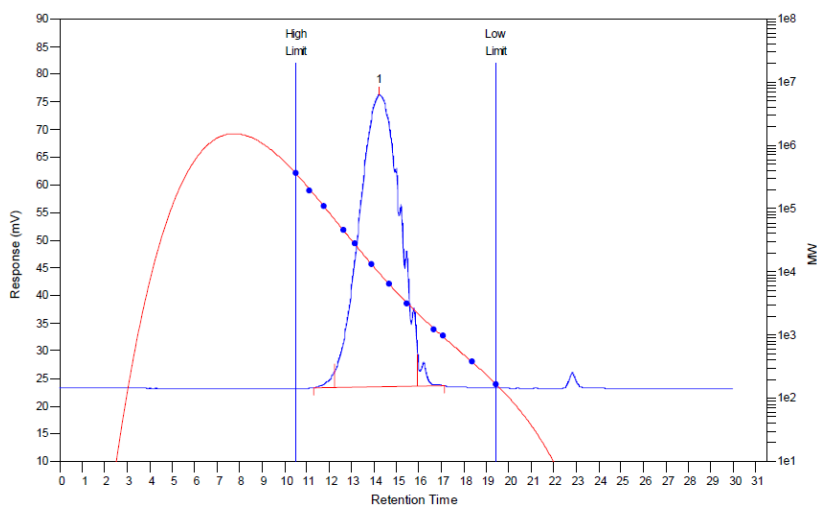
1,4-diethynyl-2,5-bis(octyloxy)benzene (50 mg, 0.13 mmol), **mTT3** (118 mg, 0.13 mmol), CuI (1 mg, 3 μ mol), and PdCl₂(PPh₃)₂ (2 mg, 3 μ mol) were added to a 50 mL 3-neck round bottom flask equipped with a reflux condenser, which was then evacuated and backfilled with N₂ three times. Dry, degassed triethylamine (5 mL) and THF (5 mL) were added, and the reaction mixture was heated to 85° C. After refluxing for 72 hr, the solution was concentrated and precipitated with MeOH (200 mL). The precipitate was subjected to Soxhlet extraction with MeOH (24 hr), acetone (24 hr), and CHCl₃ (24 hr). The chloroform layer was concentrated via rotovap, and precipitated with MeOH to yield a metallic red product (90 mg, 54%).

GPC Chromatographs

All polymers were characterized using conditions listed in the General Information section.

Photochromic polymers were first prepared as 1 mg/mL solutions and photo-bleached using a 617 nm light source for 20 minutes, from which a 10 μ L aliquot was immediately subjected to GPC analysis to obtain “Open” chromatographs. These 1 mg/mL solutions were then irradiated using a 254 nm light source for 3 minutes (longer than required to reach the photostationary state of each photochromic polymer), from which a 10 μ L aliquot was immediately subjected to GPC analysis to obtain “closed” chromatographs.

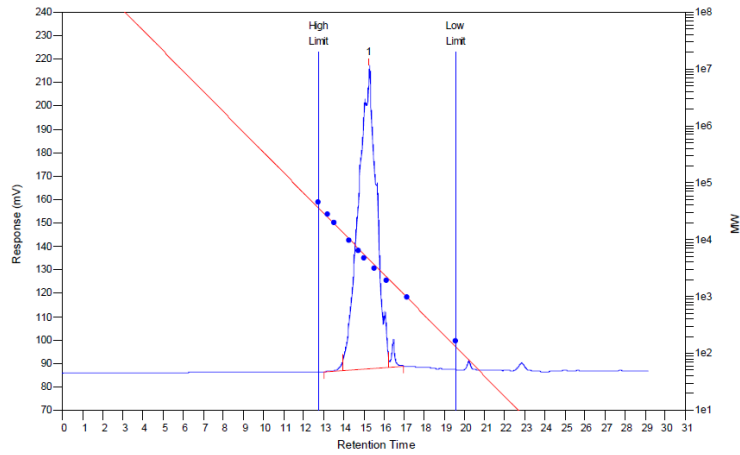
P-TT1 (No Photochromic Activity)



MW Averages

Peak No	Mp	Mn	Mw	Mz	Mz+1	Mv	PD
1	9479	7340	12213	20434	30320	11260	1.6639

P-TT2 "Open"



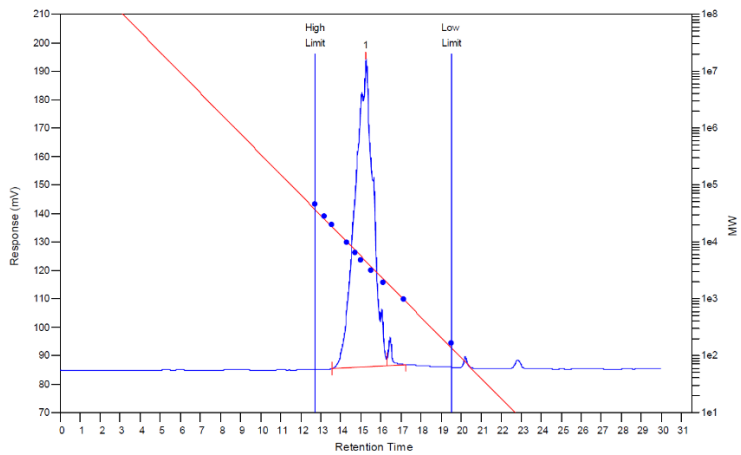
MW Averages

Peak No	Mp	Mn	Mw	Mz	Mz+1	Mv	PD
1	4511	4689	5352	6122	6962	5244	1.14139

Processed Peaks

Peak No	Name	Start RT (mins)	Max RT (mins)	End RT (mins)	Pk Height (mV)	% Height	Area (mV.secs)	% Area
1		13.92	15.26	16.22	129.335	0	8224.46	100

P-TT2 "Closed"



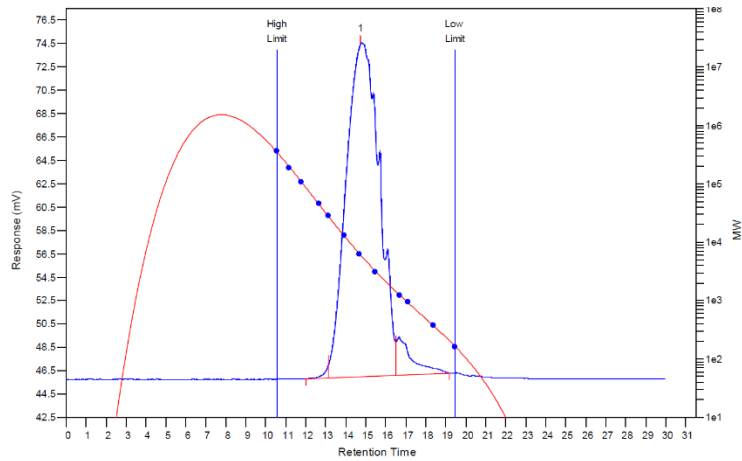
MW Averages

Peak No	Mp	Mn	Mw	Mz	Mz+1	Mv	PD
1	4527	4706	5397	6219	7151	5284	1.14683

Processed Peaks

Peak No	Name	Start RT (mins)	Max RT (mins)	End RT (mins)	Pk Height (mV)	% Height	Area (mV.secs)	% Area
1		13.56	15.26	16.29	108.142	0	6914.02	100

P-TT3 "Open"



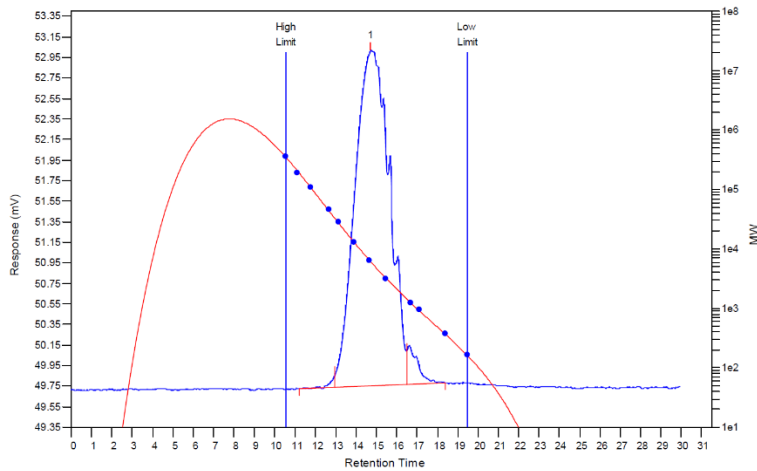
MW Averages

Peak No	Mp	Mn	Mw	Mz	Mz+1	Mv	PD
1	5993	4442	6485	9319	12413	6121	1.45993

Processed Peaks

Peak No	Name	Start RT (mins)	Max RT (mins)	End RT (mins)	Pk Height (mV)	% Height	Area (mV.secs)	% Area
1		13.13	14.74	16.50	28.5847	0	3361.78	100

P-TT3 "Closed"



MW Averages

Peak No	Mp	Mn	Mw	Mz	Mz+1	Mv	PD
1	6154	4537	6790	10084	13865	6379	1.49658

Processed Peaks

Peak No	Name	Start RT (mins)	Max RT (mins)	End RT (mins)	Pk Height (mV)	% Height	Area (mV.secs)	% Area
1		12.98	14.71	16.51	3.27842	0	392.92	100

References

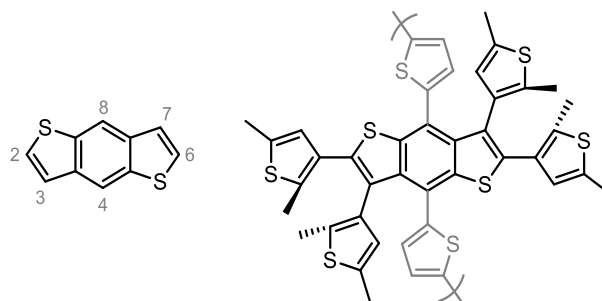
1. Kawai, T.; Nakashima, Y.; Irie, M. A Novel Photoresponsive π -Conjugated Polymer Based on Diarylethene and its Photoswitching Effect in Electrical Conductivity. *Advanced Materials* **2005**, *17* (3), 309-314.

CHAPTER IV

Alternative Switch Cores and Future Directions for Pendant Photochromic Polymers

Throughout the years, several photochromic targets besides those concerned with thieno[3,4-*b*]thiophene (**TT**) have been explored both computationally and experimentally. Historically, pendant switching monomers have been notoriously difficult to not only synthesize, but also demonstrate strong photochromic activity. This problem was encountered in almost all targets before **TT**. While none of the several targets conceptualized and synthesized seemed as desirable as the **TT**-based switches, there may be potential modifications or improvements to both the synthesis or design that would allow for similar switch targets to be realized and incorporated into pendant π -conjugated materials.

The first photochromic target I pursued when I joined the lab involved the fused conjugated core benzo[1,2-*b*:4,5-*b'*]dithiophene (**BDT**, **Scheme 4.1**). The literature is rich with examples of its incorporation into π -conjugated materials for organic field-effect transistors (OFETs) and organic photovoltaics (OPVs), though most involved π -extension from the 2- and 6-positions.¹ This is not a viable option if one is trying to impart a diarylethene switching motif onto the molecule, however, as there wouldn't be contiguous carbons bridged by a double bond remaining. If π -extension was performed from the 4- and 8- positions of **BDT**, however, then it leaves the potential to build a double switch, one at the 2- and 3- positions, and the other at the 4- and 7- positions. This represents a rather ambitious target molecule to begin with. At the time, lack of experience meant little attention was paid to the photophysics of dealing with a double switch. For example, will both cyclize? Will the cyclization event of one inhibit that of the other? If one diarylethene portion is cyclized, will the other be triggered at a different wavelength? Substitution at the β -position of the **BDT** thiophenes seems sterically hindered, will that interfere with parallel versus anti-parallel conformations? Many of these questions also apply to the cycloreversion event as well. If these questions are ignored, there is the obvious attraction of a double switch core which could impact the electronics of the core (and the resulting polymer) more so than an individual switch.



Scheme 4.1 Benzo[1,2-b:4,5-b']dithiophene numbering scheme and locations for switch functionalization and π -extension for the double switch core.

Calculations were performed very early on to demonstrate the differences in frontier molecular orbital topology of an open and closed **BDT** switch featuring a slight π -extension with alkyne groups to simplify the computation. The HOMO and LUMO of the open switch has surface distribution across the **BDT** and the alkyne, with minimal distribution over the switching motif. Lack of distribution across the switches is most likely due to rotation out of planarity to avoid steric congestion. Upon ring closure, the majority of the distribution is spread across the switching motifs and the bridging **BDT** core. As discussed in previous chapters, it is highly deceptive to interpret frontier molecular orbital surfaces, as this only describes the beginning and end goals of the cyclization process, but provides no information on the path taken. In addition, had the conjugated backbone been extended further with more traditional groups (thiophene, benzene, etc.), there is a possibility that there may have been less distribution across the switching unit. Regardless, it is beneficial to see that if the switch does cyclize, one would expect a significant impact on the electronics of the molecule.

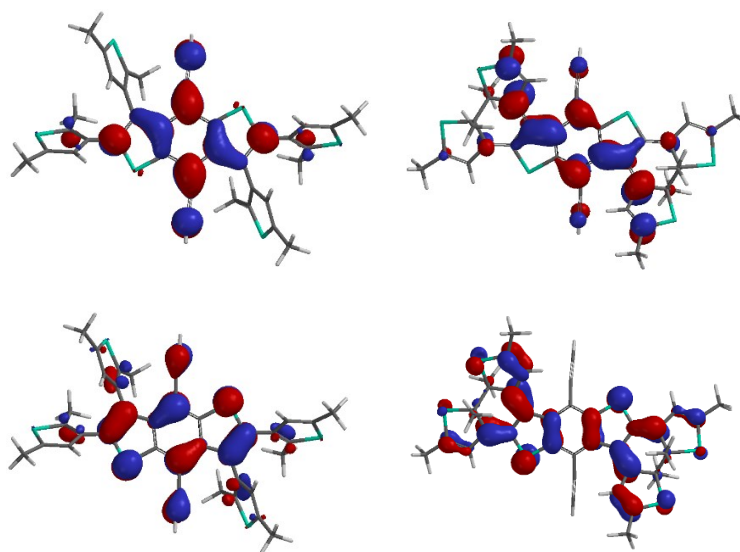
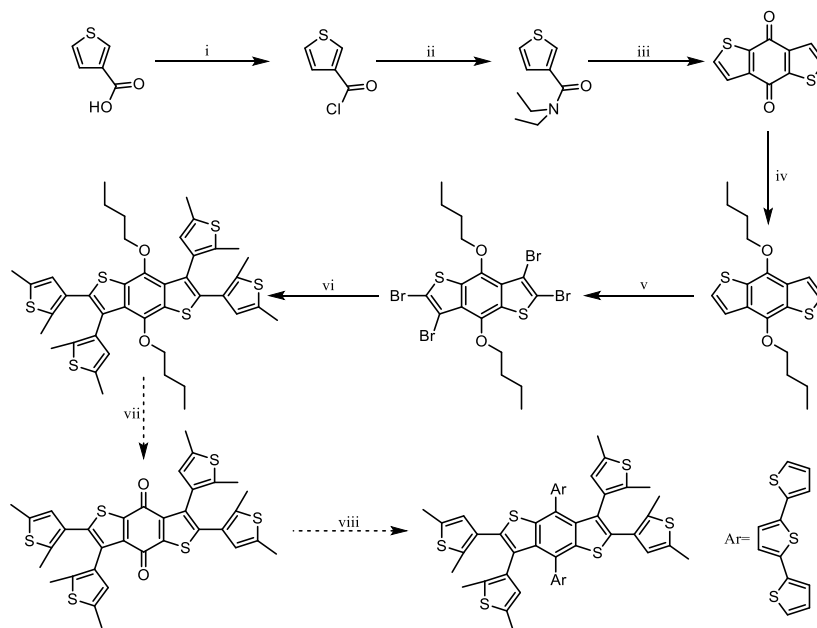


Figure 4.1 Early low level calculations demonstrating LUMO (top) and HOMO (bottom) MOs of open (left) and closed (right) benzodithiophenes, in which a simple alkyne is used as a model for the conjugated backbone.

The first proposed synthetic route is shown in **Scheme 4.2**. The synthesis begins with thiophene-3-carboxylic acid, which can be converted to the acid chloride with oxalyl chloride. The amide was then made with diethylamine rather easily due to the high reactivity of the acid chloride. Addition of *n*-butyllithium deprotonates the thiophene at the 2- position, allowing the species to condense with another identical molecule, forming the benzodithiophene-4,8-dione. Ideally, the switching units would be synthesized next if the dione were to be used as the monomer. This would be accomplished by coupling 2,5-dimethyl thiophene to 2,3,6,7-tetrabromobenzo[1.2-*b*:4.5-*b'*]dithiophene-4,8-dione. The first problem came in the form of the bromination. Under several halogenation conditions, only the dione starting material was recovered. It is believed that the strong electron deficiency of the dione effectively prevents halogenation. Thus, an attempt was made to protect each dione by conversion to an acetal. The benzodithiophene core would still be electron poor though induction, but it was predicted that loss of electron withdrawal through resonance may allow halogenation to occur. However, the product decomposed with no recovery of starting material. The goal now was to convert the dione to a species that could later be reconverted back to the dione. The use of zinc as a reducing agent

and butyl p-toluenesulfonate allowed for the conversion to the dialkoxy species, producing an electron-rich substrate as opposed to an electron deficient one. This intermediate was readily tetra-brominated using molecular bromine in chloroform. With the aryl halide at hand, 2,5-dimethylthien-3-yl boronic acid (a common heteroaromatic ring frequently used in diarylethene switches) was synthesized to carry out the tetra-coupling reaction under standard Suzuki-Miyaura conditions. Unfortunately, there were not isolable products and NMR data was inconclusive. Several other coupling reaction conditions were tried, with a successful synthesis coming from Buchwald et al, in which sterically hindered aryl halides can be coupled to boronic acids by using $\text{Pd}_2(\text{dba})_3$ and S Phos as the ligand. The reaction yielded two photoresponsive compounds. The first is the desired compound, as determined by mass spec. The other seems to be the product of tri-coupling, potentially from residual tri-brominated species (also determined by mass spec). The desired compound **vii** (orange powdery solid, yellow in solution) turns pinkish red upon irradiation with a common UV lamp.

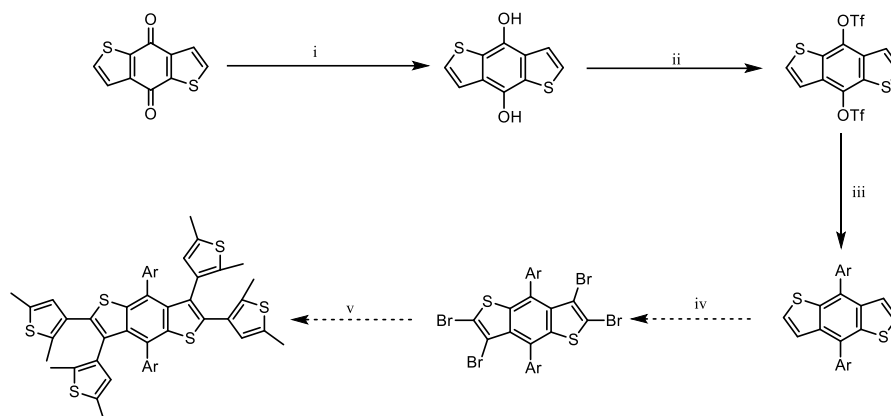


Scheme 4.2 First synthetic design of the double switch monomer. i) $(\text{COCl})_2$, DCM, r.t. ii) diethylamine, DCM, r.t. iii) n-BuLi, THF, 0°C . iv) Zn, NaOH, butyl p-toluenesulfonate, EtOH, 105°C . v) Br_2 , CHCl_3 , r.t. vi) 2,5-dimethylthien-3-yl boronic acid, $\text{Pd}_2(\text{dba})_3$, SPhos, K_3PO_4 ,

toluene, 100°C. vii) 4-iodophenoxyacetic acid, oxone viii) Ar, SnCl₂, H₂O.

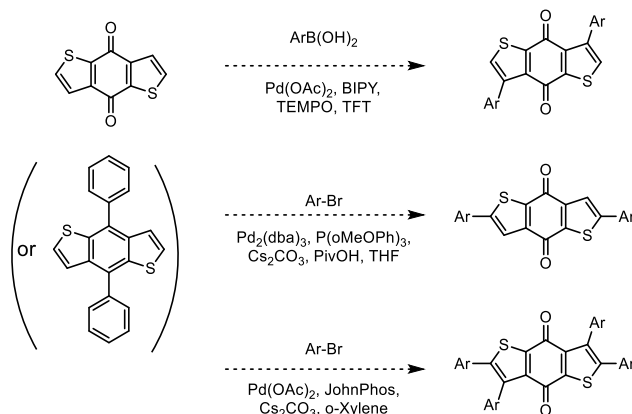
With the double switch intermediate in hand, the next step was to re-oxidize the species from the di-butyloxy species back to the dione. Reaction with aryl-lithium species and subsequent reductive aromatization would allow for π -extension along the conjugated backbone. Mild oxidation reactions (such as the use of hypervalent iodine species) were first attempted, as aggressive oxidations may generate sulfoxides on the switching motif thiophenes. Unfortunately, these proved ineffective at producing the desired species. Most procedures involved converting a di-hydroxy or di-methoxy species to the dione, which did not seem to extend to the di-butoxy compound at hand. More aggressive oxidations led to decomposition of the starting material. While being close to the desired end molecule, it seemed as though the synthesis needed to be re-engineered to avoid using butyloxy groups.

Operating under the case in which oxidation of the species doesn't work, backbone functionalization *before* incorporating the switch components was attempted through the use of the BDT di-triflate species (**Scheme 4.3**). This species, for example, acts as the "aryl bromide" species in Suzuki coupling reactions. The triflate was successfully synthesized, and coupling to this backbone has been successful for short aromatic backbones (phenyl and biphenyl). According to mass data, bromination of these backbone-functionalized species were also successful. The problem came in the form of coupling to this pre-functionalized species. Conditions that were successful in the tetra-coupling reaction (Buchwald-type Suzuki coupling) were not applicable here. Other sterically hindered coupling conditions, such as those involving PEPPSI catalysts, proved ineffective as well. It could be possible that the phenyl rings are producing too much steric hindrance for these reactions to occur in any appreciable yield. Other backbone groups were considered, but they seem to induce more problems than they solve. For example, both thiophene and alkyne groups can be extended from the phenyl core, but undesirable bromination of these compounds will occur in subsequent steps.



Scheme 4.3 Second synthetic pathway towards the double switch core. i) NaBH_4 , EtOH, 85°C ii) Tf_2O , pyridine, DCM, 0°C iii) phenylboronic acid, $\text{Pd}(\text{PPh}_3)_4$, 85°C iv) Br_2 , CHCl_3 , r.t. v) 2,5-dimethylthien-3-yl boronic acid, $\text{Pd}_2(\text{dba})_3$, SPhos, K_3PO_4 , toluene, 100°C .

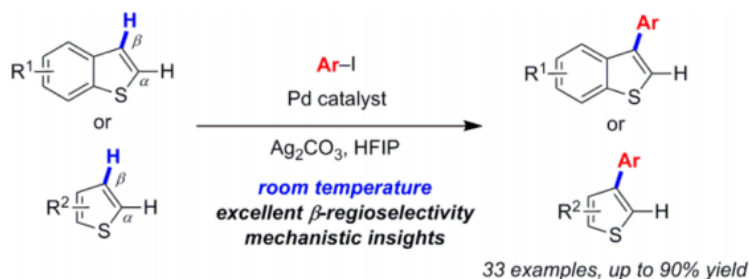
The issues ran into above could be avoided entirely if the compounds did not need to be prepped for coupling (such as aryl bromide and aryl triflate) beforehand. C-H arylation of thiophenes seemed to have the most desirable means to obtain the tetra-coupled species. In principle, the thiophene positions could be functionalized selectively^{8,9} (leading to two different switch components) or non-selectively¹⁰ (identical switch components) without the need of preparatory syntheses for traditional coupling reactions like bromination, boronic acid formation, etc. Many C-H arylations are reported in the literature, most of which are selective for one thiophene location or the other. While regioselectivity is not necessarily important for switch formation, it opens open several combinations for varying switch designs from the same BDT core (i.e. if 2,5-dimethylthiophene and 2-methylbenzo[b]thiophene switching components pendant from a thiophene of BDT) (**Scheme 4.4**).



Scheme 4.4 Selected C-H arylation conditions used for various thiophene substrates applied to two BDT cores, aimed at selectively functionalizing the β -positions.

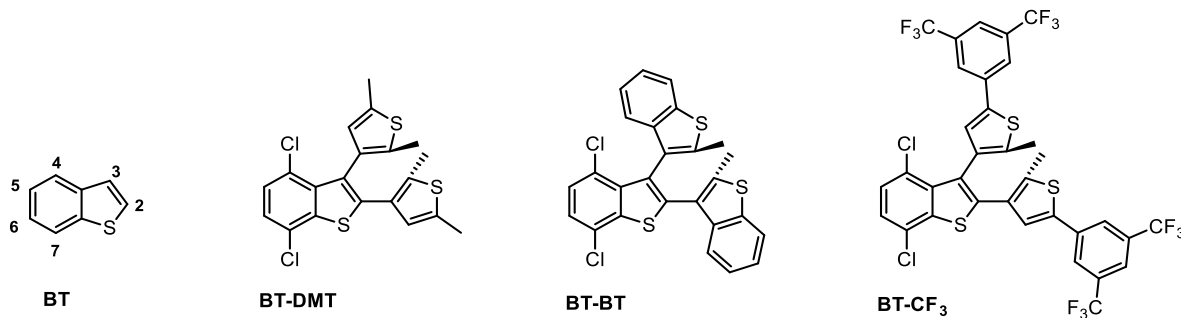
Two different cores were chosen to determine the most appropriate arylation conditions: BDT Dione, and BDT di-phenyl. BDT di-alkoxy was ignored, as although it provides a more electron-rich substrate, one can ultimately provide no functionalization of this species. From these two species, several regioselective C-H arylation procedures were performed first, with a larger volume of literature focused on the 2- and 5-position of thiophenes. These positions are analogous to the 2- and 6-positions of BDT. In all cases attempted, there was no desired product formation. This could possibly be attributed to the electron-deficient nature of the BDT's used compared to thiophene. C-H arylation of the 3- and 7-positions (analogous to the 3- or 4-positions of thiophene) were attempted next. The much smaller volume of literature for this made running through all possible conditions fairly easy, though none of these were successful either. It became clear after these attempts that the regioselective nature of the 2- and 5- position functionalizations were not by design, but simply because these locations were easier to functionalize. The literature was then searched for conditions under which selectivity was lost. A few promising conditions were found and attempted, but again these yielded no appreciable result. C-H arylation conditions seem to be *very* substrate dependant, and conditions that led to any activation of the BDT's above seem to be nonexistent at the time. An excellent potential reaction involves the selective 3-

position arylation of benzo[b]thiophenes with aryl iodides (**Scheme 4.5**), which was reported by Colletto *et. al.*² The conditions are mild for potentially sensitive substrates (room temperature, anaerobic conditions are not required, etc.) with the added benefit of common reagents.¹¹ The structural similarity to the cores presented earlier (both BT and BDT) make this an attractive option, but here again, the reactions proved unsuccessful.



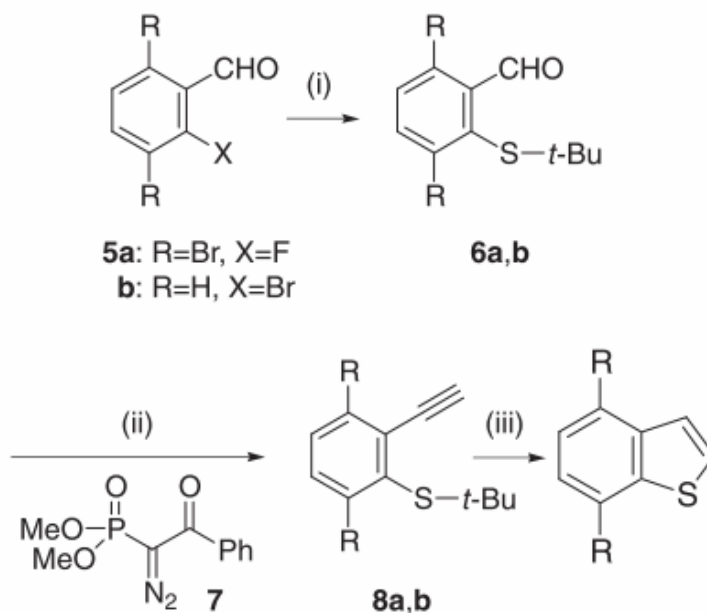
Scheme 4.5 C-H arylation of thiophenes and benzo[b]thiophenes with high regioselectivity proposed by Colletto *et. al.* [Adapted from reference 4.2]

Several months were invested into trying to make C-H activation work on this substrate without success, a synthetic endeavor shared by several other members in the lab. Due to the success in making a photochromic intermediate during the exploration of **BDT** switches, other switches were explored that proved to be more synthetically tractable and less complicated, including **BT**, shown in **Scheme 4.6**.



Scheme 4.6 Benzo[b]thiophene numbering and target photochromic cores, where polymerization occurs from the 4- and 7-positions while the switch is built from the 2- and 3-positions.

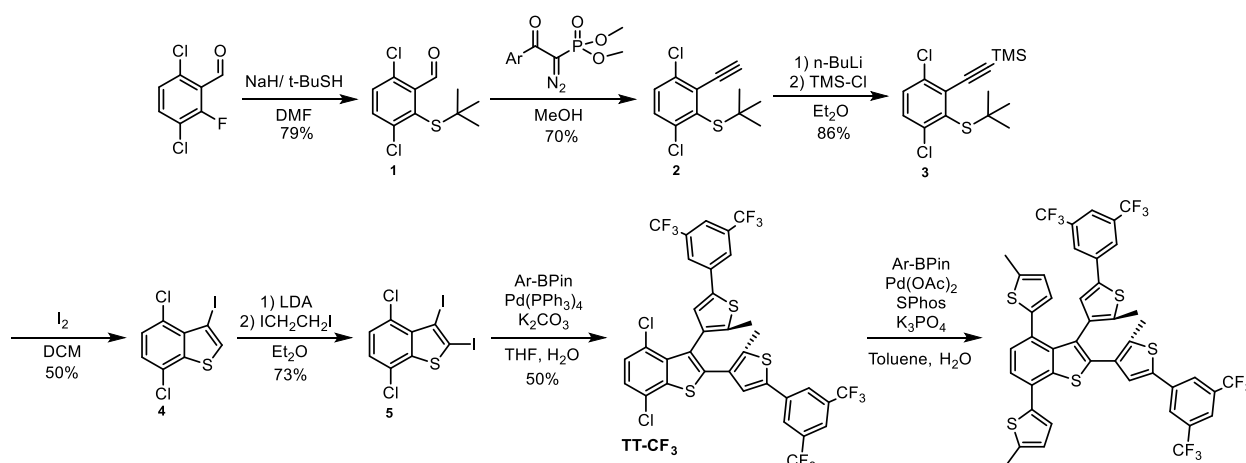
This is similar to the **TT**-based switch discussed and expanded upon in previous chapters, where the switching motif is built off of the 2- and 3- position of a fused thiophene. Here, the key difference is that the fusion is to a benzene as opposed to another thiophene. π -extension occurs from the only possible para- substitution locations on the benzene portion: the 4- and 6- positions. There are a few key differences between **BT** and **TT**. Firstly, although both species are 10π aromatic systems, it is likely that the fused thiophene from which the switch is built in each system is less impactful on the benzene in **BT** than it would be on a thiophene in **TT**, as benzene often behaves as an isolated aromatic system due to the high stabilization energy relative to other aromatic molecules. Second, the 4-position substitution is likely to create steric hindrance with the switch substitution at the 3- position of **BT** as it would in the case of **BDT** discussed earlier. This is not seen in **TT** switches since substitutions are angled away from the switching motif by the natural geometry of thiophenes. Finally, one would expect regiocontrol over functionalization to be very difficult on **BT**, as there are not substantial electronic differences between the 4-7 positions to warrant high selectivity. Many of these reasons contributed to why **TT** was the primary focus as opposed to **BT**. Morita *et. al.* published a synthesis of **BT** in which the 4- and 7- are pre-functionalized with bromines (**Scheme 4.7**).³



Scheme 4.7 Synthetic route reported by Morita *et. al.* on the synthesis of a 4- 7- dihalogenated **BT** core. Reagents and conditions: (i) *t*-BuSNa, N,N-dimethylformamide (DMF), -30 °C, 7 h; (ii) K₂CO₃, MeOH, 0 °C to r.t.; (iii) AuCl (5mol%), 1,4-dioxane, H₂O, r.t., 10 min.

While this synthetic route allows access to a core with the prerequisite functionalization for π -extension, the bromines would interfere with the cross coupling reactions necessary to introduce the switching motif at the 4- and 7- positions. The synthesis was therefore modified to feature a 4- 7- dichlorinated **BT**, as opposed to the dibrominated version. The selectivity from cross coupling reactions greatly favors bromine over chlorine, so in theory the chlorine atoms will stay unreacted under normal coupling conditions but will react under aggressive conditions. The trade-off for more difficult cross coupling reactions for π -extension is a simpler construction of the switching motif. The di-chlorinated core was synthesized following the analogous procedure, where the fused thiophene was formed in the presence of gold (I) chloride. Several bromination attempts were made, but the tetra-halogenated compound was never obtained. Due to the similarity to Larock-type ring-closures, the synthetic procedure was modified to more closely resemble a traditional cyclization. As in the case of **TT**, this would result in a key halogen placed at the hardest to functionalize location. The modified synthesis is shown in **Scheme 4.8**. The

synthesis begins as reported in the literature with substitution of the fluorine atom with a *tert*-butylsulfide group. There was some concern that the selectivity for fluorine on the di-chlorinated substrate may not be as selective as the di-brominated species, but the fluorinated carbon is still the most electrophilic site on the molecule. The aldehyde was then converted to the alkyne by way of a Seyferth-Gilbert homologation in 70% yield. While it wasn't clear if the Larock-type ring closure would occur with an unsubstituted alkyne, simple lithium-halogen exchange and quench with trimethylsilyl chloride for protection. The iodine-mediated ring closure in this case was unfamiliar, since the leaving group is a *t*-butyl as opposed to a methyl. In theory, this should be a worse leaving group as it will generate the *t*-butyl anion, and it is also more sterically hindered. The reaction proceeded well however, albeit with lower yields compared to previous cyclizations. The α -position of thiophene was then deprotonated with LDA (as *n*-BuLi will result in lithium-halogen exchange) and quenched with diiodoethane, allowing easy access to the tetra-halogenated compound. This was then coupled under standard Suzuki cross-coupling conditions with the bis(trifluoromethyl)benzene-substituted thiophene switching arm to result in **BT-CF₃**. As this was the first switch in this series, this switching motif was chosen to simplify NMR interpretation, as the bistrifluoromethylated benzene protons show up in very distinct areas.



Scheme 4.8 Synthetic path towards the di-chlorinated **BT** switch core, featuring a modified Larock-type ring closure with a *t*-butyl group (as opposed to a methyl group) as the leaving

group.

Photophysical data for **BT-CF₃** is shown in **Figure 4.3**. The open switch is entirely contained in the ultraviolet region, similar to other switches with small conjugated cores and moderately conjugated switching arms. Irradiation with 254 nm resulted in immediate blue coloration, as defined by the broad visible absorption seen in the UV-Vis spectrum. This absorbance profile is similar to that seen in **TT2** which shares an identical switching motif, though for some unexplained reason the photostationary state and bleach takes longer with this core.

With the core assembled with correct, albeit non-ideal, functionalization for π -extension, a test coupling was performed using a methylated thiophene. This heteroarene was chosen again for simplicity in spectral interpretation, as the methyl groups would appear in a region substantially different from other protons on the molecule. While NMR confirmed the product was made, this compound proved tricky to purify and therefore difficult to quantify the yield. Regardless, this switch core can indeed be incorporated into polymeric species, and represents a good comparison molecule to the **TT** series. This switch core was not pursued in light of successes with the **TT** series, but seemed like the second most promising core out of the several explored due to photochromic activity.

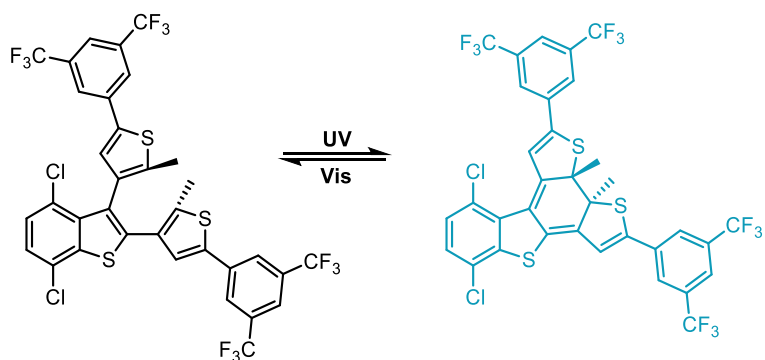
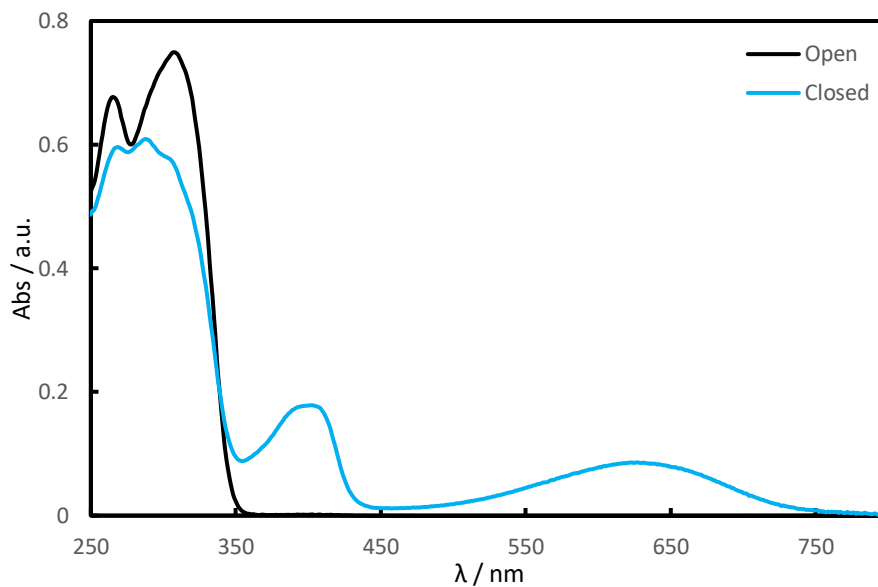


Figure 4.2 Photophysical response of **BT-CF₃** in acetonitrile solution, where photoirradiation occurred with a handheld UV lamp and cycloreversion with a white LED.

Many other switches were attempted or conceptualized to a lesser degree than those discussed above, the first of which utilizes a quinoxaline (**Q**) core (**Figure 4.3**).

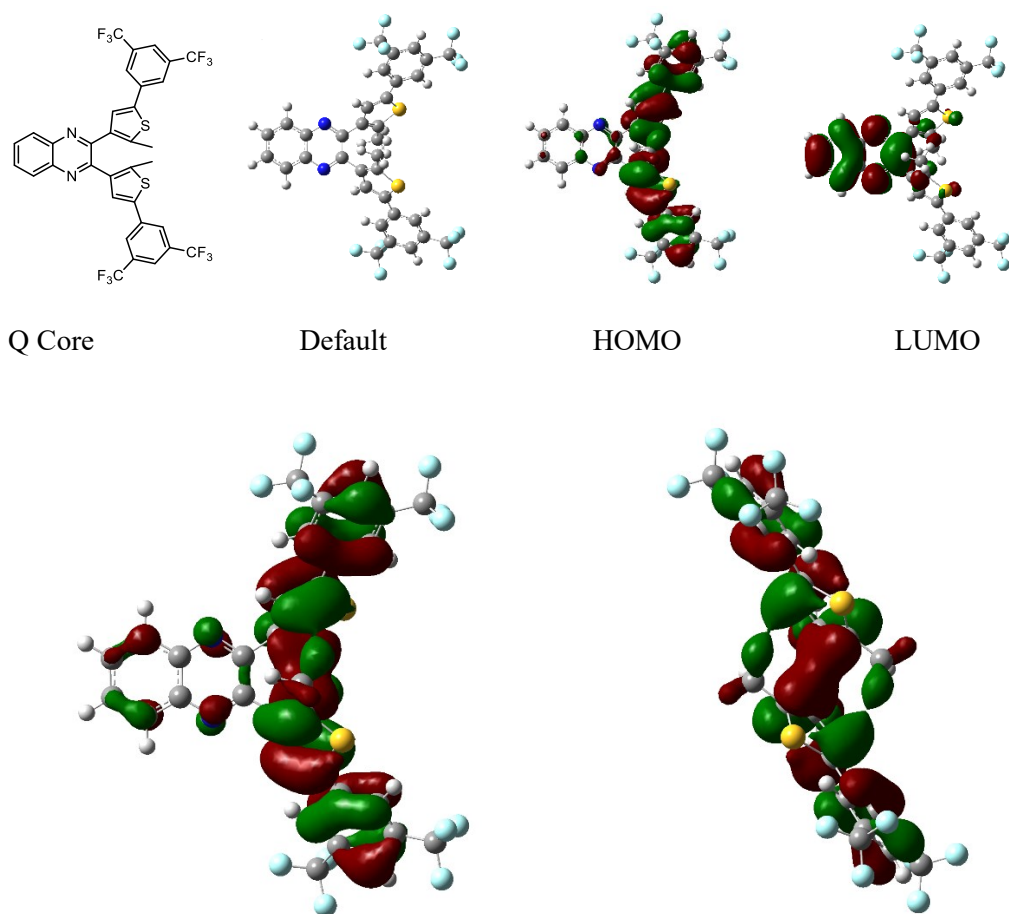
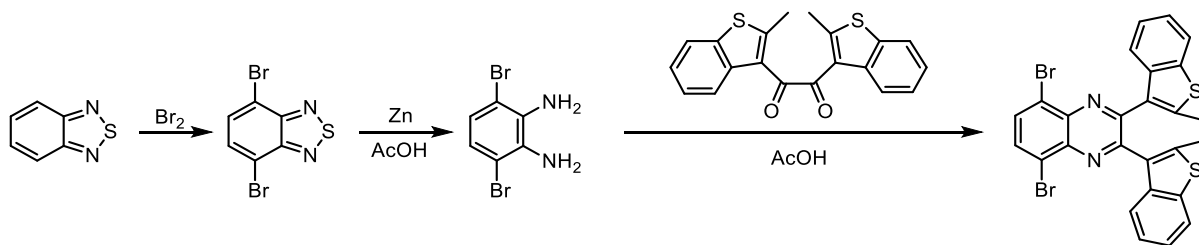


Figure 4.3 Top: Frontier orbitals for the stabilized Q core. Bottom: HOMO-1 surface topology and its side-view. B3LYP 6-31G*.

At the outset, the **Q** posed an interesting question: does the absence of a formal double bond bridging the switching motifs prevent cyclization, even though the electrons are present and, in theory, fluxional? One can view this system as a 10 π aromatic system, or a benzene with two adjacent imines. The former would mean that the electrons are constantly distributed around the outer edge of the fused system, which would mean there should be *some* ethene-like characteristic across the carbons bridging the switch arms. The frontier molecular orbitals do not show ideal distribution, but previous cases have shown that the presence of electron-withdrawing groups on the switch makes frontier-molecular orbital interpretation inaccurate as these groups tend to dominate the LUMO. DFT calculations indicated that the LUMO for quinoxaline switches do not

have the right symmetry to proceed through cyclization (**Figure 4.4**), but the synthetic pathway (**Scheme 4.9**) was simple enough to confirm. An added benefit was the ease of which any switching motif can be incorporated into the core through the straightforward synthesis from oxalyl chloride.



Scheme 4.9 Synthesis of the Quinoxaline core, containing a benzo[b]thiophene switching motif.

Synthesis of the quinoxaline core begins with 2,1,3-benzothiadiazole, to which bromine is added extremely slowly (approximately 4 drops per minute) to form the para-dibrominated species. Faster addition rates, or an excess of bromine, resulted in the major product being the tri-brominated species. After purification, refluxing the dibrominated species in the presence of zinc in acetic acid efficiently desulfurized the heteroaromatic compound, resulting in an air stable diamine. The compound was washed several times, concentrated to dryness, and immediately dissolved in the fresh solvent for the following double Schiff base condensation with the prefunctionalized dione. It is assumed that water need not be removed during the course of the reaction due to the reestablishment of aromaticity in the system (quinoxaline core).

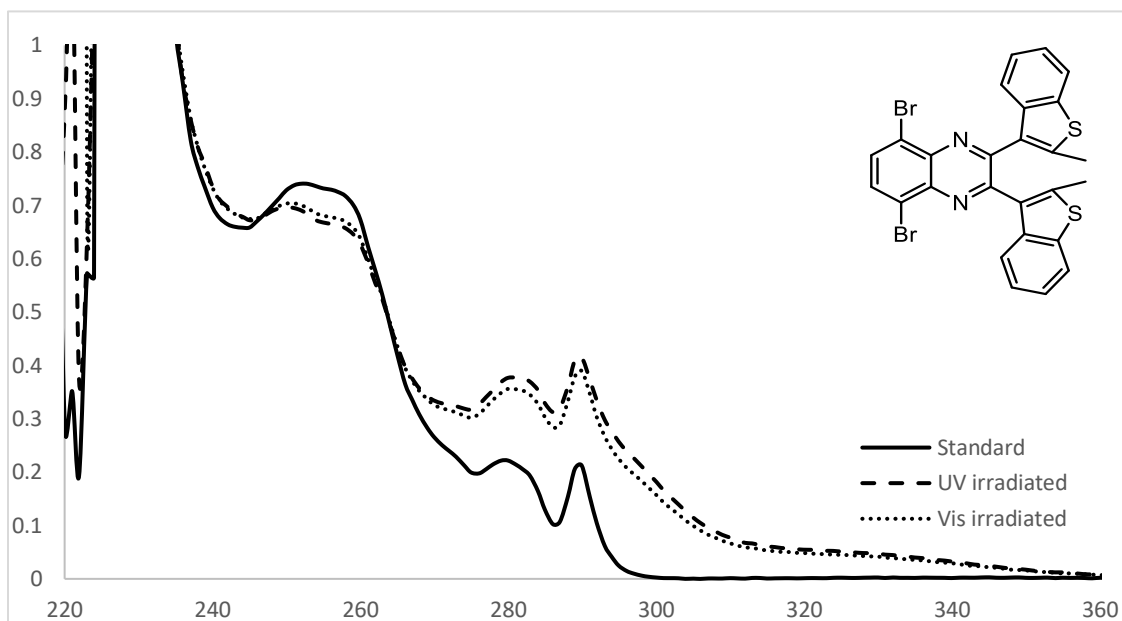
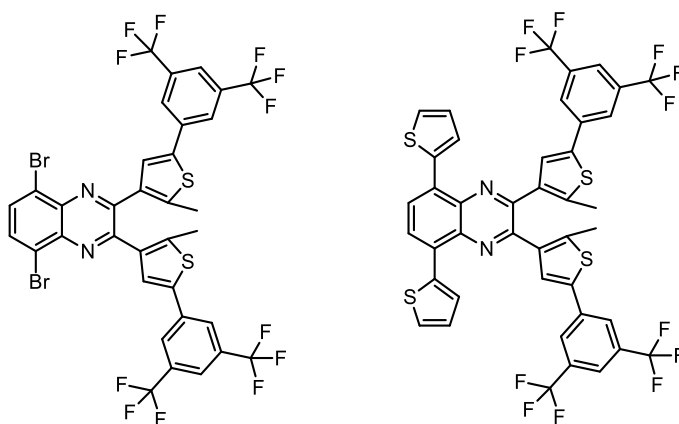


Figure 4.4 UV-Vis spectra of the quinoxaline (Q) switch core featuring benzo[b]thiophene switching motif.

The dione initially chosen contained 2-methylbenzo[b]thiophene as the switching motif. UV-Vis (**Figure 4.4**) showed possible photochromic activity due to alternating peak heights about two inflection points, but quickly decomposed, with peaks at 280 nm and 290 nm developing while a broad shoulder extending to 360 nm persisted. Focus was immediately turned to the development of a more robust switching motif. The trifluoromethylated phenyl derivatives have been demonstrated to be more fatigue resistant than benzo[b]thiophene, which was previously considered to be the most stable switching motif. The quinoxaline core was rebuilt with the new switching motif with the intent of creating a more stable core (**Scheme 4.10**). While the new quinoxaline core is *very* stable, it demonstrated no photochromic activity upon irradiation possibly due to the heavy atom effect. With this in mind, the core was functionalized with thiophene units. Unfortunately, the compound remained incapable of switching, but demonstrated very strong fluorescence and possessed a Stokes shift in excess of 200 nm. Feringa *et al.*⁴, amongst others, showed that diarylethene compounds can be made to switch through oxidation. This returns to the argument of whether or not the symmetry is correct for the cyclization to

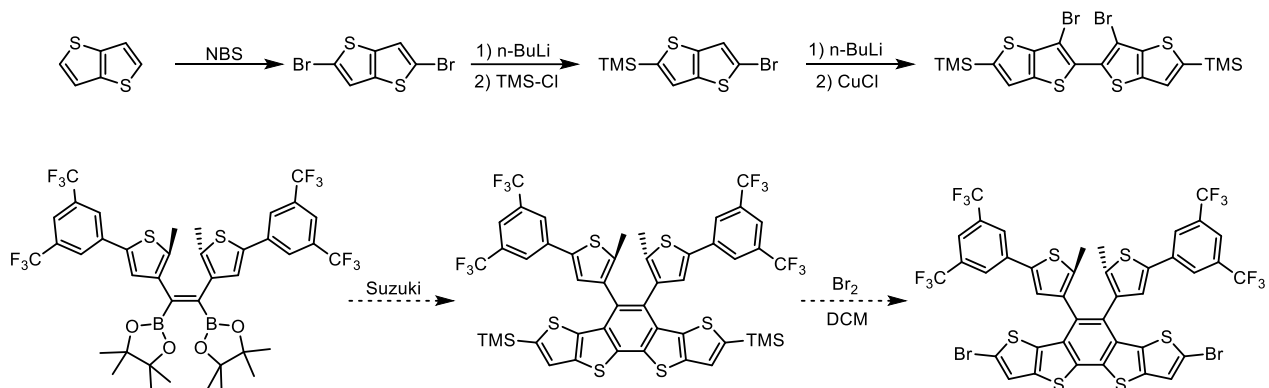
occur. While the frontier molecular orbitals for some switches may not have the right symmetry, the HOMO -1 has the orbital densities very similar to that of other model systems. The issue lies in the method of oxidation (chemical or electrochemical) and how much the species must be oxidized. Ideally, a two-electron oxidation will make the ground state HOMO-1 the new HOMO, giving the species the best orbital densities for cyclization. It may be worth exploring this switch core in the future for chemical or electrochemical switching, as opposed to photochemical cyclization.



Scheme 4.10 Bis(trifluoromethyl)phenyl switching component derivatives.

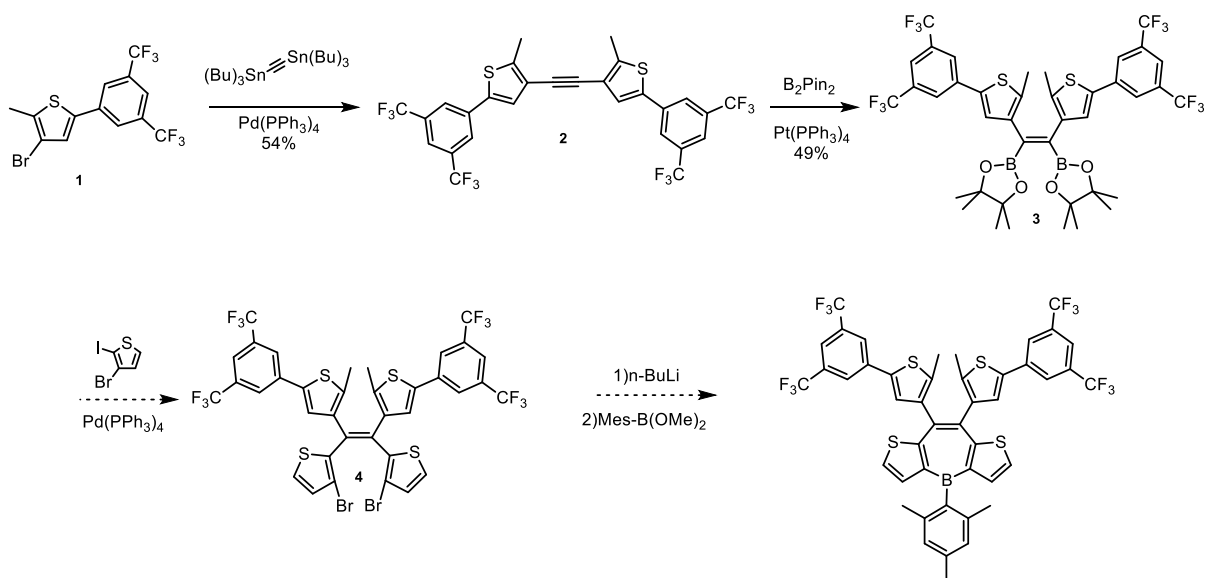
Some extended fused cores were explored that would facilitate more planarity for potential quinoidal species, with an example being dithienobenzodithiophene (**DTBDT**, **Scheme 4.11**). Almost all steps in this synthesis are literature, with the major difference being a switch-based diborylated species is incorporated instead of alkyl chains as in the literature. The diborylated quinoxaline was synthesized, but the attempted synthesis of this core yielded a white insoluble solid that was not photochromic. With the switching concept developed for **TT** in mind, it is very likely that the switching motif used in the design of this switch is not conjugated enough to compete with the low energy absorption of the switch core, especially since the fused nature of the **DTBDT** ensures planarity and effective conjugation along the “backbone”. Regardless, due to

the synthetic simplicity this switch may represent a potential switch monomer for pendant photochromic polymers.



Scheme 4.11 Proposed synthesis of switch core **DTBDT**, where the diarylethene is built from the center of the long conjugated fused acene dithienobenzodithiophene.

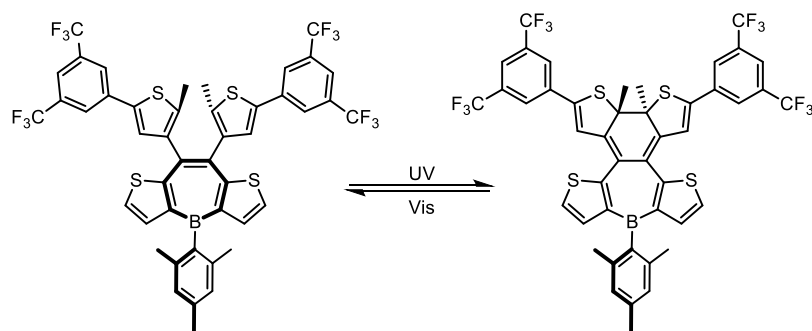
Molecules featuring non-classical aromaticity also represent interesting areas for pendant photochromic switches, as it may result in novel impacts on the π system and overall electronics of the molecule. One of the first envisioned concepts is shown in **Scheme 4.12**, where a diarylethene is built off the borepin ring in a dithienoborepin.



Scheme 4.12 Potential switch borepin, where a fatigue-resistant diarylethene switching motif is fused to a dithienoborepin.

As the aromaticity of the borepin ring may not be as high as a benzene or thiophene, cyclization may be easier as the cost of breaking aromaticity is lower. The dithienoborepins are easily di-halogenated, making this an excellent potential monomer for polymerization. In addition, this molecule may also function as a potential probe for *relative* aromaticity. There are several methods for probing the aromaticity of a compound, with some key examples being proton chemical shifts of those on the aromatic ring under investigation, and nucleus-independent chemical shift (NICS) values. It is rather difficult, however, to compare the aromaticity of a borepin to benzene or thiophene. For example, although they all feature 6π electrons and are roughly planar, they possess different ring sizes which makes comparison of NICS values rather tricky. Therefore, it may be worth it to compare the NICS values between different substituted borepins, a study that has been performed before for different fusions. An alternative method would be to compare an “aromatic” borepin to a “non-aromatic” borepin, where one of the double bonds is removed. A fused diarylethene provides this opportunity, as the bridging ethene between switching motifs is also a key double bond in the borepin system (**Scheme 4.13**). Thus, it is

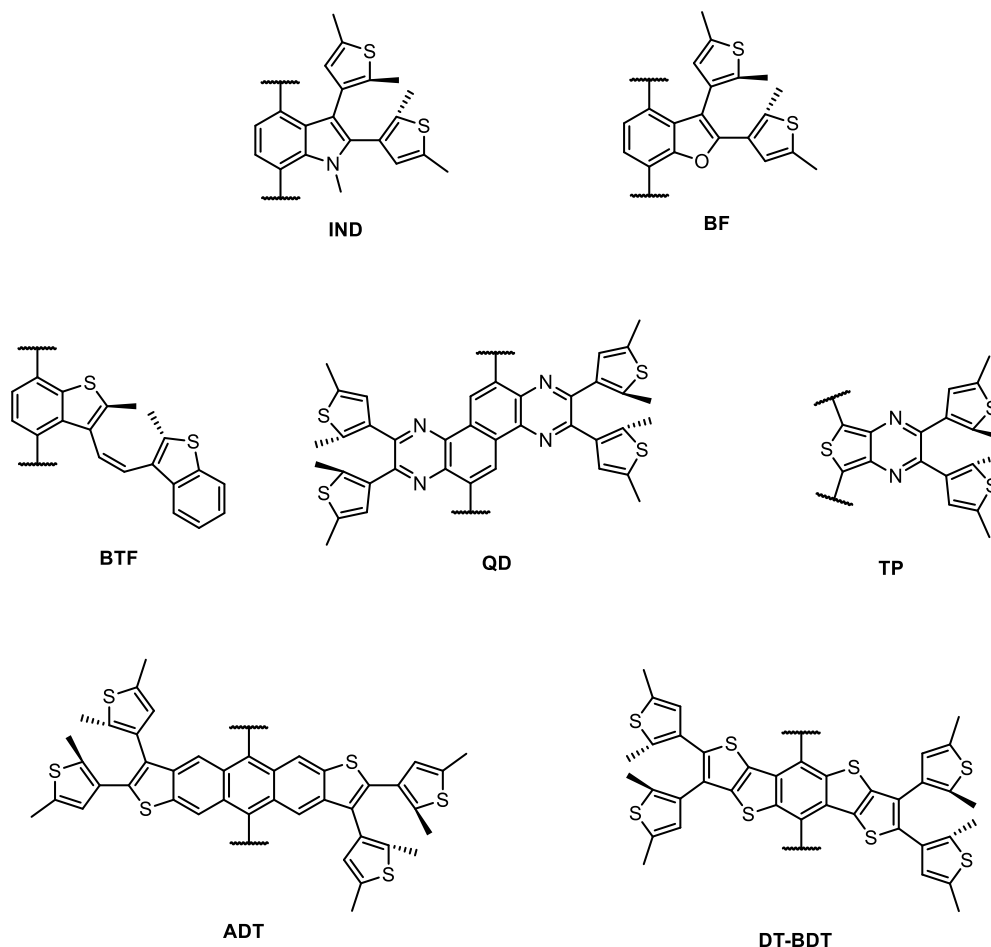
expected that the aromaticity of the borepin will be interrupted upon cyclization. Computational probes for aromaticity may provide insights into the differences in aromaticity of this borepin between open and closed structures. Other potential borepins in which substitutions do not constitute replacement of all protons along the borepin ring would allow for NMR to be used as a tool, as the chemical shift of these protons between the open and closed should also provide insight into the aromaticity. Unfortunately, this is not applicable to this ring due to the fused thiophenes and the diarylethene substitution.



Scheme 4.13 “Open” and “closed” structures for the diarylethene functionalized dithienoborepin, demonstrating the interruption of the aromaticity in the borepin core.

There are several switch concepts that were either briefly attempted or conceptually developed, but success with other switches meant these had to be placed lower on the priority list. Some of these switches are shown in **Scheme 4.14**, featuring **BT** derivatives including **IND** and **BF**, which may offer electronic differences that may affect the switch performance relative to the parent compound. **BTF** represents an interesting switch that may have three isomeric forms due to the potential for cis-trans isomerization. **QD** and **TP** present a similar situation as **Q** in that they may be another switch controlled electrochemically instead of photochemically due to the unusual bonding order in the neutral state, but ideal symmetry in an oxidized or reduced state. **ADT** and **DT-BDT'** represent a potentially interesting take on the extended conjugation issue

required to make the **TT** switches function properly. Instead of extending the conjugation along the switching arms, it may be possible to localize the transitions on an orthogonally extended fused acene containing a diarylethene motif on either ends. Here, slight rotation of the polymeric backbone may immediately favor the switching monomer due to its long conjugated system, but these are untested molecules that would need further investigation.



Scheme 4.14 Other potential pendant photochromic molecules that may prove valuable in the development of switchable polymers.

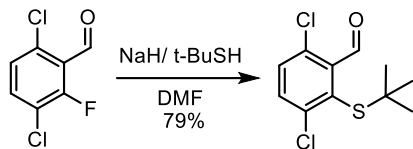
Conclusion

Several years of investigation into pendant photochromic polymers have brought many fruitful compounds to light. Although not thoroughly investigated to the extent of thieno[3,4-

b]thiophene photochromes, other switch cores involving benzo[1,2-*b*:4,5-*b'*]dithiophene and benzo[*b*]thiophene have high potential for switchable polymers. Non-traditional switch cores, such as those involving quinoxaline, may offer alternative routes to cyclization through chemical or electrochemical oxidation. Due to the simplicity of the diarylethene switching motif, it may also be possible to incorporate these photochromics into non-traditional aromatic species such as borepins. While it wasn't possible to explore all envisioned switches, several ideas are provided that lay the foundation for other potential pendant photochromes.

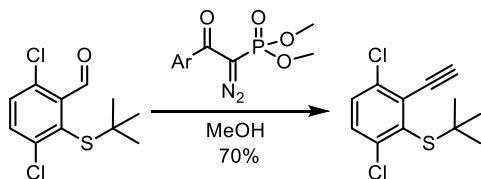
Experimental

2-(tert-butylthio)-3,6-dichlorobenzaldehyde



Sodium hydride (1.14 g, 28.5 mmol) and dry, degassed DMF (25 mL) were added to a dry 100 mL Schlenk flask. The solution was cooled to 0°C, and t-butyl thiol (2.57 g, 28.5 mmol) was added dropwise over 15 minutes. The reaction was allowed to stir at 0°C for 30 min, then cooled to -40°C. A solution of 3,6-dichloro-2-fluorobenzaldehyde (5g, 25.9 mmol) in 10 mL DMF was also cooled to -40°C, then added to the thiol solution in a constant stream via cannula. The solution was allowed to stir at -40°C for 7 hr. After warming to room temperature, the solution was poured into sat. NH₄Cl (100 mL) and extracted with diethyl ether (3x 100 mL). The organic layer was washed with brine (100 mL), dried over MgSO₄, and concentrated to a yellow oil. Product was purified via column chromatography (50:50 Hexanes:dichloromethane) to yield an oil (5.35 g, 20.3 mmol, 79% yield). ¹H NMR (400 MHz, CDCl₃): δ 10.54 (s, 1H), 7.60 (d, 1H), 7.43 (d, 1H), 1.32 (s, 9H).

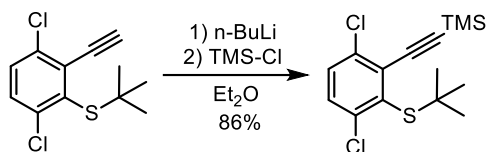
3,6-dichloro-2-(t-butylsulfanyl)(ethynyl)benzene



To a mixture of dimethyl 1-diazo-2-oxo-2-phenylethylphosphonate (1.16 g, 4.56 mmol) and K₂CO₃ (1.57 g, 11.39 mmol) in methanol (30 mL) was added a solution of 2-(tert-butylthio)-3,6-dichlorobenzaldehyde (1g, 3.79 mmol) in methanol (10 mL) at 0°C. The reaction mixture was

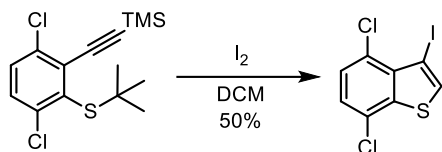
stirred at RT for 2 hr. The solution was diluted with DI H₂O (100 mL) and extracted with diethyl ether (3x 50 mL). The organic layer was washed with brine (2x 50 mL) and dried over MgSO₄, then concentrated via rotovap. Product was purified by column chromatography (70:30 hexanes:DCM) to yield a pale yellow oil (685 mg, 2.64 mmol, 70% yield). ¹H NMR (400 MHz, CDCl₃): δ 7.43 (d, 1H), 7.37 (d, 1H), 3.67 (s, 1H), 1.41 (s, 9H). ¹³C (¹H) NMR (100 MHz, CDCl₃): δ 141.3, 136.7, 136.2, 132.1, 130.8, 130.5, 88.1, 80.5, 52.7, 31.9.

((2-(tert-butylthio)-3,6-dichlorophenyl)ethynyl)trimethylsilane



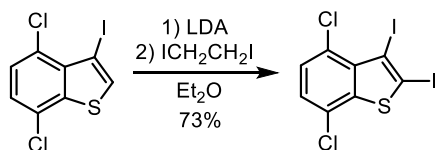
To a solution of 3,6-dichloro-2-(t-butylsulfanyl)(ethynyl)benzene (5.48g, 21.1 mmol) in dry, degassed diethyl ether (200 mL) at -78°C was added *n*-BuLi (13.6 mL, 1.63 M in hexanes) dropwise over 20 min. The solution was allowed to stir at this temperature for 0.5 h, and then chlorotrimethylsilane (2.52g, 23.2 mmol) was added dropwise over 5 min. The reaction mixture was allowed to slowly warm to room temperature over 18 h, after which it was washed twice with DI H₂O (100 mL), and once with brine (100 mL). The organic layer was dried over anhydrous MgSO₄, filtered, and concentrated under reduced pressure. The crude orange oil was purified by column chromatography (silica, 80:20 hexanes:dichloromethane) to yield the target as a yellow oil (6.36g, 19.2 mmol, 91%). ¹H NMR (400 MHz, CDCl₃): δ 7.36 (d, 1H), 7.32 (d, 1H), 1.40 (s, 3H), 0.29 (s, 3H). ¹³C (¹H) NMR (100 MHz, CDCl₃): δ 141.1, 136.4, 135.9, 133.1, 130.6, 129.9, 106.4, 101.4, 52.4, 32.0, -0.15.

4,7-dichloro-3-iodobenzo[b]thiophene



To a solution of ((2-(tert-butylthio)-3,6-dichlorophenyl)ethynyl)trimethylsilane (6.36g, 19.2 mmol) in dichloromethane (200 mL) was added iodine (9.74g, 38.4 mmol) in dichloromethane (200 mL) over 15 min. The solution was then refluxed for 72 h. The reaction mixture was allowed to cool to room temperature before washing once with sat. $\text{Na}_2\text{S}_2\text{O}_3$ (100 mL) and twice with DI H_2O (100 mL). The organic layer was dried over anhydrous MgSO_4 , filtered, and concentrated under reduced pressure. The crude product was purified by column chromatography (silica, hexanes) to yield the target as a white solid (463 mg, 1.41 mmol, 50%). ^1H NMR (400 MHz, CDCl_3): δ 7.79 (s, 1H), 7.36 (d, 1H), 7.29 (d, 1H).

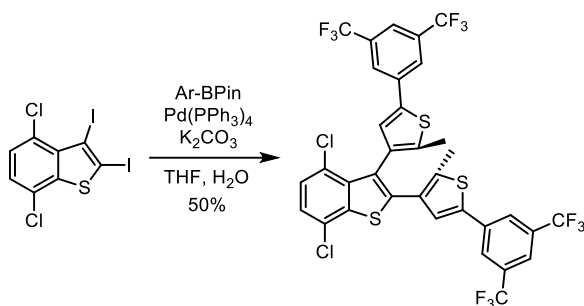
4,7-dichloro-2,3-diiodobenzo[b]thiophene



To a solution of 4,7-dichloro-3-iodobenzo[b]thiophene (50. mg, 0.15 mmol) in diethyl ether (5 mL) at -78°C was added lithium diisopropylamine (0.50 mL, 0.33 M in hexanes) dropwise over 1 min. The reaction mixture was allowed to stir at this temperature for 2 h, and then 1,2-diiodoethane (52 mg, 0.18 mmol) was added in one portion. The reaction mixture was then allowed to warm to room temperature over 18 h, and after diluting with diethyl ether to 25 mL, the mixture was washed twice with DI H_2O (25 mL) and once with brine (25 mL). The organic layer was dried over anhydrous MgSO_4 , filtered, and concentrated under reduced pressure. The

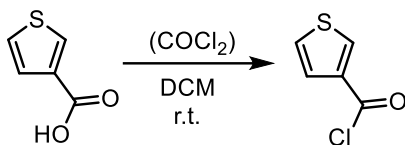
off-white solid was purified by column chromatography (silica, hexanes) to yield the product as a white solid (50. mg, 0.11 mmol, 73%). ^1H NMR (400 MHz, CDCl_3): δ 7.36 (d, 1H), 7.23 (d, 1H).

2,3-bis(5-(3,5-bis(trifluoromethyl)phenyl)-2-methylthiophen-3-yl)-4,7-dichlorobenzo[b]thiophene (BT- CF_3)



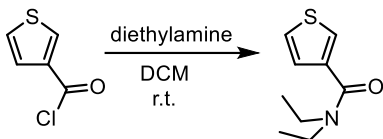
4,7-dichloro-2,3-diiodobenzo[b]thiophene (237 mg, 0.521 mmol), CF_3 boronate ester (500 mg, 1.15 mmol), and $\text{Pd(PPh}_3)_4$ (15.0 mg, 1.30×10^{-5} mol) were added to a 50 mL Schlenk flask, which was evacuated and backfilled with N_2 three times. THF (20 mL) and sat K_2CO_3 solution (10 mL) were added, and the reaction mixture was refluxed for 24 h. At this point, an equivalent amount of $\text{Pd(PPh}_3)_4$ was added, and the mixture was refluxed for another 24 h. The mixture was diluted with diethyl ether (25 mL), washed twice with DI H_2O (30 mL) and once with brine (30 mL). The organic layer was dried over anhydrous MgSO_4 , filtered, and concentrated under reduced pressure. The yellow solid was purified by column chromatography (80:20 hexanes:DCM) to yield the product as a slightly yellow solid (211 mg, 0.257 mmol, (50%). ^1H NMR (400 MHz, CDCl_3): δ 7.92 (s, 2H), 7.73 (s, 1H), 7.72 (s, 2H), 7.69 (s, 1H), 7.36 (d, 1H), 7.33 (s, 1H), 7.33 (d, 1H), 6.98 (s, 1H), 2.56 (s, 3H), 2.13 (s, 3H). HRMS (EI) found $m/z = 432.0127$ (M^+), calculated for $\text{C}_{34}\text{H}_{16}\text{Cl}_2\text{F}_{12}\text{S}_3$: 817.9600.

thiophene-3-carbonyl chloride



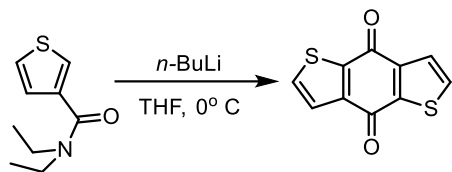
A 100 mL round-bottom flask was charged with thiophene-3-carboxylic acid (10 g, 78.03 mmol) and dichloromethane (DCM, 16 mL) and submerged in a 0°C cooling bath. Oxalyl chloride (13.4 mL, 156.60 mmol) was added in one portion, and the mixture was allowed to stir at room temperature overnight. The mixture was concentrated via rotovap, dissolved in DCM (26 mL), and used in the next step without further purification. ¹H NMR (400 MHz, CDCl₃): δ 8.37 (d, 1H), 7.57 (d, 1H), 7.39 (d, 1H).

N,N-diethylthiophene-3-carboxamide



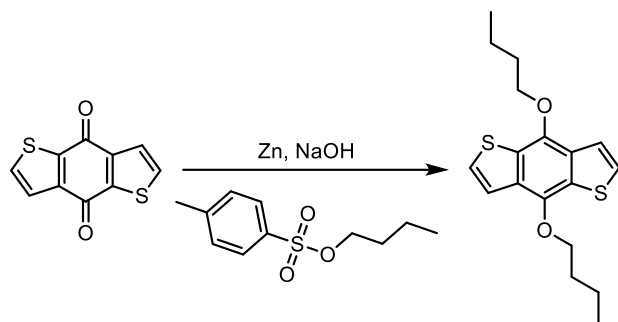
A 200 mL pear-bottom flask was charged with diethylamine (16.2 mL, 156.6 mmol) and DCM (26 mL), and submerged in a 0°C cooling bath. Thiophene-3-carbonyl chloride (26 mL solution prepared previously) was added dropwise over 20 minutes. The mixture was then allowed to stir at room temperature for 45 min. The resulting solution was washed with water (200 mL) and dried over MgSO₄. After concentrating, the amide was purified by vacuum distillation (40 mtorr, 110°C) to yield a pale pink oil (12.82 g). ¹H NMR (400 MHz, CDCl₃):

4,8-dihydrobenzo[1,2-b:4,5-b']dithiophene-4,8-dione



A 500 mL round-bottom flask was charged with N,N-diethylthiophen-3-carboxamide (12.82 g, 69.96 mmol) and tetrahydrofuran (THF, 70 mL), and the mixture was submerged in a 0°C cooling bath. *n*-butyllithium (*n*-BuLi, 37 mL, 1.6 M in hexane) was added dropwise over 20 minutes, and the resulting dark red solution was allowed to stir at room temperature for 30 min. The reaction mixture was then poured into ice cold water (170 mL) and allowed to stir overnight. The crude product was filtered and washed, sequentially, with DI H₂O (200 mL), methanol (MeOH, 20 mL), and hexane (20 mL). The product was finally dried under reduced pressure (50 mtorr) overnight to yield a yellow powder (2.86 g). ¹H NMR (400 MHz, CDCl₃): δ 7.67 (d, 2H), 7.55 (d, 2H).

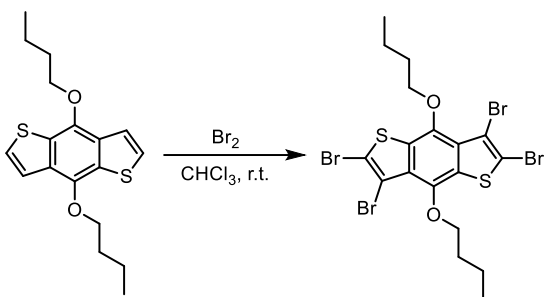
4,8-bis(butoxy)benzo[1,2-b:4,5-b']dithiophene



A 100 mL pear-bottom flask was charged with 4,8-dihydrobenzo[1,2-b:4,5-b']dithiophene-4,8-dione (1.00 g, 4.54 mmol) and zinc dust (0.66g). NaOH (15 mL, 20% w/v in DI H₂O) and ethanol (EtOH, 4 mL) were added, and the mixture was allowed to reflux for 1 h. Through the reflux condenser, butyl p-toluenesulfonate (3.75 mL) was added, and the reaction mixture was allowed to cool to room temperature. The solution was filtered, and the filtrate was poured into DI H₂O (200 mL), followed by extraction with CHCl₃ (100 mL). After concentrating the solution, the

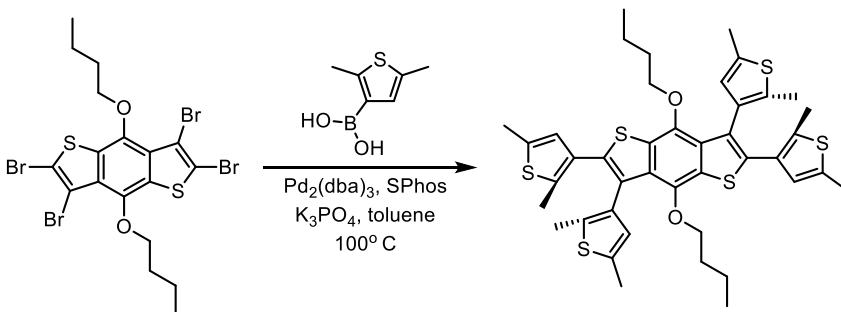
product was purified by flash column chromatography (75:25 hexane:DCM), and a pale oil (812.5 mg) was obtained. ^1H NMR (400 MHz, CDCl_3): δ 7.47 (d, 2H), 7.36 (d, 2H), 4.28 (t, 2H), 1.87 (p, 2H), 1.61 (sex, 2H), 1.01 (t, 3H). MS (nominal): 334.1 Calcd: 334.1061.

2,3,6,7-tetrabromo-4,8-bis(butoxy)benzo[1,2-b:4,5-b']dithiophene



A 100 mL pear-bottom flask was charged with 4,8-bis(butoxy)benzo[1,2-b:4,5-b']dithiophene (812.5 mg, 2.43 mmol) and CHCl_3 (23 mL) and wrapped with aluminum foil. A bromine solution (0.77 mL Br_2 in 6 mL CHCl_3) was added dropwise over 15 minutes at room temperature, and the solution was allowed to stir in the dark overnight. The reaction mixture was then poured into saturated sodium thiosulfate solution (30 mL), and extracted with DCM (45 mL). After concentrating under reduced pressure, the crude solid was purified by flash column chromatography (90:10 hexane:DCM) to yield a white powder (1.14 g). ^1H NMR (400 MHz, CDCl_3): δ 4.14 (t, 3H), 1.93 (p, 2H), 1.61 (sex, 2H), 1.03 (t, 3H).

4,8-dibutoxy-2,3,6,7-tetrakis(2,5-dimethylthiophen-3-yl)benzo[1,2-b:4,5-b']dithiophene



To a 25 mL pear-bottom flask, 2,3,6,7-tetrabromo-4,8-bis(butoxy)benzo[1,2-b:4,5-b']dithiophene (38.2 mg, 0.06 mmol), 2,5-dimethylthien-3-yl boronic acid (55 mg, 0.35 mmol), Pd₂(dba)₃ (8.7 mg, 4 mol%), S Phos (7.7 mg, 8 mol%), and K₃PO₄ (150.4 mg, 0.18 mmol) were added, and the flask was evacuated and backfilled with nitrogen three times. Toluene (2 mL) was added, and the mixture was submerged in a 100°C heating bath. After stirring for 72 hours, the reaction was cooled to room temperature and Et₂O (10 mL) was added. The mixture was passed through a coarse frit with a thin layer of silica (Et₂O as the eluent). The filtrate was concentrated to dryness, and the product was purified by flash column chromatography (70:30 hexane:DCM) to yield an orange solid (11.2 mg). MS (nominal): 774.2 Calcd: 774.1822.

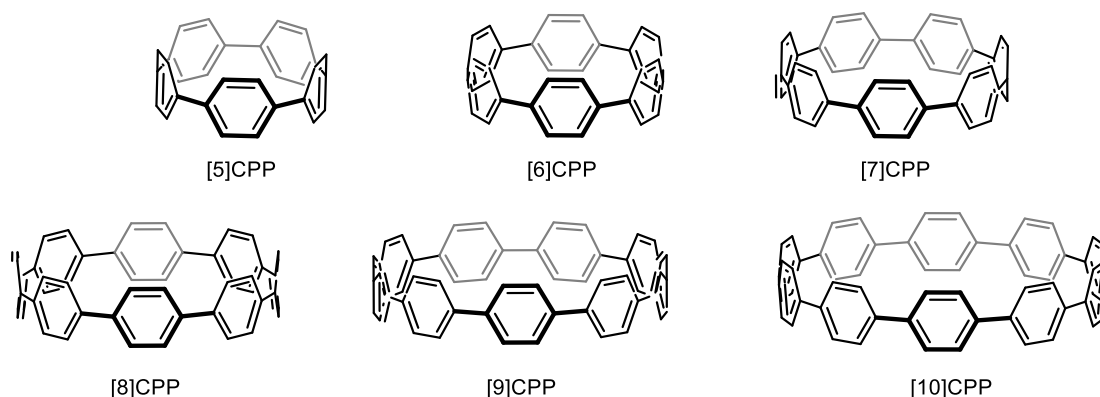
References

1. Liang, Y. Y.; Feng, D. Q.; Wu, Y.; Tsai, S. T.; Li, G.; Ray, C.; Yu, L. P. Highly Efficient Solar Cell Polymers Developed via Fine-Tuning of Structural and Electronic Properties. *Journal of the American Chemical Society* **2009**, *131* (22), 7792-7799.
2. Colletto, C.; Islam, S.; Juliá-Hernández, F.; Larrosa, I. Room-Temperature Direct β -Arylation of Thiophenes and Benzo[b]thiophenes and Kinetic Evidence for a Heck-type Pathway. *Journal of the American Chemical Society* **2016**, *138* (5), 1677-1683.
3. Yamamoto, T.; Katsuta, H.; Toyota, K.; Iwamoto, T.; Morita, N. Preparation of 4,7-Dibromobenzo[b]thiophene as a Versatile Building Block and Synthetic Application to a Bis(ethynylthienyl)oligoarene System. *Bulletin of the Chemical Society of Japan* **2012**, *85* (5), 613-623.
4. Browne, W. R.; de Jong, J. J. D.; Kudernac, T.; Walko, M.; Lucas, L. N.; Uchida, K.; van Esch, J. H.; Feringa, B. L. Oxidative Electrochemical Switching in Dithienylcyclopentenes, Part 2: Effect of Substitution and Asymmetry on the Efficiency and Direction of Molecular Switching and Redox Stability. *Chemistry – A European Journal* **2005**, *11* (21), 6430-6441.

CHAPTER V

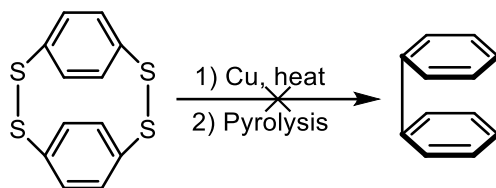
Synthesis and Characterization of Conjugated Copolymers involving Cycloparaphenylenes

[n]Cycloparaphenylenes ([n]CPPs) and other curved aromatic molecules can be thought of as diametral segments of (n,n) armchair carbon nanotubes (**Scheme 5.1**). More specifically, CPPs feature strained *para*-linked phenylenes in which the p-orbitals are distributed radially, allowing for new topological π interactions compared to planar counterparts (oligo- and polyphenylenes).



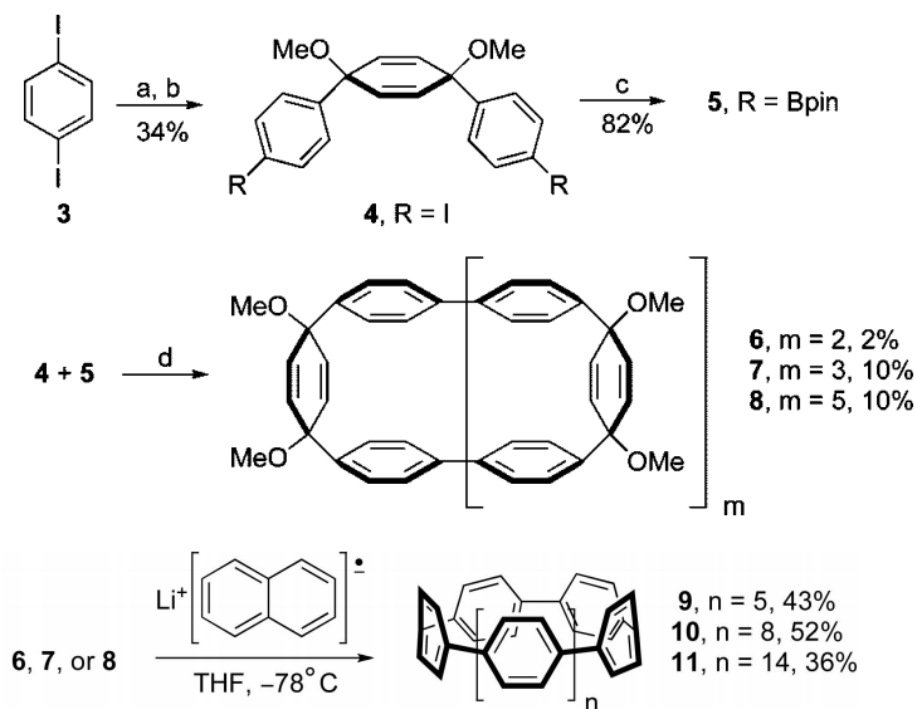
Scheme 5.1 Structures of [5]-[10] cycloparaphenylenes (CPPs), depicting para-linked benzenes in a hoop-like structure.

The earliest synthetic attempts towards these hoop-like molecules were those by Parekh and Guha, where [2]CPP was attempted by sequential desulfurization (**Scheme 5.2**).¹ The synthetic strategy involves forming the unstrained macrocycle first, which contains para-linked benzenes, and then progressively removing intermediate functionalities while simultaneously introducing the strain associated with bending sp^2 hybridized centers out of plane. While the smaller CPPs may appear far too strained and electronically congested (via superimposed π -electrons) to be synthesized, such as [2]-[4]CPP, this work proposed a reasonable synthetic concept that would later be generalized to larger CPP's by Vögtle *et. al.* almost six decades later.²



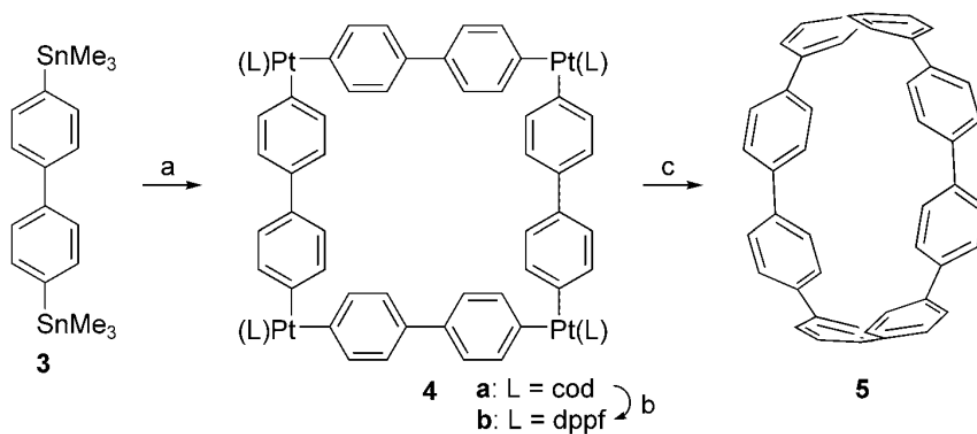
Scheme 5.2 Attempted synthesis of [2]CPP via two routes of desulfurization, proposed by Parekh and Guha in 1934.

Unfortunately, the desulfurization method proved fruitless, and it wasn't until 2008 and later that other synthetic methods were developed that led to the realization of CPPs of various sizes.³ The first synthesis was reported by Jasti and Bertozzi, where [9]-, [12]-, and [18]CPP were prepared in good yields (**Scheme 5.3**). This route is somewhat similar to that proposed by Parekh and Guha in that the macrocycle was formed first, featuring both benzenes and cyclohexadienes. The cyclohexadiene allows for the relief of ring strain due to the sp^3 hybridized linkages, featuring alkoxy substituents as the fourth substitution. These alkoxy substituents are then removed during a final reductive aromatization to produce the first reported cycloparaphenylenes. In the following year, Itami and coworkers used a similar approach to synthesize [12]CPP, in that it also involved a strain-reduced macrocyclization with sp^3 -hybridized centers and a final reductive aromatization, but the synthetic pathway taken formed only [12]CPP specifically.⁴



Scheme 5.3 Synthesis of [9], [10], and [11]CPP reported by Jasti and Bertozzi in 2008. Reagents and conditions: (a) (i) *n*-BuLi, THF, -78°C , (ii) benzoquinone; (b) (i) NaH, THF, 0°C , (ii) MeI, 0°C to rt; (c) (i) *n*-BuLi, THF, -78°C , (ii) isopropyl pinacol borate (Bpin), -78°C ; (d) Pd(PPh₃)₄, Cs₂CO₃, toluene/methanol (10:1), 80°C . [Adapted from reference 5.3]

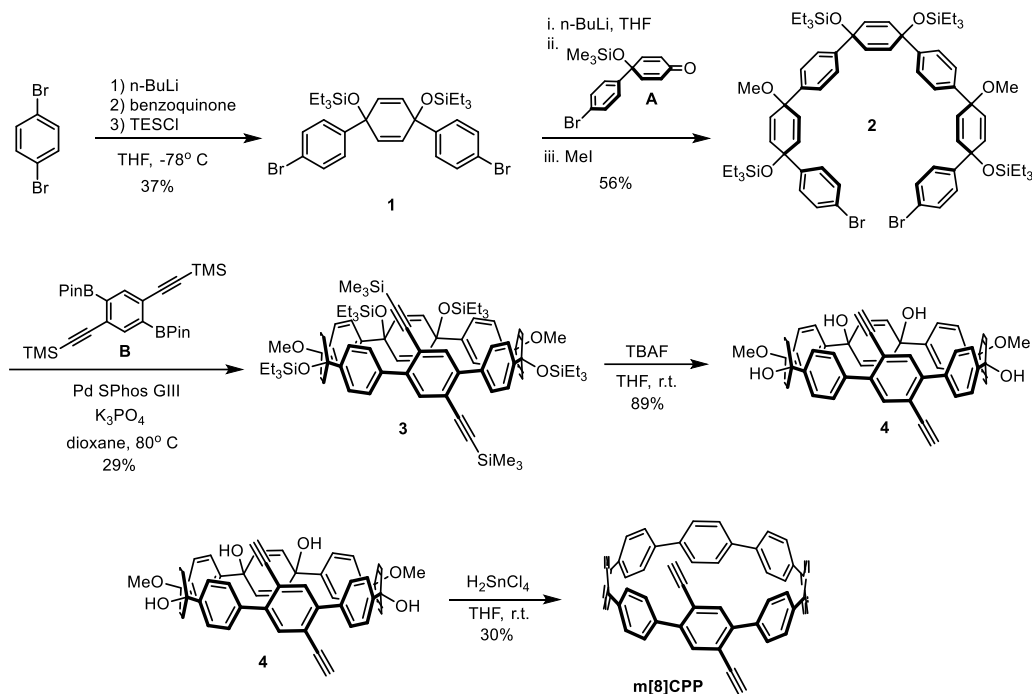
Yamago *et. al.* later reported a novel route towards CPPs that also involved assembly of a relatively strain-free macrocycle prior to the completion of the CPP (**Scheme 5.4**).⁵ In this case, all of the rings are already aromatized, and the ring strain is instead relieved by complexation with platinum centers, allowing the molecule to adopt a square shape. A bromine-induced reductive elimination was utilized to produce the completed macrocycle [8]CPP in 49% yield.



Scheme 5.4 Synthesis of [8]CPP from a square-shaped platinum complex a) $[\text{PtCl}_2(\text{cod})]$ (1 equiv), THF, reflux, 35 h, 57%. b) dppf (4.0 equiv), CH_2Cl_2 , RT, 20 h, 91%. c) Br_2 (7 equiv), toluene, 95°C , 17 h, 49%. [Adapted from reference 5.5]

These syntheses of [n]CPPs in have catalyzed several investigations into the properties and applications of these curved systems including in-plane aromaticity, strain-assisted reactivity, and supramolecular complexes. These and many other studies demonstrate that atomic control over [n]CPP structure allows for new architectures and reactivities beyond models for graphene-like derivatives. Despite all of these advances, the use of CPP radial conjugation has not been utilized in the design of pi-conjugated polymeric materials, where the nature of the pi-electron circuit plays a critical role in the nature of the resulting electronic properties. Given that radical ions created within CPPs are known to delocalize partially or entirely around the cyclic frameworks depending on the molecular size, we felt this would be an attractive motif to extend delocalization in conjugated polymer systems whereby excitons or charge carriers would freely migrate along the linear pi-conjugated backbone as well as radially through the CPP structure. This combination of radial and linear conjugation could open up new possibilities for inter-polymer energy migration or even supramolecular sensing schemes that blend the molecular selectivity expected for CPPs with the sensitivity enhancements known for pi-conjugated electronic sensors.

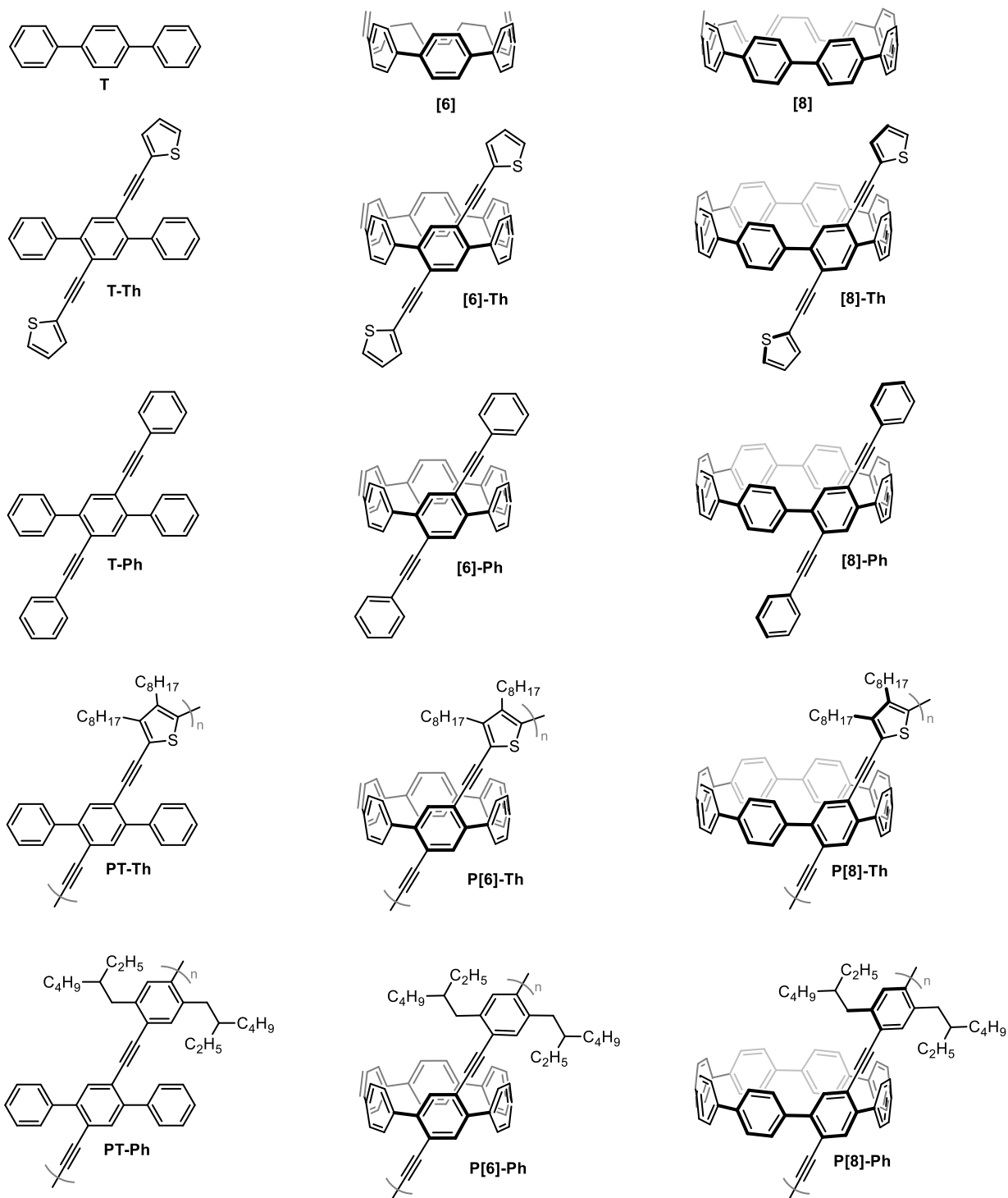
Recently, unpublished synthetic efforts by the Jasti lab have allowed for late-stage functionalization of macrocycle intermediates towards [6]- and [8]CPP, allowing for a *para*-substituted dialkyne motif to be imparted onto the structure prior to final reductive aromatization to generate **m[6]** and **m[8]**, respectively (Scheme 5.5).



Scheme 5.5 Representative synthesis of **m[8]** designed by the Jasti lab, featuring macrocyclization with a dialkyne-functionalized benzene prior to deprotection and aromatization.

Model compound **mT** was synthesized as a “linear” analogue of **m[6]** and **m[8]** to observe the change in photophysical properties of having a curved system present. The dialkynylated terphenyl model system **mT** was prepared with relative ease starting from 1,4-dibromo-2,5-diiodobenzene, which was subjected to double Suzuki cross coupling with iodine selectivity to assemble the terphenyl core. Subsequent Sonogashira cross coupling and deprotection allowed access to the terphenyl monomer. With the three monomers **mT**, **m[6]**, and **m[8]** in hand, further π -extension was accomplished through Sonogashira cross coupling

reactions to obtain a series of both “oligomeric” and polymeric linear and curved conjugated systems (**Scheme 5.6**). While these reactions performed well, there was a fair amount of insoluble compound obtained from the polymerization reactions. This insoluble material was similar in appearance to the soluble polymers reported here, and potentially represents higher molecular weight material that may have been crosslinked during polymerization.



Scheme 5.6 Linear and curved oligomeric and polymeric species investigated in this study, involving π extension through the incorporation of alkynes and either thiophene or benzene rings.

The model systems were first studied to determine the expected effect of extending π conjugation along the alkyne path with a planarizable orthogonal conjugated system present (**Figure 5.1**). The core terphenyl species (**T**) features a major absorbance ($\lambda_{\text{max}} = 281 \text{ nm}$) corresponding to the longest conjugation pathway across the three phenylene moieties. π -extension with phenylacetylene substituents (**T-Ph**) led to a new lower-energy absorbance ($\lambda_{\text{abs}} = 334 \text{ nm}$) corresponding to the new longest conjugation pathway while still retaining the high-energy absorbance of the orthogonal terphenyl system ($\lambda_{\text{abs}} = 281 \text{ nm}$) coincident with that of **T**. A further bathochromic shift was observed upon polycondensation to yield the analogous polymer **PT-Ph**, whose major absorbance ($\lambda_{\text{max}} = 392 \text{ nm}$) now extends into the visible region, while the absorbance attributed to the terphenyl moiety remains prominent ($\lambda_{\text{abs}} = 285 \text{ nm}$). Similar energetic trends are observed when π -extension is accomplished with thiophene to generate **T-Th** and **PT-Th**. In the thiophene-containing series, however, increase in conjugation is accompanied by a substantial decrease in molar attenuation of the higher-energy terphenyl absorbance relative to that of the conjugated backbone.

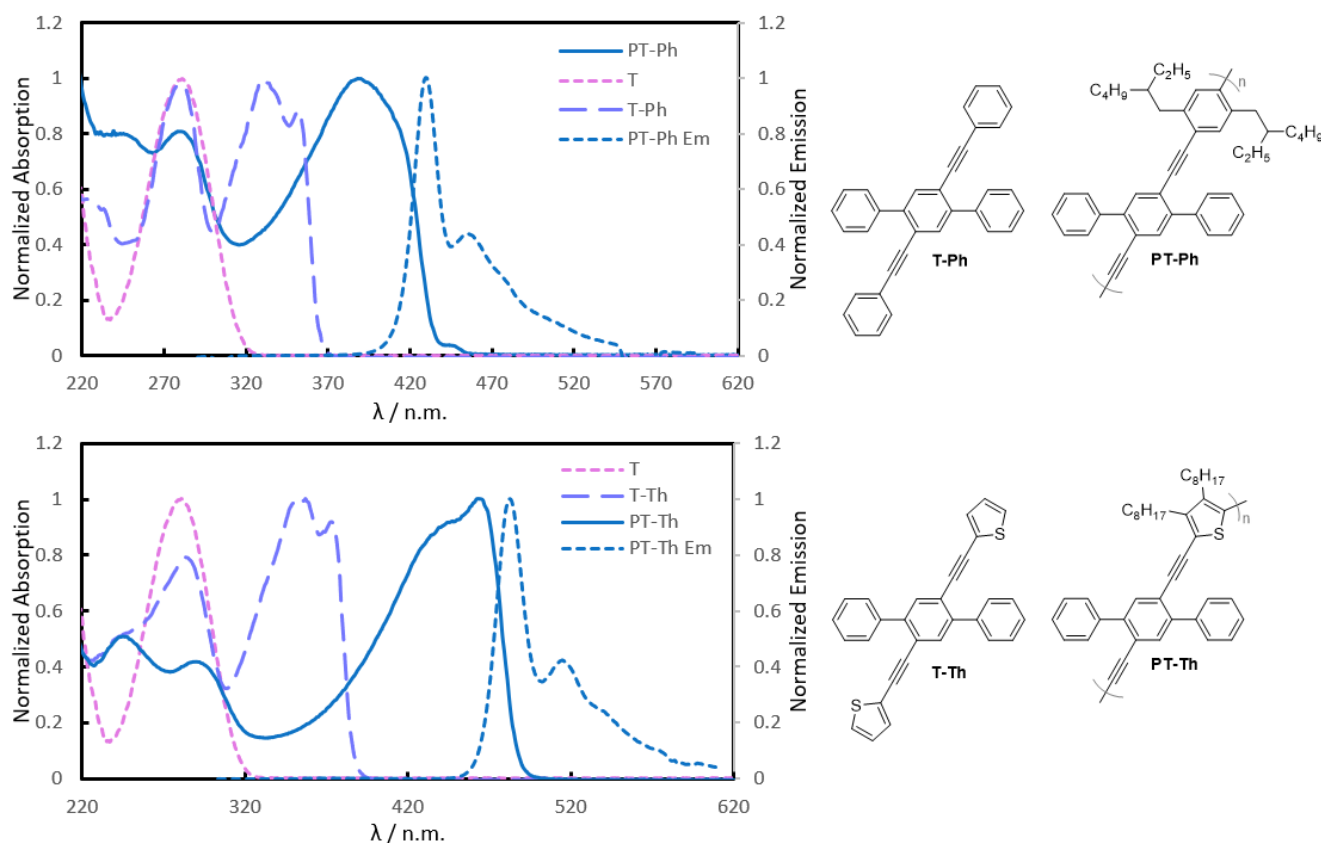


Figure 5.1 UV-Vis absorptions of model terphenyl species with π -extensions, and photoluminescence spectra for polymers.

Extension of conjugation in **m[6]** and **m[8]** along the alkyne-containing pathway was also an amalgamation of the orthogonal π -systems, but with subtle differences (**Figure 5.2**). In general, [n]CPPs have a characteristic absorbance at roughly the same energy ($\lambda_{\text{abs}} \approx 340$ nm) regardless of size. This corresponds to HOMO -1 and HOMO-2 to LUMO, or HOMO to LUMO+1 or LUMO+2 transitions, as the HOMO-LUMO transition is for the most part forbidden.⁶ Diarylated monomers **[6]-Ph** and **[6]-Th** possessed broadened absorbances that encompasses the absorbance main CPP absorbance, though **[6]-Ph** has a more pronounced blue-shift ($\lambda_{\text{max}} = 322$ nm and $\lambda_{\text{max}} = 338$ nm, respectively). Smaller CPPs, As in **[6]**, feature a low energy absorption ($\lambda_{\text{abs}} = 462$ nm). Yamago *et. al.* proposes that this may be a minor contribution from the HOMO-LUMO transition.⁶ Both **[6]-Ph** and **[6]-Th** also have this feature, though now it is bathochromically shifted ($\lambda_{\text{abs}} = 475$ nm) with increased molar absorptivity. **[8]-Ph** and **[8]-Th**

demonstrated a more pronounced blue-shift compared to parent CPP [8] ($\lambda_{\text{max}} = 321$ nm and $\lambda_{\text{max}} = 329$ nm vs $\lambda_{\text{max}} = 338$, respectively). The low-energy shoulder seen in [8] may still be present in [8]-Ph and [8]-Th, but possibly concealed by the broad net absorption of the systems.

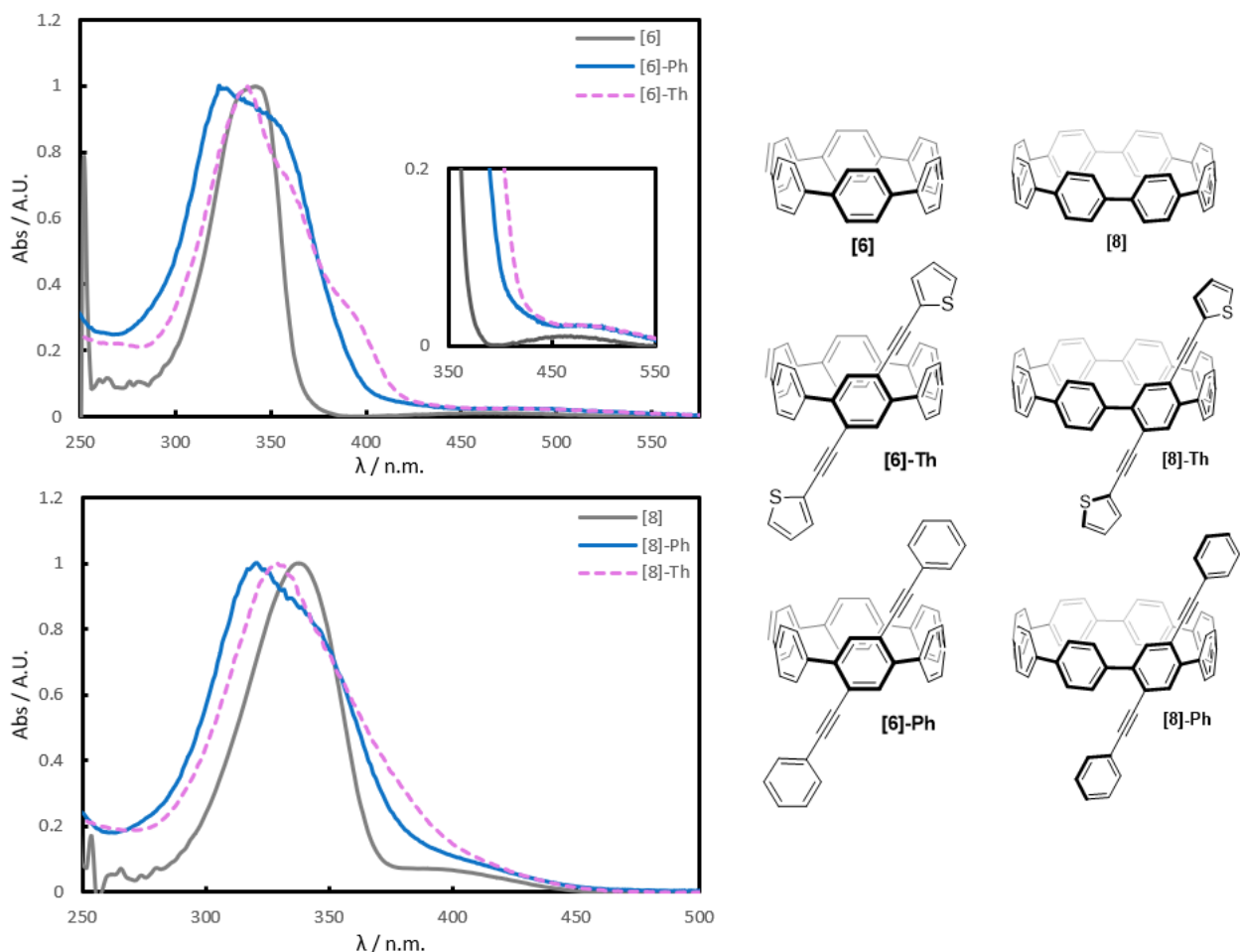


Figure 5.2 UV-Vis spectra for oligomeric [6]- and [8]CPP units in comparison with the respective core ring structure.

The broadness of the absorptions can be attributed to the superimposition of the alkyne-containing linear system with that of the macrocycle. The diphenylated CPPs [6]-Ph and [8]-Ph appears to have stronger contributions from the linear segment compared to thienylated species [6]-Th and [8]-Th, where CPP is clearly the major contributor (Figure 5.3).

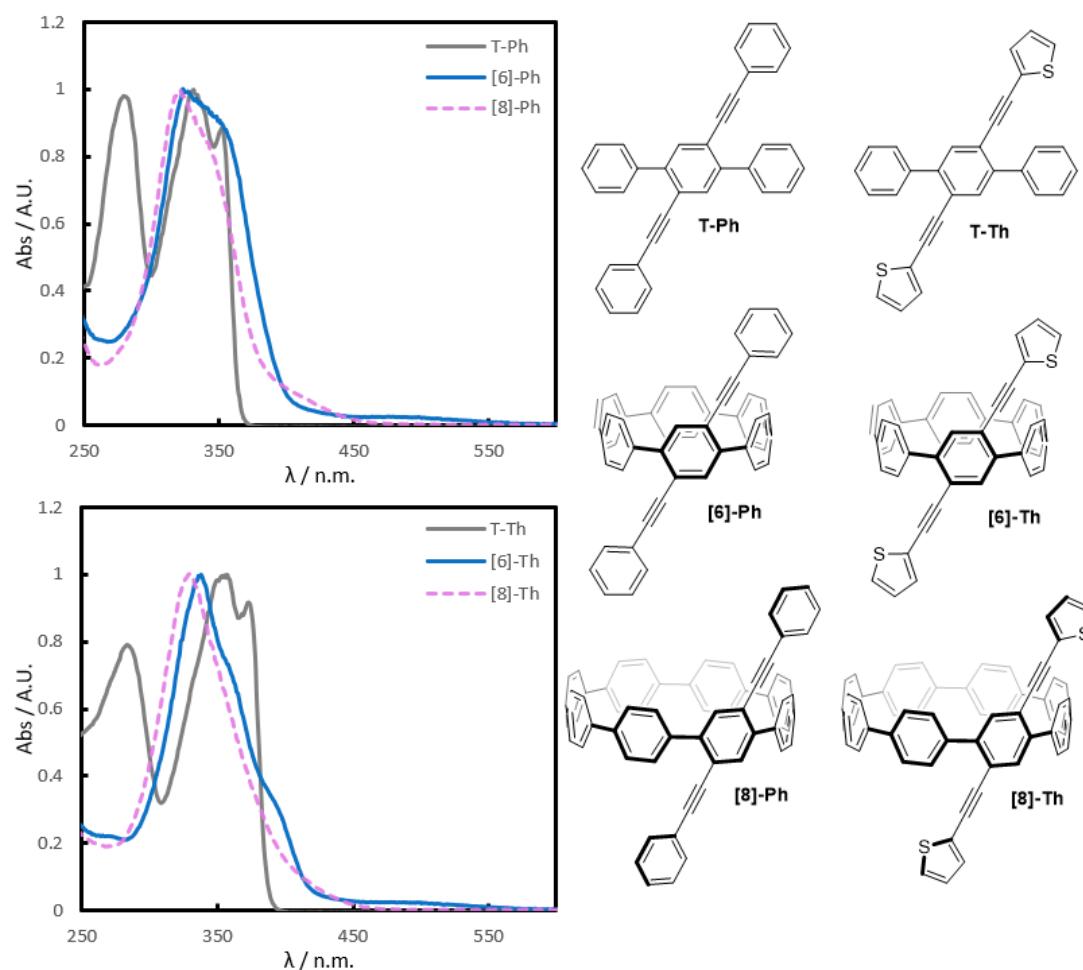


Figure 5.3 UV-Vis spectral comparison for both the di-phenylated and di-thienylated models and core CPPs.

Photoluminescence data was also collected for the oligomeric models (**Figure 5.4**).

Overall, [6]CPP derivatives demonstrated very little fluorescence compared to their [8]CPP counterparts. According to the Laporte selection rule, transitions are forbidden in molecules that contain a high degree of centrosymmetry in the molecular orbital topology of the HOMO and LUMO. This is true for smaller CPP cores (fewer than seven phenylene units). It was hypothesized that both the dialkyne substitution and further π -extension through cross coupling reactions would break the highly symmetric nature of [6]CPP's frontier molecular orbitals. This was not the case, however, as both [6]-Ph and [6]-Th demonstrated little to no fluorescence.

[8]CPP, which has enough phenylene rings to break centrosymmetry (more than six phenylene units) is in fact fluorescent, and this is retained in the substituted species.

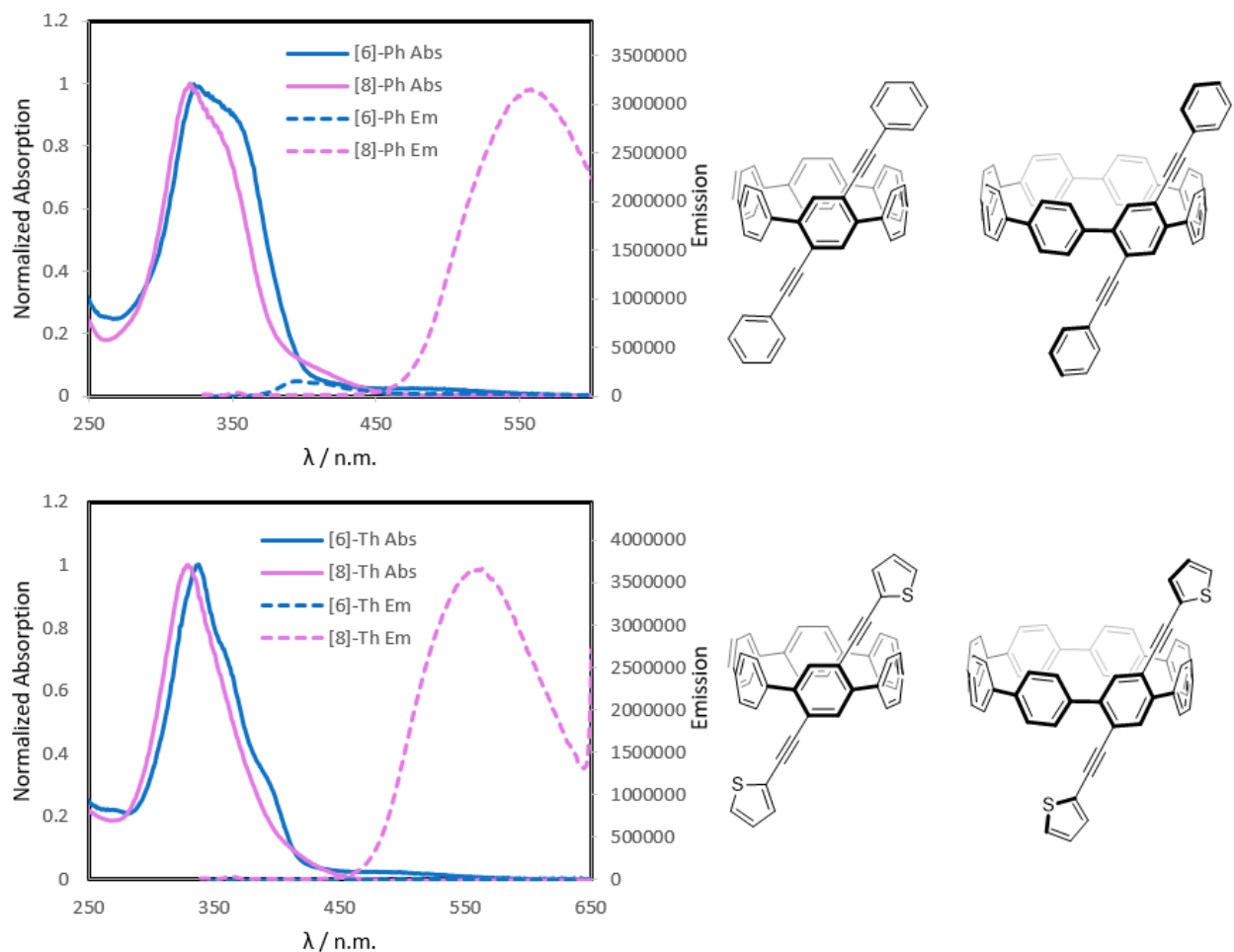


Figure 5.4 Absorption and emission spectra for both the phenylated and thienylated [6]- and [8]CPP cores, where [6]CPP species demonstrate very minimal fluorescence.

Short π -extensions through addition of benzene or thiophene on the dialkynylated core had subtle impacts on the photophysical response of the species, and one would expect these to be built upon once polymerized. **m[6]** and **m[8]** were polymerized with either a dialkylated phenyl or thienyl co-monomer. In the model species **PT-Ph**, the maximum absorbance ($\lambda_{\text{abs}} = 389$ nm) is related to the conjugated backbone of the polymer, while the higher-energy transitions are attributed to the terphenyl moiety. **P[6]-Ph** possessed an intense absorbance ($\lambda_{\text{abs}} = 348$ nm) which correlates with the pendant macrocycle along the polymer backbone (**Figure 5.5**). A low-energy

shoulder on this peak ($\lambda_{\text{abs}} = 338 \text{ nm}$) was also present, though one can attribute this to the conjugated polymer backbone. While the shoulder is further red-shifted compared to that of the model polymer, this can simply be attributed to differences in the extent of polymerization where **P[6]-Ph** features longer polymer chains. The analogous polymer for thiophenes **P[6]-Th** was also synthesized and demonstrated similar photophysical response, though now the transition corresponding to the alkyne-containing conjugated pathway is more coincident with that of the model species **PT-Th**.

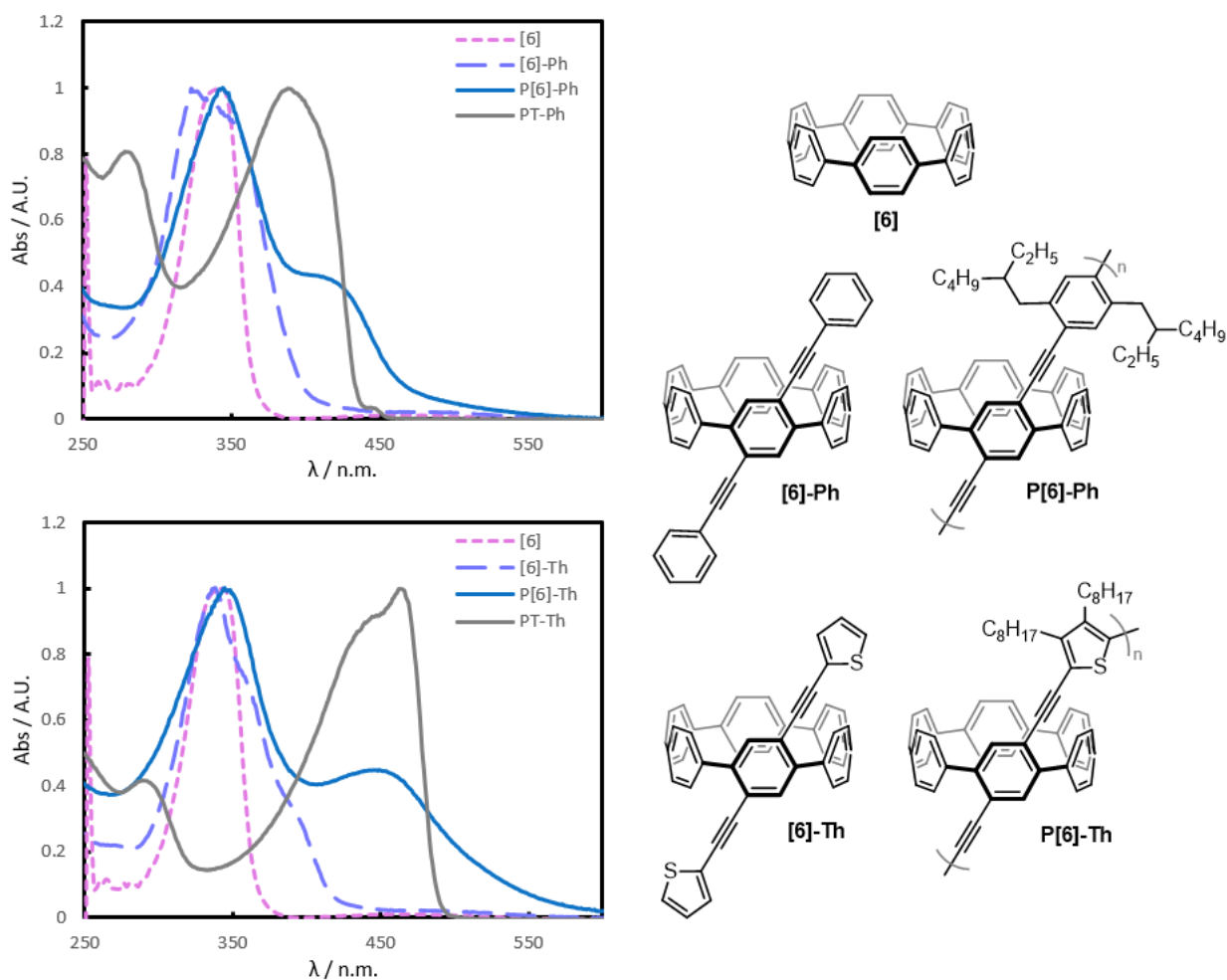


Figure 5.5 Absorption spectra bare and functionalized [6]CPP cores illustrating the impact of gradually extending the orthogonal conjugated system.

As with [6]CPP containing polymers **P[6]-Ph** and **P[6]-Th**, there is little change in the energy of the major transition upon polymerization of **m[8]** (Figure 5.6). Both **P[8]-Ph** and **P[8]-Th** contain a characteristic transition corresponding to the macrocycle seen in all CPPs and the main polymer backbone, with variances in the latter due to the extent of polymerization. Since the low energy shoulder associated with [8]CPPs extends to a lesser degree into the visible region than [6]CPP, it is more effectively masked by the absorbance of the polymer. It is difficult to say if the low energy shoulder belonging to core CPPs is affected by polymerization of **m[6]** or **m[8]**, as it is dwarfed by the polymer absorbance in all cases.

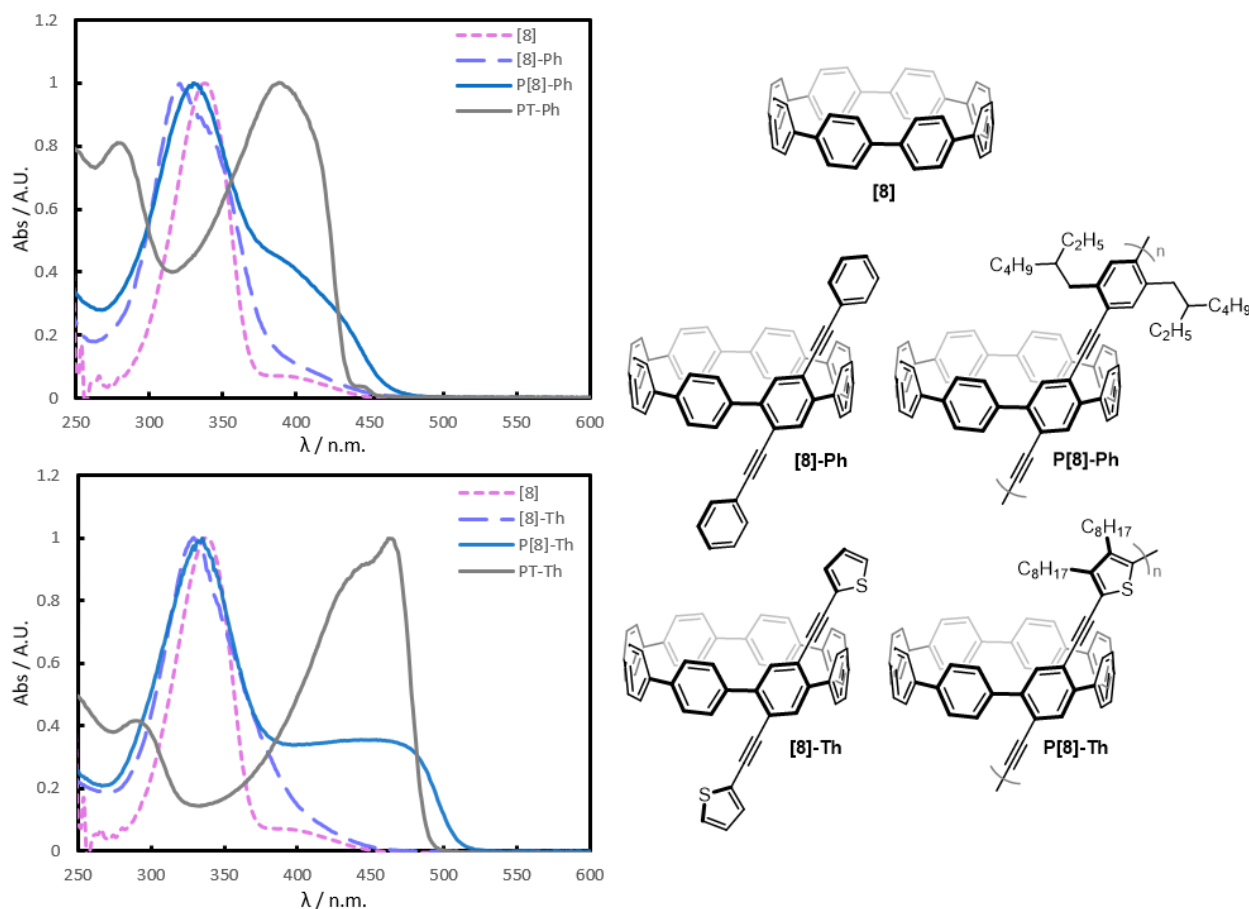


Figure 5.6 Absorption spectra bare and functionalized [8]CPP cores illustrating the impact of gradually extending the orthogonal conjugated system.

The emission spectra for the phenylated [8]CPP compounds are shown in **Figure 5.7**.

The emission profile for the oligomeric and polymeric [8]CPPs are very similar, though the latter is slightly more blue-shifted. The similarities can arise from similarities on conformation adopted for both species, or the fact that the polymers obtained were fairly low in molecular weight and thus more closely resemble oligomers. It is very clear from the comparison between the emission profile of the CPP-containing species with that of the linear system that the key fluorescence transition is located along the CPP ring itself.

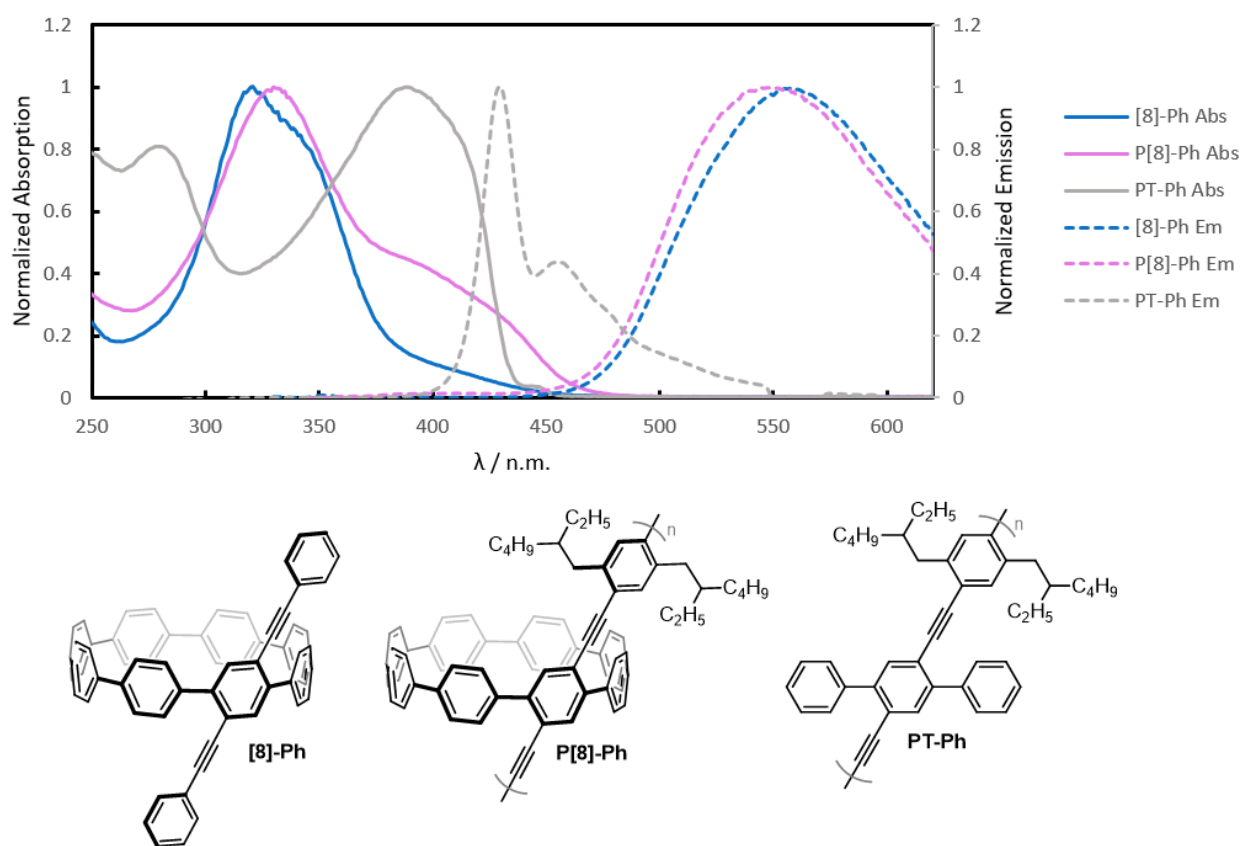


Figure 5.7 UV-Vis absorption and emission spectra for phenylated [8]CPPs compared to that of the linear analogue.

Interestingly, the emission profile for the thienylated [8]CPP analogues demonstrate larger differences. **[8]-Th** fluorescence occurs in a region familiar to [8]CPPs, but the polymeric

species is more drastically blue-shifted compared to the change seen in the phenylated systems (Figure 5.8).

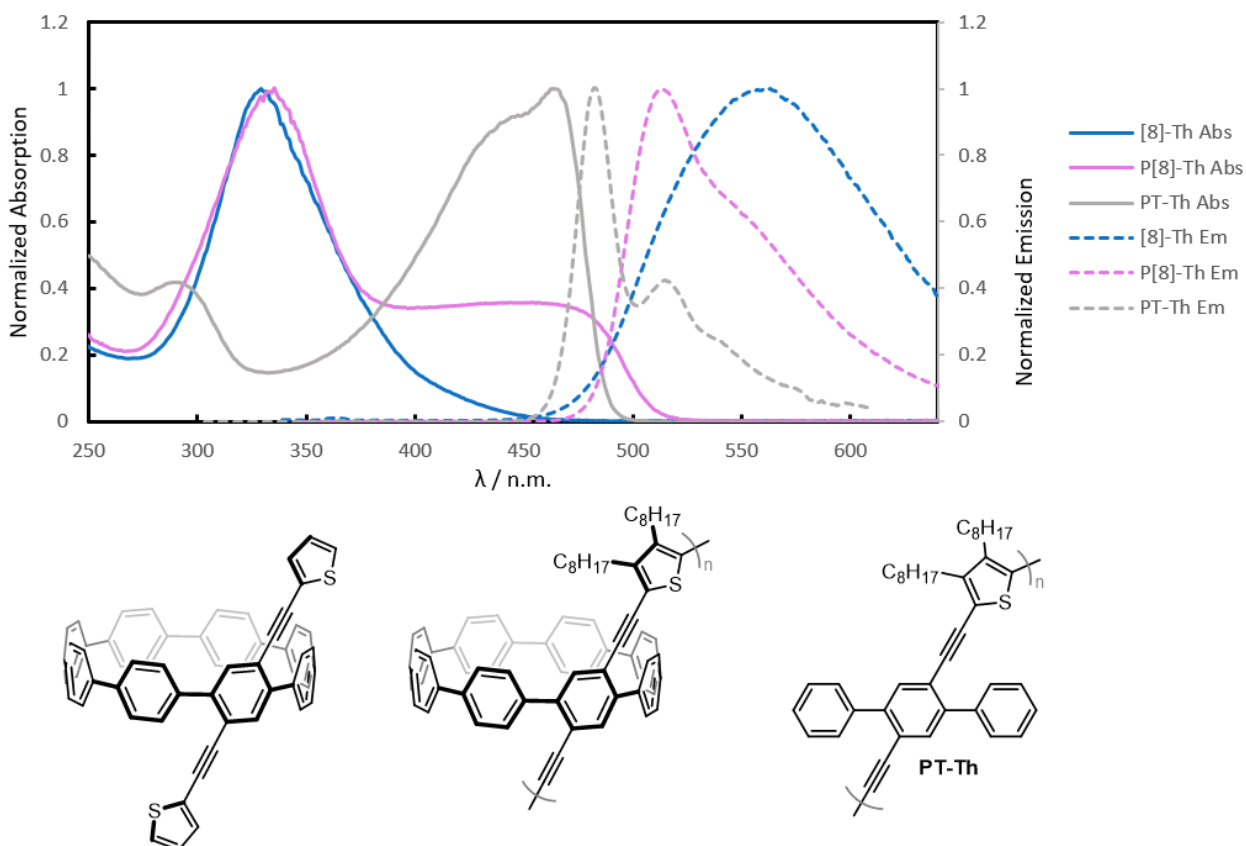


Figure 5.8 UV-Vis absorption and emission spectra for phenylated [8]CPPs compared to that of the linear analogue.

This was an unexpected result, especially in light of the mild changes seen in the phenylated species. From just the emission spectrum, it is unclear whether photoluminescence originated exclusively from cycloparaphenylenes under the influence of linear conjugated pathways with thiophene units, or from a holistic contribution of the entire system. Thus, the excitation spectrum was also obtained (Figure 5.9). Besides a subtle peak ($\lambda=473$ nm) on the excitation spectrum, it effectively traces the absorption profile of the polymer, indicating that the species overall is influenced instead of just the cycloparaphenylene units. This could be an indication that the thiophene allows for more effective communication between the curved and

linear π surfaces compared to the phenylated analogues. This could also be due to a slightly higher degree of polymerization seen in **P[8]-Th** relative to **P[8]-Ph**.

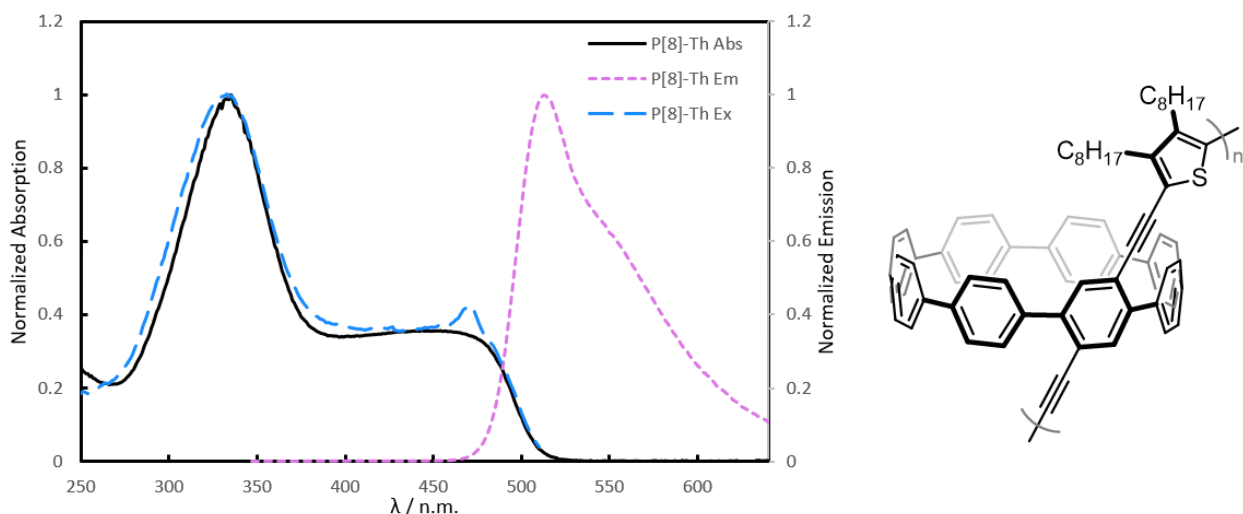


Figure 5.9 UV-Vis absorption, emission, and excitation of P[8]-Th to determine the source of photoluminescence.

Conclusion

Diversification of the synthesis of [6]- and [8]CPPs has allowed for access to linear π -extension orthogonal to the curved macrocycle through a di-alkyne-functionalized subunit. Small extensions to the conjugated system were made through the incorporation of common aromatic molecules benzene and thiophene to investigate the interplay of the linear and curved π surfaces. Further extension of the conjugated systems were accomplished through Sonogashira polycondensations, where alkyl chains were also incorporated for solubility. Absorption spectra for the hybrid systems featuring both a linear and curved π system reflect an additive effect of each contributor. Fluorescence in [6]CPP-containing structures were minimal compared to that of [8]CPP analogues, consistent with the that of the unsubstituted cores. Emission of the [8]CPP substituted cores, however, could be impacted based on the substituent incorporated. While **P[8]-Ph** shared a similar emission profile as the oligomeric version **[8]-Ph**, the thiophene analogue **P[8]-Th** demonstrated a emission between that of the oligomeric version and the linear model

compound, indicating that thiophene substitution may facilitate greater communication between the linear and curved π surfaces.

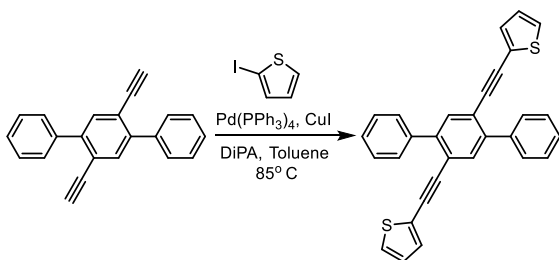
Experimental

General Information

2',5'-diethynyl-1,1':4',1''-terphenyl (**mT**) was prepared according to the literature procedure. Toluene was purified using an Innovative Technologies SPS-400-6 Solvent Purification System and further dried over Acros Organic 4Å molecular sieves prior to use. All other solvents and reagents were purchased from Sigma-Aldrich, Fisher Scientific, Alfa Aesar, or Oakwood chemicals and used without further purification.

¹H NMR spectra were obtained on either a Bruker Avance 400 MHz Spectrometer or a Bruker Avance III 400 MHz Spectrometer, with residual protio-solvent resonances used as the internal standard (CHCl₃: 7.26 ppm, CHDCl₂: 5.32 ppm). Data are reported as: Chemical shift (multiplicity, integration, coupling constant). ¹³C NMR spectra were obtained on either a Bruker Avance 400 MHz Spectrometer (100 MHz) or a Bruker Avance III 400 MHz Spectrometer (100 MHz), with solvent resonances used as the internal standard (CDCl₃: 77.2 ppm, CD₂Cl₂: 53.8). Data are reported as chemical shifts (ppm). High resolution mass spectrometry (HRMS) was performed on a VG-70SE Magnetic Sector Mass Spectrometer. Matrix-assisted laser desorption/ionization spectrometry (MALDI) was performed on a Bruker AutoFlex III MALDI-ToF/ToF Mass Spectrometer using α-cyano-4-hydroxycinnamic acid (CHCA) as the matrix. UV-Vis data were collected on a Cary 50 Bio UV-Vis Spectrophotometer. Photoluminescence data were collected on a Photon Technology International (PTI) Fluorometer (QuantaMaster 40) with a 75-W Ushio Xenon short arc lamp, using Felix32 version 4.9 software. Gel permeation chromatography was performed on an Agilent 1260 Infinity Series (degasser, iso pump, TCC, DAD) using unstabilized THF at 40° C vs. Agilent EasiVial PS-M polystyrene standards. Flash Chromatography was performed under manual air pressure on silica (SiO₂, 40-63 μm, 230-400 mesh).

2',5'-bis(phenylethynyl)-1,1':4',1''-terphenyl (T-Ph)



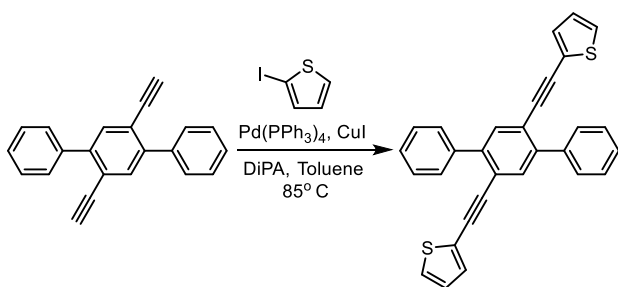
mT (25 mg, 90. μmol), Pd(PPh₃)₄ (5 mg, 4 μmol), and copper (I) iodide (2 mg, 9 μmol) were added to a Schlenk flask, which was then evacuated and backfilled with N₂ three times.

Iodobenzene (38 mg, 0.19 mmol), dry and degassed diisopropylamine (2 mL) and toluene (2 mL) were added, and the reaction mixture was stirred at 85° C for 8 h. The solution was then cooled to

room temperature, diluted with diethyl ether (10 mL), washed twice with sat. NH_4Cl (10 mL), once with brine (10 mL) and dried over MgSO_4 before concentrating under reduced pressure. Purification by column chromatography (silica, 80:20 hexanes:DCM) afforded **T-Ph** (32 mg, 74 μmol , 83%) as a white solid.

^1H NMR (400 MHz, CD_2Cl_2): δ 7.76 (dd, 4H, 7.2 Hz), 7.75 (s, 2H), 7.53 (t, 4H, 7.2 Hz), 7.46 (t, 2H, 7.4 Hz), 7.39-7.32 (m, 10H). **^{13}C (^1H) NMR (100 MHz, CD_2Cl_2):** δ 142.8, 139.8, 134.2, 131.7, 129.7, 128.9, 128.8, 128.5, 128.3, 123.4, 122.1, 94.1, 89.4. **HRMS (EI):** found m/z : 430.1723 ; calc. for $\text{C}_{34}\text{H}_{22}$: 430.1722.

2',5'-bis(thiophen-2-ylethynyl)-1,1':4',1''-terphenyl (T-Th)

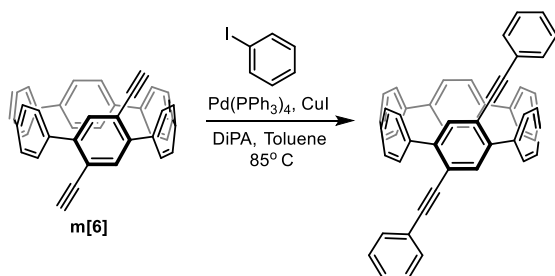


2',5'-diethynyl-1,1':4',1''-terphenyl (**mT**, 25 mg, 90. μmol), $\text{Pd}(\text{PPh}_3)_4$ (5 mg, 4 μmol), and copper (I) iodide (2 mg, 9 μmol) were added to a Schlenk flask, which was then evacuated and backfilled with N_2 three times. 2-iodothiophene (38 mg, 0.18 mmol), dry and degassed diisopropylamine (2 mL) and toluene (2 mL) were added, and the reaction mixture was stirred at 85° C for 14 h. The solution was then cooled to room temperature, diluted with diethyl ether (10 mL), washed twice with sat. NH_4Cl (10 mL), once with brine (10 mL) and dried over MgSO_4 before concentrating under reduced pressure. Purification by column chromatography (silica, 80:20 hexanes:DCM) afforded **T-Th** (35 mg, 79 μmol , 88%) as a pearl-white solid.

^1H NMR (400 MHz, CD_2Cl_2): δ 7.74-7.71 (m, 4H), 7.71 (s, 2H), 7.51 (t, 4H, 7.2 Hz), 7.44 (t, 2H, 7.2 Hz), 7.32 (dd, 2H, 5.2 Hz), 7.16 (dd, 2H, 3.6 Hz), 7.00 (dd, 2H, 5.2 Hz). **^{13}C (^1H) NMR**

(100 MHz, CD₂Cl₂): δ 142.5, 139.5, 133.7, 132.4, 129.5, 128.5, 128.3, 128.2, 127.6, 123.3, 121.8, 93.1, 87.6. **HRMS (EI)**: found m/z : 442.0851; calc. for C₃₀H₁₈S₂: 442.0850.

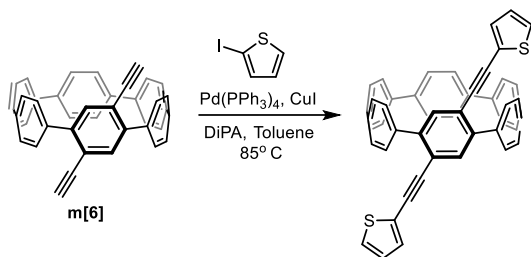
[6]-Ph



m[6] (1 mL, 8 mM in toluene, 9 μ mol), iodobenzene (0.1 mL, 0.2 M in toluene, 20 μ mol), Pd(PPh₃)₄ (0.1 mL, 4 mM in toluene, 0.4 μ mol) and copper (I) iodide (0.1 mL, 11 mM in toluene, 0.9 μ mol) were added to a Schlenk flask under nitrogen atmosphere, followed by dry and degassed toluene (0.7 mL) and diisopropylamine (2 mL). The reaction mixture was stirred at 85° C for 16 h. The solution was then cooled to room temperature, diluted with diethyl ether (10 mL), washed twice with sat. NH₄Cl (10 mL), once with brine (10 mL) and dried over MgSO₄ before concentrating under reduced pressure. Purification by column chromatography (silica, 90:10 hexanes:DCM) afforded **[6]-Ph** (5 mg, 8 μ mol, 88%) as a red solid.

¹H NMR (400 MHz, CDCl₃): δ 7.79 (s, 2H), 7.67-7.50 (m, 22H), 7.48-7.42 (m, 6H). **¹³C (¹H) NMR (100 MHz, CDCl₃)**: δ 137.5, 137.1, 135.8, 135.6, 135.3, 134.1, 133.9, 131.6, 128.9, 128.7, 128.6, 128.1, 127.9, 127.6, 127.6, 127.4, 127.3, 127.3, 127.2, 123.3, 119.6, 96.6, 89.8. **MALDI**: found m/z : 657.178; calc. for [C₅₂H₃₂ + H]⁺: 657.2504.

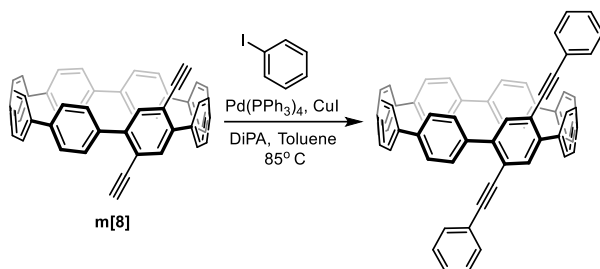
[6]-Th



m[6] (1 mL, 8 mM in toluene, 9 μmol), 2-iodothiophene (0.1 mL, 0.2 M in toluene, 20 μmol), $\text{Pd(PPh}_3)_4$ (0.1 mL, 4 mM in toluene, 0.4 μmol) and copper (I) iodide (0.1 mL, 9 mM in toluene, 0.9 μmol) were added to a Schlenk flask under nitrogen atmosphere, followed by dry and degassed toluene (0.7 mL) and diisopropylamine (2 mL). The reaction mixture was stirred at 85°C for 18 h. The solution was then cooled to room temperature, diluted with diethyl ether (10 mL), washed twice with sat. NH_4Cl (10 mL), once with brine (10 mL) and dried over MgSO_4 before concentrating under reduced pressure. Purification by column chromatography (silica, 90:10 hexanes:DCM) afforded **[6]-Th** (4 mg, 6 μmol , 69%) as a red solid.

^1H NMR (400 MHz, CDCl_3): δ 7.73 (s, 2H), 7.66-7.49 (m, 18H), 7.41 (dd, 2H, 5.2 Hz), 7.39 (dd, 2H, 4.6 Hz), 7.11 (dd, 2H, 5.2 Hz). **^{13}C (^1H) NMR (100 MHz, CDCl_3):** δ 137.7, 137.2, 135.8, 135.7, 135.4, 134.1, 133.6, 132.3, 128.7, 128.2, 128.0, 127.9, 127.64, 127.59, 127.58, 127.5, 127.4, 127.3, 127.2, 123.3, 119.5, 93.6, 90.0. **HRMS (EI):** found m/z : 668.1639; calc. for $\text{C}_{48}\text{H}_{28}\text{S}_2$: 668.1632.

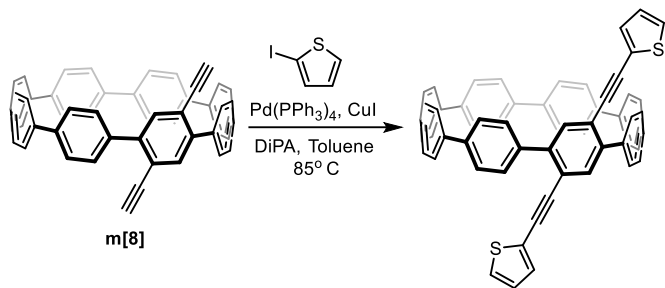
[8]-Ph



m[8] (1 mL, 9 mM in toluene, 9 μ mol), iodobenzene (0.1 mL, 0.2 M in toluene, 20 μ mol), $\text{Pd}(\text{PPh}_3)_4$ (0.1 mL, 4 mM in toluene, 0.4 μ mol) and copper (I) iodide (0.1 mL, 9 mM in toluene, 0.9 μ mol) were added to a Schlenk flask under nitrogen atmosphere, followed by dry and degassed toluene (0.7 mL) and diisopropylamine (2 mL). The reaction mixture was stirred at 75° C for 19 h. The solution was then cooled to room temperature, diluted with diethyl ether (10 mL), washed twice with sat. NH_4Cl (10 mL), once with brine (10 mL) and dried over MgSO_4 before concentrating under reduced pressure. Purification by column chromatography (silica, 90:10 hexanes:DCM) afforded **[6]-Th** (5 mg, 6 μ mol, 68%) as a red solid.

^1H NMR (400 MHz, CDCl_3): δ 7.70 (d, 4H, 8.6 Hz), 7.51-7.42 (m, 30H), 7.40-7.35 (m, 6H). **^{13}C (^1H) NMR (100 MHz, CDCl_3):** δ 140.6, 139.5, 138.3, 138.0, 137.9, 137.6, 137.0, 134.9, 131.5, 130.0, 128.6, 128.5, 128.0, 127.7, 127.6, 127.5, 127.3, 123.4, 121.3, 94.4, 89.6. **MALDI:** found m/z : 809.214; calc. for $[\text{C}_{64}\text{H}_{40} + \text{H}]^+$: 809.3130.

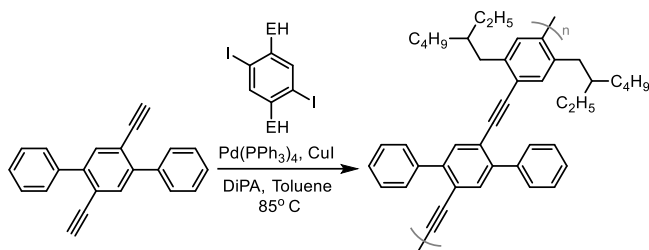
[8]-Th



m[8] (1 mL, 9 mM in toluene, 9 μ mol), 2-iodothiophene (0.1 mL, 0.2 M in toluene, 20 μ mol), $\text{Pd}(\text{PPh}_3)_4$ (0.1 mL, 5 mM in toluene, 0.4 μ mol) and copper (I) iodide (0.1 mL, 9 mM in toluene, 0.9 μ mol) were added to a Schlenk flask under nitrogen atmosphere, followed by dry and degassed toluene (0.7 mL) and diisopropylamine (2 mL). The reaction mixture was stirred at 75° C for 16 h. The solution was then cooled to room temperature, diluted with diethyl ether (10 mL), washed twice with sat. NH_4Cl (10 mL), once with brine (10 mL) and dried over MgSO_4 before concentrating under reduced pressure. Purification by column chromatography (silica, 90:10 hexanes:DCM) afforded **[6]-Ph** (6 mg, 8 μ mol, 80%) as a red solid.

^1H NMR (400 MHz, CD_2Cl_2): δ 7.68 (d, 4H, 8.5 Hz), 7.57-7.45 (m, 26 H), 7.40 (dd, 2H, 5.2 Hz), 7.28 (dd, 2H, 3.6 Hz), 7.07 (dd, 2H, 5.2 Hz). **^{13}C (^1H) NMR (100 MHz, CD_2Cl_2):** δ 140.5, 139.7, 138.4, 138.1, 138.0, 137.9, 137.7, 136.9, 134.6, 132.1, 129.9, 128.1, 127.9, 127.72, 127.70, 127.6, 127.4, 123.5, 121.1, 93.4, 87.9. **MALDI:** found m/z : 821.004; calc. for $[\text{C}_{60}\text{H}_{36}\text{S}_2 + \text{H}]^+$: 821.2258.

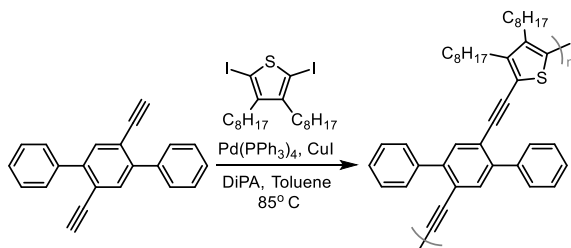
PT-Ph



2',5'-diethynyl-1,1':4,1''-terphenyl (**mT**, 25 mg, 90 μmol), 1,4-Bis(2-ethylhexyl)-2,5-diiodobenzene (50. mg, 90 μmol), $\text{Pd}(\text{PPh}_3)_4$ (5 mg, 4 μmol), and copper (I) iodide (2 mg, 9 μmol) were added to a Schlenk flask, which was then evacuated and backfilled with N_2 three times. Dry and degassed diisopropylamine (4 mL) and toluene (4 mL) were added, and the reaction mixture was stirred at 80° C for 72 h. The solution was then cooled to room temperature and concentrated to approximately 0.5 mL before being rapidly added to MeOH (50 mL). The precipitate was collected by filtration, and was purified by Soxhlet extraction: methanol (24 h), acetone (24 h), chloroform (2 h). The chloroform extract was concentrated and precipitated with 30 mL MeOH. Filtration yielded **PT-Ph** as a bright yellow solid (32 mg).

^1H NMR (400 MHz, CDCl_3): δ 7.81-7.68 (m), 7.55-7.35 (m), 7.09 (m), 2.62-0.45 (m).

PT-Th

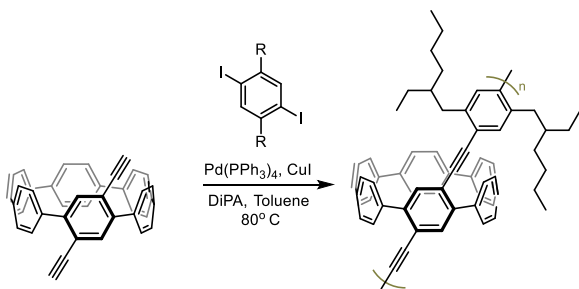


2',5'-diethynyl-1,1':4,1''-terphenyl (**mT**, 25 mg, 90 μmol), 2,5-diiodo-3,4-dioctylthiophene (50. mg, 90 μmol), $\text{Pd}(\text{PPh}_3)_4$ (5 mg, 4 μmol), and copper (I) iodide (2 mg, 9 μmol) were added to a Schlenk flask, which was then evacuated and backfilled with N_2 three times. Dry and degassed

diisopropylamine (4 mL) and toluene (4 mL) were added, and the reaction mixture was stirred at 80° C for 72 h. The solution was then cooled to room temperature and concentrated to approximately 0.5 mL before being rapidly added to MeOH (50 mL). The precipitate was collected by filtration, and was purified by Soxhlet extraction: methanol (24 h), acetone (24 h), chloroform (2 h). The chloroform extract was concentrated and precipitated with 30 mL MeOH. Filtration yielded **PT-Th** as an orange solid (28 mg).

¹H NMR (400 MHz, CDCl₃): δ 7.71-7.60 (m), 7.52-7.39 (m), 1.31-1.09 (m)

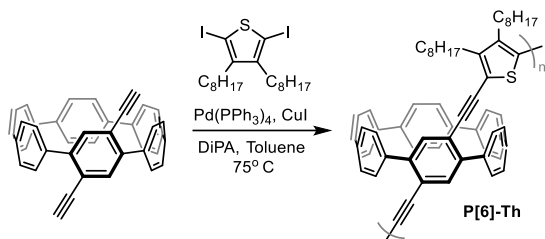
P[6]-Ph



m[6] (12 mg, 20. μmol), 1,4-Bis(2-ethylhexyl)-2,5-diiodobenzene (13 mg, 20. μmol), Pd(PPh₃)₄ (1 mg, 1 μmol), and copper (I) iodide (0.5 mg, 2 μmol) were added to a Schlenk tube, which was then evacuated and backfilled with N₂ three times. Dry and degassed diisopropylamine (2 mL) and toluene (2 mL) were added, and the reaction mixture was stirred at 80° C for 72 h. The solution was then cooled to room temperature and concentrated to approximately 0.5 mL before being rapidly added to MeOH (50 mL). The precipitate was collected by filtration, and was purified by Soxhlet extraction: methanol (24 h), acetone (24 h), chloroform (2 h). The chloroform extract was concentrated and precipitated with 30 mL MeOH. Filtration yielded **P[6]-Ph** as a red solid (6 mg).

¹H NMR (400 MHz, CDCl₃): δ 7.84-7.60 (m), 1.38-1.02 (m), 0.93-0.61 (m).

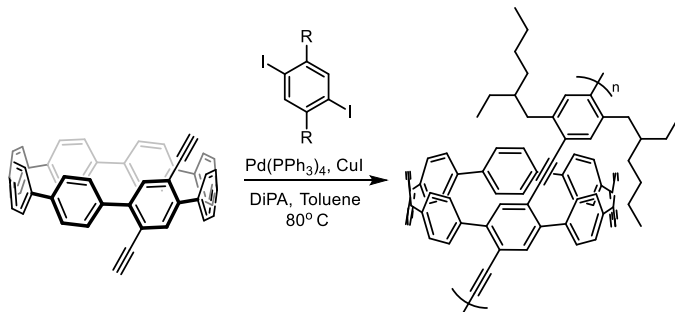
P[6]-Th



m[6] (12 mg, 20. μmol), 2,5-diiodo-3,4-dioctylthiophene (13 mg, 20. μmol), $\text{Pd(PPh}_3)_4$ (1 mg, 1 μmol), and copper (I) iodide (0.5 mg, 2 μmol) were added to a Schlenk tube, which was then evacuated and backfilled with N_2 three times. Dry and degassed diisopropylamine (2 mL) and toluene (2 mL) were added, and the reaction mixture was stirred at 80°C for 72 h. The solution was then cooled to room temperature and concentrated to approximately 0.5 mL before being rapidly added to MeOH (50 mL). The precipitate was collected by filtration, and was purified by Soxhlet extraction: methanol (24 h), acetone (24 h), chloroform (2 h). The chloroform extract was concentrated and precipitated with 30 mL MeOH. Filtration yielded **P[6]-Th** as a red solid.

$^1\text{H NMR}$ (400 MHz, CDCl_3): δ 7.91-7.34 (m), 2.10-0.51 (m), 0.86 (t).

P[8]-Ph

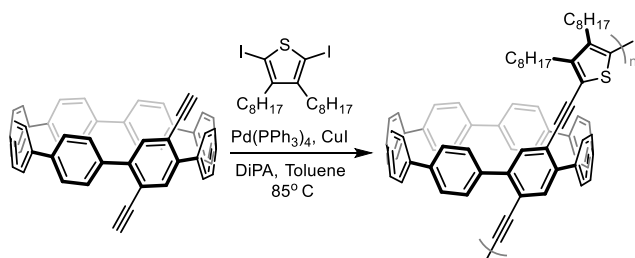


m[8] (13 mg, 20. μmol), 1,4-bis(2-ethylhexyl)-2,5-diiodobenzene (11 mg, 20. μmol), $\text{Pd(PPh}_3)_4$ (1 mg, 1 μmol), and copper (I) iodide (0.4 mg, 2 μmol) were added to a Schlenk tube, which was then evacuated and backfilled with N_2 three times. Dry and degassed diisopropylamine (2 mL)

and toluene (2 mL) were added, and the reaction mixture was stirred at 80° C for 72 h. The solution was then cooled to room temperature and concentrated to approximately 0.5 mL before being rapidly added to MeOH (50 mL). The precipitate was collected by filtration, and was purified by Soxhlet extraction: methanol (24 h), acetone (24 h), chloroform (2 h). The chloroform extract was concentrated and precipitated with 30 mL MeOH. Filtration yielded **P[8]-Ph** as a bright yellow solid.

¹H NMR (400 MHz, CDCl₃): δ 7.89-7.28 (m), 1.89-1.07 (m), 1.01-0.56 (m).

P[8]-Th



m[8] (12 mg, 20. μmol), 2,5-diiodo-3,4-dioctylthiophene (12 mg, 20. μmol), Pd(PPh₃)₄ (1 mg, 1 μmol), and copper (I) iodide (0.4 mg, 2 μmol) were added to a Schlenk tube, which was then evacuated and backfilled with N₂ three times. Dry and degassed diisopropylamine (2 mL) and toluene (2 mL) were added, and the reaction mixture was stirred at 80° C for 72 h. The solution was then cooled to room temperature and concentrated to approximately 0.5 mL before being rapidly added to MeOH (50 mL). The precipitate was collected by filtration, and was purified by Soxhlet extraction: methanol (24 h), acetone (24 h), chloroform (2 h). The chloroform extract was concentrated and precipitated with 30 mL MeOH. Filtration yielded **P[8]-Th** as an orange solid.

¹H NMR (400 MHz, CDCl₃): δ 7.80-7.33 (m), 2.42-0.78 (m).

References

1. Parekh, V. C.; Guha, P. C., *Synthesis of p,p-diphenylene disulfide*. 2019; Vol. 11, p 95-100.
2. Friederich, R.; Nieger, M.; Vögtle, F. Auf dem Weg zu makrocyclischen para-Phenylenen. *Chemische Berichte* **1993**, 126 (7), 1723-1732.
3. Jasti, R.; Bhattacharjee, J.; Neaton, J. B.; Bertozzi, C. R. Synthesis, Characterization, and Theory of [9]-, [12]-, and [18]Cycloparaphenylene: Carbon Nanohoop Structures. *Journal of the American Chemical Society* **2008**, 130 (52), 17646-17647.
4. Takaba, H.; Omachi, H.; Yamamoto, Y.; Bouffard, J.; Itami, K. Selective Synthesis of [12]Cycloparaphenylene. *Angewandte Chemie International Edition* **2009**, 48 (33), 6112-6116.
5. Yamago, S.; Watanabe, Y.; Iwamoto, T. Synthesis of [8]Cycloparaphenylene from a Square-Shaped Tetranuclear Platinum Complex. *Angewandte Chemie International Edition* **2010**, 49 (4), 757-759.
6. Iwamoto, T.; Watanabe, Y.; Sakamoto, Y.; Suzuki, T.; Yamago, S. Selective and Random Syntheses of [n]Cycloparaphenylenes (n = 8–13) and Size Dependence of Their Electronic Properties. *Journal of the American Chemical Society* **2011**, 133 (21), 8354-8361.

Computational Details

All time-dependant density functional theory calculations were performed at the B3LYP / 6-311G(d) level of theory and basis set. Higher levels of theory (i.e. camB3LYP for charge transfer characteristics) provided similar results.

CALCULATED HOMO,LUMO, LUMO+1, LUMO+2 ENERGY LEVELS

TT1-Ph Lock0					
Center	Atomic #	Atomic Type	x	y	z
1	6	0	3.178231	0.037609	-0.04275
2	6	0	1.902586	-0.45549	-0.0942
3	6	0	0.847996	0.525853	-0.03318
4	6	0	1.341425	1.812679	0.092517
5	16	0	3.091616	1.780736	0.095222
6	16	0	1.26379	-2.08889	-0.2015
7	6	0	-0.4777	-0.08655	-0.05
8	6	0	-0.40799	-1.45429	-0.14173
9	6	0	-1.48645	-2.45276	-0.19288
10	6	0	-2.51012	-2.46575	-1.11642
11	6	0	-1.54531	-3.57467	0.711182
12	16	0	-3.55779	-3.83865	-0.84723
13	6	0	-2.60137	-4.4121	0.502698
14	1	0	-0.81664	-3.73025	1.50067
15	6	0	-1.7394	0.677515	0.101008
16	6	0	-2.59401	0.549503	1.172572
17	6	0	-2.1963	1.655721	-0.8517
18	16	0	-3.96311	1.625225	0.99956
19	6	0	-3.37587	2.257038	-0.52419
20	1	0	-1.64809	1.896961	-1.75599
21	6	0	-2.779	-1.52563	-2.25204
22	1	0	-3.52093	-0.76337	-1.98573
23	1	0	-1.85882	-1.00245	-2.52754
24	1	0	-3.14702	-2.06097	-3.13433
25	6	0	-2.97566	-5.65207	1.25808
26	1	0	-2.99699	-6.53663	0.609569
27	1	0	-2.24383	-5.83605	2.051024
28	1	0	-3.96382	-5.56603	1.726807
29	6	0	-4.1251	3.316951	-1.27471
30	1	0	-4.21603	4.242445	-0.69269

31	1	0	-3.59382	3.557645	-2.20097
32	1	0	-5.13962	2.995972	-1.54202
33	6	0	-2.48315	-0.34031	2.37454
34	1	0	-1.44539	-0.6587	2.508669
35	1	0	-2.80413	0.174386	3.287229
36	1	0	-3.09309	-1.24644	2.270006
37	6	0	4.4717	-0.68603	-0.06087
38	6	0	5.683928	0.018035	0.011112
39	6	0	4.505447	-2.08698	-0.14074
40	6	0	6.900974	-0.6634	0.00467
41	1	0	5.663911	1.10243	0.07307
42	6	0	5.723185	-2.76743	-0.14642
43	1	0	3.570466	-2.63726	-0.19653
44	6	0	6.922917	-2.05713	-0.07471
45	1	0	7.831831	-0.10549	0.061824
46	1	0	5.734419	-3.85241	-0.20745
47	1	0	7.871358	-2.58771	-0.08034
48	6	0	0.659882	3.13107	0.131629
49	6	0	-0.73825	3.212519	0.031613
50	6	0	1.402284	4.32044	0.180637
51	6	0	-1.379	4.451174	0.013769
52	1	0	-1.31868	2.296082	-0.03296
53	6	0	0.761198	5.559329	0.168605
54	1	0	2.485454	4.266153	0.239113
55	6	0	-0.6306	5.627701	0.086163
56	1	0	-2.46234	4.497253	-0.06178
57	1	0	1.350195	6.471302	0.217078
58	1	0	-1.12938	6.593214	0.070742

TT1-Ph Lock45					
Center	Atomic #	Atomic Type	x	y	z
1	6	0	3.179904	0.197363	-0.02595
2	6	0	1.930179	-0.35764	-0.0827
3	6	0	0.828619	0.571359	-0.03331
4	6	0	1.257892	1.881331	0.088721
5	16	0	3.007505	1.934843	0.102397
6	16	0	1.372498	-2.02078	-0.18543
7	6	0	-0.4655	-0.10508	-0.05513
8	6	0	-0.32859	-1.46822	-0.13929
9	6	0	-1.35672	-2.51837	-0.19189
10	6	0	-2.37259	-2.58582	-1.12166

11	6	0	-1.36661	-3.63737	0.717627
12	16	0	-3.35377	-4.00688	-0.85178
13	6	0	-2.37922	-4.52634	0.506996
14	1	0	-0.63631	-3.75332	1.512398
15	6	0	-1.7639	0.59724	0.08411
16	6	0	-2.61812	0.432935	1.151032
17	6	0	-2.26184	1.547299	-0.87649
18	16	0	-4.03691	1.439706	0.963967
19	6	0	-3.47141	2.09194	-0.5594
20	1	0	-1.72025	1.810564	-1.77862
21	6	0	-2.6797	-1.66553	-2.26379
22	1	0	-3.45961	-0.93908	-2.00605
23	1	0	-1.78438	-1.09943	-2.53634
24	1	0	-3.01551	-2.22251	-3.14554
25	6	0	-2.69743	-5.77938	1.266506
26	1	0	-2.67144	-6.6671	0.622495
27	1	0	-1.96261	-5.92354	2.064901
28	1	0	-3.6916	-5.73936	1.728669
29	6	0	-4.26659	3.110337	-1.32004
30	1	0	-4.40628	4.033134	-0.74343
31	1	0	-3.74175	3.372122	-2.24426
32	1	0	-5.26251	2.738926	-1.59193
33	6	0	-2.47171	-0.44451	2.358283
34	1	0	-1.42054	-0.71121	2.500473
35	1	0	-2.82326	0.058388	3.266277
36	1	0	-3.03606	-1.37981	2.25471
37	6	0	4.507213	-0.46238	-0.03231
38	6	0	5.504272	-0.06759	0.87345
39	6	0	4.785609	-1.49854	-0.93732
40	6	0	6.749823	-0.69545	0.874635
41	1	0	5.294436	0.733833	1.576184
42	6	0	6.031405	-2.12617	-0.93475
43	1	0	4.017815	-1.80846	-1.64056
44	6	0	7.015904	-1.72532	-0.0297
45	1	0	7.512123	-0.38013	1.582094
46	1	0	6.232833	-2.92788	-1.64023
47	1	0	7.986682	-2.21387	-0.02892
48	6	0	0.512631	3.16507	0.116753
49	6	0	-0.64863	3.296801	0.894926
50	6	0	0.902979	4.238298	-0.69809
51	6	0	-1.38205	4.483001	0.882797

52	1	0	-0.97208	2.460622	1.509013
53	6	0	0.172747	5.426861	-0.70596
54	1	0	1.789571	4.13749	-1.3173
55	6	0	-0.97062	5.552442	0.084944
56	1	0	-2.27758	4.569968	1.492654
57	1	0	0.493962	6.252448	-1.33539
58	1	0	-1.54271	6.476472	0.073999

TT1-Ph Lock90					
Center	Atomic #	Atomic Type	x	y	z
1	6	0	-3.17298	0.03535	0.025962
2	6	0	-1.88986	-0.46431	-0.01737
3	6	0	-0.83536	0.515066	-0.06901
4	6	0	-1.32982	1.814146	-0.10181
5	16	0	-3.07844	1.783671	-0.03814
6	16	0	-1.24524	-2.09698	0.039458
7	6	0	0.491228	-0.0965	-0.03497
8	6	0	0.423135	-1.46611	0.020573
9	6	0	1.497943	-2.46965	0.085627
10	6	0	2.460016	-2.53744	1.070172
11	6	0	1.609862	-3.5425	-0.87101
12	16	0	3.517981	-3.9015	0.795878
13	6	0	2.647527	-4.39729	-0.64031
14	1	0	0.932629	-3.65184	-1.71245
15	6	0	1.761408	0.66695	-0.03199
16	6	0	2.742509	0.564304	-0.99167
17	6	0	2.099172	1.610039	1.003148
18	16	0	4.08452	1.621861	-0.61199
19	6	0	3.314168	2.208857	0.847144
20	1	0	1.438542	1.830713	1.835423
21	6	0	2.659218	-1.6582	2.267376
22	1	0	3.425811	-0.89417	2.091227
23	1	0	1.727806	-1.13716	2.505948
24	1	0	2.960026	-2.24137	3.144748
25	6	0	3.063781	-5.59977	-1.43352
26	1	0	3.035194	-6.51717	-0.83268
27	1	0	2.386241	-5.73451	-2.28258
28	1	0	4.081998	-5.49956	-1.82937
29	6	0	3.968316	3.237887	1.719688

30	1	0	4.113517	4.188466	1.191508
31	1	0	3.337833	3.43504	2.592415
32	1	0	4.950541	2.909307	2.081145
33	6	0	2.778701	-0.28621	-2.22654
34	1	0	1.765348	-0.59961	-2.494
35	1	0	3.204936	0.257218	-3.0775
36	1	0	3.374172	-1.19583	-2.07939
37	6	0	-4.463	-0.65497	0.1017
38	6	0	-5.15647	-1.03352	-1.06412
39	6	0	-5.04391	-0.96187	1.347224
40	6	0	-6.38129	-1.69076	-0.98649
41	1	0	-4.73928	-0.79178	-2.03792
42	6	0	-6.27476	-1.6105	1.420198
43	1	0	-4.51541	-0.71656	2.263069
44	6	0	-6.95055	-1.9794	0.255786
45	1	0	-6.89781	-1.96953	-1.90116
46	1	0	-6.70161	-1.83717	2.393624
47	1	0	-7.90945	-2.48669	0.315089
48	6	0	-0.67293	3.125129	-0.24144
49	6	0	-0.29674	3.862034	0.896544
50	6	0	-0.46045	3.697298	-1.50856
51	6	0	0.282403	5.123781	0.770828
52	1	0	-0.44739	3.431423	1.882777
53	6	0	0.125738	4.954956	-1.63122
54	1	0	-0.76499	3.151936	-2.39512
55	6	0	0.499181	5.674216	-0.49351
56	1	0	0.5696	5.6742	1.662918
57	1	0	0.281813	5.378245	-2.61982
58	1	0	0.951605	6.657367	-0.59192

TT1-DMPH					
Center	Atomic #	Atomic Type	x	y	z
1	6	0	-2.87993	-0.36629	-0.06785
2	6	0	-1.55492	-0.7426	-0.04245
3	6	0	-0.59571	0.3304	-0.09185
4	6	0	-1.20807	1.57447	-0.19428
5	16	0	-2.94724	1.379733	-0.19651
6	16	0	-0.76291	-2.30337	0.102749
7	6	0	0.779804	-0.15036	0.016842
8	6	0	0.838243	-1.51741	0.123177
9	6	0	1.998795	-2.41102	0.268501
10	6	0	2.920948	-2.35206	1.291079
11	6	0	2.250796	-3.50137	-0.64052
12	16	0	4.112765	-3.61789	1.110997
13	6	0	3.353515	-4.2447	-0.33703
14	1	0	1.622607	-3.70435	-1.50238
15	6	0	1.971515	0.730305	0.038663
16	6	0	2.997205	0.687872	-0.87798
17	6	0	2.175706	1.737194	1.048366
18	16	0	4.217014	1.881248	-0.48875
19	6	0	3.334621	2.443216	0.91576
20	1	0	1.463049	1.923097	1.845467
21	6	0	2.98652	-1.41618	2.459786
22	1	0	3.684747	-0.58925	2.283435
23	1	0	2.001171	-0.9782	2.641969
24	1	0	3.303744	-1.93674	3.370143
25	6	0	3.913567	-5.42924	-1.06614
26	1	0	3.946064	-6.32344	-0.43148
27	1	0	3.287774	-5.6578	-1.93463
28	1	0	4.933557	-5.24646	-1.4263

29	6	0	3.852262	3.560024	1.771876
30	1	0	3.92961	4.500903	1.212928
31	1	0	3.170107	3.726828	2.611441
32	1	0	4.844996	3.339504	2.183254
33	6	0	3.164663	-0.19832	-2.0764
34	1	0	2.197262	-0.6161	-2.37005
35	1	0	3.573259	0.352925	-2.93098
36	1	0	3.836166	-1.04129	-1.87114
37	6	0	-4.10153	-1.17332	-0.01469
38	6	0	-5.30088	-0.6467	0.502574
39	6	0	-4.109	-2.50093	-0.48415
40	6	0	-6.45933	-1.41741	0.549301
41	6	0	-5.26794	-3.27198	-0.42595
42	6	0	-6.44933	-2.73624	0.089731
43	1	0	-7.37129	-0.98844	0.956038
44	1	0	-5.24819	-4.29377	-0.79566
45	1	0	-7.35235	-3.33879	0.132551
46	6	0	-0.6718	2.936354	-0.35973
47	6	0	-1.17355	4.001619	0.410338
48	6	0	0.308378	3.215836	-1.32888
49	6	0	-0.70281	5.300535	0.224769
50	6	0	0.782499	4.513532	-1.50653
51	6	0	0.279516	5.561542	-0.73202
52	1	0	-1.10091	6.108158	0.833475
53	1	0	1.540816	4.707463	-2.26032
54	1	0	0.64748	6.573848	-0.87623
55	6	0	-5.32436	0.792567	1.0499
56	1	0	-4.49745	0.935218	1.713803
57	1	0	-5.25254	1.484529	0.236925
58	1	0	-6.23942	0.957962	1.579259
59	6	0	-2.8335	-3.09837	-1.10686
60	1	0	-2.26711	-2.32059	-1.575
61	1	0	-2.24393	-3.55736	-0.34093
62	1	0	-3.10323	-3.83226	-1.8373
63	6	0	-2.23991	3.718293	1.484676
64	1	0	-3.20192	3.645618	1.021904
65	1	0	-2.01173	2.797486	1.979594
66	1	0	-2.24701	4.514919	2.198984
67	6	0	0.849836	2.071165	-2.20532
68	1	0	1.838407	2.312289	-2.53621
69	1	0	0.875495	1.166456	-1.63458

70	1	0	0.211815	1.939426	-3.05413
----	---	---	----------	----------	----------

DTT3					
Center	Atomic #	Atomic Type	x	y	z
1	6	0	-2.76508	6.566546	0.836152
2	6	0	-2.23934	5.396924	0.412336
3	6	0	-0.84786	5.513816	-0.15859
4	6	0	-0.37376	6.775252	-0.22624
5	16	0	-1.51183	7.831671	0.662682
6	6	0	-0.32278	4.124866	-0.51976
7	6	0	-1.18563	3.143281	-0.19578
8	16	0	-2.80484	3.711578	0.345162
9	6	0	-0.56733	1.736937	-0.34273
10	6	0	0.731659	1.823373	-0.79117
11	16	0	1.164193	3.505812	-1.2337
12	6	0	-1.29707	0.420249	-0.01806
13	6	0	-0.69389	-0.73904	0.416645
14	6	0	-2.71527	0.261433	-0.13825
15	16	0	-1.81173	-1.95768	0.664642
16	6	0	-3.1129	-1.00963	0.2124
17	1	0	-3.37916	1.062285	-0.46876
18	6	0	1.694498	0.625793	-0.89287
19	6	0	1.379146	-0.60813	-1.41702
20	6	0	3.052526	0.673023	-0.44066
21	16	0	2.683482	-1.65277	-1.35715
22	6	0	3.69565	-0.52727	-0.64644
23	1	0	3.501036	1.561057	0.008327
24	6	0	0.011094	-1.01545	-1.99506
25	1	0	-0.7415	-0.90396	-1.24268
26	1	0	-0.22397	-0.38923	-2.83022
27	1	0	0.048221	-2.03616	-2.31391
28	6	0	0.815148	-0.93094	0.656605
29	1	0	1.344513	-0.7772	-0.26048
30	1	0	1.152928	-0.22479	1.3861
31	1	0	0.996491	-1.92416	1.010917
32	6	0	5.16002	-0.8357	-0.283
33	6	0	5.692809	-2.09813	-0.54546
34	6	0	5.953739	0.147015	0.30846
35	6	0	7.01883	-2.3779	-0.21589
36	1	0	5.06657	-2.87291	-1.01106

37	6	0	7.280473	-0.13237	0.637295
38	1	0	5.534031	1.142113	0.515227
39	6	0	7.813063	-1.39462	0.37536
40	1	0	8.858573	-1.61542	0.635076
41	6	0	-4.56144	-1.53234	0.20332
42	6	0	-4.8308	-2.84752	0.583089
43	6	0	-5.60417	-0.69096	-0.18445
44	6	0	-6.14254	-3.32133	0.574413
45	1	0	-4.00843	-3.51082	0.888011
46	6	0	-6.91647	-1.16447	-0.19224
47	1	0	-5.39207	0.345687	-0.48363
48	6	0	-7.18578	-2.47946	0.18697
49	1	0	-8.21997	-2.85325	0.180264
50	6	0	8.156637	0.953084	1.289772
51	6	0	7.606771	-3.77163	-0.50475
52	6	0	-8.0675	-0.23503	-0.61989
53	6	0	-6.43987	-4.77329	0.992748
54	9	0	8.30715	1.985219	0.432718
55	9	0	9.367283	0.435273	1.587614
56	9	0	7.563545	1.390292	2.420962
57	9	0	7.408068	-4.08359	-1.80309
58	9	0	6.996895	-4.68809	0.276694
59	9	0	8.930753	-3.76499	-0.24107
60	9	0	-7.77469	-4.97498	1.000577
61	9	0	-5.86172	-5.62157	0.11601
62	9	0	-5.94383	-4.99614	2.228379
63	9	0	-7.70453	0.452187	-1.72374
64	9	0	-9.16518	-0.97305	-0.88994
65	9	0	-8.3418	0.630545	0.379135
66	1	0	0.52115	7.087636	-0.72269
67	1	0	-3.76013	6.712806	1.201358

DTT3-Ph2					
Center	Atomic #	Atomic Type	x	y	z
1	6	0	3.23124	4.902995	-0.52829
2	6	0	2.462792	3.783668	-0.38581
3	6	0	1.130329	4.049327	0.11415
4	6	0	0.919214	5.387762	0.33959
5	16	0	2.330853	6.312002	-0.05301
6	6	0	0.395345	2.819166	0.238558

7	6	0	1.106874	1.697548	-0.13656
8	16	0	2.75566	2.059365	-0.69025
9	6	0	0.380571	0.466243	-0.06307
10	6	0	-0.90733	0.682549	0.405648
11	16	0	-1.21399	2.393266	0.725226
12	6	0	0.96196	-0.83037	-0.47439
13	6	0	0.427324	-1.67846	-1.42422
14	6	0	2.203431	-1.31296	0.055812
15	16	0	1.445237	-3.07593	-1.64673
16	6	0	2.610231	-2.51772	-0.46167
17	1	0	2.750057	-0.7847	0.829545
18	6	0	-1.9864	-0.27262	0.693192
19	6	0	-1.86349	-1.38215	1.510332
20	6	0	-3.31531	-0.11909	0.174647
21	16	0	-3.37403	-2.24282	1.613004
22	6	0	-4.19207	-1.09932	0.565654
23	1	0	-3.58433	0.681813	-0.5057
24	6	0	-0.67374	-1.86024	2.286346
25	1	0	-0.1008	-2.61436	1.733226
26	1	0	-0.00119	-1.02224	2.49097
27	1	0	-0.9725	-2.30191	3.242751
28	6	0	-0.81755	-1.52071	-2.24443
29	1	0	-1.66218	-2.07343	-1.81516
30	1	0	-1.10225	-0.46599	-2.28928
31	1	0	-0.66967	-1.87971	-3.2685
32	6	0	-5.60675	-1.25095	0.209486
33	6	0	-6.23923	-2.50502	0.219302
34	6	0	-6.36811	-0.12742	-0.15713
35	6	0	-7.58309	-2.62894	-0.1294
36	1	0	-5.6786	-3.39374	0.489937
37	6	0	-7.70799	-0.26056	-0.51303
38	1	0	-5.91425	0.857184	-0.15061
39	6	0	-8.32817	-1.51074	-0.50166
40	1	0	-9.37189	-1.60985	-0.77518
41	6	0	3.815713	-3.28754	-0.13761
42	6	0	3.88741	-4.67382	-0.35296
43	6	0	4.941497	-2.64308	0.404736
44	6	0	5.042001	-5.38693	-0.03478
45	1	0	3.034807	-5.20471	-0.76344
46	6	0	6.087569	-3.36415	0.730126
47	1	0	4.927137	-1.57041	0.560782

48	6	0	6.1502	-4.74125	0.512434
49	1	0	7.045637	-5.29872	0.76077
50	6	0	-8.52057	0.967108	-0.83794
51	6	0	-8.21688	-3.99595	-0.17964
52	6	0	7.302377	-2.6382	1.249936
53	6	0	5.068928	-6.88327	-0.21636
54	9	0	-9.11329	1.474337	0.266278
55	9	0	-9.50236	0.694142	-1.72354
56	9	0	-7.75668	1.949486	-1.36335
57	9	0	-7.65336	-4.84258	0.708804
58	9	0	-8.08076	-4.55754	-1.40232
59	9	0	-9.53929	-3.94266	0.086196
60	9	0	6.311859	-7.32817	-0.49905
61	9	0	4.664367	-7.52502	0.903381
62	9	0	4.253468	-7.28144	-1.21652
63	9	0	6.966137	-1.51506	1.920906
64	9	0	8.025614	-3.41337	2.086162
65	9	0	8.125453	-2.26689	0.24364
66	6	0	4.682457	5.038553	-1.02547
67	6	0	5.282235	6.296433	-1.09237
68	6	0	5.3973	3.903826	-1.4088
69	6	0	6.596338	6.419538	-1.54314
70	1	0	4.718141	7.190918	-0.79081
71	6	0	6.712143	4.026689	-1.85881
72	1	0	4.924794	2.912324	-1.35597
73	6	0	7.311684	5.284287	-1.92616
74	1	0	7.068947	7.411047	-1.59649
75	1	0	7.275658	3.131787	-2.16059
76	1	0	8.347814	5.381592	-2.28149
77	6	0	-0.34484	6.092389	0.866146
78	6	0	-0.35548	7.478319	1.02601
79	6	0	-1.47913	5.345094	1.183141
80	6	0	-1.49996	8.116654	1.503407
81	1	0	0.539194	8.067104	0.776737
82	6	0	-2.62438	5.983576	1.659761
83	1	0	-1.47098	4.252776	1.057035
84	6	0	-2.63492	7.369119	1.820061
85	1	0	-1.50821	9.208988	1.630034
86	1	0	-3.5187	5.394153	1.909227
87	1	0	-3.53721	7.87265	2.1964

DTT3-Th2					
Center	Atomic #	Atomic Type	x	y	z
1	6	0	-3.19791	4.98929	0.733105
2	6	0	-2.50386	3.903557	0.328747
3	6	0	-1.11672	4.208896	-0.17963
4	6	0	-0.81157	5.522549	-0.2217
5	16	0	-2.11713	6.410679	0.619811
6	6	0	-0.39695	2.905094	-0.52223
7	6	0	-1.13527	1.814969	-0.24028
8	16	0	-2.83746	2.158919	0.230546
9	6	0	-0.33018	0.504239	-0.36481
10	6	0	0.964095	0.766	-0.75502
11	16	0	1.188522	2.494974	-1.17191
12	6	0	-0.89229	-0.90043	-0.07749
13	6	0	-0.16015	-1.97378	0.379296
14	6	0	-2.27035	-1.24433	-0.26087
15	16	0	-1.11625	-3.33187	0.573203
16	6	0	-2.51077	-2.56008	0.067263
17	1	0	-3.0196	-0.53527	-0.61754
18	6	0	2.080714	-0.29266	-0.81835
19	6	0	1.954782	-1.55245	-1.36038
20	6	0	3.399588	-0.07044	-0.30634
21	16	0	3.382274	-2.41586	-1.24663
22	6	0	4.204494	-1.1731	-0.48779
23	1	0	3.706498	0.864847	0.165254
24	6	0	0.679182	-2.13171	-1.99984
25	1	0	-0.11346	-2.12788	-1.28109
26	1	0	0.399607	-1.53424	-2.84231
27	1	0	0.86511	-3.13549	-2.32041
28	6	0	1.349164	-1.96659	0.685087
29	1	0	1.892743	-1.73552	-0.20712
30	1	0	1.558376	-1.22888	1.431352
31	1	0	1.645054	-2.93039	1.04349
32	6	0	-4.66675	5.003502	1.195613
33	6	0	-5.36867	6.114788	1.606833
34	16	0	-5.61055	3.624359	1.253626
35	6	0	-6.71346	5.782121	1.969936
36	1	0	-4.97107	7.130019	1.657403
37	6	0	-6.96022	4.436021	1.815702
38	1	0	-7.43595	6.520351	2.322614

39	1	0	-7.90354	3.935509	2.025001
40	6	0	0.435209	6.145321	-0.8769
41	6	0	0.736914	7.488583	-0.91397
42	16	0	1.606016	5.231128	-1.64476
43	6	0	1.970669	7.731215	-1.5995
44	1	0	0.127991	8.284888	-0.48218
45	6	0	2.539115	6.559285	-2.04683
46	1	0	2.389424	8.729572	-1.73836
47	1	0	3.475531	6.476765	-2.59501
48	6	0	5.679676	-1.2885	-0.06103
49	6	0	6.38602	-2.46681	-0.30422
50	6	0	6.309686	-0.21504	0.568499
51	6	0	7.721875	-2.57179	0.082685
52	1	0	5.888825	-3.31321	-0.79986
53	6	0	7.646227	-0.31953	0.954695
54	1	0	5.753176	0.713788	0.760083
55	6	0	8.352329	-1.4977	0.712029
56	1	0	9.405627	-1.58068	1.016945
57	6	0	-3.87546	-3.26973	-0.00778
58	6	0	-3.98428	-4.61251	0.35496
59	6	0	-5.00272	-2.57008	-0.43826
60	6	0	-5.21999	-5.25559	0.286554
61	1	0	-3.09523	-5.16403	0.693571
62	6	0	-6.23907	-3.21295	-0.50581
63	1	0	-4.91717	-1.51171	-0.72402
64	6	0	-6.34785	-4.55553	-0.14362
65	1	0	-7.32207	-5.06277	-0.19742
66	6	0	8.341608	0.866092	1.649205
67	6	0	8.501387	-3.87269	-0.18491
68	6	0	-7.48353	-2.43997	-0.9806
69	6	0	-5.34004	-6.73801	0.686088
70	9	0	8.390972	1.917109	0.803375
71	9	0	9.596153	0.510216	1.998444
72	9	0	7.647285	1.210298	2.754618
73	9	0	8.402299	-4.19593	-1.49189
74	9	0	7.985094	-4.86912	0.565478
75	9	0	9.800107	-3.69343	0.137109
76	9	0	-6.63541	-7.11459	0.63413
77	9	0	-4.61705	-7.49403	-0.16727
78	9	0	-4.8729	-6.90493	1.941642
79	9	0	-7.16736	-1.70039	-2.06483

80	9	0	-8.46091	-3.31414	-1.3016
81	9	0	-7.91324	-1.62776	0.008425

TT2					
Center	Atomic #	Atomic Type	x	y	z
1	6	0	-0.49629	6.101527	-0.27367
2	6	0	-0.12089	4.771952	-0.29558
3	6	0	-1.05111	3.846883	0.291609
4	6	0	-2.17591	4.493879	0.812964
5	16	0	-2.05519	6.222939	0.523342
6	16	0	1.299439	3.949095	-0.90694
7	6	0	-0.59364	2.464425	0.190129
8	6	0	0.624031	2.374084	-0.41371
9	6	0	1.434466	1.19162	-0.72919
10	6	0	1.017554	0.139662	-1.50521
11	6	0	2.798156	1.050833	-0.2879
12	16	0	2.295276	-1.03968	-1.66451
13	6	0	3.40429	-0.09478	-0.69533
14	1	0	3.294207	1.791304	0.331414
15	6	0	-1.36596	1.293727	0.657639
16	6	0	-0.93516	0.39726	1.601929
17	6	0	-2.67534	0.978237	0.14982
18	16	0	-2.1401	-0.84215	1.859538
19	6	0	-3.23225	-0.1386	0.687034
20	1	0	-3.17796	1.584886	-0.59615
21	6	0	-0.29674	-0.07065	-2.19383
22	1	0	-0.97563	-0.69348	-1.59861
23	1	0	-0.79272	0.891249	-2.35376
24	1	0	-0.16334	-0.55309	-3.16812
25	6	0	0.346749	0.377698	2.379318
26	1	0	0.81993	1.363183	2.34336
27	1	0	0.174371	0.119946	3.430391
28	1	0	1.062733	-0.34628	1.970528
29	6	0	4.838092	-0.5779	-0.40827
30	6	0	5.279026	-1.79786	-0.92182
31	6	0	5.695957	0.204172	0.365026
32	6	0	6.577327	-2.2359	-0.66151
33	1	0	4.602208	-2.41456	-1.53079
34	6	0	6.995005	-0.23339	0.624679
35	1	0	5.348654	1.165806	0.769711

36	6	0	7.435748	-1.45328	0.111684
37	1	0	8.459388	-1.79883	0.316742
38	6	0	-4.61343	-0.75724	0.402041
39	6	0	-5.00639	-1.92103	1.063585
40	6	0	-5.4716	-0.15406	-0.51734
41	6	0	-6.25699	-2.48183	0.805243
42	1	0	-4.32929	-2.39675	1.787782
43	6	0	-6.72301	-0.71435	-0.77515
44	1	0	-5.16211	0.763289	-1.0387
45	6	0	-7.11575	-1.87812	-0.11415
46	1	0	-8.10178	-2.32044	-0.31764
47	6	0	7.94203	0.630637	1.478022
48	6	0	7.063851	-3.58291	-1.22759
49	6	0	-7.67043	-0.04776	-1.78986
50	6	0	-6.69049	-3.76692	1.534761
51	9	0	8.167783	1.804625	0.850895
52	9	0	9.112336	-0.01996	1.650084
53	9	0	6.868842	-3.60652	-2.56323
54	9	0	8.378829	-3.73402	-0.96208
55	9	0	6.370379	-4.58903	-0.65372
56	9	0	7.376156	0.864676	2.681148
57	9	0	-6.39045	-4.84005	0.772609
58	9	0	-8.02156	-3.73093	1.75715
59	9	0	-6.03948	-3.85634	2.714037
60	9	0	-8.59765	-0.94172	-2.19435
61	9	0	-8.28383	1.004984	-1.20852
62	9	0	-6.96035	0.377793	-2.85625
63	1	0	-0.00728	6.977444	-0.64588
64	1	0	-3.03679	4.161487	1.354539

TT3-D1					
Center	Atomic #	Atomic Type	x	y	z
1	6	0	2.227843	-2.9081	-0.08793
2	6	0	1.950083	-1.58935	-0.13518
3	6	0	0.492707	-1.26039	-0.1016
4	6	0	-0.30774	-2.34394	-0.21077
5	16	0	0.686499	-3.79966	0.040788
6	16	0	2.901003	-0.10858	-0.26556
7	6	0	0.266678	0.252832	0.022701
8	6	0	1.460361	0.939302	0.013999

9	6	0	1.509038	2.457924	0.241078
10	6	0	0.680977	3.073247	1.117719
11	6	0	2.482588	3.453662	-0.45745
12	16	0	0.876658	4.821217	1.048438
13	6	0	2.298935	4.731203	-0.00476
14	1	0	3.211232	3.168919	-1.18708
15	6	0	-1.0985	0.946977	0.161234
16	6	0	-1.40743	2.109168	-0.46887
17	6	0	-2.27489	0.409703	1.015474
18	16	0	-2.98567	2.707164	0.051532
19	6	0	-3.36095	1.230821	0.953429
20	1	0	-2.23616	-0.50118	1.575985
21	6	0	-0.2936	2.339132	2.054903
22	1	0	-1.23994	2.2174	1.56683
23	1	0	0.103907	1.376046	2.302125
24	1	0	-0.42635	2.91018	2.949477
25	6	0	-0.51072	2.799001	-1.50791
26	1	0	0.065276	2.061662	-2.02794
27	1	0	-1.1171	3.336503	-2.2067
28	1	0	0.14801	3.479893	-1.00985
29	6	0	3.169012	5.96466	-0.32504
30	6	0	2.933844	7.142289	0.396351
31	6	0	4.173561	5.934673	-1.30594
32	6	0	3.715034	8.281097	0.167756
33	1	0	2.154901	7.168122	1.131785
34	6	0	4.927678	7.094359	-1.56726
35	1	0	4.365003	5.036867	-1.85521
36	6	0	4.706617	8.262174	-0.82185
37	1	0	5.292195	9.137874	-1.01006
38	6	0	-4.73681	0.939759	1.5735
39	6	0	-5.80883	1.792474	1.28853
40	6	0	-4.91968	-0.15928	2.422422
41	6	0	-7.06941	1.537977	1.837018
42	1	0	-5.66402	2.638472	0.645931
43	6	0	-6.1739	-0.39387	3.003715
44	1	0	-4.10133	-0.81696	2.63057
45	6	0	-7.25301	0.448556	2.700905
46	1	0	-8.21675	0.261754	3.130314
47	6	0	5.998146	7.082903	-2.67395
48	6	0	3.483811	9.548437	1.009685
49	6	0	-6.3628	-1.57591	3.974683

50	6	0	-8.2516	2.455147	1.484951
51	9	0	7.177155	6.67792	-2.15744
52	9	0	6.132311	8.326903	-3.18327
53	9	0	3.064568	9.196734	2.245857
54	9	0	4.638325	10.24165	1.10496
55	9	0	2.544212	10.31672	0.418569
56	9	0	5.617542	6.236619	-3.65437
57	9	0	-8.3069	3.474834	2.365867
58	9	0	-9.39879	1.74649	1.539566
59	9	0	-8.08347	2.944998	0.237265
60	9	0	-7.32946	-1.27653	4.868951
61	9	0	-6.71799	-2.67853	3.280907
62	9	0	-5.20398	-1.80847	4.627803
63	6	0	3.620124	-3.5478	-0.13605
64	6	0	3.842677	-4.88508	-0.26355
65	16	0	5.151989	-2.6605	-0.00964
66	6	0	5.32209	-5.23682	0.006175
67	1	0	3.085808	-5.60335	-0.50267
68	6	0	6.070513	-4.14067	0.284582
69	6	0	-1.80659	-2.33784	-0.53938
70	6	0	-2.53905	-3.46525	-0.75436
71	16	0	-2.80331	-0.88345	-0.73573
72	6	0	-3.91155	-3.12965	-1.38417
73	1	0	-2.19874	-4.45698	-0.53872
74	6	0	-4.10598	-1.79079	-1.50817
75	6	0	5.943058	-6.64414	-0.00162
76	6	0	7.227199	-6.72773	0.405391
77	6	0	8.014371	-5.51489	0.878746
78	6	0	7.513421	-4.26003	0.801837
79	6	0	9.385798	-5.94232	1.448255
80	1	0	10.1047	-5.26441	1.848791
81	6	0	9.564877	-7.30198	1.399874
82	1	0	10.3971	-7.79809	1.856886
83	16	0	8.261498	-8.15246	0.500991
84	6	0	-5.32242	-1.21169	-2.24817
85	6	0	-6.19661	-2.11648	-2.75237
86	6	0	-6.05172	-3.61013	-2.4961
87	6	0	-4.97576	-4.14137	-1.87137
88	6	0	-7.421	-1.84077	-3.64309
89	1	0	-7.72209	-0.86492	-3.96105
90	6	0	-8.07637	-2.99543	-3.99987

91	1	0	-8.86578	-3.01758	-4.71849
92	16	0	-7.46517	-4.44378	-3.14224
93	8	0	5.211198	-7.79857	-0.41181
94	8	0	8.293152	-3.12596	1.18469
95	8	0	-4.84462	-5.55549	-1.68041
96	8	0	-5.51064	0.202611	-2.39537
97	6	0	5.695909	-8.93775	0.297547
98	1	0	6.744699	-9.05258	0.115633
99	1	0	5.530487	-8.80373	1.346853
100	1	0	5.177193	-9.81011	-0.03761
101	6	0	9.188214	-3.52167	2.229289
102	1	0	8.623597	-3.87863	3.065196
103	1	0	9.828705	-4.30247	1.873968
104	1	0	9.779598	-2.68408	2.53002
105	6	0	-5.46542	-6.24552	-2.77145
106	1	0	-5.4203	-7.29996	-2.59994
107	1	0	-6.48979	-5.94073	-2.85087
108	1	0	-4.95343	-6.00857	-3.68069
109	6	0	-6.09654	0.482248	-3.66652
110	1	0	-7.03067	-0.03303	-3.75411
111	1	0	-6.26208	1.534651	-3.75658
112	1	0	-5.43591	0.156375	-4.44083

TT2-D2					
Center	Atomic #	Atomic Type	x	y	z
1	6	0	1.41062	3.899142	-0.05364
2	6	0	1.439008	2.544676	0.010988
3	6	0	0.098507	1.9064	0.176048
4	6	0	-0.89749	2.771593	0.455241
5	16	0	-0.30773	4.409614	0.044675
6	16	0	2.690194	1.297158	-0.03176
7	6	0	0.177213	0.389298	0.003069
8	6	0	1.485813	-0.04982	-0.14233
9	6	0	1.859314	-1.5343	-0.38151
10	6	0	1.155208	-2.37318	-1.1973
11	6	0	3.091131	-2.24147	0.255372
12	16	0	1.79113	-4.01545	-1.11077
13	6	0	3.214644	-3.51715	-0.18633
14	1	0	3.77045	-1.77869	0.943896
15	6	0	-1.04887	-0.52674	-0.04944

16	6	0	-1.04242	-1.76183	0.484044
17	6	0	-2.4147	-0.16244	-0.70155
18	16	0	-2.51116	-2.63878	0.035343
19	6	0	-3.2905	-1.1952	-0.64694
20	1	0	-2.64341	0.787667	-1.13932
21	6	0	-0.0293	-1.95874	-2.08316
22	1	0	-0.94027	-2.06085	-1.53479
23	1	0	0.094969	-0.94451	-2.3854
24	1	0	-0.06453	-2.5877	-2.94943
25	6	0	0.106385	-2.28706	1.36522
26	1	0	0.556267	-1.46351	1.881964
27	1	0	-0.27496	-2.98656	2.076047
28	1	0	0.839488	-2.76342	0.752289
29	6	0	4.424409	-4.422	0.062499
30	6	0	4.518194	-5.61036	-0.65566
31	6	0	5.423496	-4.06768	0.985756
32	6	0	5.61788	-6.44675	-0.47943
33	1	0	3.747512	-5.87595	-1.34715
34	6	0	6.506791	-4.92976	1.201892
35	1	0	5.358884	-3.14748	1.52678
36	6	0	6.612377	-6.11204	0.452114
37	1	0	7.451719	-6.76136	0.590991
38	6	0	-4.75802	-1.14784	-1.11194
39	6	0	-5.53184	-2.29226	-0.93803
40	6	0	-5.32106	0.002292	-1.70861
41	6	0	-6.85643	-2.31576	-1.36821
42	1	0	-5.10823	-3.15317	-0.46936
43	6	0	-6.66777	-0.01788	-2.13379
44	1	0	-4.73215	0.886857	-1.83526
45	6	0	-7.42246	-1.18739	-1.97881
46	1	0	-8.43402	-1.21815	-2.32559
47	6	0	7.574882	-4.57641	2.262847
48	6	0	5.734524	-7.73279	-1.31343
49	6	0	-7.32999	1.232549	-2.76899
50	6	0	-7.6869	-3.59001	-1.16508
51	9	0	8.548045	-3.82813	1.699072
52	9	0	8.113752	-5.71183	2.757852
53	9	0	5.137369	-7.552	-2.51144
54	9	0	7.038317	-8.02458	-1.5013
55	9	0	5.130948	-8.74683	-0.6606
56	9	0	6.99846	-3.87971	3.265701

57	9	0	-7.55023	-4.39351	-2.24121
58	9	0	-8.98382	-3.2563	-1.00879
59	9	0	-7.25296	-4.23896	-0.06308
60	9	0	-8.30426	0.840965	-3.61911
61	9	0	-7.8679	2.000082	-1.79501
62	9	0	-6.40717	1.950343	-3.44508
63	6	0	2.637887	4.833773	-0.17798
64	6	0	2.549381	6.206862	-0.27734
65	16	0	4.350866	4.276252	-0.22669
66	6	0	3.930684	6.80336	-0.61453
67	1	0	1.651252	6.775414	-0.15881
68	6	0	4.899976	5.911709	-0.59517
69	6	0	6.187292	6.639329	-0.8757
70	6	0	5.89702	7.925532	-0.94007
71	16	0	7.898881	6.292325	-1.07879
72	6	0	7.149081	8.820448	-0.93233
73	6	0	8.288735	8.04297	-0.9038
74	1	0	7.138867	9.892773	-0.94613
75	1	0	9.280108	8.433702	-0.78422
76	6	0	-2.27035	2.39321	1.06022
77	6	0	-3.27388	3.295117	1.357854
78	16	0	-2.72325	0.713543	1.546781
79	6	0	-4.3872	2.600671	2.175497
80	1	0	-3.26681	4.325773	1.079316
81	6	0	-4.23022	1.293534	2.24828
82	6	0	-5.46969	0.728555	2.893797
83	6	0	-6.28033	1.736559	3.142873
84	16	0	-6.12648	-0.83593	3.355369
85	6	0	-7.69071	1.278665	3.587362
86	6	0	-7.74247	-0.10502	3.638014
87	1	0	-8.51122	1.93287	3.812645
88	1	0	-8.63051	-0.67169	3.82198
89	7	0	4.423646	8.166635	-0.97954
90	7	0	-5.61825	3.05576	2.906452
91	6	0	3.945256	9.235202	-0.0906
92	1	0	4.436547	10.15265	-0.33924
93	1	0	2.888508	9.352592	-0.21061
94	1	0	4.162499	8.978164	0.925093
95	6	0	-6.44138	4.026462	2.170866
96	1	0	-7.47604	3.840264	2.370184
97	1	0	-6.19034	5.017874	2.485476

98	1	0	-6.25693	3.927813	1.121512
----	---	---	----------	----------	----------

TT2-D3					
Center	Atomic #	Atomic Type	x	y	z
1	6	0	0.986045	3.880962	-0.37369
2	6	0	1.240567	2.557613	-0.32345
3	6	0	0.043679	1.693804	-0.06835
4	6	0	-1.07387	2.391601	0.239234
5	16	0	-0.77219	4.105699	-0.17005
6	16	0	2.679628	1.55894	-0.47485
7	6	0	0.380814	0.199759	-0.22916
8	6	0	1.733864	0.020391	-0.48111
9	6	0	2.372362	-1.35705	-0.74474
10	6	0	1.903909	-2.24974	-1.65495
11	6	0	3.630276	-1.88798	-0.00331
12	16	0	2.74398	-3.79954	-1.49555
13	6	0	3.968891	-3.14625	-0.39815
14	1	0	4.170884	-1.32572	0.72608
15	6	0	-0.6547	-0.94205	-0.16258
16	6	0	-0.38764	-2.19148	0.310968
17	6	0	-2.12543	-0.80604	-0.64259
18	16	0	-1.7358	-3.28745	-0.02962
19	6	0	-2.80895	-1.98092	-0.55283
20	1	0	-2.55167	0.10751	-1.00066
21	6	0	0.800363	-1.95592	-2.68402
22	1	0	-0.15399	-2.19215	-2.26036
23	1	0	0.826056	-0.91978	-2.94942
24	1	0	0.960798	-2.5526	-3.55703
25	6	0	0.901392	-2.60609	1.041297
26	1	0	1.296126	-1.76764	1.57505
27	1	0	0.68326	-3.39698	1.729246
28	1	0	1.62074	-2.94464	0.324798
29	6	0	5.234683	-3.9129	0.038295
30	6	0	5.428081	-5.22998	-0.40265
31	6	0	6.185896	-3.30595	0.872272
32	6	0	6.562621	-5.94778	0.000212
33	1	0	4.704915	-5.68845	-1.04616
34	6	0	7.331587	-4.01916	1.260553
35	1	0	6.037617	-2.30127	1.210168
36	6	0	7.515001	-5.34011	0.828305

37	1	0	8.383891	-5.88523	1.131604
38	6	0	-4.30664	-2.1664	-0.86937
39	6	0	-4.8769	-3.44638	-0.80392
40	6	0	-5.09612	-1.06638	-1.22958
41	6	0	-6.23125	-3.63019	-1.12194
42	1	0	-4.27621	-4.28219	-0.51517
43	6	0	-6.45397	-1.24799	-1.53039
44	1	0	-4.66393	-0.08934	-1.27505
45	6	0	-7.01705	-2.53051	-1.48601
46	1	0	-8.04976	-2.66993	-1.72999
47	6	0	8.390621	-3.35594	2.162897
48	6	0	6.763666	-7.40465	-0.46356
49	6	0	-7.32865	-0.04039	-1.91048
50	6	0	-6.85682	-5.04052	-1.0742
51	9	0	9.308323	-2.73171	1.394374
52	9	0	8.998746	-4.29992	2.912841
53	9	0	6.187319	-7.57681	-1.67226
54	9	0	8.084344	-7.67175	-0.55063
55	9	0	6.193818	-8.24333	0.428018
56	9	0	7.794028	-2.45513	2.972798
57	9	0	-6.7205	-5.63628	-2.27794
58	9	0	-8.16947	-4.941	-0.76895
59	9	0	-6.23039	-5.78135	-0.13543
60	9	0	-8.30613	-0.43901	-2.75064
61	9	0	-7.8793	0.481788	-0.79356
62	9	0	-6.56706	0.89382	-2.51745
63	6	0	2.025679	5.000865	-0.56029
64	6	0	1.59472	6.341071	-0.6462
65	6	0	3.408807	4.683497	-0.6495
66	6	0	2.56204	7.326182	-0.81587
67	1	0	0.555451	6.591981	-0.59122
68	6	0	4.367788	5.711964	-0.76616
69	1	0	3.723586	3.662901	-0.62242
70	6	0	3.900333	7.018781	-0.80472
71	1	0	5.415141	5.494206	-0.815
72	6	0	4.658497	8.33282	-0.8034
73	6	0	6.02511	8.580329	-0.7673
74	6	0	3.721	9.33812	-0.80961
75	6	0	6.439197	9.921533	-0.63878
76	1	0	6.736813	7.783824	-0.82689
77	6	0	4.094319	10.66856	-0.62942

78	6	0	5.475528	10.96085	-0.54724
79	1	0	7.482234	10.1568	-0.60647
80	1	0	3.360157	11.44481	-0.56208
81	1	0	5.796643	11.97334	-0.41691
82	6	0	-2.36974	1.823088	0.854123
83	6	0	-3.44524	2.69442	1.140234
84	6	0	-2.47257	0.43487	1.146713
85	6	0	-4.57995	2.156261	1.742932
86	1	0	-3.38658	3.738822	0.909675
87	6	0	-3.65693	-0.0875	1.709761
88	1	0	-1.65042	-0.21593	0.937591
89	6	0	-4.69596	0.802485	1.955454
90	1	0	-3.75388	-1.12857	1.935952
91	6	0	-6.1139	0.548341	2.436957
92	6	0	-6.75166	-0.64101	2.775603
93	6	0	-6.75223	1.767312	2.466383
94	6	0	-8.13101	-0.57869	3.06272
95	1	0	-6.22019	-1.56817	2.809607
96	6	0	-8.12584	1.85234	2.688261
97	6	0	-8.82119	0.661066	2.991639
98	1	0	-8.66021	-1.46934	3.331214
99	1	0	-8.63818	2.790089	2.638751
100	1	0	-9.87541	0.692205	3.173005
101	7	0	2.356324	8.783895	-1.02568
102	7	0	-5.78488	2.876025	2.239811
103	6	0	1.340713	9.360252	-0.13701
104	1	0	1.264452	10.41135	-0.31824
105	1	0	0.395322	8.895631	-0.32674
106	1	0	1.622538	9.192912	0.881238
107	6	0	-5.48749	3.558804	3.511218
108	1	0	-4.74407	4.310315	3.349218
109	1	0	-6.38031	4.015798	3.887192
110	1	0	-5.12389	2.84791	4.223828

TT2-D4					
Center	Atomic #	Atomic Type	x	y	z
1	6	0	-1.81428	-3.42381	-0.08059
2	6	0	-1.71643	-2.07907	-0.01454
3	6	0	-0.32209	-1.56878	0.122711
4	6	0	0.576241	-2.52921	0.41026

5	16	0	-0.1666	-4.10837	0.043201
6	16	0	-2.84741	-0.7278	-0.02818
7	6	0	-0.26049	-0.05357	-0.09176
8	6	0	-1.52524	0.485441	-0.19823
9	6	0	-1.74468	1.979996	-0.45637
10	6	0	-0.95875	2.690483	-1.29973
11	6	0	-2.86615	2.843337	0.179637
12	16	0	-1.3526	4.41379	-1.22623
13	6	0	-2.80164	4.13557	-0.23544
14	1	0	-3.60705	2.464293	0.853821
15	6	0	1.029495	0.771244	-0.21181
16	6	0	1.154083	2.056903	0.215609
17	6	0	2.338094	0.238802	-0.85026
18	16	0	2.690379	2.749186	-0.3252
19	6	0	3.308473	1.192802	-0.89966
20	1	0	2.46014	-0.76042	-1.20711
21	6	0	0.120122	2.058051	-2.1993
22	1	0	1.049623	2.028198	-1.6741
23	1	0	-0.17476	1.062073	-2.46111
24	1	0	0.23011	2.639973	-3.08948
25	6	0	0.109016	2.808752	1.059613
26	1	0	-0.42246	2.110283	1.672757
27	1	0	0.602434	3.526233	1.685007
28	1	0	-0.57538	3.310926	0.412014
29	6	0	-3.84067	5.219216	0.100931
30	6	0	-3.70984	6.478334	-0.4875
31	6	0	-4.90247	4.95958	0.985855
32	6	0	-4.64211	7.480415	-0.21406
33	1	0	-2.89468	6.672615	-1.15376
34	6	0	-5.832	5.973351	1.28001
35	1	0	-5.00329	3.992824	1.435029
36	6	0	-5.69915	7.234452	0.677628
37	1	0	-6.40431	8.007397	0.893473
38	6	0	4.746655	0.975668	-1.39254
39	6	0	5.645212	2.045703	-1.35557
40	6	0	5.156052	-0.27144	-1.88484
41	6	0	6.956484	1.877898	-1.81006
42	1	0	5.329674	2.993853	-0.97739
43	6	0	6.467575	-0.43958	-2.35461
44	1	0	4.47142	-1.09376	-1.90625
45	6	0	7.371344	0.634881	-2.30901

46	1	0	8.375632	0.505535	-2.65783
47	6	0	-6.99419	5.708916	2.265657
48	6	0	-4.49892	8.851424	-0.89495
49	6	0	6.916464	-1.80185	-2.9221
50	6	0	7.935141	3.066473	-1.75978
51	9	0	-8.06023	5.232585	1.58703
52	9	0	-7.33406	6.861978	2.881777
53	9	0	-3.91652	8.692489	-2.10332
54	9	0	-5.72029	9.402138	-1.05355
55	9	0	-3.73467	9.65851	-0.13005
56	9	0	-6.60889	4.803041	3.189347
57	9	0	7.86219	3.759177	-2.91663
58	9	0	9.193339	2.609788	-1.58717
59	9	0	7.60476	3.875715	-0.73015
60	9	0	7.865415	-1.6066	-3.86345
61	9	0	7.419032	-2.56196	-1.92726
62	9	0	5.856266	-2.42758	-3.47623
63	6	0	-3.09658	-4.24953	-0.23513
64	6	0	-3.09479	-5.61712	-0.25195
65	16	0	-4.74847	-3.57301	-0.46225
66	6	0	-4.50013	-6.12771	-0.56722
67	1	0	-2.23903	-6.23255	-0.08828
68	6	0	-5.45964	-5.18018	-0.60983
69	6	0	-6.95171	-5.73433	-0.71577
70	6	0	-7.06405	-7.0839	-0.71236
71	16	0	-8.545	-4.98014	-0.79349
72	6	0	-8.49466	-7.60614	-0.53546
73	6	0	-9.36756	-6.54176	-0.45815
74	1	0	-8.77199	-8.63854	-0.4744
75	1	0	-10.4073	-6.63334	-0.22011
76	6	0	1.974801	-2.30352	1.000082
77	6	0	2.813019	-3.32639	1.375471
78	16	0	2.676499	-0.68852	1.357591
79	6	0	4.00115	-2.74827	2.158334
80	1	0	2.6477	-4.36515	1.175016
81	6	0	4.094038	-1.40075	2.124119
82	6	0	5.443021	-0.79635	2.711281
83	6	0	6.336633	-1.70954	3.150833
84	16	0	6.083862	0.836876	2.890149
85	6	0	7.732556	-1.14953	3.447154
86	6	0	7.73419	0.212882	3.236826

87	1	0	8.574832	-1.72611	3.761763
88	1	0	8.609837	0.824278	3.268178
89	6	0	-4.81159	-9.26882	0.266505
90	1	0	-5.408	-10.1277	0.046627
91	1	0	-3.77992	-9.50587	0.113829
92	1	0	-4.96327	-8.97875	1.282336
93	6	0	6.433979	-4.92459	2.486476
94	1	0	7.297878	-5.11408	3.094016
95	1	0	5.798377	-5.78734	2.497608
96	1	0	6.739797	-4.71792	1.482249
97	14	0	-5.31568	-7.80712	-0.90822
98	14	0	5.461418	-3.39499	3.194244
99	6	0	-4.98199	-8.43615	-2.70873
100	1	0	-5.2328	-7.66757	-3.41086
101	1	0	-3.9464	-8.68789	-2.80766
102	1	0	-5.58114	-9.30325	-2.89686
103	6	0	4.926442	-3.86778	5.000026
104	1	0	4.302262	-4.73524	4.974536
105	1	0	5.798502	-4.07211	5.585077
106	1	0	4.384591	-3.05278	5.438465

TT2-D5					
Center	Atomic #	Atomic Type	x	y	z
1	6	0	-2.34701	-2.81015	-0.24649
2	6	0	-2.00919	-1.49775	-0.14655
3	6	0	-0.54528	-1.24754	0.053832
4	6	0	0.161465	-2.35801	0.355449
5	16	0	-0.85156	-3.77387	-0.04073
6	16	0	-2.86917	0.045776	-0.17402
7	6	0	-0.19966	0.239921	-0.13041
8	6	0	-1.344	1.011207	-0.25516
9	6	0	-1.27517	2.540107	-0.45754
10	6	0	-0.32416	3.120142	-1.23047
11	6	0	-2.24773	3.589954	0.158438
12	16	0	-0.39485	4.881929	-1.10776
13	6	0	-1.91406	4.865979	-0.19721
14	1	0	-3.08174	3.342622	0.781315
15	6	0	1.227973	0.815207	-0.22171
16	6	0	1.595983	2.022085	0.287691
17	6	0	2.410408	0.096972	-0.92683

18	16	0	3.217304	2.464495	-0.26706
19	6	0	3.526055	0.874443	-0.97935
20	1	0	2.354366	-0.8927	-1.33104
21	6	0	0.67086	2.337075	-2.10475
22	1	0	1.55372	2.126245	-1.53939
23	1	0	0.221717	1.417315	-2.42037
24	1	0	0.927301	2.920469	-2.96402
25	6	0	0.730486	2.886785	1.219596
26	1	0	0.102703	2.255085	1.812655
27	1	0	1.365974	3.460986	1.860691
28	1	0	0.123771	3.544925	0.634369
29	6	0	-2.72958	6.132996	0.144132
30	6	0	-2.31809	7.382836	-0.34512
31	6	0	-3.87797	6.042308	0.947337
32	6	0	-3.04351	8.539157	-0.02031
33	1	0	-1.44922	7.454314	-0.96333
34	6	0	-4.59785	7.200199	1.277792
35	1	0	-4.20301	5.09114	1.311505
36	6	0	-4.18018	8.446734	0.793331
37	1	0	-4.72908	9.330449	1.045393
38	6	0	4.875898	0.457307	-1.59108
39	6	0	5.939348	1.368761	-1.59857
40	6	0	5.039158	-0.81522	-2.15744
41	6	0	7.1536	1.024945	-2.20468
42	1	0	5.82279	2.33126	-1.14374
43	6	0	6.256479	-1.15914	-2.76546
44	1	0	4.235046	-1.52105	-2.1295
45	6	0	7.311444	-0.23844	-2.79039
46	1	0	8.237399	-0.49841	-3.25487
47	6	0	-5.8463	7.101316	2.175246
48	6	0	-2.5944	9.911683	-0.55802
49	6	0	6.433387	-2.54626	-3.41092
50	6	0	8.312517	2.036889	-2.23303
51	9	0	-6.94036	6.917978	1.406188
52	9	0	-5.9816	8.242644	2.884528
53	9	0	-1.99006	9.751846	-1.75523
54	9	0	-3.67031	10.7139	-0.7012
55	9	0	-1.72735	10.47367	0.311095
56	9	0	-5.71028	6.058823	3.020918
57	9	0	8.22049	2.794515	-3.34642
58	9	0	9.488736	1.375319	-2.23479

59	9	0	8.242891	2.829985	-1.1424
60	9	0	7.304648	-2.45555	-4.43846
61	9	0	6.91009	-3.41323	-2.49265
62	9	0	5.241954	-2.98436	-3.86924
63	6	0	-3.75441	-3.39972	-0.49997
64	6	0	-4.01041	-4.75201	-0.56503
65	16	0	-5.25406	-2.43324	-0.76258
66	6	0	-5.52014	-4.99398	-0.72424
67	1	0	-3.26531	-5.51549	-0.51205
68	6	0	-6.28331	-3.87175	-0.70586
69	6	0	-7.86707	-4.11005	-0.60831
70	6	0	-8.26886	-5.40749	-0.54068
71	16	0	-9.26707	-3.04116	-0.52581
72	6	0	-9.74595	-5.61468	-0.17971
73	6	0	-10.3619	-4.38944	-0.04622
74	1	0	-10.2229	-6.56478	-0.04716
75	1	0	-11.3642	-4.2574	0.303456
76	6	0	1.576792	-2.37723	0.972017
77	6	0	2.226116	-3.51601	1.406416
78	16	0	2.551887	-0.89324	1.276132
79	6	0	3.515575	-3.1169	2.148455
80	1	0	1.875951	-4.51738	1.268769
81	6	0	3.846349	-1.80252	2.056834
82	6	0	5.299732	-1.40623	2.602548
83	6	0	6.049399	-2.42779	3.08359
84	16	0	6.206639	0.105079	2.690241
85	6	0	7.522733	-2.09163	3.339607
86	6	0	7.744827	-0.76143	3.056505
87	1	0	8.264336	-2.78621	3.678067
88	1	0	8.712465	-0.30423	3.050261
89	6	0	-6.4004	-8.07653	0.285504
90	1	0	-7.18855	-8.78898	0.161986
91	1	0	-5.46455	-8.53124	0.036655
92	1	0	-6.37583	-7.74465	1.3033
93	6	0	5.629842	-5.7101	2.548912
94	1	0	6.454491	-6.01038	3.161529
95	1	0	4.867005	-6.45803	2.586037
96	1	0	5.962671	-5.58967	1.538559
97	6	0	-6.74478	-7.26402	-2.76101
98	1	0	-6.91254	-6.47504	-3.46286
99	1	0	-5.80602	-7.73294	-2.96878

100	1	0	-7.52997	-7.98669	-2.84174
101	6	0	4.319276	-4.32155	5.095055
102	1	0	3.570742	-5.08524	5.106071
103	1	0	5.16016	-4.63809	5.676995
104	1	0	3.916684	-3.42143	5.511424
105	32	0	-6.71961	-6.52118	-0.91458
106	32	0	4.900617	-3.98401	3.218307

TT2-D6A					
Center	Atomic #	Atomic Type	x	y	z
1	6	0	1.569742	3.304143	-0.49683
2	6	0	1.59251	1.96037	-0.36858
3	6	0	0.246345	1.322548	-0.22737
4	6	0	-0.7716	2.205045	-0.13243
5	16	0	-0.13987	3.823369	-0.55368
6	16	0	2.850643	0.73105	-0.30549
7	6	0	0.344325	-0.2108	-0.22402
8	6	0	1.659528	-0.62597	-0.34199
9	6	0	2.057753	-2.10481	-0.4995
10	6	0	1.331731	-3.01278	-1.20479
11	6	0	3.338708	-2.72863	0.112143
12	16	0	2.004016	-4.63966	-1.0068
13	6	0	3.463028	-4.04665	-0.19647
14	1	0	4.047546	-2.18275	0.698565
15	6	0	-0.85805	-1.16655	-0.13536
16	6	0	-0.80353	-2.4038	0.42712
17	6	0	-2.27345	-0.83203	-0.67471
18	16	0	-2.30566	-3.29079	0.12555
19	6	0	-3.14319	-1.86407	-0.5062
20	1	0	-2.53665	0.103667	-1.12189
21	6	0	0.098079	-2.67151	-2.06089
22	1	0	-0.78419	-2.74052	-1.45862
23	1	0	0.192475	-1.67672	-2.44223
24	1	0	0.027773	-3.36134	-2.87571
25	6	0	0.39588	-2.95601	1.219204
26	1	0	0.909806	-2.14874	1.697844
27	1	0	0.04728	-3.64576	1.959331
28	1	0	1.063784	-3.45756	0.550462
29	6	0	4.70705	-4.89624	0.113255

30	6	0	4.756644	-6.24581	-0.26327
31	6	0	5.793007	-4.31241	0.775257
32	6	0	5.897703	-7.00974	0.022291
33	1	0	3.925591	-6.6922	-0.76832
34	6	0	6.9303	-5.07493	1.063638
35	1	0	5.752997	-3.28198	1.061207
36	6	0	6.984007	-6.42379	0.687125
37	1	0	7.85376	-7.00578	0.90733
38	6	0	-4.64724	-1.80564	-0.82191
39	6	0	-5.44015	-2.94681	-0.64699
40	6	0	-5.22209	-0.61617	-1.28829
41	6	0	-6.80537	-2.90466	-0.95732
42	1	0	-5.00187	-3.85142	-0.27933
43	6	0	-6.58991	-0.57158	-1.58989
44	1	0	-4.61694	0.257407	-1.41521
45	6	0	-7.38071	-1.717	-1.4275
46	1	0	-8.42342	-1.6848	-1.6624
47	6	0	8.120111	-4.42819	1.794639
48	6	0	5.958988	-8.49167	-0.39406
49	6	0	-7.22307	0.735407	-2.10103
50	6	0	-7.67409	-4.16354	-0.7848
51	9	0	8.973602	-3.90496	0.889291
52	9	0	8.759289	-5.36321	2.528686
53	9	0	5.220064	-8.67725	-1.5085
54	9	0	7.240577	-8.83662	-0.64134
55	9	0	5.470623	-9.26011	0.602833
56	9	0	7.669629	-3.4483	2.607213
57	9	0	-7.66539	-4.87644	-1.93162
58	9	0	-8.94017	-3.79909	-0.49132
59	9	0	-7.17884	-4.91927	0.21809
60	9	0	-8.26028	0.444634	-2.9147
61	9	0	-7.66375	1.461607	-1.05195
62	9	0	-6.30045	1.44547	-2.78443
63	6	0	2.798908	4.227349	-0.56406
64	6	0	2.627465	5.614214	-0.6718
65	6	0	4.089294	3.678973	-0.52081
66	6	0	3.746897	6.454295	-0.72376
67	1	0	1.642596	6.029752	-0.71686
68	6	0	5.207564	4.521716	-0.55168
69	1	0	4.219777	2.618148	-0.46209
70	6	0	5.027718	5.907937	-0.62029

71	1	0	6.194283	4.108479	-0.5179
72	6	0	-2.21484	1.865519	0.283918
73	6	0	-3.18824	2.873523	0.362437
74	6	0	-2.55015	0.540303	0.593632
75	6	0	-4.48134	2.561588	0.810397
76	1	0	-2.94423	3.876597	0.082162
77	6	0	-3.83563	0.234826	1.058999
78	1	0	-1.82176	-0.23633	0.480108
79	6	0	-4.77982	1.256315	1.208683
80	1	0	-4.09151	-0.77456	1.303659
81	6	0	-6.15704	0.97572	1.805829
82	6	0	-6.61427	-0.33007	2.017157
83	6	0	-6.94703	2.066008	2.149778
84	6	0	-7.89685	-0.53793	2.545595
85	1	0	-5.98945	-1.16401	1.775151
86	6	0	-8.23579	1.864974	2.663144
87	6	0	-8.71187	0.560624	2.858567
88	1	0	-8.25421	-1.53209	2.709113
89	1	0	-8.85513	2.704041	2.907229
90	1	0	-9.69671	0.403598	3.248676
91	6	0	6.219834	6.860118	-0.58831
92	6	0	7.53236	6.396612	-0.73646
93	6	0	5.962256	8.212361	-0.39438
94	6	0	8.594393	7.311217	-0.72315
95	1	0	7.72324	5.351217	-0.86121
96	6	0	7.018403	9.132434	-0.39312
97	6	0	8.336481	8.681232	-0.55919
98	1	0	9.600203	6.965296	-0.83906
99	1	0	6.820913	10.17565	-0.26357
100	1	0	9.145547	9.380964	-0.55955
101	6	0	4.507627	8.67666	-0.15674
102	6	0	-6.37805	3.491424	1.982833
103	8	0	3.578266	7.871889	-0.90727
104	8	0	-5.50391	3.573165	0.839517
105	6	0	4.189296	8.551142	1.344565
106	1	0	3.186936	8.879307	1.525209
107	1	0	4.289461	7.529091	1.646091
108	1	0	4.869727	9.156732	1.905352
109	6	0	4.360942	10.14356	-0.60114
110	1	0	5.03832	10.75441	-0.04223
111	1	0	4.585323	10.22457	-1.64441

112	1	0	3.357495	10.47058	-0.42602
113	6	0	-7.54075	4.479005	1.784336
114	1	0	-8.1914	4.440849	2.633499
115	1	0	-7.15167	5.46927	1.676026
116	1	0	-8.08786	4.211193	0.903381
117	6	0	-5.58549	3.858251	3.253269
118	1	0	-4.77696	3.168522	3.381436
119	1	0	-5.19436	4.850361	3.156569
120	1	0	-6.23317	3.811068	4.104181

TT2-D6B					
Center	Atomic #	Atomic Type	x	y	z
1	6	0	1.555439	3.421315	-0.18024
2	6	0	1.61311	2.072013	-0.15543
3	6	0	0.287403	1.389872	-0.01365
4	6	0	-0.74556	2.231662	0.197204
5	16	0	-0.16716	3.897519	-0.08973
6	16	0	2.898051	0.875352	-0.23162
7	6	0	0.41361	-0.13511	-0.1448
8	6	0	1.738191	-0.50694	-0.32121
9	6	0	2.180251	-1.95913	-0.56568
10	6	0	1.526903	-2.81971	-1.38944
11	6	0	3.429879	-2.6087	0.092597
12	16	0	2.193887	-4.45001	-1.23545
13	6	0	3.585466	-3.90594	-0.28565
14	1	0	4.093023	-2.09276	0.756592
15	6	0	-0.78023	-1.11398	-0.11468
16	6	0	-0.71723	-2.37409	0.392672
17	6	0	-2.19689	-0.7764	-0.65808
18	16	0	-2.19625	-3.27064	0.01819
19	6	0	-3.05478	-1.83079	-0.55026
20	1	0	-2.46722	0.176082	-1.06381
21	6	0	0.371913	-2.42951	-2.33023
22	1	0	-0.56008	-2.5364	-1.81605
23	1	0	0.49409	-1.41273	-2.64079
24	1	0	0.379825	-3.06762	-3.18969
25	6	0	0.472193	-2.94337	1.183912
26	1	0	0.959362	-2.15016	1.710173
27	1	0	0.118551	-3.67204	1.882874
28	1	0	1.164559	-3.40304	0.509691

29	6	0	4.795105	-4.79351	0.049671
30	6	0	4.82205	-6.1137	-0.41583
31	6	0	5.860737	-4.29348	0.812173
32	6	0	5.905042	-6.94544	-0.10905
33	1	0	4.011823	-6.48668	-1.00695
34	6	0	6.952668	-5.12193	1.111069
35	1	0	5.841608	-3.28261	1.165336
36	6	0	6.97013	-6.45077	0.656815
37	1	0	7.796768	-7.0874	0.89417
38	6	0	-4.56421	-1.79841	-0.87297
39	6	0	-5.31998	-2.97771	-0.77533
40	6	0	-5.18261	-0.60381	-1.26575
41	6	0	-6.68776	-2.96426	-1.07923
42	1	0	-4.85093	-3.8904	-0.47128
43	6	0	-6.55647	-0.58627	-1.5537
44	1	0	-4.60739	0.2943	-1.34493
45	6	0	-7.3081	-1.76737	-1.46167
46	1	0	-8.35447	-1.75481	-1.6852
47	6	0	8.132112	-4.57099	1.936859
48	6	0	5.921549	-8.40292	-0.61484
49	6	0	-7.23995	0.730502	-1.96939
50	6	0	-7.50612	-4.26646	-0.99288
51	9	0	9.052791	-4.03848	1.104863
52	9	0	8.692445	-5.57333	2.646362
53	9	0	5.25923	-8.48051	-1.78995
54	9	0	7.198629	-8.80397	-0.79172
55	9	0	5.320479	-9.20233	0.292629
56	9	0	7.685517	-3.61714	2.782245
57	9	0	-7.47984	-4.89363	-2.18832
58	9	0	-8.78327	-3.97662	-0.66544
59	9	0	-6.97122	-5.07205	-0.05066
60	9	0	-8.28516	0.459231	-2.77967
61	9	0	-7.67987	1.376211	-0.86835
62	9	0	-6.35367	1.509869	-2.62461
63	6	0	2.75158	4.393726	-0.26436
64	6	0	2.509538	5.772564	-0.26627
65	6	0	4.072298	3.915769	-0.34633
66	6	0	3.57707	6.671448	-0.35874
67	1	0	1.507607	6.138554	-0.20199
68	6	0	5.141306	4.825196	-0.42222
69	1	0	4.26366	2.863528	-0.35231

70	6	0	4.882991	6.201826	-0.40951
71	1	0	6.148384	4.469844	-0.48749
72	6	0	-2.16152	1.809703	0.625081
73	6	0	-3.14493	2.774117	0.8901
74	6	0	-2.46086	0.445983	0.754425
75	6	0	-4.40901	2.365657	1.339117
76	1	0	-2.92857	3.813577	0.753705
77	6	0	-3.7253	0.046558	1.201024
78	1	0	-1.72136	-0.2884	0.515824
79	6	0	-4.67882	1.015222	1.52583
80	1	0	-3.95999	-0.99213	1.297045
81	6	0	-6.0445	0.629006	2.085243
82	6	0	-6.47725	-0.70179	2.082289
83	6	0	-6.85282	1.637528	2.611577
84	6	0	-7.75516	-1.01764	2.561118
85	1	0	-5.83648	-1.47455	1.715643
86	6	0	-8.14387	1.327427	3.06556
87	6	0	-8.59482	-0.00054	3.038422
88	1	0	-8.09118	-2.03363	2.560228
89	1	0	-8.78224	2.101759	3.436679
90	1	0	-9.57865	-0.23894	3.385823
91	6	0	6.006887	7.23777	-0.46564
92	6	0	7.321057	6.87	-0.7787
93	6	0	5.690271	8.571417	-0.19046
94	6	0	8.313654	7.85452	-0.87998
95	1	0	7.567272	5.842689	-0.94497
96	6	0	6.680008	9.558928	-0.30405
97	6	0	7.991296	9.200436	-0.6534
98	1	0	9.316919	7.57998	-1.13065
99	1	0	6.436247	10.58526	-0.12087
100	1	0	8.745855	9.954253	-0.74573
101	8	0	4.359877	8.926765	0.233381
102	8	0	-6.35294	2.983963	2.714527
103	6	0	3.315026	8.187814	-0.43046
104	6	0	-5.52154	3.396751	1.611626
105	6	0	1.972495	8.502219	0.2558
106	1	0	1.778642	9.551801	0.19493
107	1	0	1.187052	7.964538	-0.23445
108	1	0	2.019492	8.206726	1.283068
109	6	0	3.256685	8.605462	-1.91202
110	1	0	4.193774	8.387065	-2.38122

111	1	0	2.476427	8.063833	-2.40496
112	1	0	3.06045	9.654859	-1.98066
113	6	0	-4.87884	4.751123	1.959747
114	1	0	-4.26508	5.073258	1.144505
115	1	0	-5.64481	5.475395	2.13797
116	1	0	-4.27807	4.643701	2.838984
117	6	0	-6.3877	3.535974	0.344688
118	1	0	-7.15476	4.260135	0.517493
119	1	0	-5.77644	3.851942	-0.47569
120	1	0	-6.83461	2.591473	0.111861

TT2-D7					
Center	Atomic #	Atomic Type	x	y	z
1	6	0	1.016083	3.572813	-0.28344
2	6	0	1.302588	2.255424	-0.25248
3	6	0	0.1242	1.358209	-0.02846
4	6	0	-1.0142	2.022919	0.275915
5	16	0	-0.74969	3.750791	-0.09978
6	16	0	2.767777	1.295123	-0.40152
7	6	0	0.500273	-0.12408	-0.2103
8	6	0	1.860531	-0.2658	-0.44696
9	6	0	2.536312	-1.62236	-0.72552
10	6	0	2.102053	-2.51021	-1.65718
11	6	0	3.797156	-2.13518	0.02363
12	16	0	2.978051	-4.0415	-1.51304
13	6	0	4.171941	-3.37768	-0.38813
14	1	0	4.314086	-1.57268	0.769808
15	6	0	-0.50746	-1.29192	-0.17734
16	6	0	-0.21579	-2.54251	0.278274
17	6	0	-1.97468	-1.18363	-0.67479
18	16	0	-1.53184	-3.66507	-0.09928
19	6	0	-2.63005	-2.3763	-0.61446
20	1	0	-2.41867	-0.27468	-1.02287
21	6	0	1.005152	-2.22557	-2.69589
22	1	0	0.051465	-2.4925	-2.28929
23	1	0	1.008677	-1.18464	-2.94309
24	1	0	1.191725	-2.80279	-3.57676
25	6	0	1.073423	-2.93812	1.018752
26	1	0	1.440266	-2.09971	1.572104
27	1	0	0.865931	-3.74602	1.690015

28	1	0	1.810252	-3.24635	0.306345
29	6	0	5.450487	-4.12059	0.052185
30	6	0	5.682172	-5.42461	-0.40864
31	6	0	6.375385	-3.50518	0.909246
32	6	0	6.82875	-6.12133	-0.00284
33	1	0	4.979064	-5.88935	-1.06964
34	6	0	7.533186	-4.19678	1.300694
35	1	0	6.19788	-2.5105	1.262294
36	6	0	7.754873	-5.50507	0.848364
37	1	0	8.632935	-6.03395	1.153992
38	6	0	-4.11841	-2.59286	-0.95437
39	6	0	-4.65764	-3.88739	-0.91861
40	6	0	-4.93008	-1.5064	-1.30629
41	6	0	-6.00275	-4.09875	-1.25803
42	1	0	-4.04029	-4.71315	-0.63615
43	6	0	-6.27897	-1.71595	-1.62852
44	1	0	-4.52164	-0.51841	-1.32915
45	6	0	-6.81068	-3.01246	-1.61377
46	1	0	-7.83634	-3.17286	-1.87406
47	6	0	8.563574	-3.52368	2.228529
48	6	0	7.071836	-7.5645	-0.48878
49	6	0	-7.1782	-0.52368	-1.99963
50	6	0	-6.5938	-5.52461	-1.24296
51	9	0	9.475541	-2.8638	1.483315
52	9	0	9.184991	-4.46544	2.970323
53	9	0	6.515809	-7.72957	-1.70795
54	9	0	8.399745	-7.79758	-0.56255
55	9	0	6.51128	-8.43236	0.380484
56	9	0	7.934318	-2.65206	3.045624
57	9	0	-6.42702	-6.09571	-2.4548
58	9	0	-7.9124	-5.46265	-0.95384
59	9	0	-5.96159	-6.26616	-0.30865
60	9	0	-8.13443	-0.9314	-2.85965
61	9	0	-7.75619	-0.03477	-0.88147
62	9	0	-6.43207	0.439382	-2.58012
63	6	0	2.030047	4.720952	-0.43672
64	6	0	1.567224	6.05149	-0.50544
65	6	0	3.421654	4.43919	-0.51264
66	6	0	2.512015	7.062831	-0.64508
67	1	0	0.521434	6.275852	-0.46023
68	6	0	4.356342	5.492735	-0.59865

69	1	0	3.761205	3.426298	-0.49882
70	6	0	3.857243	6.788176	-0.6211
71	1	0	5.409312	5.301601	-0.63705
72	6	0	4.582581	8.120179	-0.58698
73	6	0	5.942063	8.400442	-0.52815
74	6	0	3.620661	9.102154	-0.58862
75	6	0	6.321121	9.748939	-0.37105
76	1	0	6.673973	7.622784	-0.59177
77	6	0	3.958557	10.43799	-0.3806
78	6	0	5.330915	10.76257	-0.27473
79	1	0	7.357505	10.0091	-0.3206
80	1	0	3.204595	11.19472	-0.30988
81	1	0	5.625147	11.78019	-0.12272
82	6	0	-2.30356	1.412149	0.863372
83	6	0	-3.40394	2.251722	1.149817
84	6	0	-2.37583	0.016924	1.13068
85	6	0	-4.53279	1.675456	1.727786
86	1	0	-3.36812	3.30112	0.938026
87	6	0	-3.55419	-0.54408	1.668609
88	1	0	-1.53517	-0.60978	0.921563
89	6	0	-4.61805	0.315733	1.915459
90	1	0	-3.6283	-1.59101	1.87557
91	6	0	-6.03545	0.01853	2.373304
92	6	0	-6.64797	-1.19184	2.682834
93	6	0	-6.70407	1.220789	2.415004
94	6	0	-8.03208	-1.16837	2.952292
95	1	0	-6.09421	-2.10614	2.708111
96	6	0	-8.08216	1.26823	2.619707
97	6	0	-8.75173	0.055147	2.893165
98	1	0	-8.54255	-2.07628	3.198281
99	1	0	-8.61685	2.193862	2.579369
100	1	0	-9.80869	0.057262	3.060761
101	6	0	1.231948	9.054173	0.052002
102	1	0	1.132085	10.10609	-0.11218
103	1	0	0.300908	8.569908	-0.15845
104	1	0	1.504462	8.87601	1.070945
105	6	0	-5.49784	3.024197	3.507439
106	1	0	-4.77118	3.796421	3.36843
107	1	0	-6.40654	3.452526	3.879088
108	1	0	-5.12613	2.310075	4.2126
109	14	0	-5.76156	2.35667	2.220597

110	6	0	1.550214	8.964298	-2.57685
111	1	0	2.116139	8.465363	-3.33559
112	1	0	0.52843	8.651218	-2.63011
113	1	0	1.60739	10.02219	-2.72687
114	6	0	-6.42315	3.739491	1.031605
115	1	0	-7.48716	3.808128	1.121526
116	1	0	-5.98166	4.677817	1.295288
117	1	0	-6.16554	3.495217	0.022216
118	14	0	2.273063	8.51851	-0.83261

TT2-DAPh2					
Center	Atomic #	Atomic Type	x	y	z
1	6	0	-0.36642	3.457982	-0.24009
2	6	0	0.242165	2.224354	-0.30457
3	6	0	-0.57317	1.100555	0.077602
4	6	0	-1.85215	1.488437	0.457764
5	16	0	-2.01485	3.22182	0.303943
6	16	0	1.86886	1.718968	-0.73584
7	6	0	0.145686	-0.16699	-0.03087
8	6	0	1.440007	0.013437	-0.45138
9	6	0	2.492539	-0.97714	-0.73089
10	6	0	2.381347	-2.02185	-1.62925
11	6	0	3.788326	-0.91557	-0.11874
12	16	0	3.860356	-2.93997	-1.69346
13	6	0	4.649334	-1.90699	-0.51665
14	1	0	4.043339	-0.17068	0.627432
15	6	0	-0.45825	-1.48741	0.260148
16	6	0	0.024219	-2.39928	1.17806
17	6	0	-1.64493	-1.95046	-0.39765
18	16	0	-0.97591	-3.82874	1.217638
19	6	0	-2.06286	-3.19418	-0.00254
20	1	0	-2.15941	-1.36674	-1.15255
21	6	0	1.228135	-2.39685	-2.50971
22	1	0	0.607814	-3.17961	-2.05696
23	1	0	0.587775	-1.5262	-2.6764
24	1	0	1.571644	-2.76214	-3.4833
25	6	0	1.207288	-2.29171	2.092998
26	1	0	1.482909	-1.24154	2.223759
27	1	0	0.990237	-2.715	3.079865
28	1	0	2.084033	-2.81462	1.691852

29	6	0	6.028977	-2.14401	-0.07906
30	6	0	6.611404	-3.42295	-0.13477
31	6	0	6.808495	-1.08434	0.410775
32	6	0	7.922461	-3.62808	0.28616
33	1	0	6.034933	-4.26543	-0.50231
34	6	0	8.117148	-1.30033	0.842668
35	1	0	6.399413	-0.0796	0.433593
36	6	0	8.68719	-2.5699	0.782142
37	1	0	9.70894	-2.73082	1.103096
38	6	0	-3.26594	-3.92139	-0.42202
39	6	0	-3.31481	-5.32514	-0.46053
40	6	0	-4.42106	-3.2063	-0.77481
41	6	0	-4.48272	-5.985	-0.83811
42	1	0	-2.43535	-5.90504	-0.20001
43	6	0	-5.58601	-3.87414	-1.14966
44	1	0	-4.41836	-2.12354	-0.71909
45	6	0	-5.62952	-5.26685	-1.1837
46	1	0	-6.53885	-5.78393	-1.4647
47	6	0	8.901046	-0.12392	1.366089
48	6	0	8.50471	-5.01854	0.275515
49	6	0	-6.81639	-3.05576	-1.44325
50	6	0	-4.49262	-7.4886	-0.94048
51	9	0	8.951596	0.876096	0.45767
52	9	0	10.17005	-0.45279	1.680525
53	9	0	7.923471	-5.80098	-0.65885
54	9	0	9.831861	-4.99997	0.026912
55	9	0	8.33528	-5.63292	1.468457
56	9	0	8.327319	0.390343	2.477707
57	9	0	-4.16824	-7.90069	-2.18738
58	9	0	-5.71109	-8.00002	-0.66121
59	9	0	-3.60683	-8.05661	-0.09396
60	9	0	-7.80129	-3.79135	-1.99657
61	9	0	-7.31878	-2.49744	-0.31364
62	9	0	-6.54375	-2.03526	-2.28674
63	6	0	0.153972	4.794855	-0.54392
64	6	0	-0.35249	5.937307	0.10445
65	6	0	1.176591	4.968838	-1.49556
66	6	0	0.146098	7.204124	-0.18748
67	6	0	1.680086	6.237276	-1.77677
68	6	0	1.168373	7.361163	-1.12598
69	1	0	2.468698	6.346971	-2.51632

70	1	0	1.561093	8.349414	-1.34813
71	6	0	-3.00776	0.726234	0.970356
72	6	0	-4.2659	0.832309	0.350026
73	6	0	-2.88662	-0.09013	2.108057
74	6	0	-5.36419	0.124288	0.839475
75	1	0	-4.37319	1.458613	-0.53152
76	6	0	-3.98535	-0.79575	2.595598
77	6	0	-5.22595	-0.69547	1.961642
78	1	0	-3.87216	-1.4236	3.475173
79	1	0	-6.07902	-1.25529	2.334126
80	8	0	-1.62163	-0.18682	2.767871
81	8	0	-6.62636	0.218985	0.174001
82	8	0	1.68068	3.838373	-2.21169
83	8	0	-0.3865	8.344392	0.491513
84	1	0	-1.11629	5.828991	0.845923
85	6	0	-7.45845	1.158042	0.860074
86	1	0	-7.04451	2.139817	0.761722
87	1	0	-7.51287	0.896054	1.896076
88	6	0	-8.87198	1.133381	0.249407
89	1	0	-9.3857	0.252916	0.574636
90	1	0	-8.79932	1.130102	-0.81812
91	6	0	-9.65073	2.38065	0.70709
92	1	0	-9.23802	3.250208	0.239719
93	1	0	-9.576	2.477627	1.770063
94	6	0	-11.131	2.236828	0.307553
95	1	0	-11.5536	1.388305	0.803881
96	1	0	-11.6648	3.11924	0.592766
97	1	0	-11.2032	2.103012	-0.75159
98	6	0	-1.78619	0.097695	4.159587
99	1	0	-2.14199	-0.77699	4.662809
100	1	0	-2.49378	0.891217	4.280177
101	6	0	-0.43291	0.520907	4.760535
102	1	0	0.210204	-0.33169	4.826733
103	1	0	0.019547	1.261189	4.134306
104	6	0	-0.65645	1.105765	6.167508
105	1	0	-1.10844	0.365317	6.79388
106	1	0	-1.29998	1.958054	6.101372
107	6	0	0.696747	1.529656	6.76816
108	1	0	0.546395	1.897827	7.76151
109	1	0	1.354458	0.686132	6.796162
110	1	0	1.129595	2.299532	6.164144

111	6	0	0.111483	9.538421	-0.11775
112	1	0	1.170299	9.596854	0.025063
113	1	0	-0.10678	9.522171	-1.16513
114	6	0	-0.56199	10.76359	0.528008
115	1	0	-1.61333	10.73799	0.330688
116	1	0	-0.39694	10.74549	1.585047
117	6	0	0.040134	12.05164	-0.06359
118	1	0	1.088812	12.0843	0.146434
119	1	0	-0.11203	12.06278	-1.12265
120	6	0	-0.64805	13.27662	0.566817
121	1	0	-0.21588	14.17169	0.170608
122	1	0	-1.69346	13.25453	0.339818
123	1	0	-0.51296	13.25478	1.62803
124	6	0	2.277335	4.275824	-3.43543
125	1	0	1.611493	4.946569	-3.93708
126	1	0	3.197676	4.778845	-3.22367
127	6	0	2.553598	3.057581	-4.33607
128	1	0	3.321689	2.456039	-3.89666
129	1	0	1.659822	2.477842	-4.43591
130	6	0	3.010752	3.539501	-5.72545
131	1	0	3.879402	4.155535	-5.62129
132	1	0	2.225695	4.104376	-6.18316
133	6	0	3.347595	2.321793	-6.60597
134	1	0	4.158065	1.777897	-6.16755
135	1	0	2.489836	1.686341	-6.67911
136	1	0	3.628924	2.655074	-7.58305

TT2-EDAPh2					
Center	Atomic #	Atomic Type	x	y	z
1	6	0	-1.97159	-2.45124	-0.1275
2	6	0	-1.73923	-1.12246	-0.34737
3	6	0	-0.36487	-0.72781	-0.18225
4	6	0	0.436251	-1.78847	0.17442
5	16	0	-0.48571	-3.24823	0.292255
6	16	0	-2.74287	0.253397	-0.78245
7	6	0	-0.15404	0.694945	-0.3961
8	6	0	-1.31905	1.338558	-0.72999
9	6	0	-1.55401	2.749855	-1.06828
10	6	0	-0.87313	3.453894	-2.04475
11	6	0	-2.57916	3.533459	-0.44175

12	16	0	-1.46973	5.086272	-2.15617
13	6	0	-2.66992	4.821888	-0.90466
14	1	0	-3.23198	3.12811	0.323721
15	6	0	1.177169	1.315831	-0.22619
16	6	0	1.470153	2.360151	0.628816
17	6	0	2.338201	0.830797	-0.91422
18	16	0	3.165557	2.76248	0.557331
19	6	0	3.498282	1.500649	-0.61388
20	1	0	2.296418	-0.00483	-1.60482
21	6	0	0.216137	2.990427	-2.96371
22	1	0	1.211309	3.239865	-2.5759
23	1	0	0.170186	1.903548	-3.07613
24	1	0	0.119847	3.443201	-3.95603
25	6	0	0.561326	3.110548	1.555128
26	1	0	-0.32963	2.512428	1.764767
27	1	0	1.055947	3.335283	2.5061
28	1	0	0.227123	4.060218	1.11952
29	6	0	-3.58837	5.882693	-0.47764
30	6	0	-3.87255	6.986038	-1.3003
31	6	0	-4.21648	5.815672	0.7779
32	6	0	-4.75227	7.981559	-0.8809
33	1	0	-3.42031	7.061543	-2.28349
34	6	0	-5.10789	6.806365	1.183573
35	1	0	-3.99414	4.996	1.451494
36	6	0	-5.3824	7.898929	0.360852
37	1	0	-6.07029	8.671909	0.682625
38	6	0	4.84664	1.272386	-1.14393
39	6	0	5.993591	1.673321	-0.43735
40	6	0	5.023762	0.635179	-2.38377
41	6	0	7.266769	1.44219	-0.95325
42	1	0	5.894804	2.151824	0.531169
43	6	0	6.30082	0.392047	-2.88557
44	1	0	4.15942	0.34591	-2.97083
45	6	0	7.433277	0.794296	-2.17777
46	1	0	8.424765	0.610145	-2.57427
47	6	0	-5.81989	6.671479	2.505628
48	6	0	-4.99012	9.190281	-1.75007
49	6	0	6.455428	-0.3564	-4.18503
50	6	0	8.480714	1.939588	-0.21037
51	9	0	-6.98163	5.992367	2.373189
52	9	0	-6.12346	7.875376	3.035197

53	9	0	-4.76182	8.926649	-3.05433
54	9	0	-6.25835	9.6407	-1.63893
55	9	0	-4.17648	10.21307	-1.40307
56	9	0	-5.0728	6.002237	3.41105
57	9	0	8.875728	3.149435	-0.66685
58	9	0	9.530131	1.102202	-0.35602
59	9	0	8.243245	2.072506	1.112106
60	9	0	7.606084	-0.03823	-4.81405
61	9	0	6.468739	-1.69391	-3.98513
62	9	0	5.437959	-0.09602	-5.03542
63	6	0	-3.28888	-3.24523	-0.2045
64	6	0	-4.31636	-3.86455	-0.26456
65	6	0	1.947194	-1.79872	0.471988
66	6	0	3.125729	-1.80671	0.704091
67	6	0	-5.63365	-4.65854	-0.34157
68	6	0	-6.3169	-4.99133	0.828427
69	6	0	-6.14375	-5.0449	-1.58095
70	6	0	-7.50964	-5.7109	0.758998
71	6	0	-7.33735	-5.76384	-1.65063
72	1	0	-5.60546	-4.78254	-2.5032
73	6	0	-8.02025	-6.097	-0.48093
74	1	0	-8.04792	-5.97379	1.681191
75	1	0	-8.96073	-6.66429	-0.53543
76	6	0	4.636672	-1.81696	1.001659
77	6	0	5.505961	-2.52714	0.173139
78	6	0	5.136158	-1.11618	2.099373
79	6	0	6.874333	-2.53705	0.442738
80	1	0	5.111771	-3.08015	-0.69175
81	6	0	6.505038	-1.12518	2.368623
82	6	0	7.374122	-1.83556	1.54062
83	1	0	6.898624	-0.57222	3.233956
84	1	0	8.453079	-1.84347	1.752957
85	8	0	-5.79307	-4.5959	2.098915
86	8	0	-7.86029	-6.1593	-2.92147
87	8	0	4.245372	-0.38801	2.948583
88	8	0	7.765313	-3.26561	-0.40594
89	6	0	-6.46787	-5.31129	3.137071
90	1	0	-7.49264	-5.00557	3.172929
91	1	0	-6.41569	-6.36143	2.938628
92	6	0	-5.79478	-5.01029	4.489085
93	1	0	-4.79223	-5.38408	4.479445

94	1	0	-5.77965	-3.95294	4.652416
95	6	0	-6.58636	-5.69312	5.619898
96	1	0	-6.59645	-6.75102	5.459755
97	1	0	-7.59054	-5.32368	5.62577
98	6	0	-5.91814	-5.38509	6.972747
99	1	0	-4.91289	-5.75159	6.96568
100	1	0	-5.91102	-4.32739	7.134405
101	1	0	-6.46623	-5.86225	7.758122
102	6	0	-8.79047	-7.23058	-2.74248
103	1	0	-9.66399	-6.86497	-2.24429
104	1	0	-8.33887	-8.00013	-2.15193
105	6	0	-9.18495	-7.80289	-4.11669
106	1	0	-9.58698	-7.02103	-4.72659
107	1	0	-8.32048	-8.21725	-4.59198
108	6	0	-10.245	-8.90411	-3.92904
109	1	0	-11.1051	-8.49222	-3.44387
110	1	0	-9.83927	-9.69107	-3.32822
111	6	0	-10.651	-9.4655	-5.30438
112	1	0	-11.3928	-10.2257	-5.17449
113	1	0	-11.0501	-8.6771	-5.90774
114	1	0	-9.79226	-9.8838	-5.78652
115	6	0	4.555879	-0.66603	4.316497
116	1	0	5.401208	-0.08245	4.616078
117	1	0	4.783281	-1.70579	4.426406
118	6	0	3.346342	-0.30888	5.200275
119	1	0	3.101475	0.724429	5.069072
120	1	0	2.508677	-0.9124	4.919239
121	6	0	3.69484	-0.5703	6.677369
122	1	0	3.95122	-1.6011	6.806299
123	1	0	4.524997	0.041971	6.961726
124	6	0	2.479536	-0.22937	7.559637
125	1	0	2.212607	0.79706	7.417866
126	1	0	1.654361	-0.85346	7.286711
127	1	0	2.72724	-0.39481	8.587339
128	6	0	8.38203	-4.3179	0.340553
129	1	0	9.121052	-3.90515	0.995067
130	1	0	7.639547	-4.82831	0.917698
131	6	0	9.05117	-5.31056	-0.6282
132	1	0	9.803315	-4.80325	-1.19549
133	1	0	8.314511	-5.71277	-1.29186
134	6	0	9.69802	-6.45446	0.174707

135	1	0	10.40473	-6.04842	0.867956
136	1	0	8.940095	-6.98797	0.709328
137	6	0	10.41859	-7.41493	-0.7896
138	1	0	11.18564	-6.88458	-1.31427
139	1	0	10.85638	-8.21712	-0.23307
140	1	0	9.714415	-7.81041	-1.49148

TT2-EDOT2					
Center	Atomic #	Atomic Type	x	y	z
1	6	0	-0.81242	4.357969	-0.22683
2	6	0	-0.08924	3.223497	-0.1283
3	6	0	-0.89759	1.988979	0.130722
4	6	0	-2.20718	2.23267	0.371468
5	16	0	-2.53821	3.934067	-0.05521
6	16	0	1.62203	2.822764	-0.22277
7	6	0	-0.0262	0.727013	0.054595
8	6	0	1.297373	1.048555	-0.19639
9	6	0	2.369728	-0.02396	-0.43782
10	6	0	2.142779	-1.13067	-1.18672
11	6	0	3.818699	0.023145	0.121156
12	16	0	3.51532	-2.24407	-1.08949
13	6	0	4.548579	-1.05853	-0.27265
14	1	0	4.198354	0.818079	0.729305
15	6	0	-0.54187	-0.7173	0.203686
16	6	0	0.157838	-1.7024	0.824982
17	6	0	-1.91172	-1.22213	-0.32941
18	16	0	-0.63297	-3.26506	0.605881
19	6	0	-2.10305	-2.54432	-0.06268
20	1	0	-2.62216	-0.60298	-0.83583
21	6	0	0.860008	-1.36529	-2.00632
22	1	0	0.128534	-1.84749	-1.39215
23	1	0	0.478169	-0.42354	-2.34352
24	1	0	1.078891	-1.98319	-2.85189
25	6	0	1.456613	-1.49534	1.615748
26	1	0	1.45335	-0.52209	2.060009
27	1	0	1.523814	-2.23773	2.38239
28	1	0	2.295191	-1.58386	0.957384

29	6	0	-0.2615	5.774606	-0.44433
30	6	0	-1.03308	6.878826	-0.61015
31	16	0	1.45649	6.204299	-0.54027
32	6	0	-0.21875	8.120806	-0.94278
33	6	0	1.105777	7.855863	-1.08497
34	6	0	-3.23612	1.227744	0.927526
35	6	0	-4.52348	1.52812	1.258035
36	16	0	-2.91557	-0.4877	1.239786
37	6	0	-5.21047	0.396392	2.019811
38	6	0	-4.43115	-0.70958	2.133978
39	6	0	6.063878	-1.24267	-0.05745
40	6	0	6.683606	-2.39946	-0.54765
41	6	0	6.824114	-0.26863	0.61153
42	6	0	8.063889	-2.57765	-0.39314
43	1	0	6.099108	-3.14823	-1.04067
44	6	0	8.209701	-0.44482	0.759017
45	1	0	6.350405	0.605971	1.007275
46	6	0	8.827465	-1.59862	0.255229
47	1	0	9.884034	-1.73318	0.366264
48	6	0	-3.40626	-3.33007	-0.29405
49	6	0	-3.45044	-4.68795	0.043526
50	6	0	-4.53901	-2.70244	-0.83218
51	6	0	-4.62754	-5.42012	-0.14074
52	1	0	-2.57983	-5.16703	0.444099
53	6	0	-5.72509	-3.43059	-1.01145
54	1	0	-4.50042	-1.66825	-1.10519
55	6	0	-5.76876	-4.79463	-0.66868
56	1	0	-6.67055	-5.35703	-0.80824
57	6	0	9.058686	0.628113	1.46993
58	6	0	8.746928	-3.84636	-0.93799
59	6	0	-6.97372	-2.72423	-1.58204
60	6	0	-4.65855	-6.91206	0.242245
61	9	0	9.488549	1.532556	0.564348
62	9	0	10.12289	0.042498	2.060482
63	9	0	8.088801	-4.27834	-2.03473
64	9	0	10.02622	-3.5623	-1.26344
65	9	0	8.72651	-4.81086	0.007184
66	9	0	8.310727	1.248602	2.406299
67	9	0	-4.27338	-7.65734	-0.81573
68	9	0	-5.9114	-7.25924	0.605124
69	9	0	-3.81475	-7.12691	1.274952

70	9	0	-7.73233	-3.61341	-2.25862
71	9	0	-7.6959	-2.1987	-0.56847
72	9	0	-6.58768	-1.73678	-2.41815
73	1	0	1.829012	8.542166	-1.46822
74	1	0	-4.68954	-1.58429	2.691866
75	8	0	-0.83815	9.387475	-1.0775
76	8	0	-2.45104	6.92527	-0.53271
77	8	0	-5.21052	2.735984	0.970292
78	8	0	-6.51416	0.554247	2.559537
79	6	0	-2.24924	9.245663	-1.35076
80	1	0	-2.69838	10.21441	-1.27583
81	1	0	-2.39826	8.85728	-2.33685
82	6	0	-2.91435	8.277859	-0.32499
83	1	0	-2.67461	8.604758	0.666029
84	1	0	-3.97722	8.28853	-0.45753
85	6	0	-6.33077	2.918047	1.867781
86	1	0	-5.98085	3.127305	2.860115
87	1	0	-6.91187	3.743142	1.510617
88	6	0	-7.21613	1.630702	1.905911
89	1	0	-8.11269	1.829396	2.460562
90	1	0	-7.47131	1.348602	0.904538

TT4-D1					
Center	Atomic #	Atomic Type	x	y	z
1	6	0	2.177806	-2.11781	0.005838
2	6	0	1.77808	-0.80004	0.117374
3	6	0	0.370638	-0.55947	-0.05068
4	6	0	-0.3331	-1.72931	-0.32267
5	16	0	0.76291	-3.09722	-0.32778
6	16	0	2.654828	0.689945	0.415153
7	6	0	0.026625	0.847488	0.114085
8	6	0	1.135662	1.617305	0.362539
9	6	0	1.241814	3.066365	0.602689
10	6	0	0.610793	3.748237	1.625867
11	6	0	2.078245	3.917943	-0.19197
12	16	0	1.017736	5.440933	1.57951
13	6	0	2.070994	5.235247	0.192362
14	1	0	2.673677	3.541151	-1.01657
15	6	0	-1.35382	1.3797	0.045649
16	6	0	-1.79158	2.32019	-0.86433

17	6	0	-2.39375	0.945739	0.931173
18	16	0	-3.47847	2.678781	-0.6194
19	6	0	-3.60783	1.546304	0.712127
20	1	0	-2.23763	0.181214	1.684307
21	6	0	-0.29618	3.223477	2.697002
22	1	0	-1.35278	3.354983	2.434676
23	1	0	-0.12299	2.153265	2.840657
24	1	0	-0.12091	3.730392	3.651686
25	6	0	-1.03265	2.995941	-1.96674
26	1	0	-0.12899	2.426078	-2.20005
27	1	0	-1.6345	3.071046	-2.87875
28	1	0	-0.72186	4.009986	-1.68626
29	6	0	2.785236	6.365555	-0.41064
30	6	0	3.061364	7.535178	0.314894
31	6	0	3.214392	6.300616	-1.74881
32	6	0	3.736029	8.601998	-0.27871
33	6	0	3.902146	7.362295	-2.32913
34	6	0	4.164816	8.525392	-1.60204
35	6	0	-4.87179	1.332281	1.424877
36	6	0	-6.1129	1.558742	0.805976
37	6	0	-4.86768	0.884625	2.756593
38	6	0	-7.30354	1.34335	1.49698
39	6	0	-6.06276	0.655252	3.435637
40	6	0	-7.29025	0.885045	2.81448
41	6	0	3.483108	-2.72732	0.115389
42	6	0	3.864756	-3.96964	-0.32252
43	16	0	4.825714	-1.85799	0.892875
44	6	0	5.235974	-4.28082	-0.0561
45	1	0	3.20512	-4.64014	-0.8614
46	6	0	5.907902	-3.21027	0.600726
47	6	0	-1.72881	-2.00937	-0.6311
48	6	0	-2.50033	-2.99906	-0.08327
49	16	0	-2.57834	-1.15316	-1.93643
50	6	0	-3.80593	-3.10582	-0.66583
51	1	0	-2.16699	-3.61831	0.741483
52	6	0	-4.0052	-2.1472	-1.70073
53	6	0	5.948935	-5.45008	-0.37636
54	6	0	7.303869	-5.49676	-0.06053
55	6	0	7.976636	-4.42212	0.58977
56	6	0	7.25591	-3.26624	0.938559
57	6	0	9.374507	-4.70717	0.785521

58	1	0	10.06581	-4.00785	1.24075
59	6	0	9.733047	-5.92888	0.314676
60	1	0	10.7187	-6.37592	0.330431
61	16	0	8.407338	-6.82084	-0.4093
62	6	0	-5.20781	-2.03833	-2.39347
63	6	0	-6.25824	-2.9006	-2.03576
64	6	0	-6.05575	-3.86413	-1.00553
65	6	0	-4.84727	-3.98688	-0.32534
66	6	0	-7.59498	-2.96064	-2.56856
67	1	0	-7.9564	-2.29496	-3.34333
68	6	0	-8.35432	-3.91715	-1.9764
69	1	0	-9.38899	-4.15729	-2.18484
70	16	0	-7.51139	-4.81013	-0.72374
71	8	0	5.338152	-6.49701	-1.02862
72	8	0	7.87081	-2.19654	1.549308
73	8	0	-4.6901	-4.90747	0.685563
74	8	0	-5.37492	-1.07926	-3.36754
75	6	0	4.714218	-7.45218	-0.16136
76	1	0	5.447405	-7.91377	0.511242
77	1	0	3.920063	-6.98567	0.434999
78	1	0	4.282914	-8.21688	-0.81077
79	6	0	7.935721	-2.28623	2.978072
80	1	0	6.931867	-2.33718	3.417211
81	1	0	8.513256	-3.16374	3.294457
82	1	0	8.436243	-1.377	3.317517
83	6	0	-4.19618	-6.18219	0.25552
84	1	0	-4.13096	-6.80142	1.152581
85	1	0	-4.87964	-6.65009	-0.46338
86	1	0	-3.20211	-6.08755	-0.19932
87	6	0	-5.08627	-1.52884	-4.6971
88	1	0	-5.74918	-2.35287	-4.98905
89	1	0	-5.25751	-0.6722	-5.35243
90	1	0	-4.043	-1.85564	-4.78696
91	9	0	2.93531	5.209136	-2.49264
92	9	0	4.320061	7.266761	-3.60925
93	9	0	4.818724	9.559481	-2.17262
94	9	0	3.97616	9.721164	0.437042
95	9	0	2.693829	7.629719	1.610456
96	9	0	-3.69441	0.696183	3.397227
97	9	0	-6.03209	0.205831	4.708264
98	9	0	-8.44583	0.668387	3.477936

99	9	0	-8.48304	1.580813	0.884693
100	9	0	-6.15975	1.957983	-0.48279

TT4-D2					
Center	Atomic #	Atomic Type	x	y	z
1	6	0	-1.78974	-3.03891	0.050506
2	6	0	-1.5956	-1.67524	-0.05637
3	6	0	-0.2468	-1.21644	0.132775
4	6	0	0.631708	-2.25972	0.415565
5	16	0	-0.24148	-3.78516	0.40528
6	16	0	-2.69144	-0.34478	-0.38718
7	6	0	-0.12885	0.228558	-0.02989
8	6	0	-1.34028	0.811404	-0.31178
9	6	0	-1.66961	2.220074	-0.5858
10	6	0	-1.11535	2.98083	-1.59821
11	6	0	-2.67492	2.932284	0.148377
12	16	0	-1.8034	4.580901	-1.61384
13	6	0	-2.8727	4.223899	-0.27044
14	1	0	-3.2381	2.47498	0.954803
15	6	0	1.143728	0.977182	0.081477
16	6	0	1.374492	2.012376	0.965089
17	6	0	2.286912	0.688809	-0.73422
18	16	0	2.990589	2.638154	0.780028
19	6	0	3.370048	1.493953	-0.4919
20	1	0	2.28495	-0.08915	-1.48947
21	6	0	-0.08617	2.595951	-2.61695
22	1	0	0.923023	2.896389	-2.31073
23	1	0	-0.07992	1.510085	-2.74653
24	1	0	-0.29441	3.056818	-3.58821
25	6	0	0.46796	2.587775	2.011718
26	1	0	-0.31892	1.869726	2.258923
27	1	0	1.017175	2.821996	2.930022
28	1	0	-0.01941	3.508936	1.66935
29	6	0	-3.80387	5.222685	0.264434
30	6	0	-4.25883	6.298421	-0.51602
31	6	0	-4.27212	5.119993	1.58603
32	6	0	-5.14849	7.234731	0.00798
33	6	0	-5.17422	6.049866	2.097242
34	6	0	-5.61816	7.117304	1.315616
35	6	0	4.695378	1.450235	-1.11821

36	6	0	5.476631	2.607375	-1.2753
37	6	0	5.220144	0.227734	-1.56958
38	6	0	6.736259	2.541844	-1.8679
39	6	0	6.477618	0.172775	-2.16848
40	6	0	7.247319	1.325905	-2.32246
41	6	0	-2.97922	-3.8423	-0.08635
42	6	0	-3.19656	-5.11603	0.408263
43	16	0	-4.38111	-3.2374	-1.00513
44	6	0	-4.47747	-5.60406	0.059148
45	1	0	-2.4675	-5.64135	1.014865
46	6	0	-5.25567	-4.70511	-0.68914
47	6	0	-6.5003	-5.33143	-0.91888
48	6	0	-6.43907	-6.59343	-0.30662
49	16	0	-8.04171	-5.09274	-1.6917
50	6	0	-7.62664	-7.36578	-0.44699
51	6	0	-8.56942	-6.68335	-1.16793
52	1	0	-7.78675	-8.35871	-0.04265
53	1	0	-9.56481	-7.01602	-1.42928
54	6	0	2.05211	-2.31338	0.716865
55	6	0	2.984081	-3.1478	0.127751
56	16	0	2.752261	-1.38582	2.065641
57	6	0	4.260775	-3.02355	0.72947
58	1	0	2.740303	-3.7901	-0.71097
59	6	0	4.31279	-2.09524	1.783958
60	6	0	5.654491	-2.05703	2.225857
61	6	0	6.371037	-2.96764	1.43285
62	16	0	6.697288	-1.3017	3.398034
63	6	0	7.755143	-3.0555	1.756448
64	6	0	8.067633	-2.21667	2.791332
65	1	0	8.482025	-3.68492	1.256382
66	1	0	9.038223	-2.06564	3.244128
67	7	0	-5.19613	-6.7676	0.280311
68	7	0	5.516615	-3.57163	0.526951
69	6	0	-4.78325	-7.88866	1.10049
70	1	0	-5.25093	-8.80418	0.728206
71	1	0	-3.69884	-8.00973	1.032192
72	1	0	-5.05942	-7.75225	2.153997
73	6	0	5.883576	-4.50821	-0.51915
74	1	0	6.770658	-5.06515	-0.20734
75	1	0	5.069802	-5.2234	-0.67051
76	1	0	6.097223	-3.99833	-1.46388

77	9	0	4.512933	-0.9079	-1.38878
78	9	0	6.956671	-1.01147	-2.60504
79	9	0	8.468831	1.266049	-2.89415
80	9	0	7.469785	3.667029	-2.00355
81	9	0	5.002324	3.800423	-0.85796
82	9	0	-3.8267	4.124707	2.381962
83	9	0	-5.62422	5.917069	3.36309
84	9	0	-6.48447	8.022678	1.817918
85	9	0	-5.56	8.266685	-0.75898
86	9	0	-3.85547	6.420558	-1.79855

TT4-D5					
Center	Atomic #	Atomic Type	x	y	z
1	6	0	-2.12654	-2.13787	0.020001
2	6	0	-1.72165	-0.81903	-0.06907
3	6	0	-0.31492	-0.57749	0.10171
4	6	0	0.393532	-1.7495	0.363563
5	16	0	-0.71407	-3.11635	0.378058
6	16	0	-2.60011	0.665793	-0.38482
7	6	0	0.022675	0.831137	-0.06455
8	6	0	-1.08708	1.598415	-0.32118
9	6	0	-1.20068	3.045941	-0.56964
10	6	0	-0.58197	3.724387	-1.60253
11	6	0	-2.04434	3.896418	0.218696
12	16	0	-1.00932	5.412892	-1.57344
13	6	0	-2.05603	5.208981	-0.18123
14	1	0	-2.63519	3.521182	1.047332
15	6	0	1.396534	1.380837	0.000863
16	6	0	1.816514	2.34448	0.895078
17	6	0	2.437173	0.974705	-0.89738
18	16	0	3.487092	2.758914	0.620766
19	6	0	3.629271	1.6263	-0.70926
20	1	0	2.28125	0.237108	-1.67707
21	6	0	0.323966	3.197539	-2.67351
22	1	0	1.381076	3.341094	-2.41996
23	1	0	0.160063	2.124271	-2.80462
24	1	0	0.137874	3.692544	-3.63242
25	6	0	1.054477	3.001485	2.006687
26	1	0	0.172517	2.405439	2.256515
27	1	0	1.667841	3.099305	2.909006

28	1	0	0.709485	4.004408	1.726621
29	6	0	-2.79511	6.33264	0.403769
30	6	0	-3.11857	7.473625	-0.35047
31	6	0	-3.20807	6.288663	1.746069
32	6	0	-3.83049	8.526982	0.218983
33	6	0	-3.93385	7.339257	2.304271
34	6	0	-4.24968	8.467932	1.548453
35	6	0	4.879672	1.465589	-1.45843
36	6	0	5.771548	2.534802	-1.63769
37	6	0	5.206753	0.222256	-2.02911
38	6	0	6.944355	2.370336	-2.37441
39	6	0	6.374202	0.070702	-2.77251
40	6	0	7.25257	1.141222	-2.95371
41	6	0	-3.42154	-2.74841	-0.1294
42	6	0	-3.74454	-4.09804	-0.09497
43	16	0	-4.87557	-1.78043	-0.39195
44	6	0	-5.11714	-4.37058	-0.27374
45	1	0	-2.991	-4.86554	0.053109
46	6	0	-5.86165	-3.21062	-0.44805
47	6	0	-7.29154	-3.34316	-0.64471
48	6	0	-7.82902	-4.6232	-0.6463
49	16	0	-8.5059	-2.12064	-0.89111
50	6	0	-9.23625	-4.60483	-0.84911
51	6	0	-9.74589	-3.3401	-0.99687
52	1	0	-9.86009	-5.49227	-0.88615
53	1	0	-10.7734	-3.04412	-1.16159
54	6	0	1.780763	-2.05168	0.658856
55	6	0	2.497256	-3.15577	0.219956
56	16	0	2.730173	-1.14157	1.83712
57	6	0	3.78712	-3.2774	0.784217
58	1	0	2.084108	-3.84534	-0.50968
59	6	0	4.05895	-2.24785	1.677191
60	6	0	5.359979	-2.23732	2.320106
61	6	0	6.235097	-3.27394	2.028397
62	16	0	6.040642	-1.10008	3.448672
63	6	0	7.46566	-3.13872	2.728156
64	6	0	7.514338	-2.02544	3.527629
65	1	0	8.294098	-3.83529	2.647846
66	1	0	8.325014	-1.68602	4.158613
67	6	0	-6.48785	-6.88182	1.295356
68	1	0	-7.31033	-7.60163	1.232802

69	1	0	-5.55898	-7.43465	1.468881
70	1	0	-6.66576	-6.21637	2.143712
71	6	0	6.219473	-4.70864	-0.93332
72	1	0	7.067513	-5.3902	-0.80903
73	1	0	5.523488	-5.15674	-1.64994
74	1	0	6.584205	-3.76458	-1.33977
75	6	0	-6.03711	-7.06694	-1.86463
76	1	0	-5.95846	-6.50606	-2.79922
77	1	0	-5.10722	-7.62277	-1.70677
78	1	0	-6.85728	-7.78671	-1.95313
79	6	0	4.916289	-6.20501	1.555541
80	1	0	4.29667	-6.78312	0.862195
81	1	0	5.838734	-6.76468	1.741245
82	1	0	4.377333	-6.09093	2.499346
83	32	0	-6.36069	-5.86875	-0.36333
84	32	0	5.33224	-4.46536	0.780438
85	9	0	-2.87986	5.229618	2.516265
86	9	0	-4.33564	7.263575	3.59087
87	9	0	-4.94639	9.486966	2.094954
88	9	0	-4.11799	9.617005	-0.52378
89	9	0	-2.76325	7.546848	-1.65081
90	9	0	5.487852	3.743168	-1.10678
91	9	0	7.789103	3.412162	-2.52771
92	9	0	8.385064	0.986452	-3.67204
93	9	0	6.660895	-1.127	-3.32552
94	9	0	4.397936	-0.84001	-1.82932

TT4-EDOT2					
Center	Atomic #	Atomic Type	x	y	z
1	6	0	-1.00838	3.769392	-0.16697
2	6	0	-0.20474	2.644586	-0.21198
3	6	0	-0.82197	1.419934	0.211266
4	6	0	-2.13804	1.608184	0.622454
5	16	0	-2.58435	3.295364	0.447616
6	16	0	1.460926	2.388579	-0.70677
7	6	0	0.079463	0.279608	0.098165
8	6	0	1.314556	0.646435	-0.37567
9	6	0	2.49629	-0.18153	-0.67054
10	6	0	2.522376	-1.22975	-1.57097
11	6	0	3.779846	0.06895	-0.08215

12	16	0	4.115935	-1.92788	-1.6582
13	6	0	4.769842	-0.78487	-0.49939
14	1	0	3.947742	0.878399	0.620115
15	6	0	-0.3021	-1.11337	0.42358
16	6	0	0.326494	-1.91093	1.357779
17	6	0	-1.38944	-1.78297	-0.22534
18	16	0	-0.41531	-3.48715	1.428104
19	6	0	-1.58708	-3.07545	0.190364
20	1	0	-1.98354	-1.30855	-0.99832
21	6	0	1.417879	-1.76855	-2.42839
22	1	0	0.946289	-2.65062	-1.97881
23	1	0	0.641681	-1.00872	-2.55424
24	1	0	1.784934	-2.05276	-3.42029
25	6	0	1.470228	-1.58132	2.269441
26	1	0	1.562146	-0.49669	2.37415
27	1	0	1.323594	-2.0099	3.266767
28	1	0	2.42393	-1.95876	1.880279
29	6	0	-0.72066	5.130252	-0.5445
30	6	0	-1.52505	6.246008	-0.42047
31	16	0	0.817941	5.607207	-1.26095
32	6	0	-0.92441	7.455958	-0.88856
33	6	0	0.341894	7.274473	-1.36616
34	6	0	-3.11233	0.708399	1.220628
35	6	0	-4.42894	0.521131	0.856487
36	16	0	-2.79085	-0.17498	2.710429
37	6	0	-5.16114	-0.34064	1.737419
38	6	0	-4.40797	-0.79842	2.781379
39	6	0	6.177394	-0.81984	-0.08928
40	6	0	7.167586	-1.39588	-0.90121
41	6	0	6.571903	-0.26713	1.142521
42	6	0	8.501126	-1.42059	-0.49377
43	6	0	7.90737	-0.28073	1.535106
44	6	0	8.884273	-0.86141	0.723768
45	6	0	-2.60284	-4.02836	-0.26516
46	6	0	-2.42158	-5.41701	-0.15661
47	6	0	-3.80174	-3.56096	-0.83173
48	6	0	-3.40185	-6.30281	-0.60239
49	6	0	-4.77227	-4.45205	-1.28207
50	6	0	-4.58365	-5.83093	-1.17211
51	1	0	1.010823	8.018966	-1.77201
52	1	0	-4.71521	-1.47508	3.565712

53	8	0	-1.56815	8.66171	-0.82966
54	8	0	-2.79307	6.209311	0.08948
55	8	0	-4.99967	1.073811	-0.25649
56	8	0	-6.48064	-0.64163	1.54303
57	6	0	-2.98071	8.52074	-0.63642
58	1	0	-3.35021	9.511964	-0.3622
59	1	0	-3.45481	8.206818	-1.57643
60	6	0	-3.27844	7.507967	0.459712
61	1	0	-2.8092	7.819905	1.402123
62	1	0	-4.35449	7.396345	0.611774
63	6	0	-6.43352	1.055792	-0.20205
64	1	0	-6.78375	1.826475	0.497858
65	1	0	-6.77639	1.302961	-1.20957
66	6	0	-6.94205	-0.31287	0.225188
67	1	0	-8.03379	-0.32198	0.277574
68	1	0	-6.6156	-1.08001	-0.48676
69	9	0	-4.02381	-2.23228	-0.91999
70	9	0	-5.9099	-3.97667	-1.8319
71	9	0	-5.52955	-6.69184	-1.60409
72	9	0	-3.20433	-7.63274	-0.48094
73	9	0	-1.28232	-5.90874	0.375175
74	9	0	6.838255	-1.91256	-2.10415
75	9	0	9.431164	-1.9926	-1.2877
76	9	0	10.17655	-0.88482	1.113617
77	9	0	8.262086	0.273824	2.713727
78	9	0	5.645566	0.260725	1.970634

TT5-D1					
Center	Atomic #	Atomic Type	x	y	z
1	6	0	-1.6906	2.986366	0.006515
2	6	0	-1.59431	1.614293	0.136529
3	6	0	-0.2916	1.055526	-0.10378
4	6	0	0.640893	2.028604	-0.45211
5	16	0	-0.11405	3.610467	-0.43784
6	16	0	-2.76601	0.369597	0.530534
7	6	0	-0.26637	-0.38968	0.085337
8	6	0	-1.50342	-0.88117	0.420681
9	6	0	-1.92053	-2.26315	0.711991
10	6	0	-1.39796	-3.053	1.718517
11	16	0	-2.18066	-4.60846	1.748732

12	6	0	-3.2445	-4.19206	0.418055
13	6	0	0.950128	-1.2244	-0.04484
14	6	0	1.105041	-2.25596	-0.94822
15	16	0	2.678404	-2.98617	-0.78862
16	6	0	3.144655	-1.88989	0.497056
17	6	0	-0.33026	-2.73056	2.719189
18	1	0	0.650324	-3.10466	2.401366
19	1	0	-0.24661	-1.64672	2.838713
20	1	0	-0.55588	-3.16706	3.697793
21	6	0	0.144972	-2.75976	-1.98379
22	1	0	-0.61851	-2.00268	-2.18305
23	1	0	0.655705	-2.98651	-2.92578
24	1	0	-0.36972	-3.67083	-1.65427
25	6	0	-4.23304	-5.1397	-0.10739
26	6	0	-4.72149	-6.20227	0.669156
27	6	0	-4.71921	-5.00206	-1.42032
28	6	0	-5.65657	-7.097	0.148831
29	1	0	-4.38632	-6.32538	1.694085
30	6	0	-5.66501	-5.88855	-1.9268
31	1	0	-4.33991	-4.21083	-2.0566
32	6	0	-6.13881	-6.94782	-1.14967
33	1	0	-6.86586	-7.64371	-1.55055
34	6	0	4.4663	-1.95782	1.12955
35	6	0	5.582312	-2.4728	0.448385
36	6	0	4.647375	-1.49762	2.444582
37	6	0	6.831657	-2.52303	1.063312
38	1	0	5.481177	-2.81202	-0.57719
39	6	0	5.90345	-1.53546	3.046881
40	1	0	3.798043	-1.12582	3.007011
41	6	0	7.005323	-2.05062	2.364346
42	1	0	7.979272	-2.08389	2.837261
43	6	0	-6.21952	-5.68509	-3.31382
44	6	0	-6.1035	-8.26403	0.992056
45	6	0	6.075265	-0.97165	4.433985
46	6	0	7.998635	-3.13861	0.334558
47	9	0	-7.36907	-4.97392	-3.286
48	9	0	-6.49846	-6.86163	-3.91518
49	9	0	-6.23888	-7.91589	2.290609
50	9	0	-7.28633	-8.76298	0.576558
51	9	0	-5.2062	-9.27482	0.948118
52	9	0	-5.35728	-5.01441	-4.10826

53	9	0	8.085774	-4.4675	0.574978
54	9	0	9.172261	-2.59165	0.718356
55	9	0	7.893648	-2.98646	-1.00255
56	9	0	7.134439	-1.51538	5.07055
57	9	0	6.272581	0.3653	4.404648
58	9	0	4.982552	-1.18998	5.200146
59	6	0	-2.81394	3.879874	0.171008
60	6	0	-2.93024	5.168601	-0.28334
61	16	0	-4.26744	3.354242	1.050701
62	6	0	-4.17555	5.789557	0.05083
63	1	0	-2.17069	5.660993	-0.87977
64	6	0	-5.03048	4.912661	0.778251
65	6	0	2.041603	1.976802	-0.84822
66	6	0	3.050432	2.773507	-0.37666
67	16	0	2.591071	0.926193	-2.17222
68	6	0	4.307051	2.568782	-1.03573
69	1	0	2.918726	3.467022	0.445837
70	6	0	4.218238	1.57186	-2.0496
71	6	0	-4.62305	7.084968	-0.26494
72	6	0	-5.90949	7.445614	0.125941
73	6	0	-6.76657	6.564819	0.847021
74	6	0	-6.30669	5.281162	1.190402
75	6	0	-8.04814	7.165178	1.11302
76	1	0	-8.85025	6.650501	1.628683
77	6	0	-8.14872	8.427987	0.625136
78	1	0	-9.00418	9.088645	0.682936
79	16	0	-6.70316	8.980454	-0.20091
80	6	0	5.318904	1.178827	-2.80596
81	6	0	6.557957	1.784408	-2.53599
82	6	0	6.644458	2.786766	-1.52676
83	6	0	5.540453	3.194429	-0.78302
84	6	0	7.837349	1.527968	-3.14572
85	1	0	7.988936	0.783732	-3.91847
86	6	0	8.829588	2.295941	-2.62818
87	1	0	9.87661	2.289562	-2.90269
88	16	0	8.291575	3.379904	-1.35827
89	8	0	-3.83263	7.952926	-0.98358
90	8	0	-7.10889	4.391245	1.868563
91	8	0	5.660044	4.144285	0.205708
92	8	0	5.202548	0.189896	-3.75729
93	6	0	-2.95506	8.7554	-0.18377

94	1	0	-3.52069	9.384135	0.514642
95	1	0	-2.25179	8.130362	0.380768
96	1	0	-2.40296	9.389705	-0.88045
97	6	0	-7.0621	4.518621	3.295172
98	1	0	-6.04741	4.346569	3.674586
99	1	0	-7.40435	5.510338	3.616161
100	1	0	-7.73371	3.753972	3.691036
101	6	0	5.442481	5.490342	-0.23542
102	1	0	5.575874	6.123841	0.643963
103	1	0	6.167905	5.776896	-1.00646
104	1	0	4.426384	5.617356	-0.62968
105	6	0	4.940789	0.66999	-5.08174
106	1	0	5.753846	1.315434	-5.43678
107	1	0	4.871671	-0.21456	-5.71846
108	1	0	3.995436	1.224908	-5.12226
109	7	0	-2.97655	-2.91495	-0.00652
110	7	0	2.114804	-1.024	0.765896

TT5-D2					
Center	Atomic #	Atomic Type	x	y	z
1	6	0	1.111451	3.767344	0.009409
2	6	0	1.203838	2.393102	-0.0985
3	6	0	-0.00191	1.659623	0.173048
4	6	0	-1.0609	2.494106	0.522788
5	16	0	-0.53305	4.169898	0.471392
6	16	0	2.532423	1.323829	-0.51316
7	6	0	0.178343	0.221834	0.00371
8	6	0	1.464566	-0.09213	-0.36205
9	6	0	2.065977	-1.40005	-0.67114
10	6	0	1.620218	-2.26486	-1.65315
11	16	0	2.628887	-3.68283	-1.72961
12	6	0	3.684038	-3.10219	-0.45481
13	6	0	-0.89681	-0.77904	0.189754
14	6	0	-0.84478	-1.83623	1.075914
15	16	0	-2.30034	-2.79098	0.989694
16	6	0	-2.99594	-1.75805	-0.24327
17	6	0	0.468399	-2.11072	-2.59904
18	1	0	-0.43203	-2.61702	-2.23109
19	1	0	0.223933	-1.05134	-2.71691
20	1	0	0.705393	-2.5207	-3.58639

21	6	0	0.229603	-2.20244	2.05566
22	1	0	0.861096	-1.33301	2.258598
23	1	0	-0.1962	-2.54422	3.00522
24	1	0	0.877434	-3.00071	1.673074
25	6	0	4.838551	-3.87891	0.008383
26	6	0	5.458797	-4.83678	-0.81081
27	6	0	5.36001	-3.67427	1.297808
28	6	0	6.558895	-5.56128	-0.35514
29	1	0	5.095918	-5.00536	-1.81934
30	6	0	6.470042	-4.38989	1.739979
31	1	0	4.883919	-2.96657	1.96686
32	6	0	7.077709	-5.34199	0.920412
33	1	0	7.935911	-5.9032	1.270201
34	6	0	-4.33861	-1.99858	-0.78184
35	6	0	-4.86575	-3.29559	-0.89968
36	6	0	-5.13871	-0.91679	-1.1858
37	6	0	-6.14676	-3.50075	-1.40866
38	1	0	-4.26903	-4.15063	-0.59943
39	6	0	-6.41579	-1.13185	-1.70131
40	1	0	-4.76834	0.09572	-1.06845
41	6	0	-6.93232	-2.42248	-1.81675
42	1	0	-7.92845	-2.58503	-2.2105
43	6	0	7.050946	-4.0999	3.100477
44	6	0	7.161326	-6.63039	-1.23073
45	6	0	-7.27573	0.051743	-2.05517
46	6	0	-6.66497	-4.90463	-1.58812
47	9	0	7.998972	-3.13788	3.037301
48	9	0	7.632721	-5.19286	3.63891
49	9	0	7.024721	-6.33981	-2.54248
50	9	0	8.478114	-6.79659	-0.98305
51	9	0	6.566139	-7.82761	-1.02723
52	9	0	6.108417	-3.66914	3.967236
53	9	0	-6.37854	-5.38432	-2.82028
54	9	0	-8.0068	-4.96226	-1.44585
55	9	0	-6.1214	-5.75905	-0.69531
56	9	0	-8.22039	-0.25845	-2.96614
57	9	0	-7.9193	0.547386	-0.97032
58	9	0	-6.54021	1.072095	-2.5634
59	6	0	2.092307	4.804026	-0.19613
60	6	0	2.066996	6.096772	0.29626
61	16	0	3.527195	4.506433	-1.20997

62	6	0	3.189855	6.843818	-0.13021
63	1	0	1.284599	6.45797	0.954165
64	6	0	4.089988	6.127341	-0.93647
65	6	0	5.156023	7.002306	-1.24006
66	6	0	4.869264	8.225006	-0.61234
67	16	0	6.659003	7.09273	-2.11359
68	6	0	5.854594	9.23093	-0.82157
69	6	0	6.871162	8.76104	-1.60902
70	1	0	5.827001	10.23678	-0.41841
71	1	0	7.754253	9.296087	-1.93098
72	6	0	-2.43761	2.2467	0.916089
73	6	0	-3.56165	2.862406	0.397151
74	16	0	-2.8356	1.197001	2.297939
75	6	0	-4.74087	2.472736	1.079098
76	1	0	-3.51487	3.538568	-0.44905
77	6	0	-4.52597	1.558527	2.12526
78	6	0	-5.79727	1.238551	2.652821
79	6	0	-6.74074	1.973587	1.917234
80	16	0	-6.57742	0.28388	3.88242
81	6	0	-8.08782	1.767374	2.330778
82	6	0	-8.14715	0.88534	3.375177
83	1	0	-8.96265	2.226543	1.885316
84	1	0	-9.03196	0.533799	3.888401
85	7	0	3.658809	8.13406	0.055693
86	7	0	-6.09479	2.741455	0.964016
87	6	0	3.072605	9.145296	0.912259
88	1	0	3.310441	10.1377	0.519748
89	1	0	1.98505	9.033554	0.915657
90	1	0	3.43981	9.074541	1.944202
91	6	0	-6.71945	3.574989	-0.04653
92	1	0	-7.68195	3.932484	0.32779
93	1	0	-6.08724	4.445797	-0.24307
94	1	0	-6.88174	3.027801	-0.98054
95	7	0	3.245174	-1.88023	-0.01096
96	7	0	-2.12607	-0.74259	-0.54713

TT5-D5					
Center	Atomic #	Atomic Type	x	y	z
1	6	0	-2.35162	-2.80934	-0.24651
2	6	0	-2.0123	-1.49735	-0.14626

3	6	0	-0.54806	-1.24885	0.053921
4	6	0	0.157474	-2.36021	0.355092
5	16	0	-0.85723	-3.77481	-0.04129
6	16	0	-2.87053	0.047159	-0.17313
7	6	0	-0.20079	0.238265	-0.12997
8	6	0	-1.34429	1.010883	-0.25428
9	6	0	-1.27376	2.539761	-0.45624
10	6	0	-0.32224	3.118937	-1.22919
11	16	0	-0.3909	4.880768	-1.10596
12	6	0	-1.90996	4.866283	-0.19514
13	6	0	1.227471	0.811957	-0.22137
14	6	0	1.596945	2.018274	0.288303
15	16	0	3.218662	2.459001	-0.26662
16	6	0	3.525477	0.868802	-0.97942
17	6	0	0.671732	2.334989	-2.10388
18	1	0	1.554458	2.122999	-1.53874
19	1	0	0.221488	1.415828	-2.41968
20	1	0	0.928674	2.918335	-2.96303
21	6	0	0.732603	2.88369	1.220615
22	1	0	0.104215	2.252535	1.813612
23	1	0	1.368861	3.456989	1.861753
24	1	0	0.126525	3.542684	0.635687
25	6	0	-2.72398	6.134126	0.146717
26	6	0	-2.31117	7.383638	-0.34226
27	6	0	-3.87232	6.044513	0.950111
28	6	0	-3.03522	8.540689	-0.01699
29	1	0	-1.44233	7.454305	-0.96062
30	6	0	-4.59083	7.203127	1.281028
31	1	0	-4.19837	5.093611	1.314071
32	6	0	-4.17183	8.449324	0.796841
33	1	0	-4.71968	9.333589	1.049256
34	6	0	4.874732	0.450309	-1.59152
35	6	0	5.939213	1.360559	-1.59895
36	6	0	5.036443	-0.82225	-2.15827
37	6	0	7.152961	1.015538	-2.20539
38	1	0	5.823832	2.32306	-1.14384
39	6	0	6.25326	-1.16737	-2.76662
40	1	0	4.231537	-1.52717	-2.13038
41	6	0	7.309264	-0.24786	-2.79149
42	1	0	8.234836	-0.50875	-3.25621
43	6	0	-5.83922	7.105405	2.178687

44	6	0	-2.58465	9.912856	-0.55439
45	6	0	6.428474	-2.55451	-3.41251
46	6	0	8.31302	2.026175	-2.23367
47	9	0	-6.93363	6.923526	1.409783
48	9	0	-5.9731	8.246684	2.888318
49	9	0	-1.98072	9.752673	-1.75176
50	9	0	-3.65968	10.71634	-0.69715
51	9	0	-1.71679	10.47362	0.314719
52	9	0	-5.70423	6.062519	3.02404
53	9	0	8.221644	2.78422	-3.34683
54	9	0	9.488487	1.363272	-2.23584
55	9	0	8.244496	2.819041	-1.14281
56	9	0	7.299645	-2.4645	-4.44018
57	9	0	6.904365	-3.42227	-2.49457
58	9	0	5.23646	-2.99113	-3.87073
59	6	0	-3.75974	-3.39724	-0.49989
60	6	0	-4.01729	-4.74922	-0.56528
61	16	0	-5.25834	-2.42898	-0.76195
62	6	0	-5.52732	-4.98943	-0.72428
63	1	0	-3.27304	-5.51356	-0.51266
64	6	0	-6.28922	-3.86634	-0.70544
65	6	0	-7.87323	-4.10287	-0.60766
66	6	0	-8.27647	-5.39988	-0.54032
67	16	0	-9.272	-3.03242	-0.5246
68	6	0	-9.75373	-5.60549	-0.17913
69	6	0	-10.3683	-4.3796	-0.04518
70	1	0	-10.2317	-6.55509	-0.04676
71	1	0	-11.3704	-4.24652	0.304719
72	6	0	1.572892	-2.38121	0.971389
73	6	0	2.221007	-3.52085	1.405344
74	16	0	2.549727	-0.89841	1.275741
75	6	0	3.511056	-3.12341	2.147254
76	1	0	1.869681	-4.52178	1.267479
77	6	0	3.843303	-1.80938	2.055943
78	6	0	5.297237	-1.4149	2.601497
79	6	0	6.045834	-2.43744	3.08211
80	16	0	6.205873	0.095361	2.689448
81	6	0	7.519597	-2.10303	3.337946
82	6	0	7.743146	-0.773	3.055179
83	1	0	8.260475	-2.79854	3.676071
84	1	0	8.711301	-0.31689	3.048883

85	6	0	-6.41088	-8.07126	0.284758
86	1	0	-7.19986	-8.78279	0.161186
87	1	0	-5.4756	-8.52697	0.035605
88	1	0	-6.38575	-7.7397	1.302643
89	6	0	5.622455	-5.71912	2.546583
90	1	0	6.446878	-6.0205	3.15896
91	1	0	4.858778	-6.4662	2.583638
92	1	0	5.955232	-5.59878	1.536201
93	6	0	-6.75491	-7.25751	-2.76146
94	1	0	-6.92191	-6.46814	-3.46306
95	1	0	-5.81672	-7.72743	-2.96954
96	1	0	-7.54094	-7.97926	-2.84225
97	6	0	4.313941	-4.32981	5.093363
98	1	0	3.564544	-5.09265	5.104304
99	1	0	5.154574	-4.64746	5.675056
100	1	0	3.912448	-3.42935	5.510062
101	32	0	-6.72856	-6.51522	-0.91482
102	32	0	4.895314	-3.99239	3.216602
103	7	0	-2.24502	3.590536	0.160213
104	7	0	2.408959	0.092581	-0.92691

TT5-EDOT2					
Center	Atomic #	Atomic Type	x	y	z
1	6	0	-0.74204	4.249824	-0.2623
2	6	0	-0.07818	3.036796	-0.29252
3	6	0	-0.81629	1.909568	0.201877
4	6	0	-2.08293	2.266826	0.654145
5	16	0	-2.33558	3.987834	0.429127
6	16	0	1.523919	2.567923	-0.83864
7	6	0	-0.06006	0.667157	0.100621
8	6	0	1.188588	0.868119	-0.43325
9	6	0	2.251908	-0.10394	-0.73891
10	6	0	2.117449	-1.17881	-1.59727
11	16	0	3.613279	-2.06356	-1.71615
12	6	0	4.444356	-0.96617	-0.62898
13	6	0	-0.58813	-0.65848	0.495226
14	6	0	-0.01872	-1.49165	1.43627
15	16	0	-0.93635	-2.96537	1.596918
16	6	0	-2.10257	-2.46136	0.388434
17	6	0	0.922604	-1.61263	-2.39071

18	1	0	0.370209	-2.41625	-1.88908
19	1	0	0.236112	-0.77103	-2.51759
20	1	0	1.212081	-1.97299	-3.38353
21	6	0	1.192835	-1.26816	2.290718
22	1	0	1.415384	-0.19908	2.348688
23	1	0	1.038856	-1.64106	3.309087
24	1	0	2.078691	-1.76942	1.881511
25	6	0	-0.31302	5.552882	-0.70416
26	6	0	-0.97537	6.759791	-0.59463
27	16	0	1.239532	5.818631	-1.496
28	6	0	-0.25732	7.872823	-1.13261
29	6	0	0.957951	7.525848	-1.6496
30	6	0	-3.12999	1.51044	1.323633
31	6	0	-4.47353	1.467911	1.016687
32	16	0	-2.85213	0.648015	2.834342
33	6	0	-5.26411	0.730478	1.957951
34	6	0	-4.52673	0.223563	2.99042
35	6	0	5.85404	-1.15334	-0.27069
36	6	0	6.735182	-1.87084	-1.0955
37	6	0	6.36168	-0.6084	0.922544
38	6	0	8.072518	-2.03916	-0.73751
39	1	0	6.383461	-2.28555	-2.03463
40	6	0	7.701608	-0.76644	1.265178
41	1	0	5.701128	-0.07636	1.597347
42	6	0	8.569046	-1.48695	0.441642
43	1	0	9.608935	-1.61756	0.716023
44	6	0	-3.24104	-3.30252	0.00946
45	6	0	-3.21921	-4.6982	0.16632
46	6	0	-4.39962	-2.71647	-0.53006
47	6	0	-4.3142	-5.47664	-0.20693
48	1	0	-2.33898	-5.18398	0.574627
49	6	0	-5.48576	-3.50148	-0.908
50	1	0	-4.45461	-1.63924	-0.63659
51	6	0	-5.45541	-4.88827	-0.75041
52	1	0	-6.30403	-5.49607	-1.04072
53	6	0	8.237462	-0.11933	2.516765
54	6	0	8.970732	-2.87297	-1.61532
55	6	0	-6.73962	-2.83981	-1.41504
56	6	0	-4.23228	-6.97709	-0.08867
57	9	0	8.771407	1.09522	2.255165
58	9	0	9.210981	-0.86347	3.084403

59	9	0	8.669876	-2.7205	-2.92354
60	9	0	10.27153	-2.55112	-1.45437
61	9	0	8.849052	-4.19042	-1.33514
62	9	0	7.270886	0.063905	3.442425
63	9	0	-3.70135	-7.53316	-1.20165
64	9	0	-5.45036	-7.53258	0.087666
65	9	0	-3.45541	-7.35495	0.949445
66	9	0	-7.40796	-3.62134	-2.28725
67	9	0	-7.59522	-2.5506	-0.40549
68	9	0	-6.47322	-1.66663	-2.04027
69	1	0	1.691878	8.171083	-2.10946
70	1	0	-4.87802	-0.38395	3.811985
71	8	0	-0.75246	9.147707	-1.0977
72	8	0	-2.21654	6.891597	-0.0366
73	8	0	-5.02166	2.044946	-0.09529
74	8	0	-6.61673	0.5814	1.825136
75	6	0	-2.16249	9.182058	-0.84636
76	1	0	-2.40163	10.21911	-0.59817
77	1	0	-2.70895	8.893756	-1.75476
78	6	0	-2.53065	8.250824	0.299558
79	1	0	-1.98914	8.537818	1.210619
80	1	0	-3.60507	8.272961	0.496046
81	6	0	-6.44422	2.198958	0.013371
82	1	0	-6.67226	3.029814	0.694665
83	1	0	-6.79761	2.449515	-0.98966
84	6	0	-7.09117	0.916078	0.513424
85	1	0	-8.17332	1.038301	0.606893
86	1	0	-6.88681	0.091132	-0.17915
87	7	0	-1.77254	-1.21681	-0.08545
88	7	0	3.579426	0.013108	-0.20933

TT5-EPh2					
Center	Atomic #	Atomic Type	x	y	z
1	6	0	-0.35403	4.619986	-0.03427
2	6	0	-0.6408	3.274011	0.108026
3	6	0	0.426895	2.37472	-0.19422
4	6	0	1.585545	3.046045	-0.59674
5	16	0	1.313309	4.78491	-0.56974
6	16	0	-2.09065	2.428337	0.59705
7	6	0	0.041775	0.982335	-0.02944

8	6	0	-1.26118	0.862655	0.393749
9	6	0	-2.0415	-0.3434	0.710808
10	6	0	-1.66785	-1.31264	1.623708
11	16	0	-2.88522	-2.55322	1.738775
12	6	0	-3.92672	-1.7549	0.57547
13	6	0	0.940002	-0.1547	-0.33338
14	6	0	0.683439	-1.11837	-1.28778
15	16	0	1.998454	-2.25816	-1.38618
16	6	0	2.916858	-1.42232	-0.15051
17	6	0	-0.43815	-1.38839	2.476486
18	1	0	0.343039	-2.00122	2.010854
19	1	0	-0.02534	-0.38622	2.623124
20	1	0	-0.66053	-1.81594	3.459732
21	6	0	-0.506	-1.2696	-2.18799
22	1	0	-1.02139	-0.31028	-2.28834
23	1	0	-0.21116	-1.60434	-3.18835
24	1	0	-1.22872	-1.99391	-1.7923
25	6	0	-5.22494	-2.31515	0.186345
26	6	0	-5.92803	-3.19594	1.025539
27	6	0	-5.80441	-1.97369	-1.04782
28	6	0	-7.16388	-3.71323	0.642278
29	1	0	-5.51992	-3.46432	1.994309
30	6	0	-7.0481	-2.48166	-1.41681
31	1	0	-5.27202	-1.32344	-1.73276
32	6	0	-7.73776	-3.35768	-0.57821
33	1	0	-8.70123	-3.75716	-0.87133
34	6	0	4.269656	-1.84428	0.225353
35	6	0	5.135745	-2.4237	-0.71583
36	6	0	4.747884	-1.6431	1.530461
37	6	0	6.43872	-2.7723	-0.36773
38	1	0	4.798594	-2.56723	-1.73608
39	6	0	6.053468	-1.99258	1.87165
40	1	0	4.090886	-1.22489	2.285038
41	6	0	6.910524	-2.55932	0.927571
42	1	0	7.924871	-2.8283	1.19684
43	6	0	-7.67511	-2.04143	-2.71505
44	6	0	-7.86653	-4.7079	1.530694
45	6	0	6.559579	-1.70637	3.262005
46	6	0	7.334279	-3.4144	-1.39415
47	9	0	-8.40241	-0.91295	-2.55416
48	9	0	-8.50712	-2.98051	-3.21351

49	9	0	-7.55364	-4.52872	2.831996
50	9	0	-9.20899	-4.61764	1.416325
51	9	0	-7.52774	-5.97817	1.213338
52	9	0	-6.74326	-1.77852	-3.6575
53	9	0	7.209966	-4.76038	-1.39616
54	9	0	8.636263	-3.13814	-1.17004
55	9	0	7.042953	-2.99525	-2.65112
56	9	0	7.534254	-2.56714	3.628146
57	9	0	7.077265	-0.46084	3.355274
58	9	0	5.57287	-1.79257	4.181226
59	6	0	-1.17596	5.730933	0.178651
60	6	0	-1.88155	6.708318	0.359647
61	6	0	2.851894	2.573253	-0.97048
62	6	0	3.9808	2.241894	-1.29217
63	6	0	-2.72069	7.832296	0.573768
64	6	0	-2.22015	9.148959	0.375935
65	6	0	-4.05036	7.659108	0.980463
66	6	0	-3.06493	10.23501	0.591576
67	6	0	-4.89113	8.756133	1.193805
68	1	0	-4.44245	6.659698	1.133851
69	6	0	-4.3928	10.04651	0.997751
70	1	0	-2.70484	11.24686	0.447402
71	1	0	-5.01833	10.91733	1.154681
72	6	0	5.326841	1.877544	-1.57609
73	6	0	6.370962	2.501021	-0.87839
74	6	0	5.63806	0.893107	-2.55243
75	6	0	7.707759	2.169727	-1.1199
76	1	0	6.144614	3.254187	-0.13162
77	6	0	6.972891	0.559761	-2.77778
78	6	0	8.004345	1.190299	-2.07116
79	1	0	7.231567	-0.20777	-3.49719
80	1	0	9.028596	0.901432	-2.27613
81	1	0	-1.20782	9.302998	0.065501
82	1	0	-5.90463	8.608846	1.503689
83	1	0	8.493168	2.659771	-0.58335
84	1	0	4.858469	0.414137	-3.10716
85	7	0	-3.33028	-0.60019	0.135856
86	7	0	2.210912	-0.3387	0.303608

TT5-Ph2					
Center	Atomic #	Atomic Type	x	y	z

1	6	0	-0.36451	4.978638	-0.19002
2	6	0	0.073649	3.675294	-0.26544
3	6	0	-0.84992	2.673747	0.201112
4	6	0	-2.03727	3.231209	0.659601
5	16	0	-1.98583	4.968296	0.473515
6	16	0	1.58603	2.955172	-0.79617
7	6	0	-0.31027	1.321693	0.074991
8	6	0	0.9626	1.324955	-0.43925
9	6	0	1.855573	0.201181	-0.76625
10	6	0	1.54579	-0.83446	-1.62783
11	16	0	2.885495	-1.93855	-1.77172
12	6	0	3.884278	-0.99844	-0.67945
13	6	0	-1.05672	0.096186	0.44089
14	6	0	-0.63061	-0.85589	1.345776
15	16	0	-1.80118	-2.14187	1.491342
16	6	0	-2.88279	-1.39074	0.33425
17	6	0	0.293097	-1.07	-2.41587
18	1	0	-0.38852	-1.75776	-1.9012
19	1	0	-0.24004	-0.12607	-2.55954
20	1	0	0.515165	-1.49263	-3.40145
21	6	0	0.619628	-0.88879	2.172915
22	1	0	1.037101	0.118422	2.257402
23	1	0	0.421911	-1.26419	3.182955
24	1	0	1.390231	-1.52799	1.724993
25	6	0	5.249899	-1.40629	-0.3333
26	6	0	5.656977	-2.751	-0.397
27	6	0	6.192978	-0.44958	0.073871
28	6	0	6.957671	-3.11855	-0.06349
29	1	0	4.951581	-3.51691	-0.7019
30	6	0	7.490688	-0.82741	0.418757
31	1	0	5.9196	0.600175	0.099638
32	6	0	7.886376	-2.16129	0.350885
33	1	0	8.899401	-2.44889	0.603755
34	6	0	-4.19681	-1.9615	0.018336
35	6	0	-4.42893	-3.34733	0.019013
36	6	0	-5.27258	-1.10764	-0.27106
37	6	0	-5.69644	-3.85522	-0.25928
38	1	0	-3.61503	-4.03269	0.232181
39	6	0	-6.53801	-1.6238	-0.54663
40	1	0	-5.12627	-0.03373	-0.2432

41	6	0	-6.76308	-2.99931	-0.54215
42	1	0	-7.74944	-3.39784	-0.7458
43	6	0	8.455586	0.245009	0.856151
44	6	0	7.35346	-4.57306	-0.0794
45	6	0	-7.67061	-0.65678	-0.77436
46	6	0	-5.90752	-5.34615	-0.32247
47	9	0	8.568681	1.215102	-0.0787
48	9	0	9.691014	-0.24145	1.08954
49	9	0	6.610006	-5.28798	-0.95075
50	9	0	8.650389	-4.73176	-0.42038
51	9	0	7.193137	-5.14077	1.137682
52	9	0	8.035044	0.847571	1.991664
53	9	0	-5.73021	-5.81709	-1.5781
54	9	0	-7.15829	-5.68971	0.054028
55	9	0	-5.04336	-6.0111	0.474338
56	9	0	-8.77962	-1.26647	-1.23875
57	9	0	-8.01361	-0.01956	0.372998
58	9	0	-7.33052	0.305694	-1.66047
59	6	0	0.300517	6.231142	-0.56329
60	6	0	-0.00608	7.440201	0.089597
61	6	0	1.265348	6.254889	-1.58807
62	6	0	0.629212	8.626293	-0.2685
63	1	0	-0.73282	7.444469	0.897423
64	6	0	1.906475	7.442121	-1.93586
65	1	0	1.493766	5.345443	-2.13512
66	6	0	1.592471	8.633499	-1.27972
67	1	0	0.37806	9.54638	0.252266
68	1	0	2.646955	7.436079	-2.73118
69	1	0	2.092194	9.558375	-1.55377
70	6	0	-3.24129	2.634605	1.270769
71	6	0	-4.51688	2.893846	0.737235
72	6	0	-3.14429	1.827873	2.41762
73	6	0	-5.6589	2.343105	1.319948
74	1	0	-4.60612	3.514489	-0.15031
75	6	0	-4.28657	1.279547	2.9984
76	1	0	-2.16796	1.637994	2.851883
77	6	0	-5.54655	1.530532	2.4502
78	1	0	-6.63453	2.531316	0.88088
79	1	0	-4.19184	0.656569	3.883602
80	1	0	-6.43543	1.092837	2.895398
81	7	0	3.189412	0.103093	-0.24776

82	7	0	-2.33773	-0.21869	-0.12054
----	---	---	----------	----------	----------

TT5-Th2					
Center	Atomic #	Atomic Type	x	y	z
1	6	0	-0.39243	4.97118	-0.16457
2	6	0	0.054423	3.667457	-0.23416
3	6	0	-0.87002	2.665907	0.2227
4	6	0	-2.06154	3.219521	0.677405
5	16	0	-2.01689	4.962328	0.49447
6	16	0	1.561845	2.952505	-0.77847
7	6	0	-0.33347	1.315424	0.090982
8	6	0	0.937824	1.320847	-0.42786
9	6	0	1.82957	0.197653	-0.75889
10	6	0	1.516308	-0.83607	-1.6215
11	16	0	2.852778	-1.9434	-1.7668
12	6	0	3.854369	-1.00766	-0.67325
13	6	0	-1.08433	0.092027	0.453215
14	6	0	-0.66206	-0.86406	1.355204
15	16	0	-1.83814	-2.14431	1.497609
16	6	0	-2.91722	-1.38544	0.343457
17	6	0	0.262445	-1.06742	-2.40893
18	1	0	-0.42074	-1.75328	-1.89381
19	1	0	-0.26794	-0.12195	-2.55259
20	1	0	0.482771	-1.49053	-3.39466
21	6	0	0.585378	-0.90056	2.185964
22	1	0	1.004228	0.105777	2.272583
23	1	0	0.38255	-1.27442	3.195368
24	1	0	1.355499	-1.54215	1.740557
25	6	0	0.245719	6.214831	-0.53547
26	6	0	-0.10041	7.49831	-0.16186
27	16	0	1.637621	6.255442	-1.60869
28	6	0	0.738557	8.499764	-0.72227
29	1	0	-0.92345	7.712656	0.51168
30	6	0	1.72623	7.984108	-1.51672
31	1	0	0.618032	9.560654	-0.53223
32	6	0	-3.25806	2.635393	1.274059
33	6	0	-4.56267	2.763987	0.847021
34	16	0	-3.20339	1.739332	2.782748
35	6	0	-5.50878	2.12301	1.698856
36	1	0	-4.82598	3.290308	-0.06453
37	6	0	-4.92085	1.524168	2.780951

38	1	0	-6.57353	2.082373	1.497505
39	6	0	5.218435	-1.4215	-0.32789
40	6	0	5.617629	-2.7671	-0.38719
41	6	0	6.166197	-0.46623	0.078198
42	6	0	6.916938	-3.14116	-0.04921
43	1	0	4.908151	-3.53075	-0.68843
44	6	0	7.460484	-0.84903	0.422738
45	1	0	5.894975	0.583026	0.111193
46	6	0	7.848582	-2.18788	0.360968
47	1	0	8.857778	-2.48103	0.624809
48	6	0	-4.2279	-1.95594	0.013684
49	6	0	-4.45901	-3.34214	0.011767
50	6	0	-5.29964	-1.10359	-0.29477
51	6	0	-5.72048	-3.8516	-0.2893
52	1	0	-3.64835	-4.02648	0.239767
53	6	0	-6.5584	-1.62158	-0.59674
54	1	0	-5.15447	-0.02938	-0.26271
55	6	0	-6.78196	-2.99723	-0.59543
56	1	0	-7.76331	-3.39702	-0.81972
57	6	0	8.475757	0.203835	0.788369
58	6	0	7.29951	-4.59936	-0.05223
59	6	0	-7.68547	-0.65641	-0.85706
60	6	0	-5.92986	-5.34277	-0.3541
61	9	0	9.128178	0.661496	-0.30383
62	9	0	9.410854	-0.27722	1.635078
63	9	0	6.576302	-5.30646	-0.9469
64	9	0	8.604548	-4.77137	-0.35225
65	9	0	7.094219	-5.16534	1.158808
66	9	0	7.898229	1.27203	1.380025
67	9	0	-5.73871	-5.81394	-1.60756
68	9	0	-7.18468	-5.68642	0.008628
69	9	0	-5.07444	-6.00695	0.452491
70	9	0	-8.78744	-1.27061	-1.33131
71	9	0	-8.04665	-0.00242	0.275264
72	9	0	-7.32824	0.292491	-1.75104
73	1	0	2.504214	8.511215	-2.05225
74	1	0	-5.39628	0.956512	3.569987
75	7	0	3.16336	0.095973	-0.24085
76	7	0	-2.36675	-0.2145	-0.10913

EXCITATION ENERGIES AND OSCILLATOR STRENGTHS (first 5 for each system):

TT1

Excited State 1: Singlet-A 3.7746 eV 328.47 nm f=0.1229 <S**2>=0.000

92 -> 95 -0.13691

94 (H) -> 95 (L) 0.68314

This state for optimization and/or second-order correction.

Total Energy, E(TD-HF/TD-KS) = -2288.15454404

Copying the excited state density for this state as the 1-particle RhoCI density.

Excited State 2: Singlet-A 4.1585 eV 298.14 nm f=0.0347 <S**2>=0.000

93 -> 95 0.66853

94 -> 97 -0.16762

Excited State 3: Singlet-A 4.2629 eV 290.85 nm f=0.0406 <S**2>=0.000

92 -> 95 0.55282

94 -> 95 0.10618

94 -> 96 0.40211

Excited State 4: Singlet-A 4.4445 eV 278.96 nm f=0.1186 <S**2>=0.000

92 -> 95 -0.35272

93 -> 95 0.13796

94 -> 96 0.52195

94 -> 97 0.22047

Excited State 5: Singlet-A 4.4947 eV 275.85 nm f=0.0138 <S**2>=0.000

92 -> 95 0.16025

93 -> 95 0.11274

94 -> 96 -0.17665

94 -> 97 0.62760

TT2

Excited State 1: Singlet-A 3.3888 eV 365.87 nm f=0.0113 <S**2>=0.000

190 (H) -> 191 (L) 0.69976

This state for optimization and/or second-order correction.

Total Energy, E(TD-HF/TD-KS) = -4019.79417085

Copying the excited state density for this state as the 1-particle RhoCI density.

Excited State 2: Singlet-A 3.4620 eV 358.12 nm f=0.0045 <S**2>=0.000

190 -> 192 0.69834

Excited State 3: Singlet-A 3.8437 eV 322.56 nm f=0.2057 <S**2>=0.000

188 ->191	-0.11098
189 ->193	-0.11254
190 ->193	0.66052
<u>Excited State 4:</u>	Singlet-A 3.9213 eV 316.18 nm f=0.3465 <S**2>=0.000
188 ->191	-0.10214
189 ->191	0.66495
189 ->192	-0.12326
<u>Excited State 5:</u>	Singlet-A 3.9403 eV 314.65 nm f=0.0090 <S**2>=0.000
190 ->194	0.67987
190 ->195	-0.11076

TT3

<u>Excited State 1:</u>	Singlet-A 3.0201 eV 410.53 nm f=0.9772 <S**2>=0.000
178 (H) ->179 (L)	0.70145

This state for optimization and/or second-order correction.

Total Energy, E(TD-HF/TD-KS) = -4495.44195604

Copying the excited state density for this state as the 1-particle RhoCI density.

<u>Excited State 2:</u>	Singlet-A 3.0868 eV 401.66 nm f=0.1018 <S**2>=0.000
177 ->179	0.28325
178 ->180	0.63295
<u>Excited State 3:</u>	Singlet-A 3.1943 eV 388.14 nm f=1.0832 <S**2>=0.000
177 ->179	0.13540
177 ->180	0.65856
178 ->181	-0.16366
<u>Excited State 4:</u>	Singlet-A 3.2465 eV 381.91 nm f=0.0392 <S**2>=0.000
177 ->179	0.62631
177 ->180	-0.16724
178 ->180	-0.27458
<u>Excited State 5:</u>	Singlet-A 3.3689 eV 368.03 nm f=0.0215 <S**2>=0.000
176 ->179	-0.28849
177 ->180	0.11599
178 ->181	0.62249

TT-Ph

Excited State 1: Singlet-A 3.2951 eV 376.27 nm f=0.5614 <S**2>=0.000

76 (H) -> 77 (L) 0.70330

This state for optimization and/or second-order correction.

Total Energy, E(TD-HF/TD-KS) = -1489.39363887

Copying the excited state density for this state as the 1-particle RhoCI density.

Excited State 2: Singlet-A 4.0973 eV 302.60 nm f=0.0219 <S**2>=0.000

75 -> 77 0.22587

76 -> 78 0.60384

76 -> 79 0.23771

Excited State 3: Singlet-A 4.1890 eV 295.97 nm f=0.0019 <S**2>=0.000

75 -> 77 -0.27074

76 -> 78 -0.15700

76 -> 79 0.59640

76 -> 80 -0.12931

Excited State 4: Singlet-A 4.2931 eV 288.80 nm f=0.0003 <S**2>=0.000

71 -> 77 0.14077

73 -> 77 -0.13619

76 -> 79 0.11561

76 -> 80 0.65149

Excited State 5: Singlet-A 4.5835 eV 270.50 nm f=0.1195 <S**2>=0.000

72 -> 77 -0.21662

74 -> 77 -0.18544

75 -> 77 0.43872

76 -> 78 -0.20897

76 -> 79 0.16530

76 -> 81 -0.32854

76 -> 82 -0.17130

TT1-Ph

Excited State 1: Singlet-A 3.2856 eV 377.35 nm f=0.3791 <S**2>=0.000

134 (H) -> 135 (L) 0.69692

This state for optimization and/or second-order correction.

Total Energy, E(TD-HF/TD-KS) = -2750.28571582

Copying the excited state density for this state as the 1-particle RhoCI density.

Excited State 2: Singlet-A 3.6736 eV 337.50 nm f=0.0683 <S**2>=0.000

133 (H) ->135 (L) 0.68290

134 ->136 0.10895

Excited State 3: Singlet-A 3.9106 eV 317.05 nm f=0.0367 <S**2>=0.000

132 ->135 0.36531

134 ->136 0.58418

Excited State 4: Singlet-A 4.0330 eV 307.43 nm f=0.1436 <S**2>=0.000

131 ->135 0.14520

132 ->135 0.50835

133 ->135 0.12116

134 ->136 -0.31690

134 ->137 0.29342

Excited State 5: Singlet-A 4.0475 eV 306.33 nm f=0.0183 <S**2>=0.000

132 ->135 -0.26993

134 ->136 0.10574

134 ->137 0.59241

134 ->138 0.19414

TT2-Ph

Excited State 1: Singlet-A 3.1912 eV 388.52 nm f=0.0211 <S**2>=0.000

230 (H) ->231 (L) 0.69436

This state for optimization and/or second-order correction.

Total Energy, E(TD-HF/TD-KS) = -4481.91638274

Copying the excited state density for this state as the 1-particle RhoCI density.

Excited State 2: Singlet-A 3.3069 eV 374.92 nm f=0.0535 <S**2>=0.000

230 ->232 0.48452

230 ->233 0.50769

Excited State 3: Singlet-A 3.3788 eV 366.95 nm f=0.3466 <S**2>=0.000

230 ->232 0.49629

230 ->233 -0.48313

Excited State 4: Singlet-A 3.6724 eV 337.61 nm f=0.0000 <S**2>=0.000

230 ->234 0.68010

230 ->235 0.17967

Excited State 5: Singlet-A 3.6840 eV 336.55 nm f=0.0014 <S**2>=0.000

230 ->234 -0.18080

230 ->235 0.67936

TT3-Ph

Excited State 1: Singlet-A 2.9935 eV 414.17 nm f=0.3946 <S**2>=0.000

216 ->219 -0.10781

218 (H) ->219 (L) 0.67990

This state for optimization and/or second-order correction.

Total Energy, E(TD-HF/TD-KS) = -4957.55601924

Copying the excited state density for this state as the 1-particle RhoCI density.

Excited State 2: Singlet-A 3.0655 eV 404.45 nm f=0.5872 <S**2>=0.000

216 ->220 0.11497

217 ->219 -0.19800

218 ->220 -0.38273

218 ->221 0.53234

Excited State 3: Singlet-A 3.0863 eV 401.73 nm f=0.0370 <S**2>=0.000

216 ->220 -0.18699

218 ->220 0.50515

218 ->221 0.41551

Excited State 4: Singlet-A 3.1657 eV 391.65 nm f=0.6431 <S**2>=0.000

216 ->219 0.60973

216 ->220 -0.20325

217 ->219 -0.21153

217 ->220 -0.12822

218 ->219 0.12731

Excited State 5: Singlet-A 3.2166 eV 385.45 nm f=0.3003 <S**2>=0.000

216 ->219 0.30938

216 ->220 0.40077

217 ->219 0.46554

218 ->221 0.12189

TT-Th

Excited State 1: Singlet-A 2.9443 eV 421.10 nm f=0.6053 <S**2>=0.000

78 (H) -> 79 (L) 0.70633

This state for optimization and/or second-order correction.

Total Energy, E(TD-HF/TD-KS) = -2130.91686712

Copying the excited state density for this state as the 1-particle RhoCI density.

Excited State 2: Singlet-A 3.8259 eV 324.07 nm f=0.0167 <S**2>=0.000

77 -> 79 0.36183

78 -> 80 0.59902

Excited State 3: Singlet-A 4.1319 eV 300.06 nm f=0.0040 <S**2>=0.000

75 -> 79 -0.17505

76 -> 79 0.25151

78 -> 81 0.59300

78 -> 82 0.10854

78 -> 83 -0.17469

Excited State 4: Singlet-A 4.2316 eV 293.00 nm f=0.0500 <S**2>=0.000

75 -> 79 0.24231

76 -> 79 -0.15598

77 -> 79 0.35155

78 -> 80 -0.15486

78 -> 81 0.18391

78 -> 82 0.37426

78 -> 83 0.29123

Excited State 5: Singlet-A 4.2649 eV 290.71 nm f=0.0241 <S**2>=0.000

75 -> 79 -0.41320

76 -> 79 0.25634

78 -> 83 0.48774

218 -> 221 0.21790

218 -> 223 0.13928

219 -> 221 0.54783

219 -> 222 -0.24524

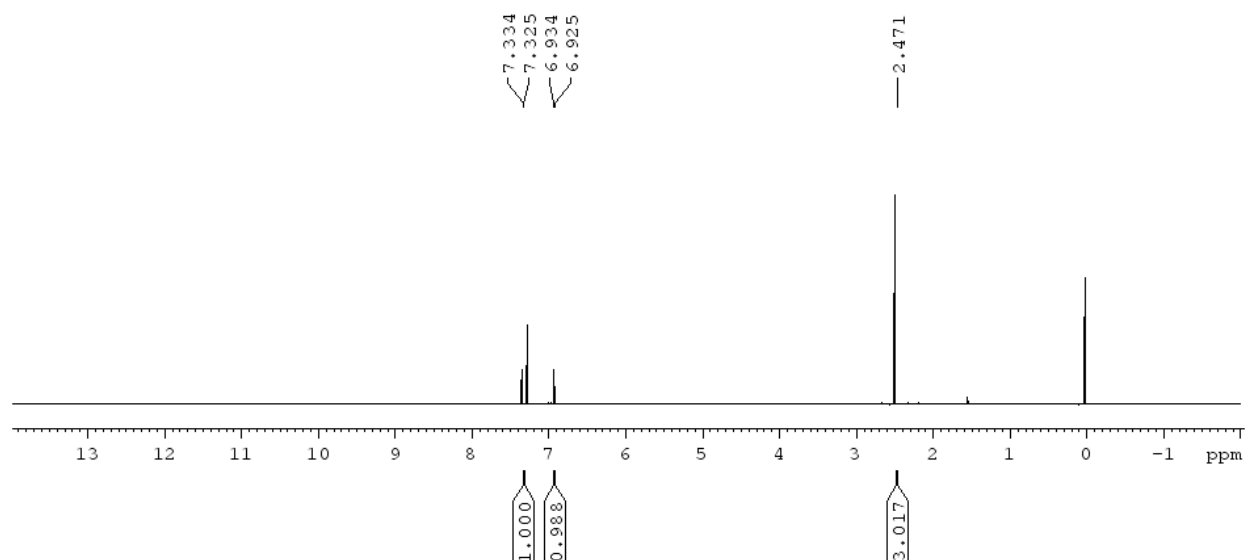
219 -> 223 0.14725

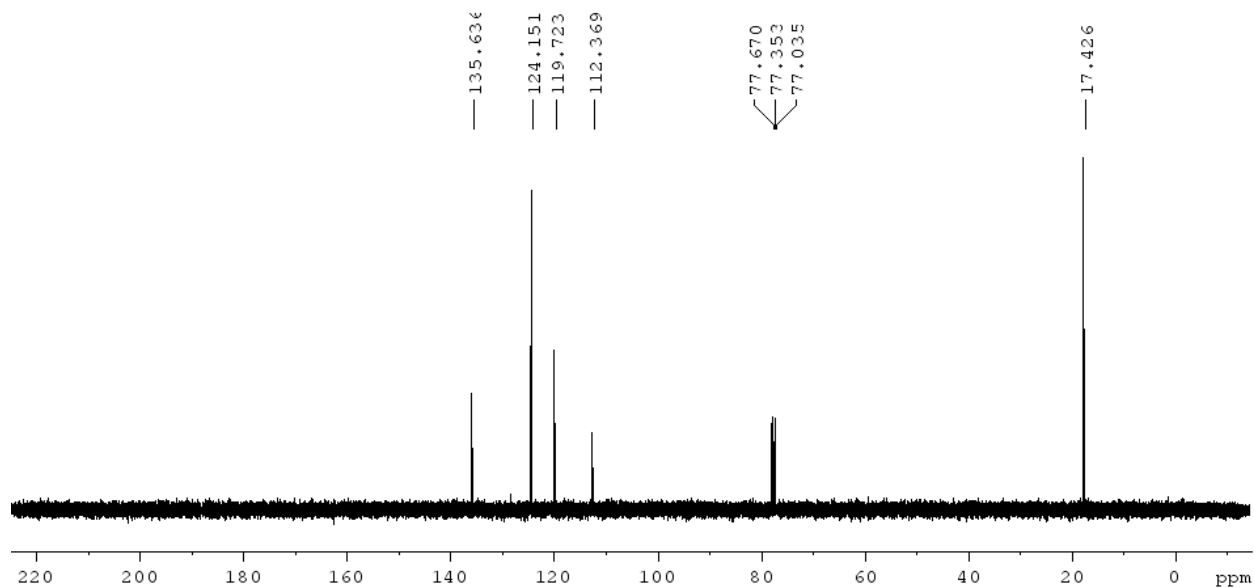
220 -> 221 -0.10058

220 -> 222 -0.17414

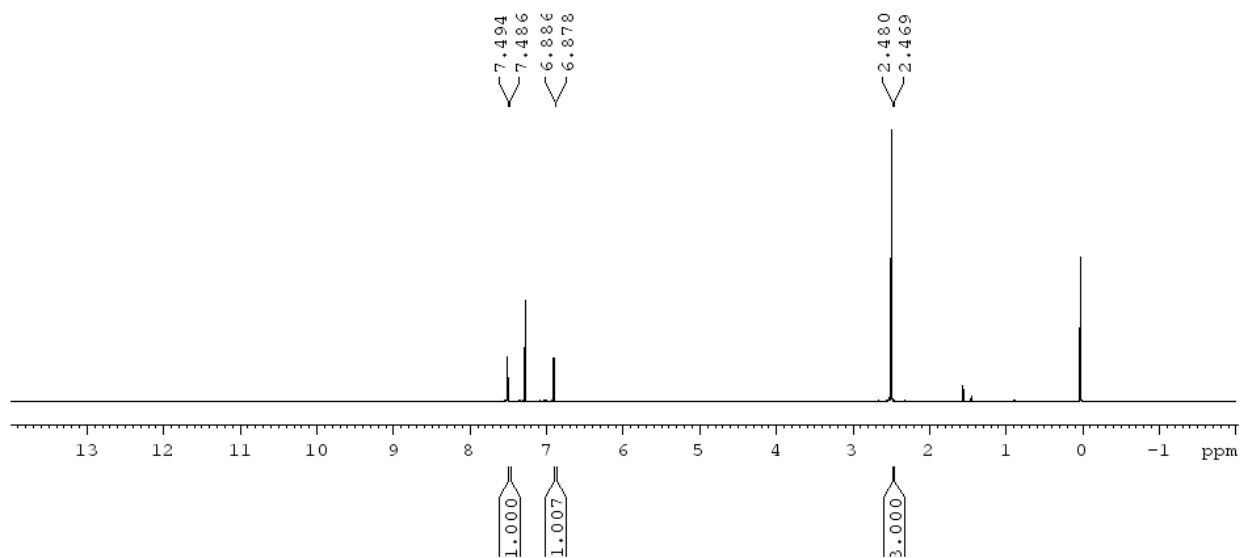
^1H and ^{13}C NMR SPECTRA

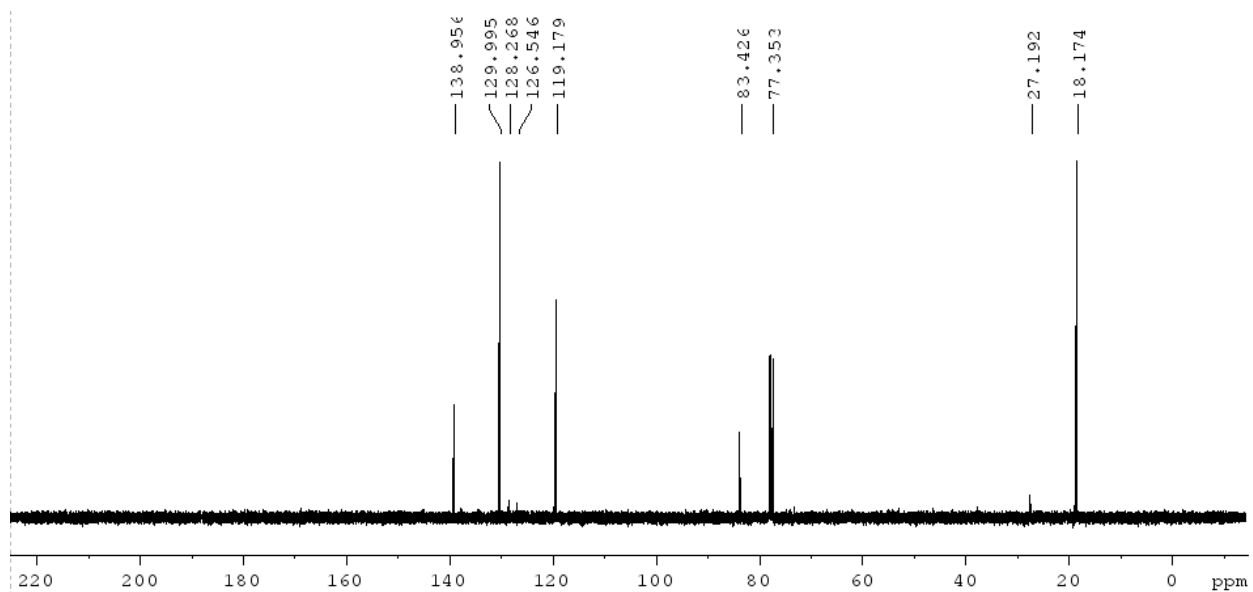
3-bromo-4-(methylthio)thiophene (1)



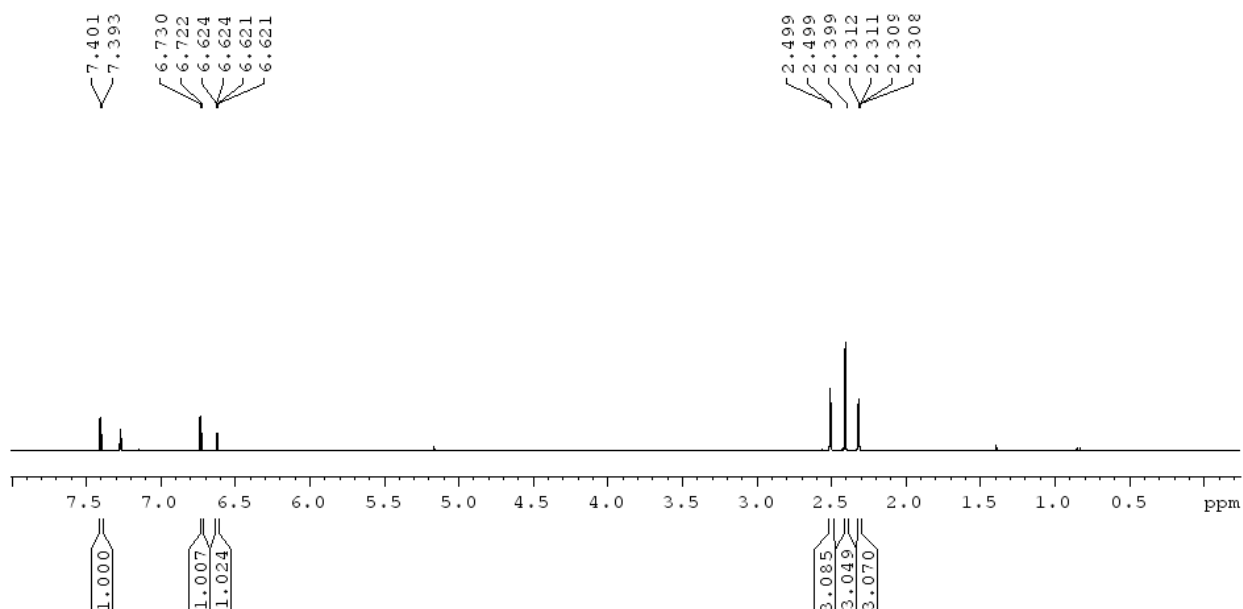


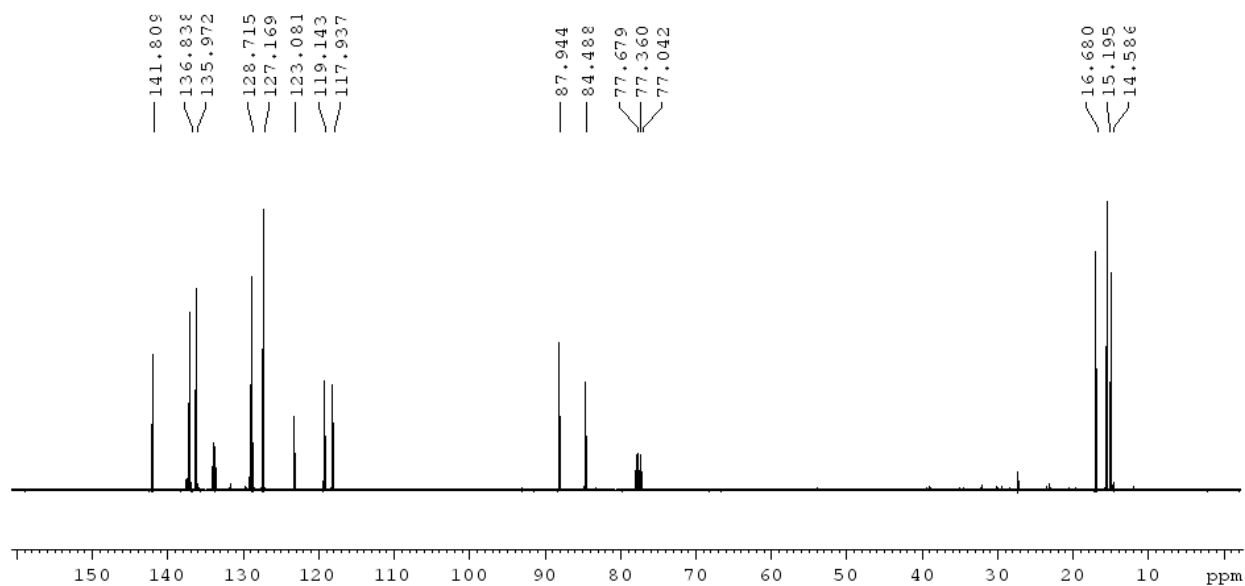
3-iodo-4-(methylthio)thiophene (2)



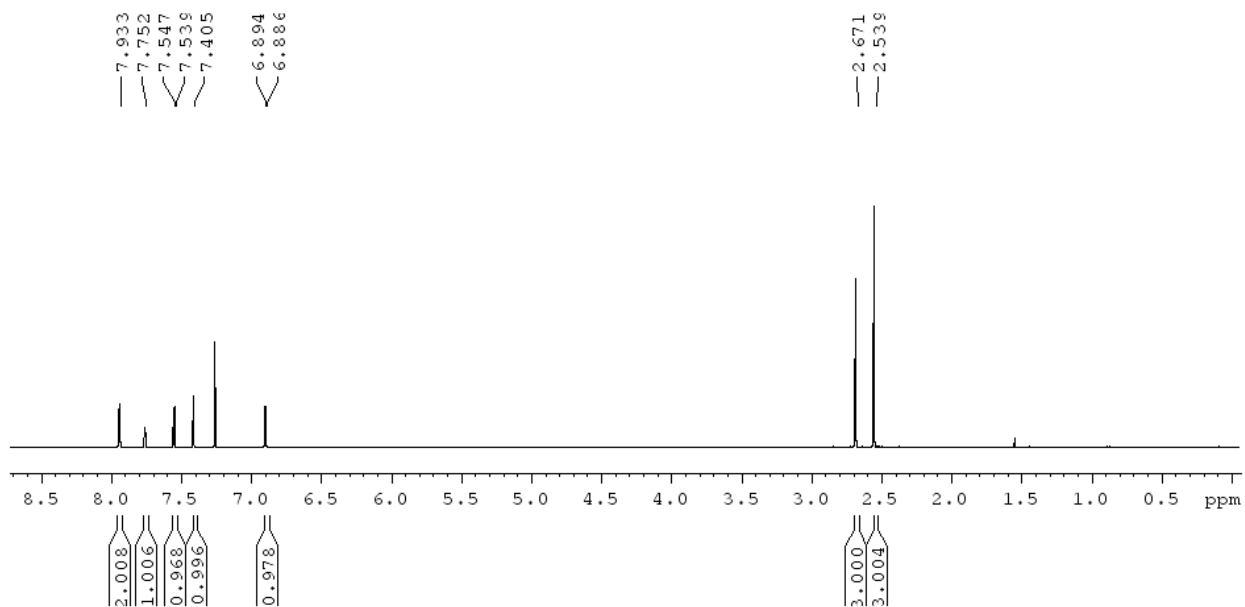


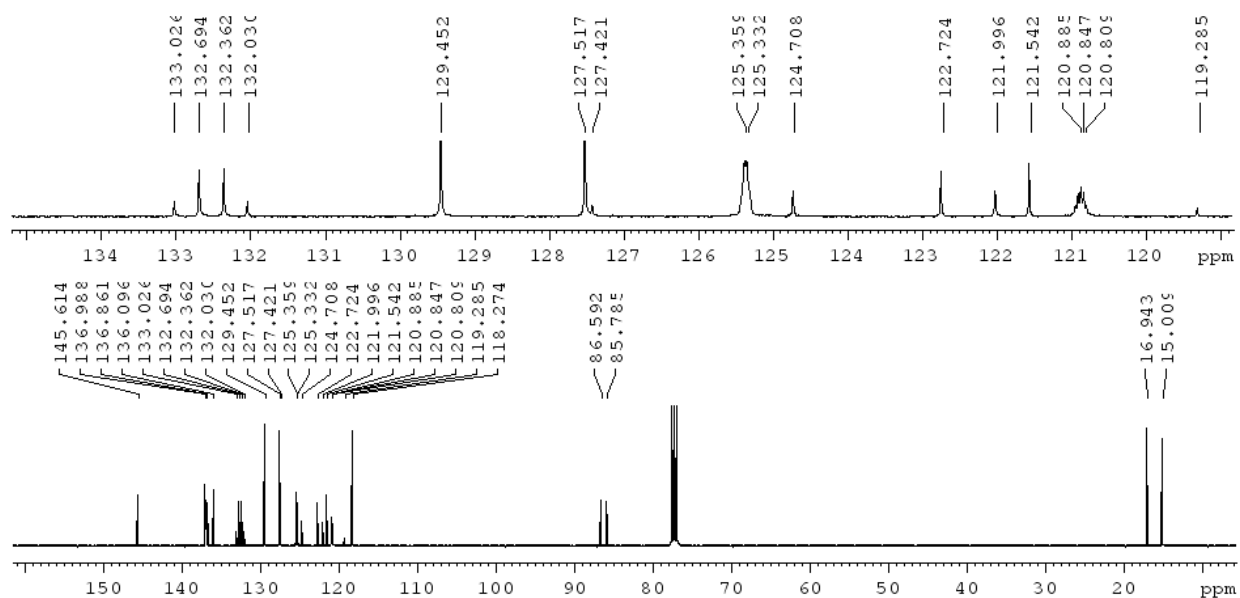
2,5-dimethyl-3-((4-(methylthio)thiophen-3-yl)ethynyl)thiophene (3a)



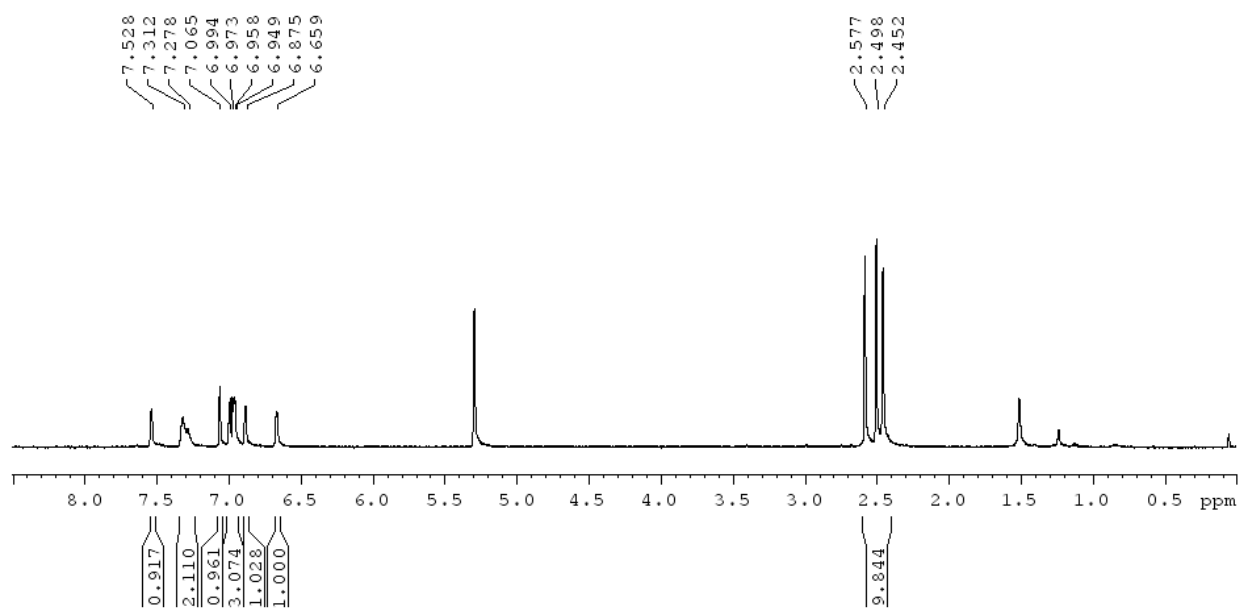


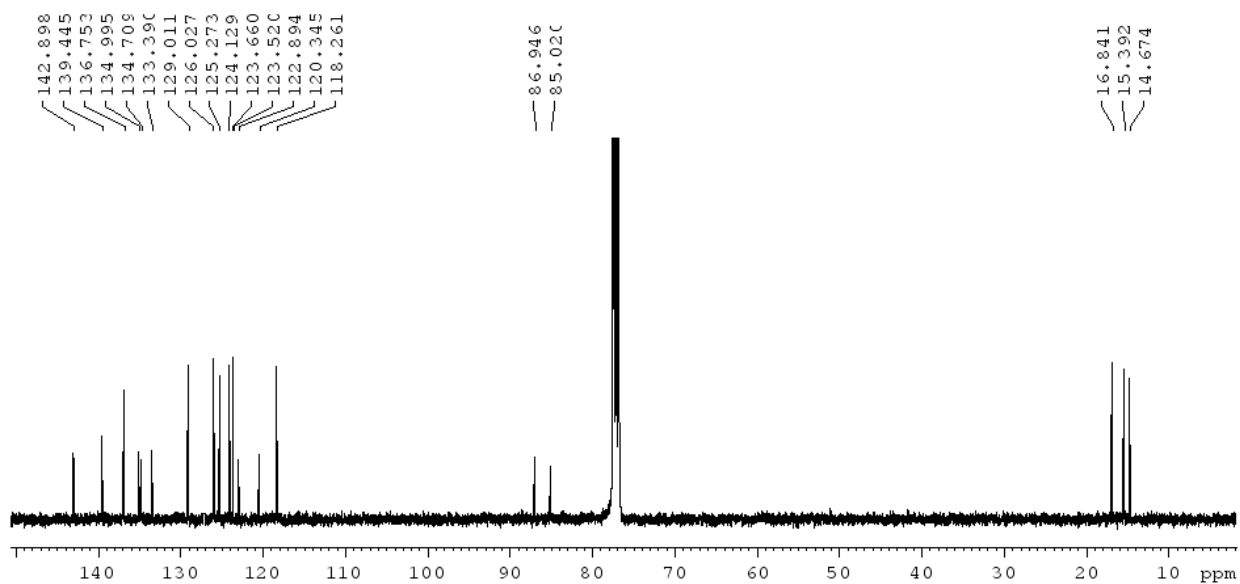
5-(3,5-bis(trifluoromethyl)phenyl)-2-methyl-3-((4-(methylthio)thiophen-3-yl)ethynyl)thiophene (3b)



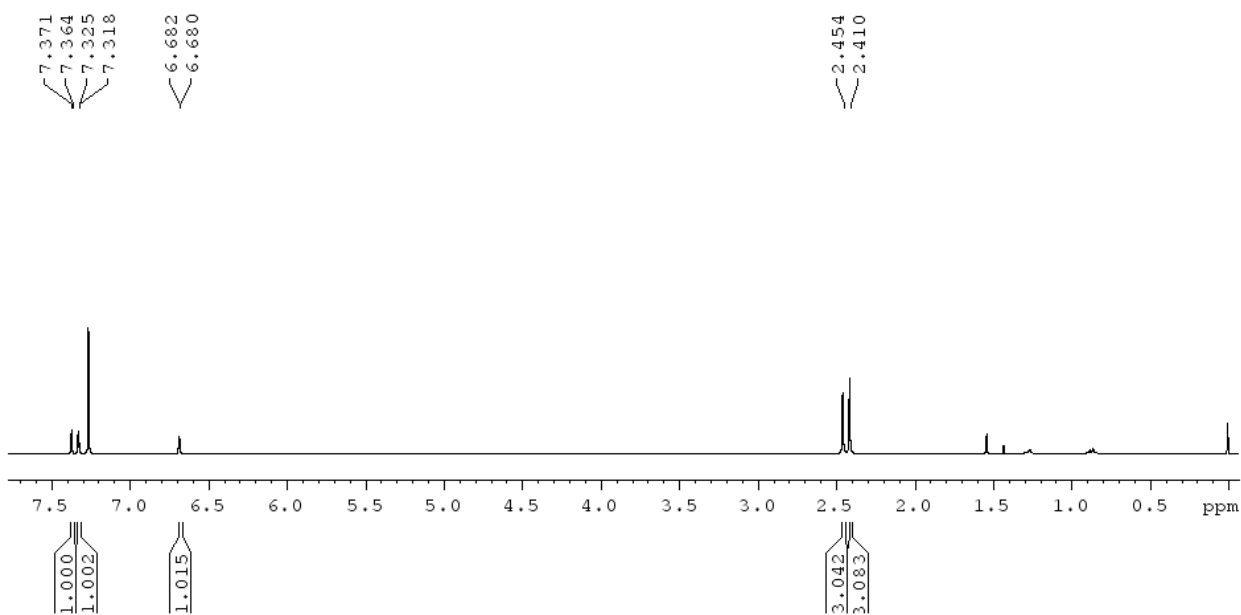


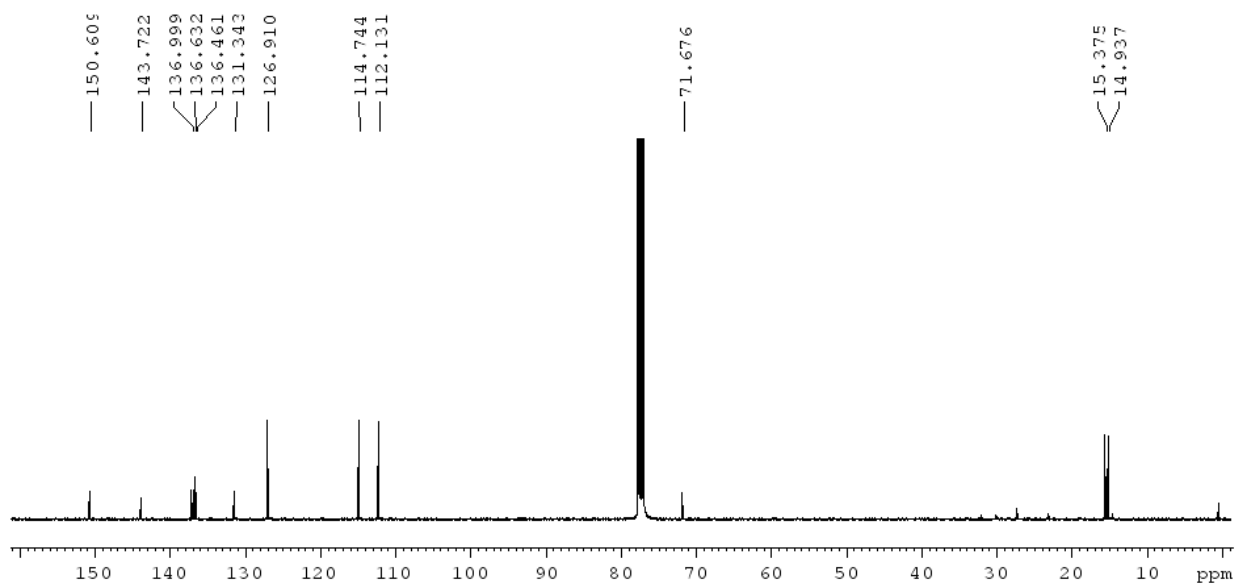
5,5''-dimethyl-4-((4-(methylthio)thiophen-3-yl)ethynyl)-2,2':5',2''-terthiophene (3c)



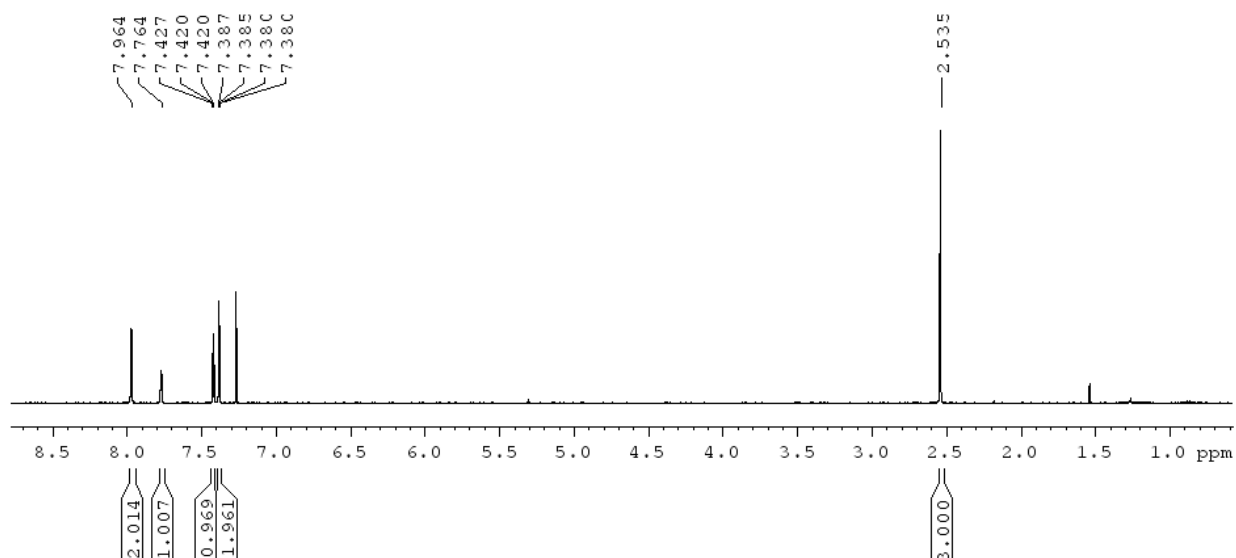


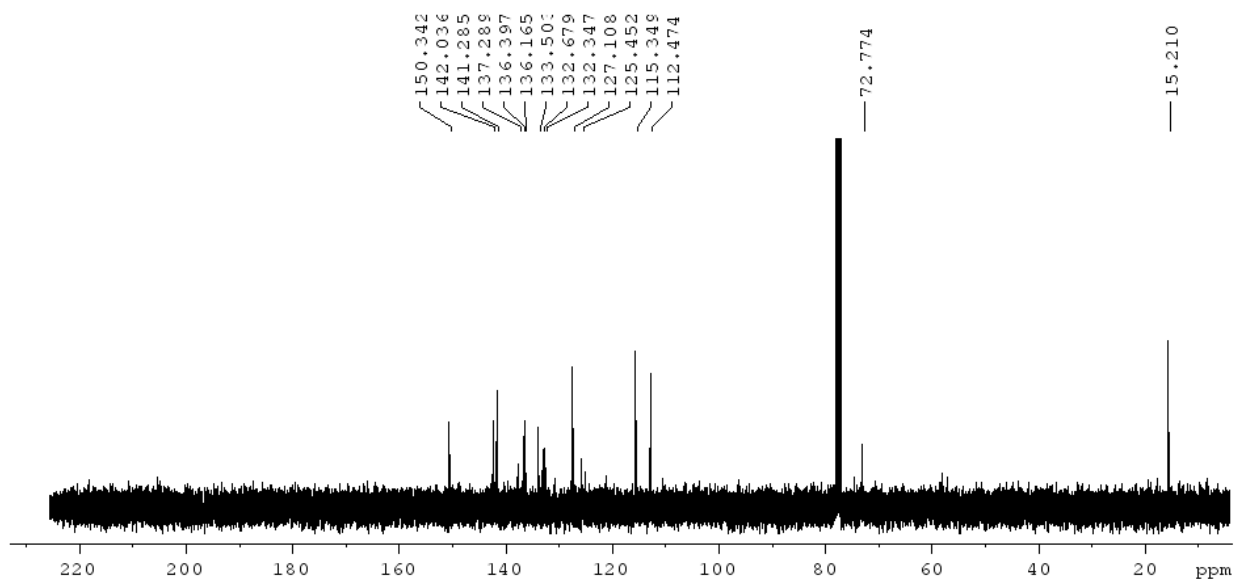
2-(2,5-dimethylthiophen-3-yl)-3-iodothiopheno[3,4-b]thiophene (4a)



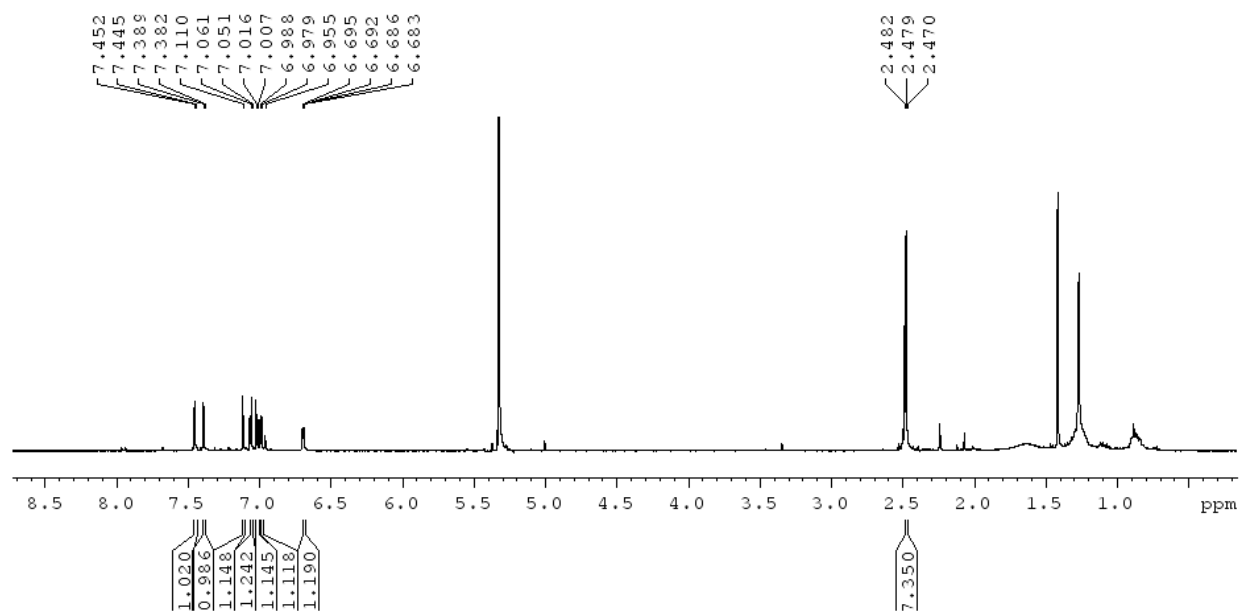


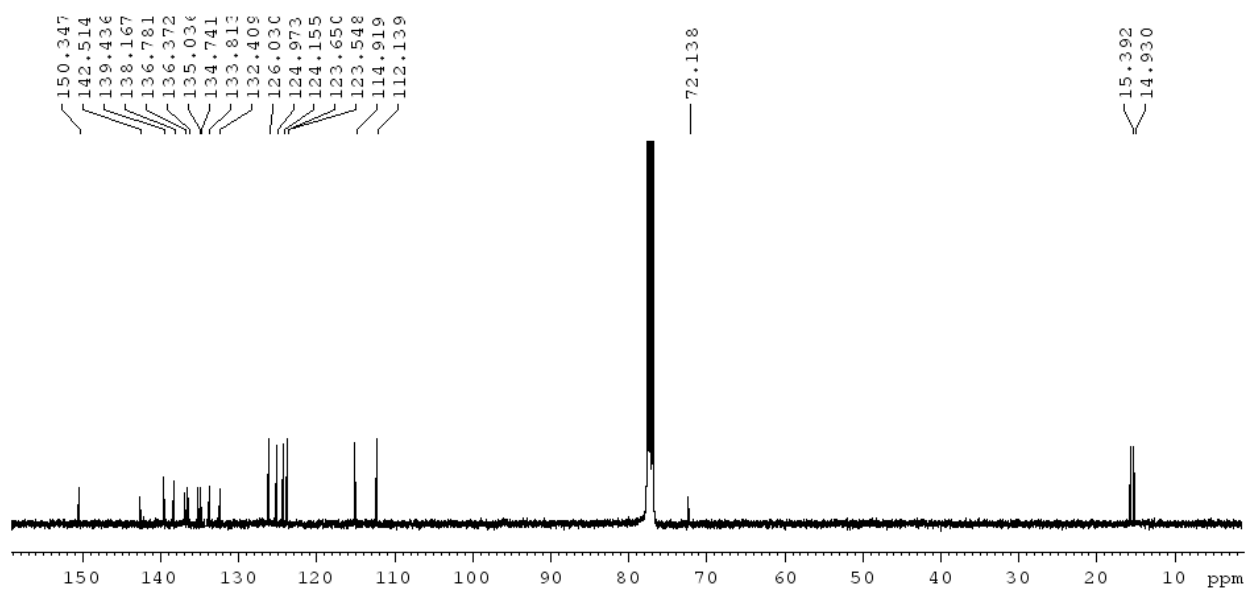
2-(5-(3,5-bis(trifluoromethyl)phenyl)-2-methylthiophen-3-yl)-3-iodothieno[3,4-b]thiophene (4b)



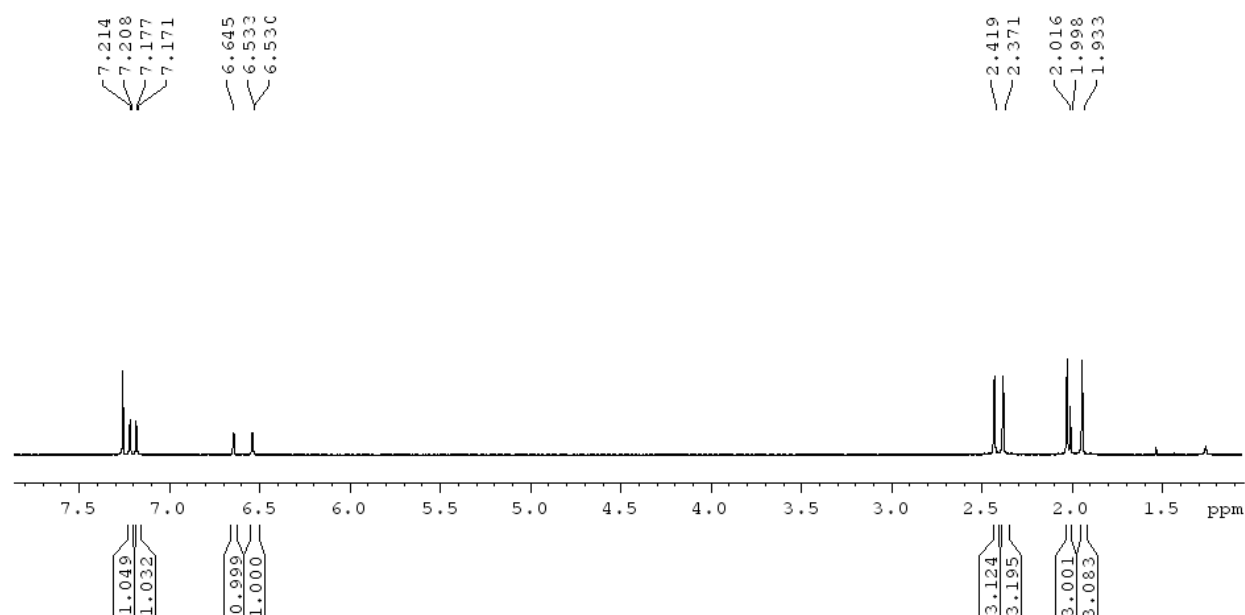


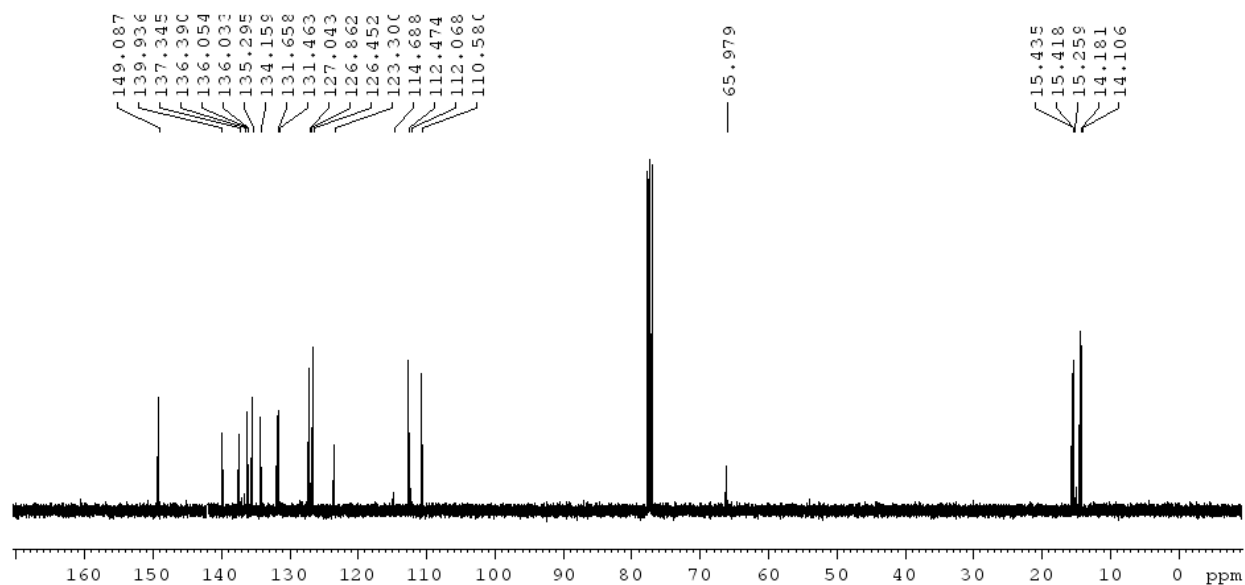
2-(5,5'-dimethyl-[2,2':5',2''-terthiophen]-4-yl)-3-iodothiopheno[3,4-b]thiophene (4c)



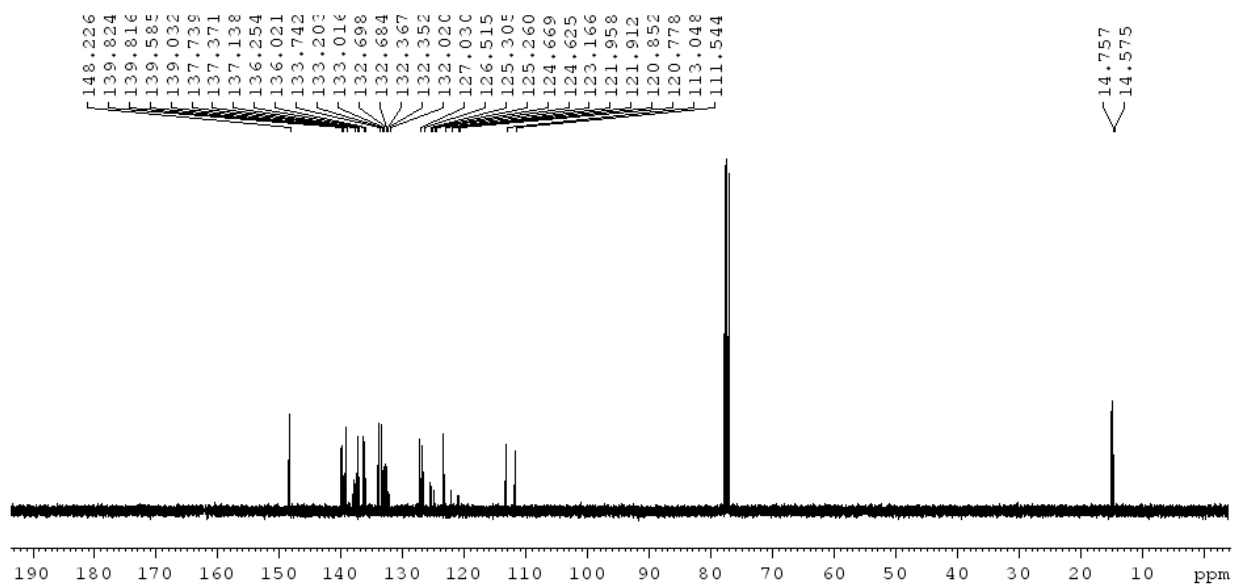
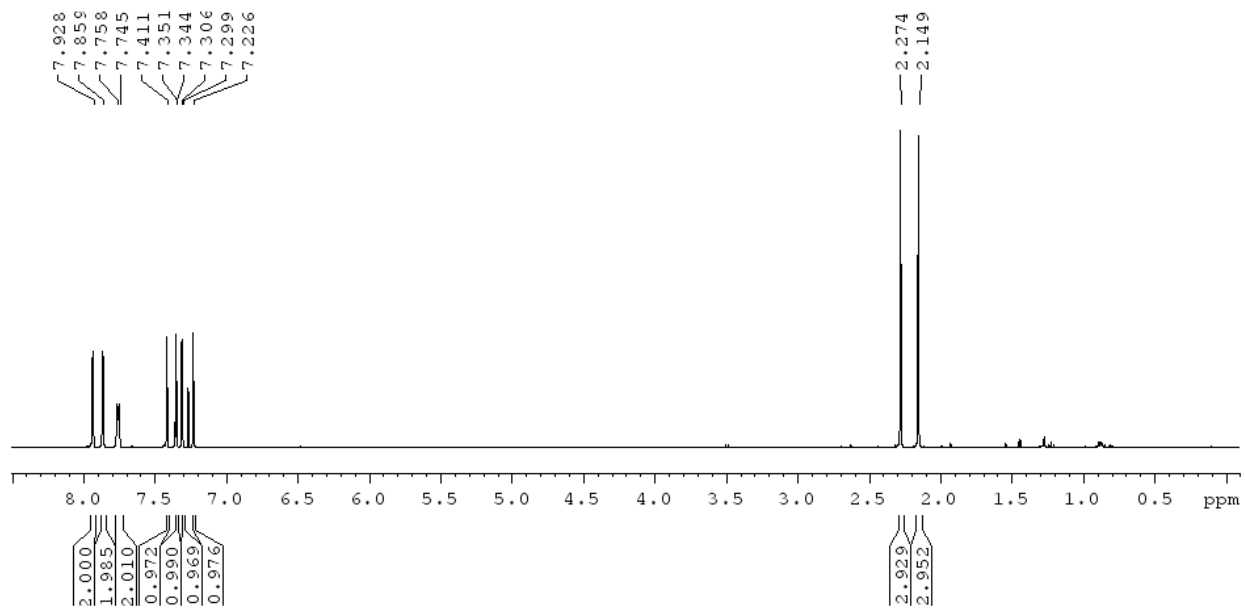


2,3-bis(2,5-dimethylthiophen-3-yl)thieno[3,4-b]thiophene (TT1)

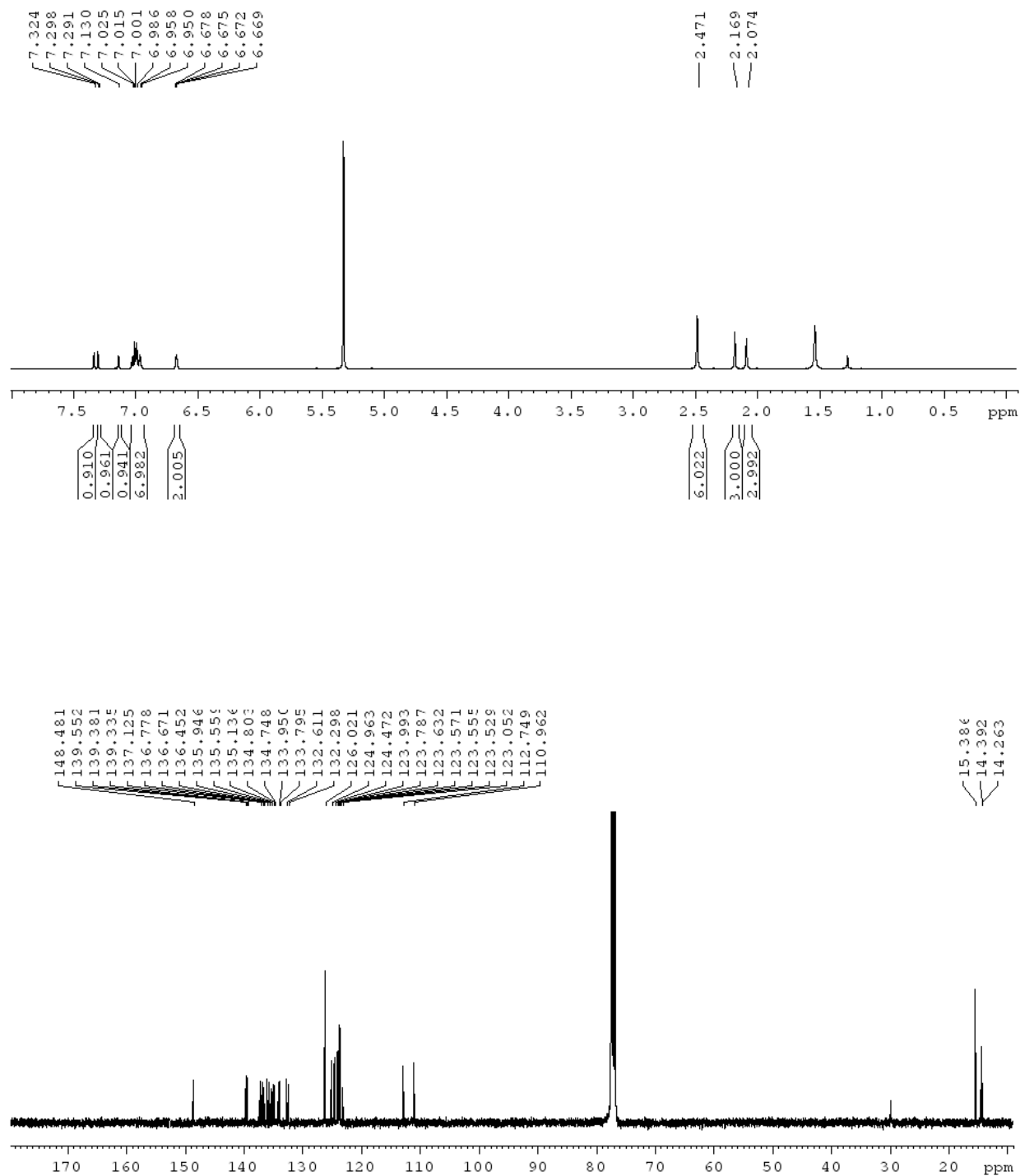




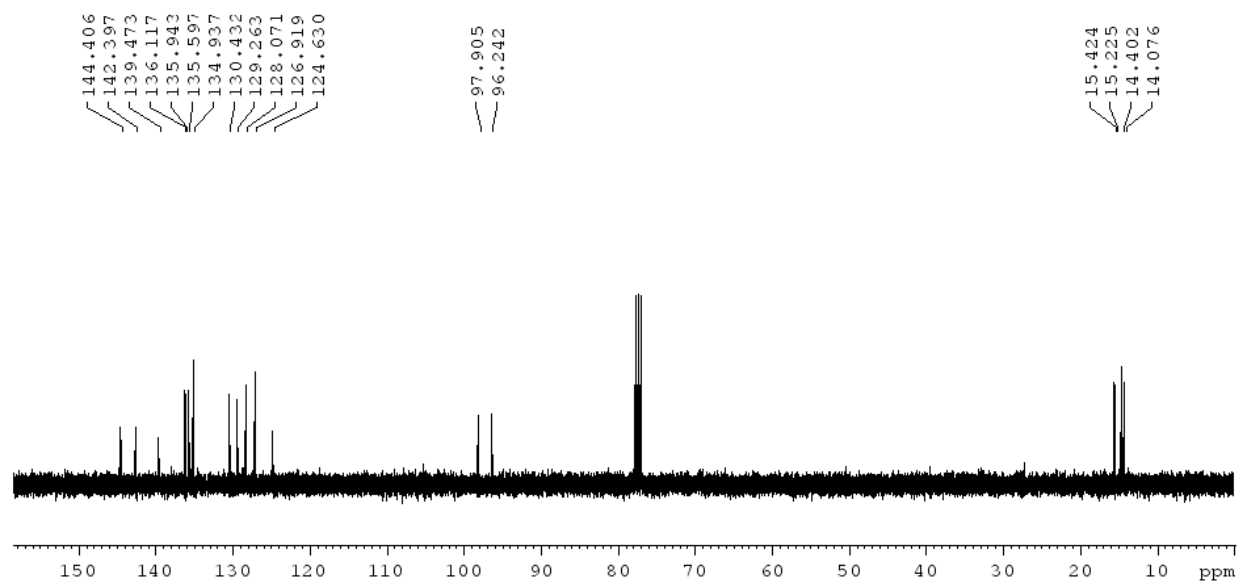
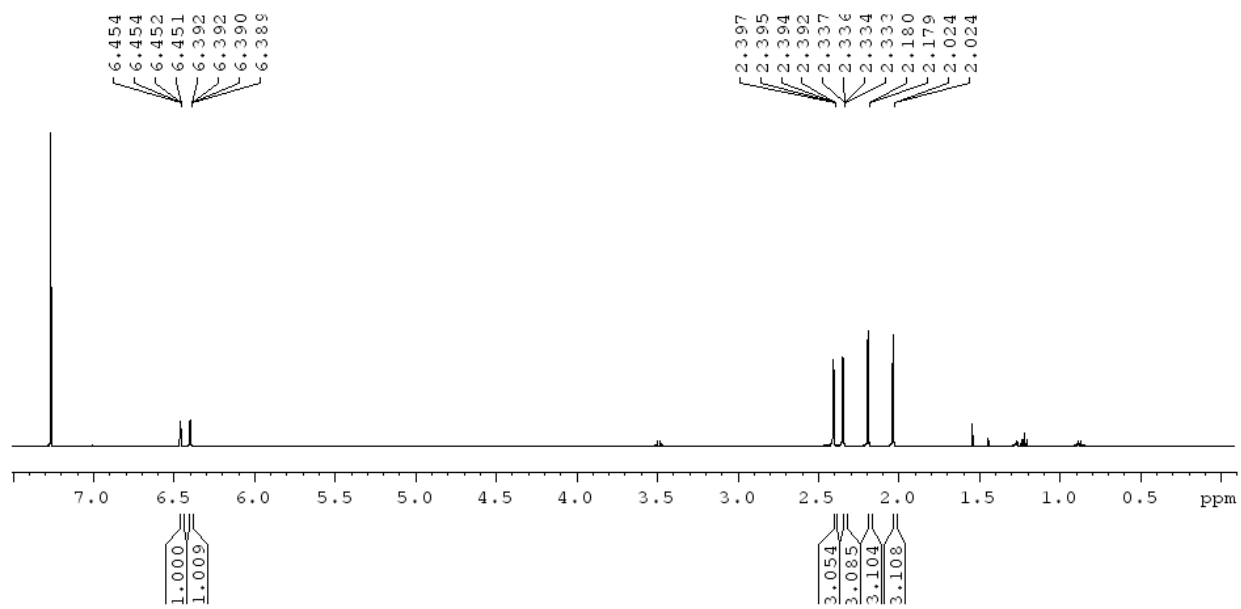
2,3-bis(5-(3,5-bis(trifluoromethyl)phenyl)-2-methylthiophen-3-yl)thieno[3,4-b]thiophene (TT2)



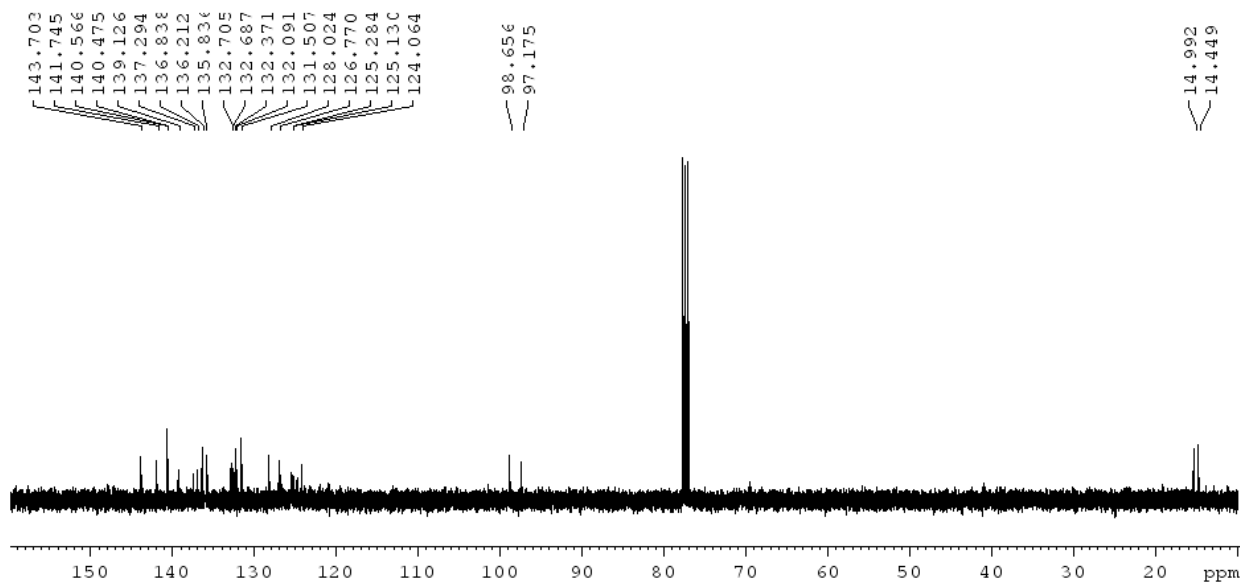
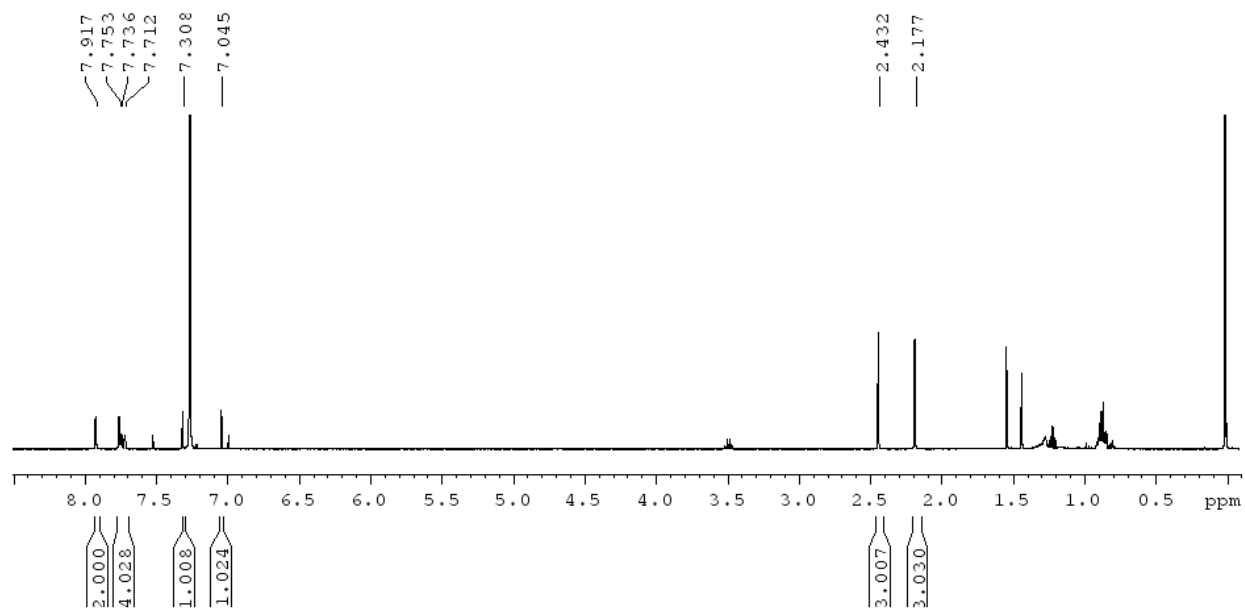
2,3-bis(5,5'-dimethyl-[2,2':5',2''-terthiophen]-4-yl)thieno[3,4-b]thiophene (TT3)



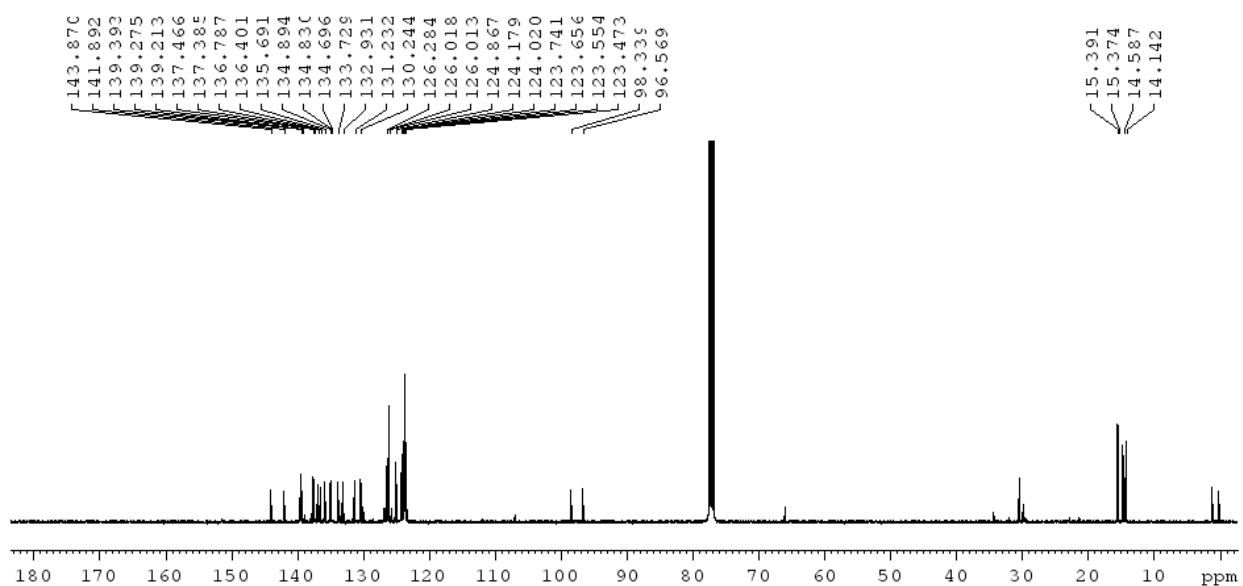
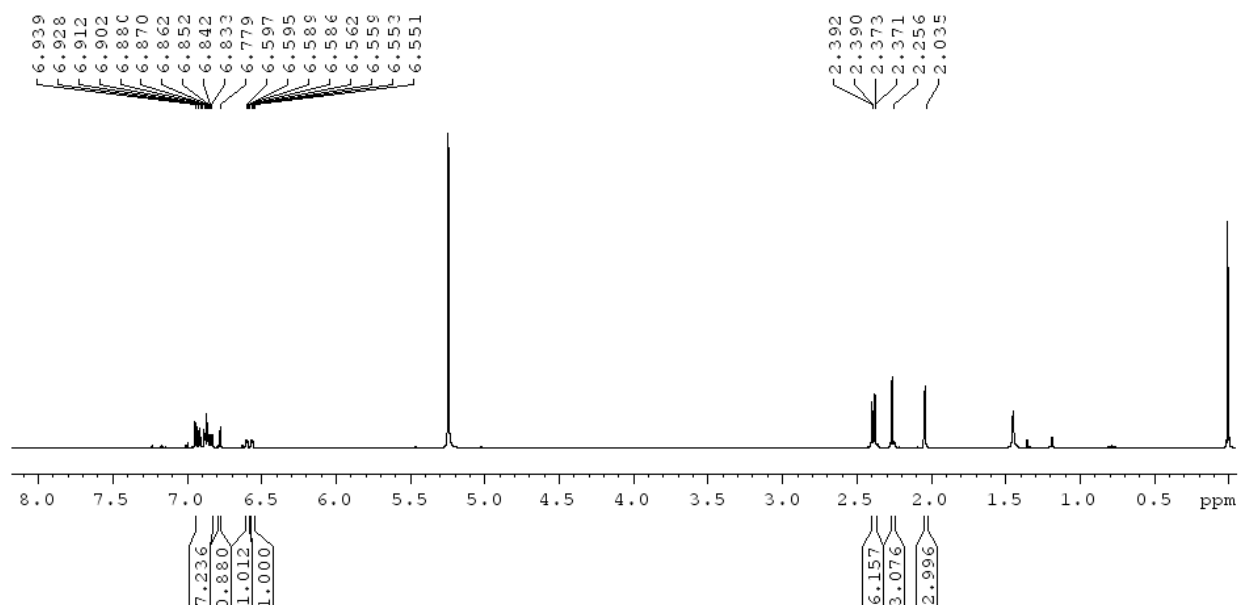
4,6-dibromo-2,3-bis(2,5-dimethylthiophen-3-yl)thieno[3,4-b]thiophene (TT1-Br)



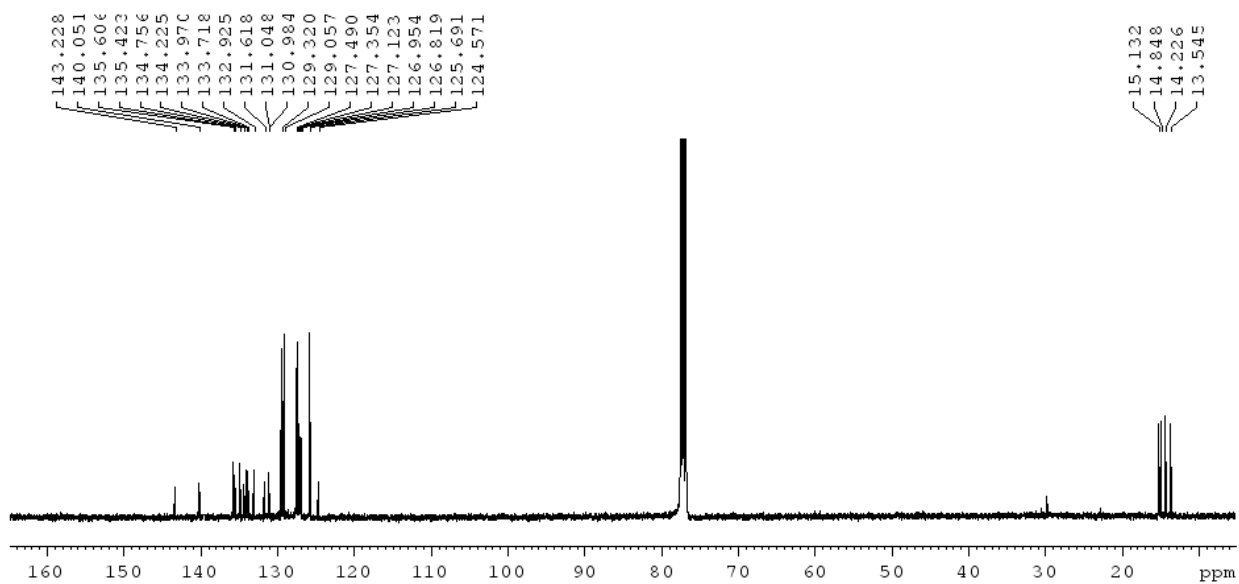
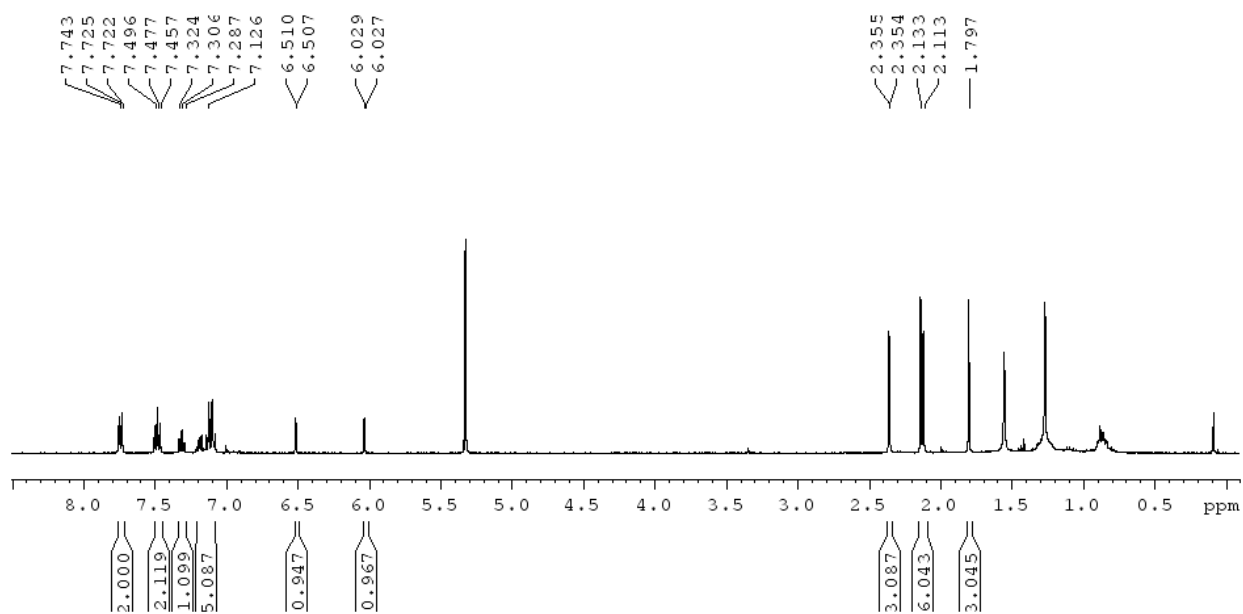
2,3-bis(5-(3,5-bis(trifluoromethyl)phenyl)-2-methylthiophen-3-yl)-4,6-dibromothiopheno[3,4-b]thiophene (TT2-Br)



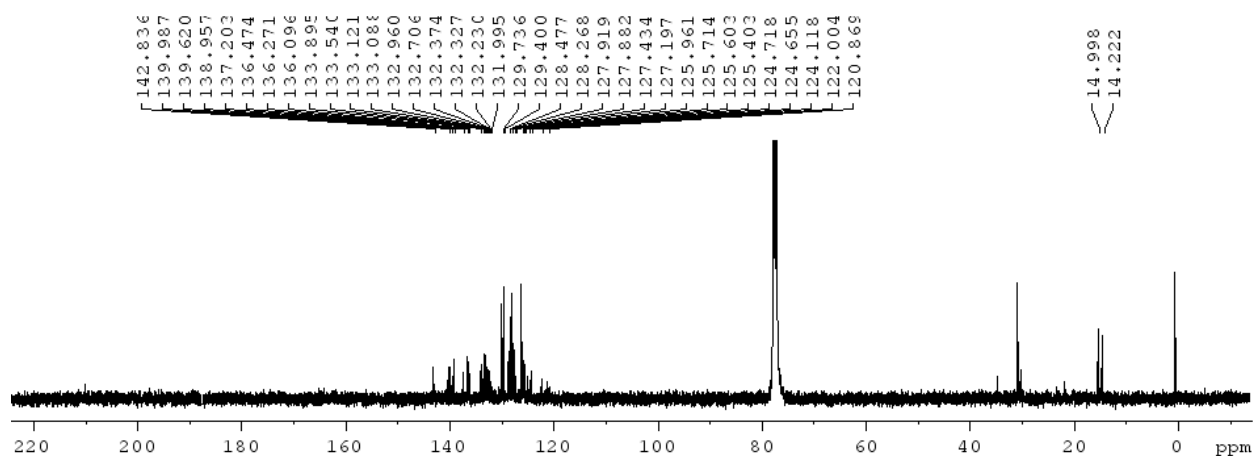
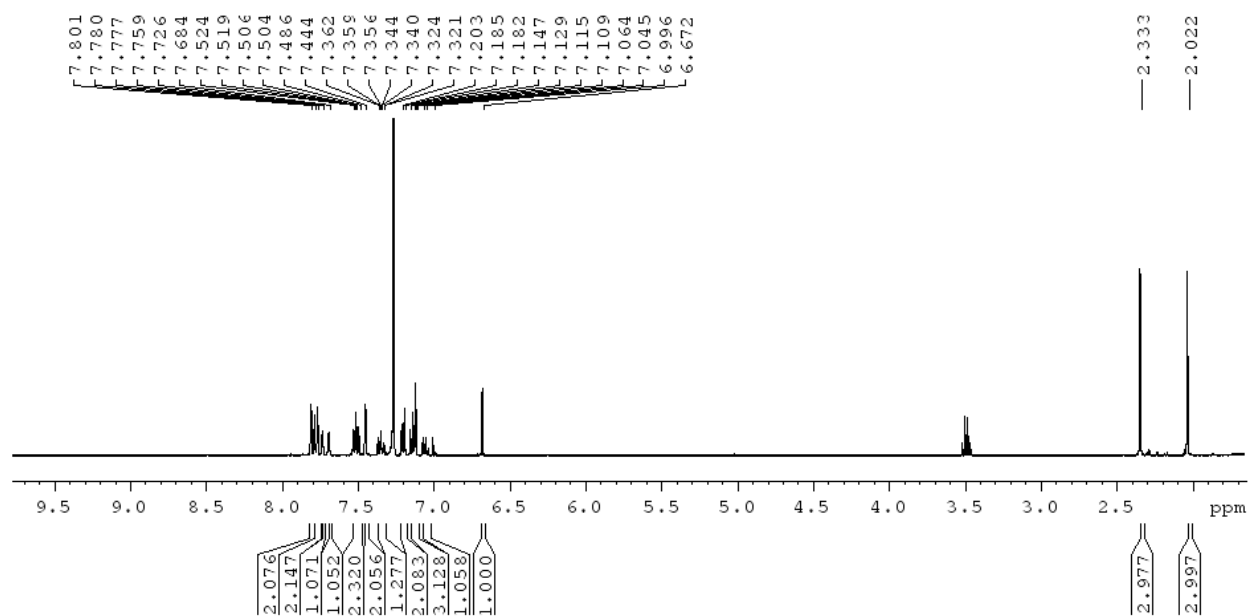
4,6-dibromo-2,3-bis(5,5''-dimethyl-[2,2':5',2''-terthiophen]-4-yl)thieno[3,4-b]thiophene (TT3-Br)



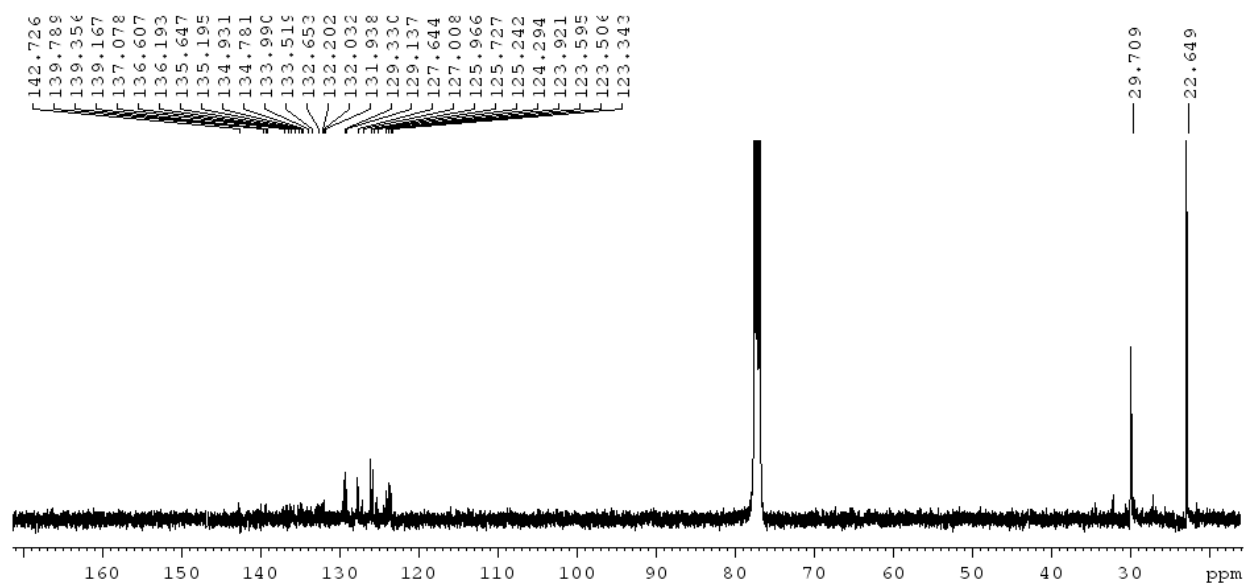
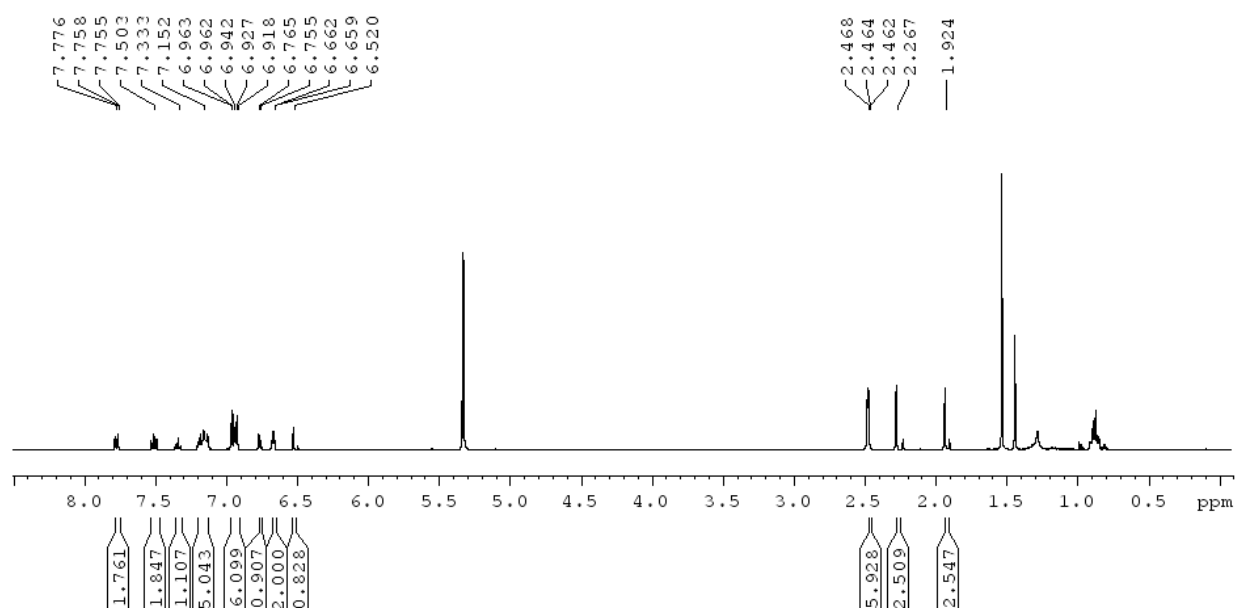
2,3-bis(2,5-dimethylthiophen-3-yl)-4,6-diphenylthieno[3,4-b]thiophene (TT1-Ph)



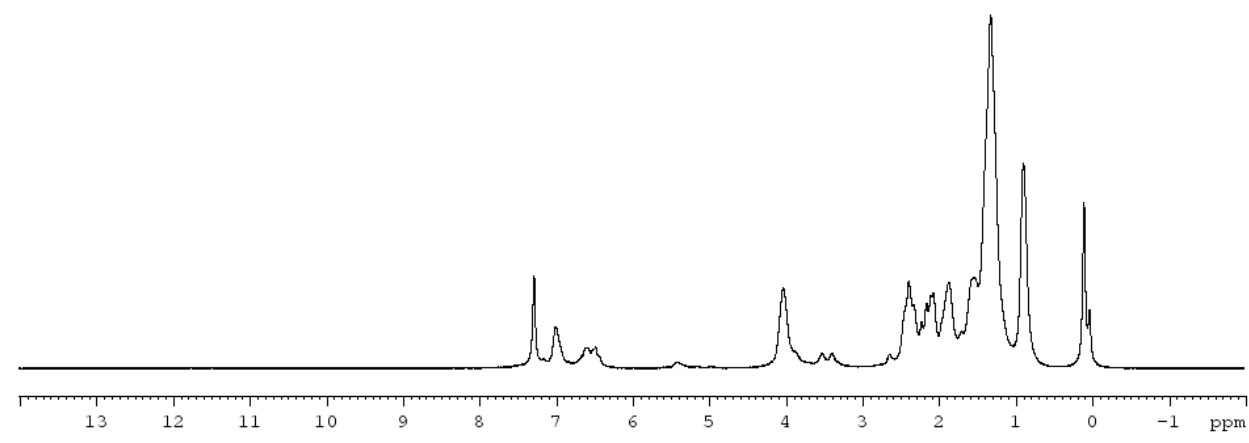
2,3-bis(5-(3,5-bis(trifluoromethyl)phenyl)-2-methylthiophen-3-yl)-4,6-diphenylthieno[3,4-b]thiophene (TT2-Ph)



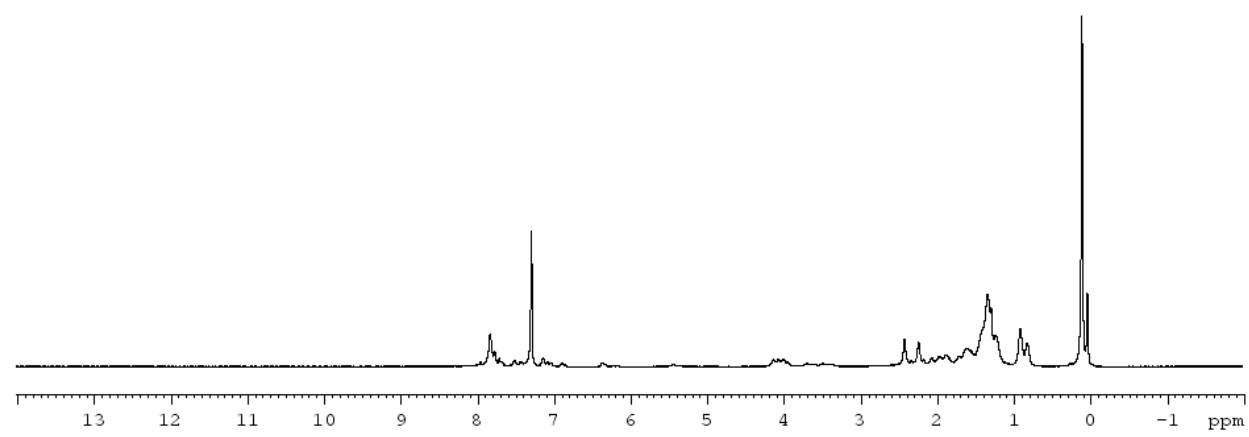
2,3-bis(5,5''-dimethyl-[2,2':5',2''-terthiophen]-4-yl)-4,6-diphenylthieno[3,4-b]thiophene (TT3-Ph)



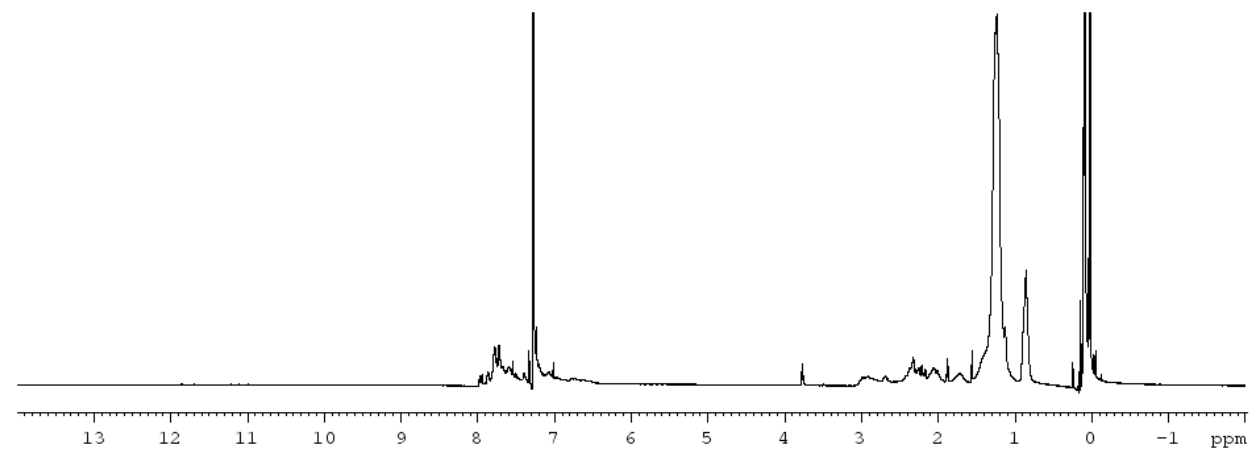
P-TT1



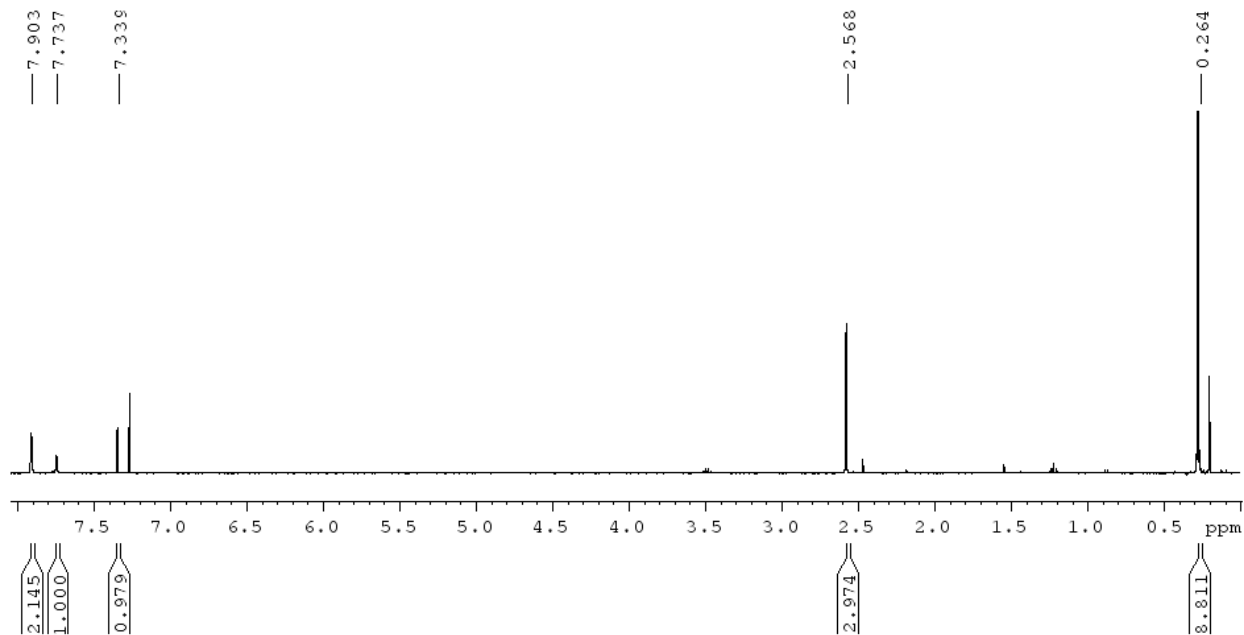
P-TT2

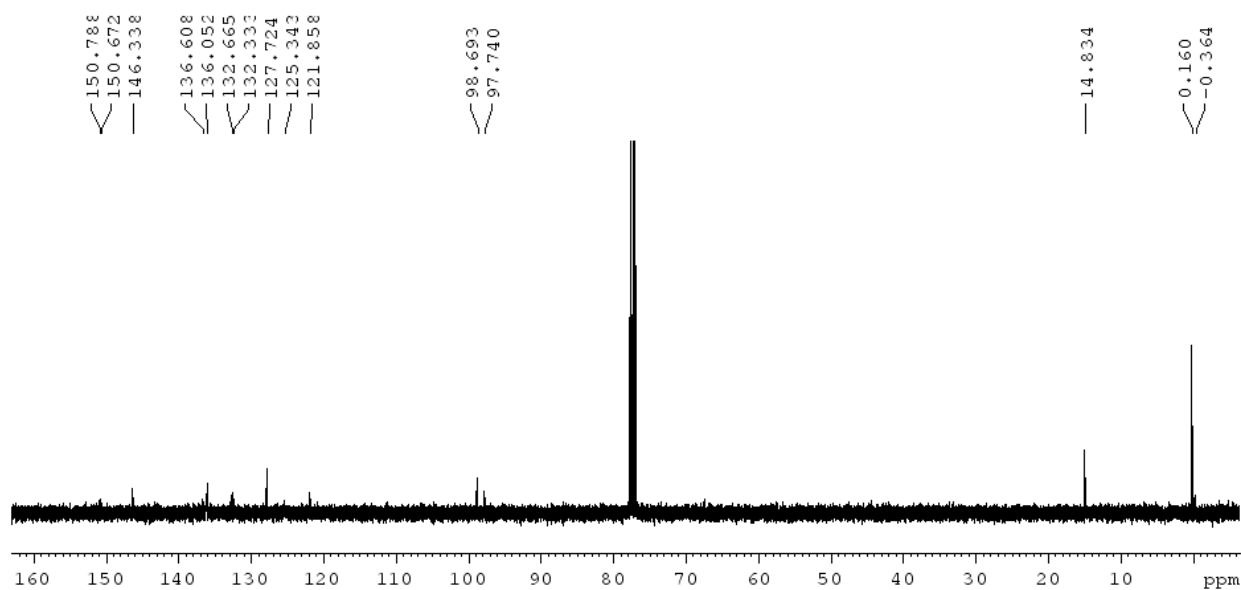


P-TT3

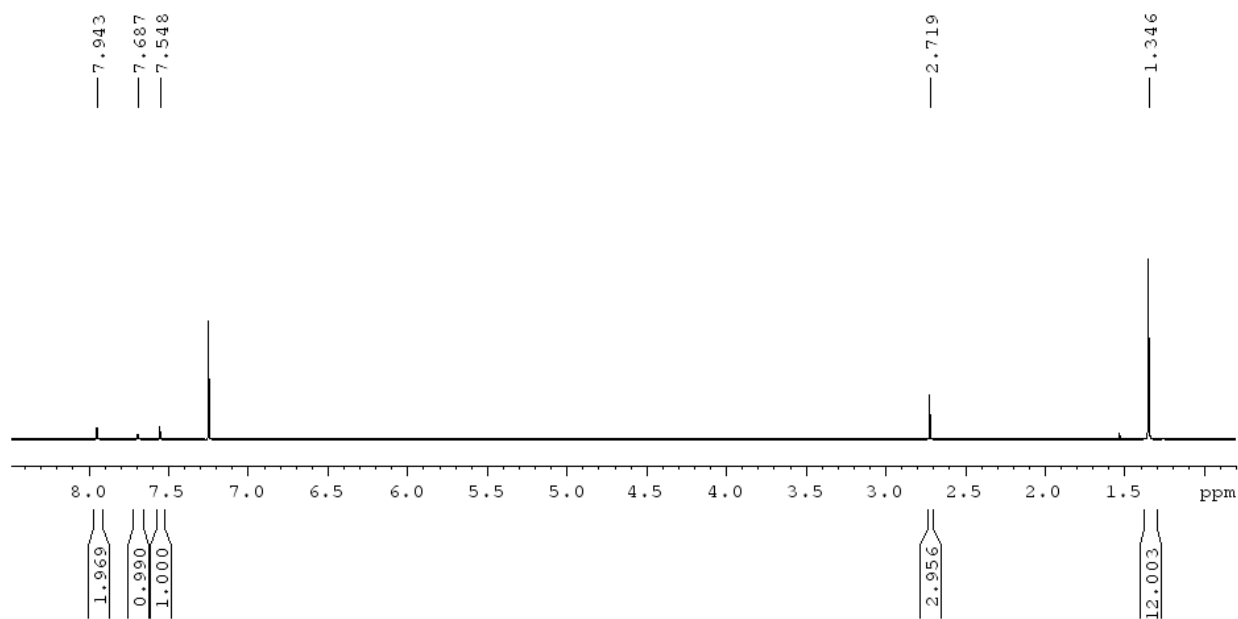


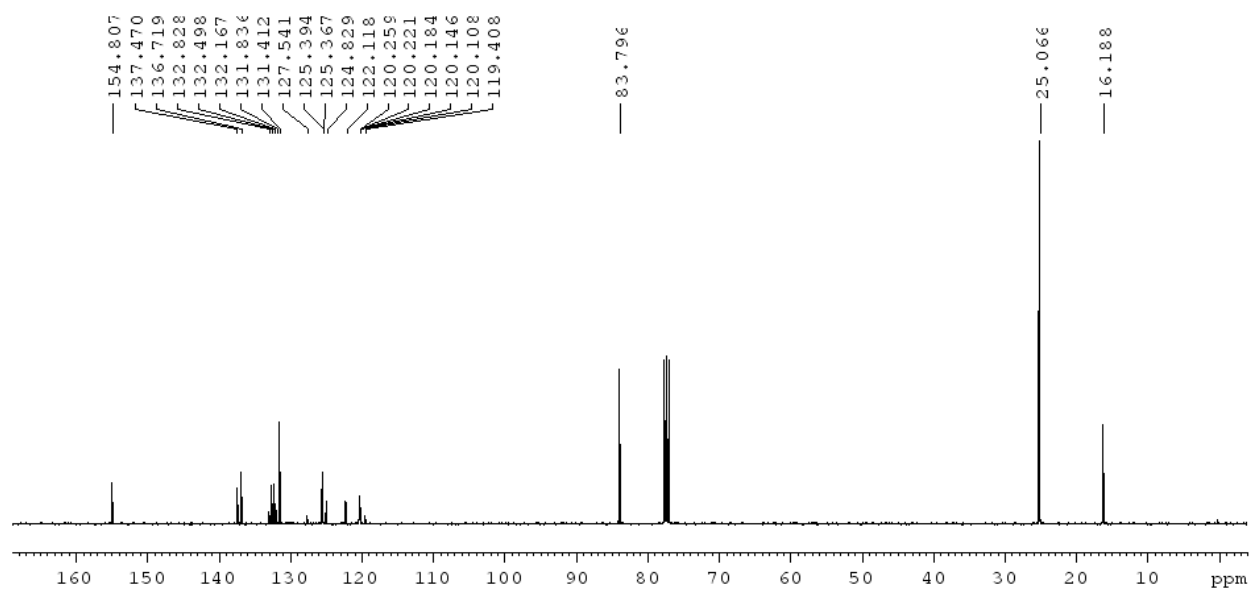
((5-(3,5-bis(trifluoromethyl)phenyl)-2-methylthiophen-3-yl)ethynyl)trimethylsilane (6)



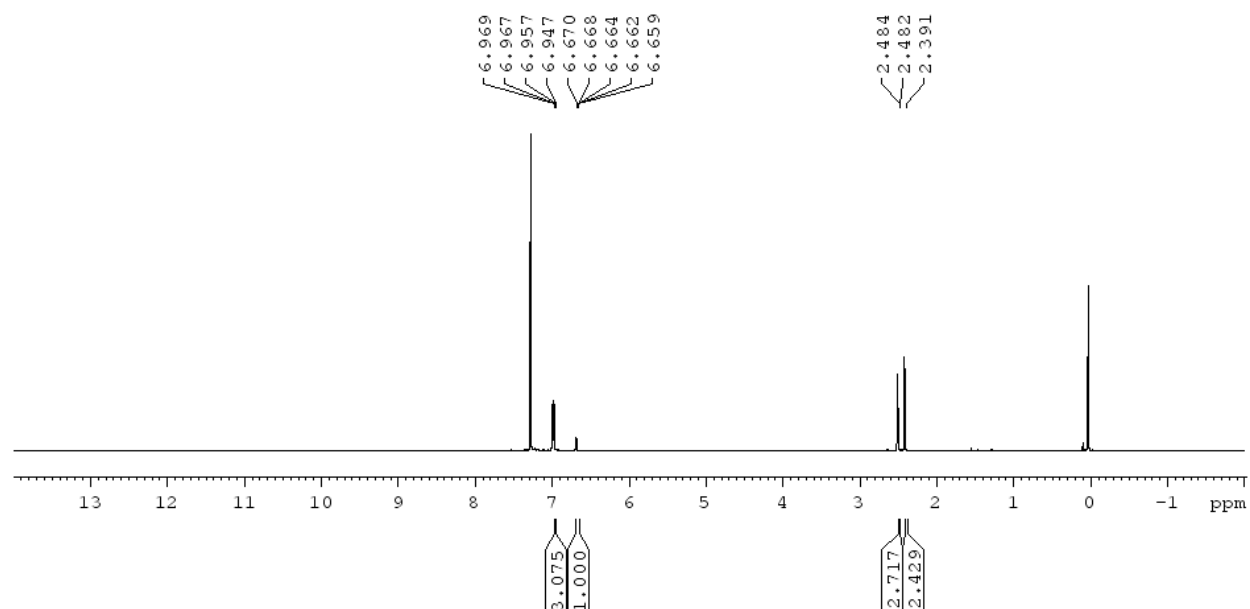


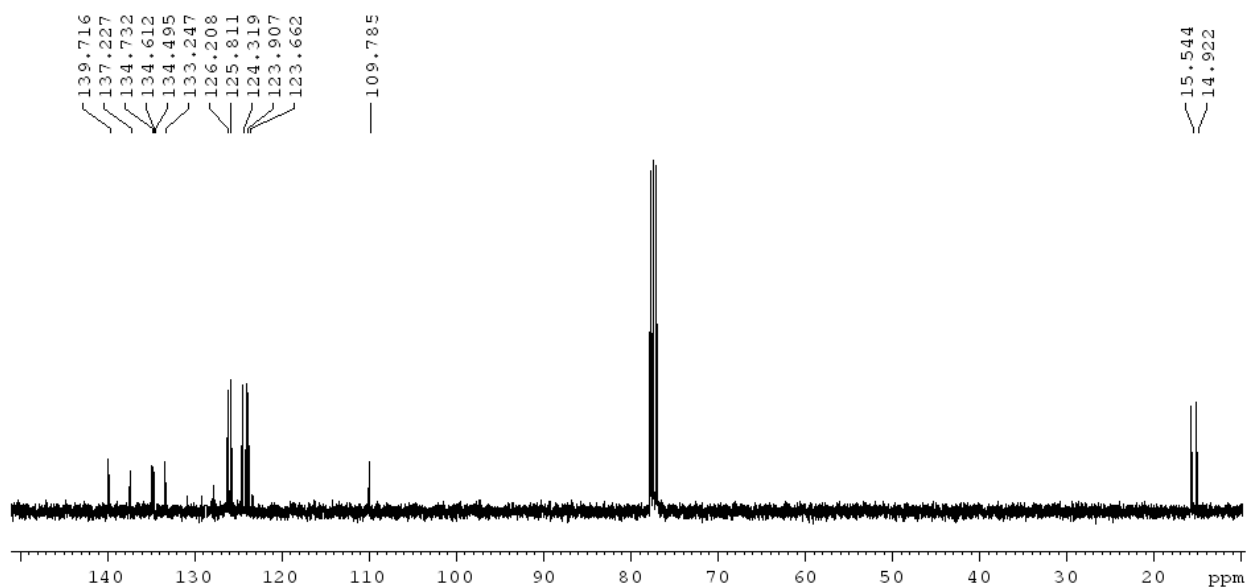
2-(5-(3,5-bis(trifluoromethyl)phenyl)-2-methylthiophen-3-yl)-4,4,5,5-tetramethyl-1,3,2-dioxaborolane (7)



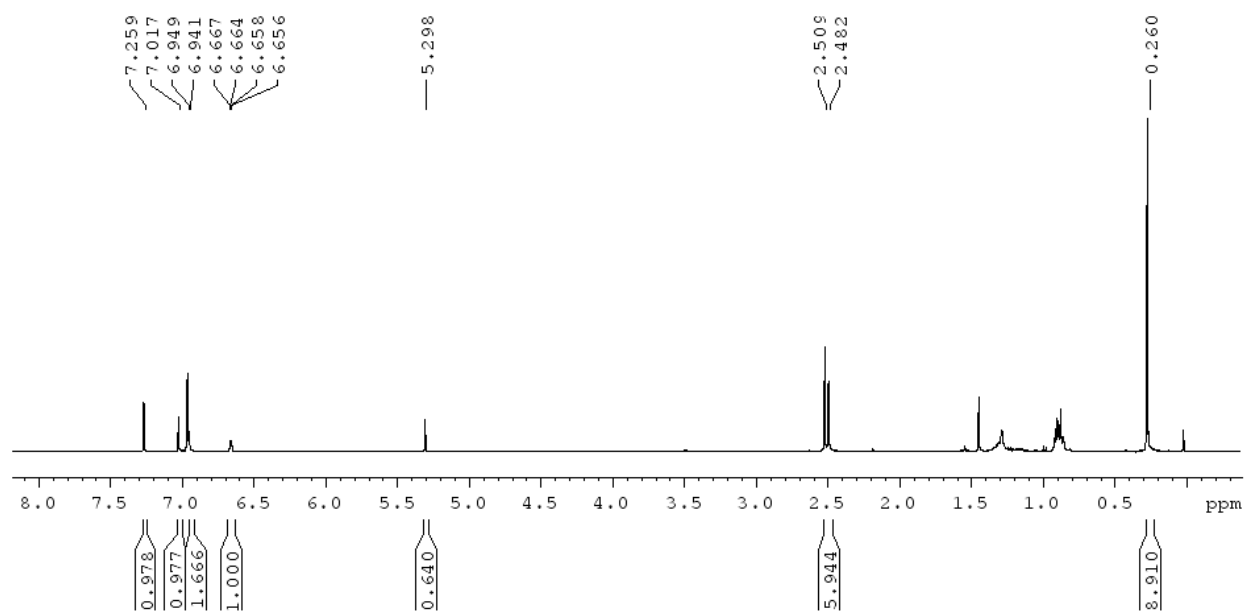


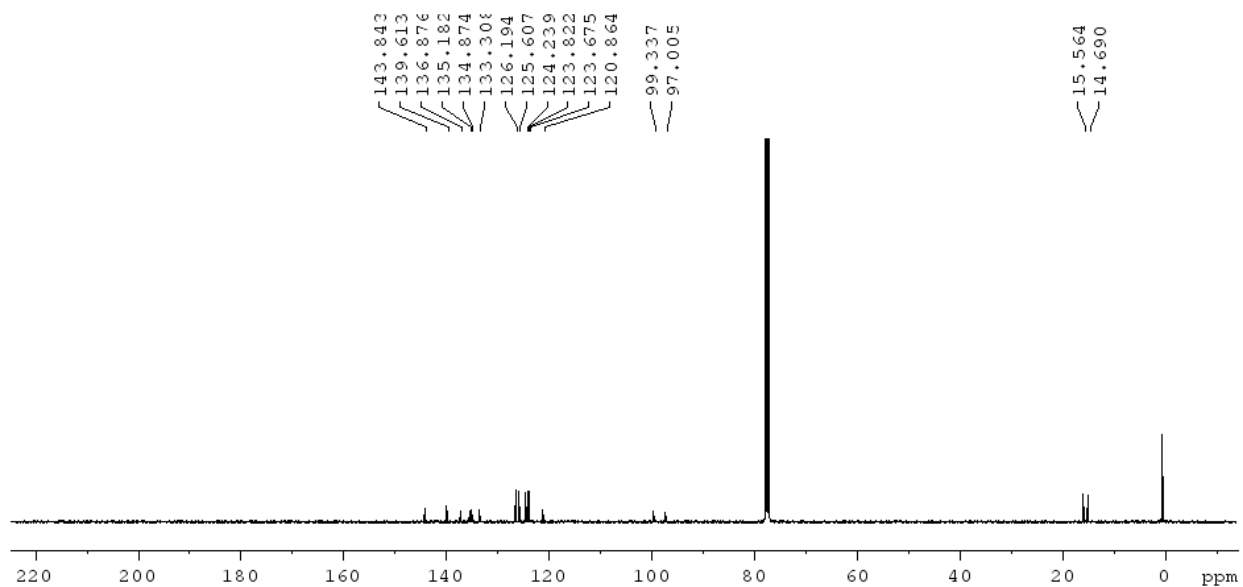
4-bromo-5,5''-dimethyl-2,2':5',2''-terthiophene (10)



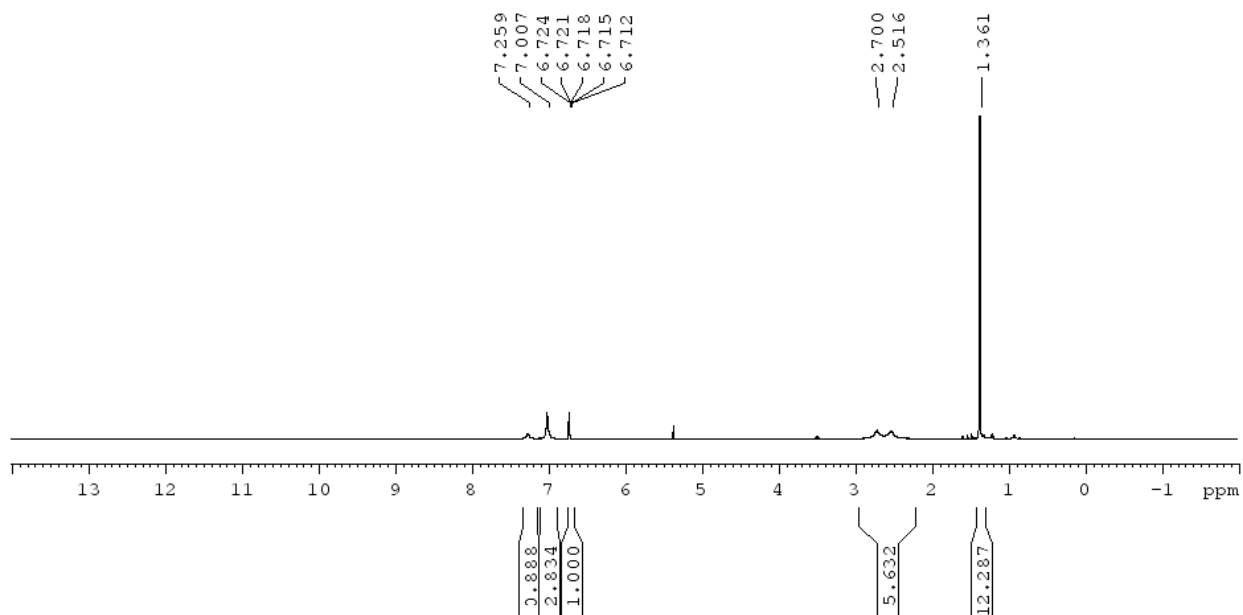


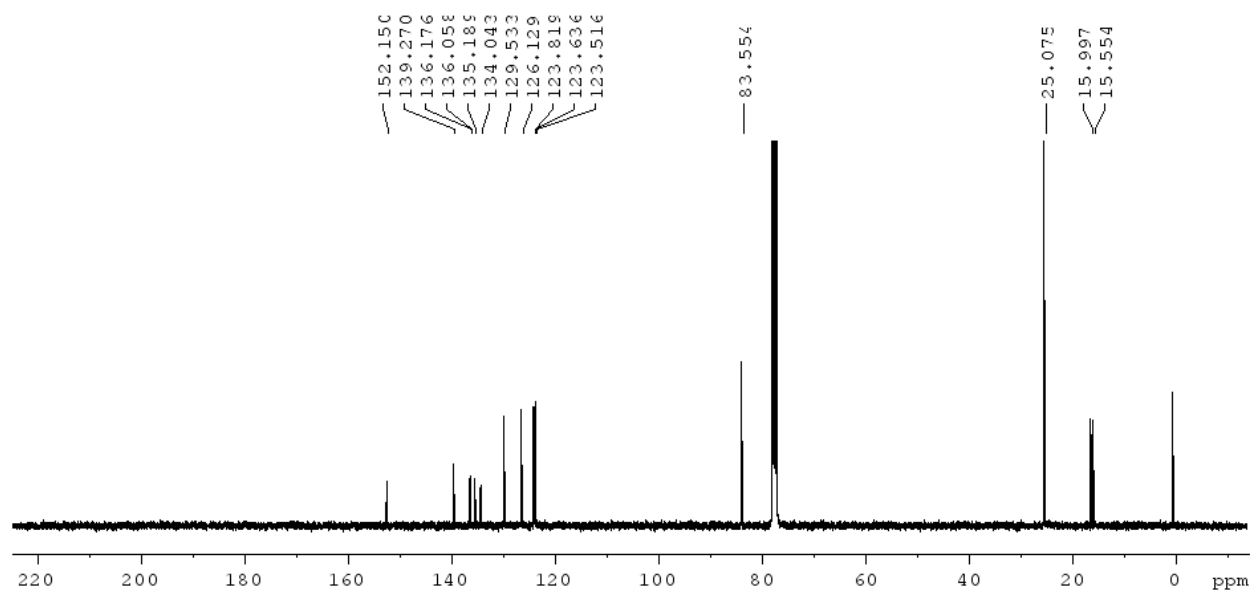
((5,5''-dimethyl-[2,2':5',2''-terthiophen]-4-yl)ethynyl)trimethylsilane (11)



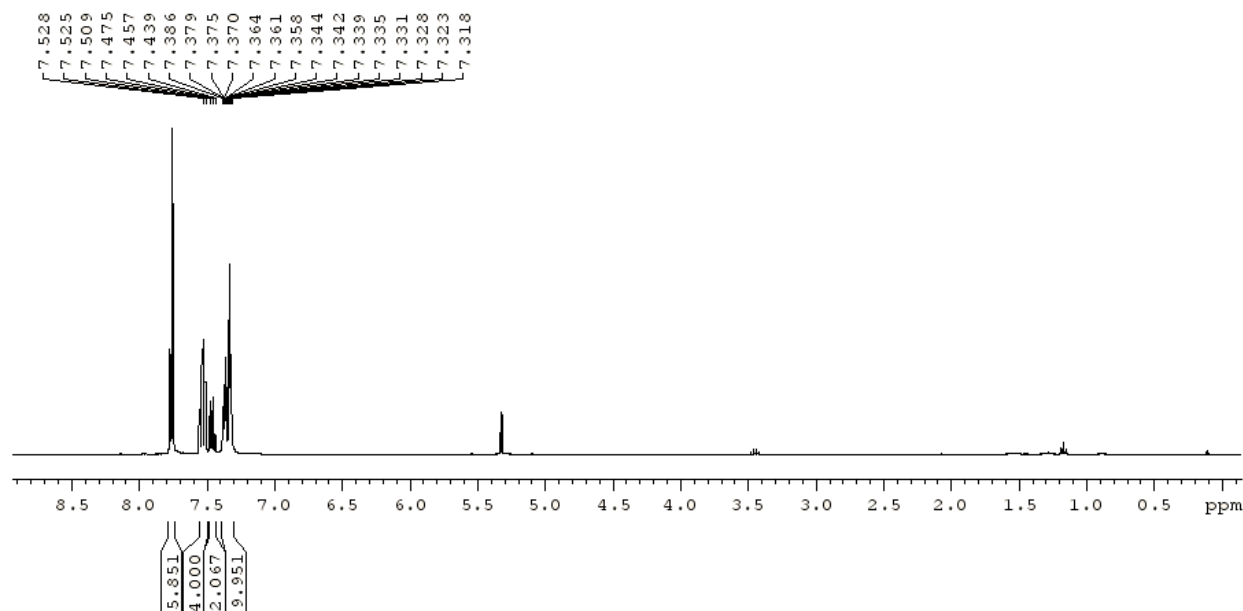


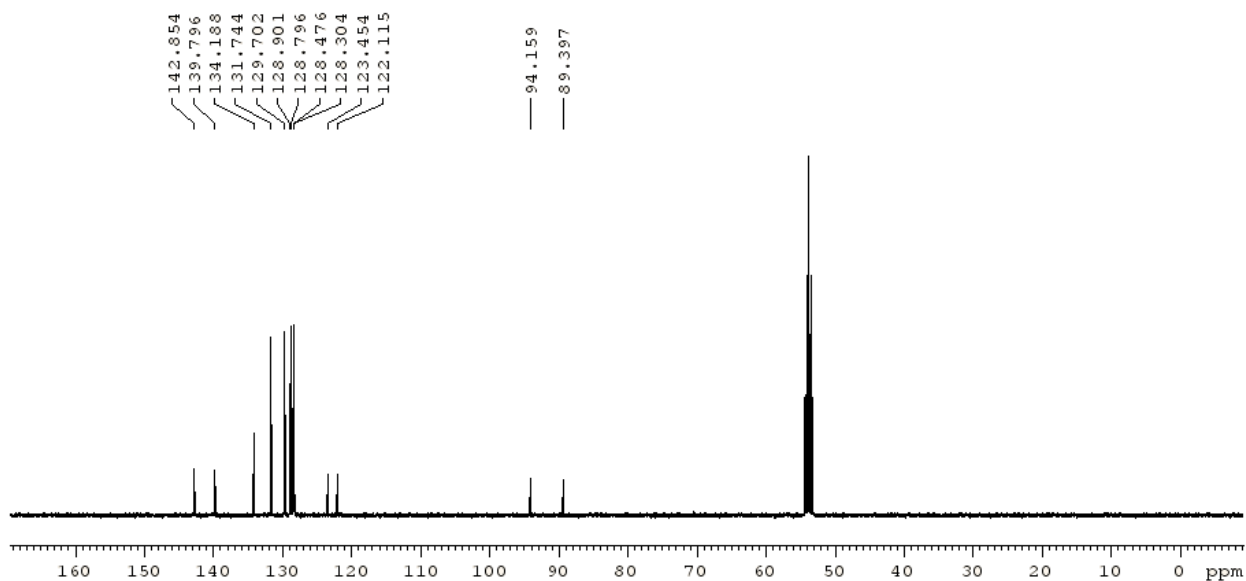
2-(5,5''-dimethyl-[2,2':5',2''-terthiophen]-4-yl)-4,4,5,5-tetramethyl-1,3,2-dioxaborolane (12)



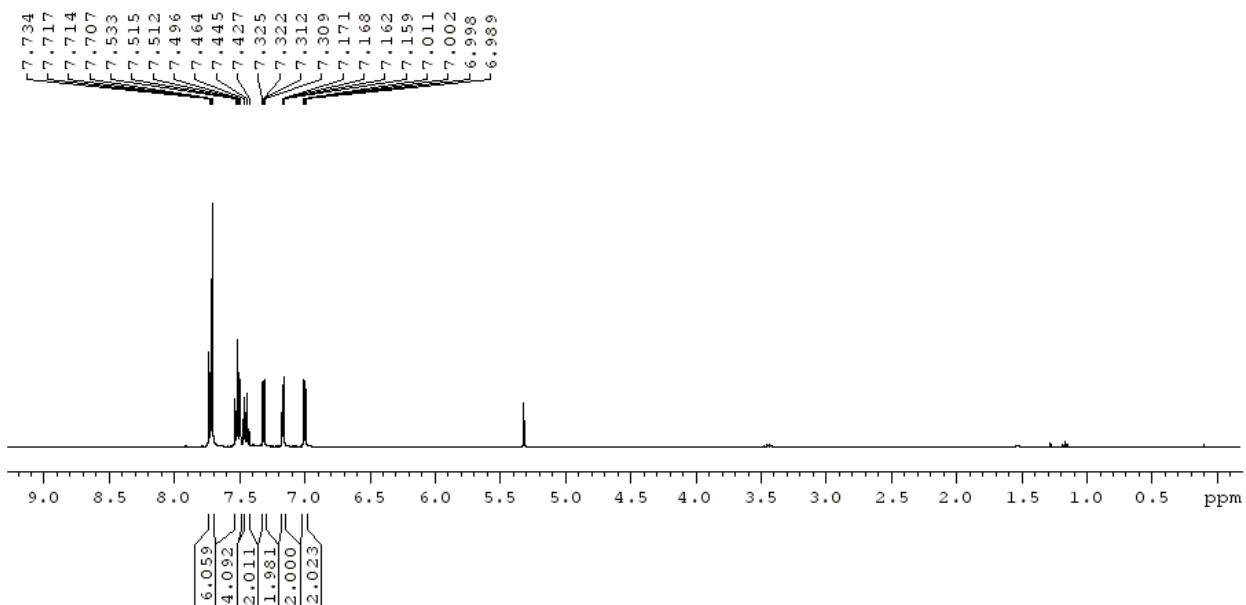


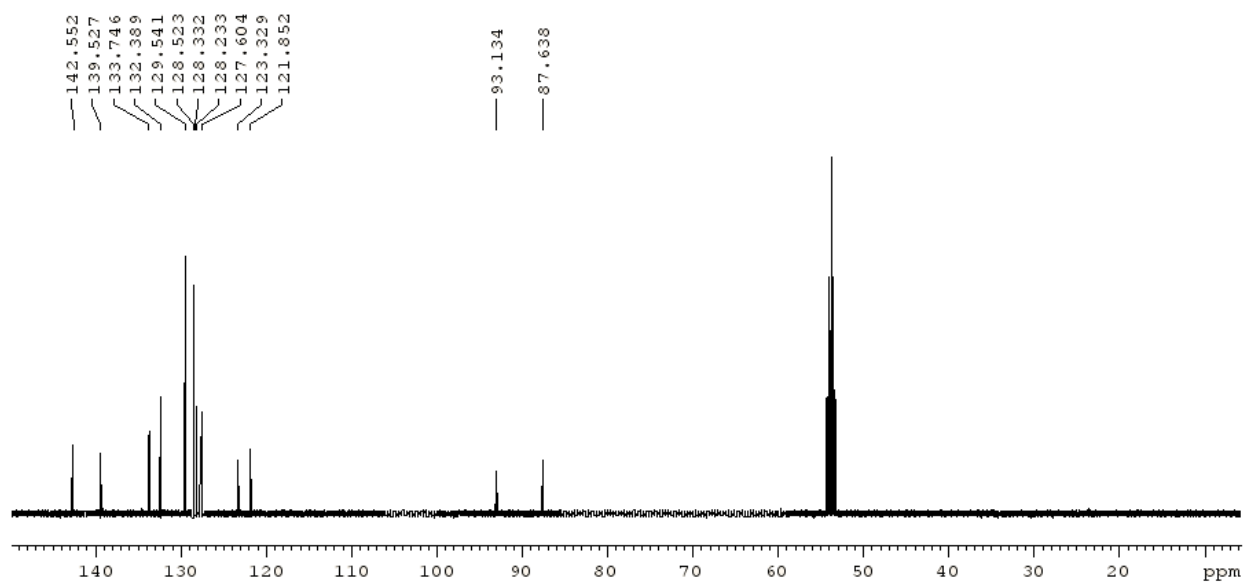
2',5'-bis(phenylethynyl)-1,1':4',1''-terphenyl (T-Ph)



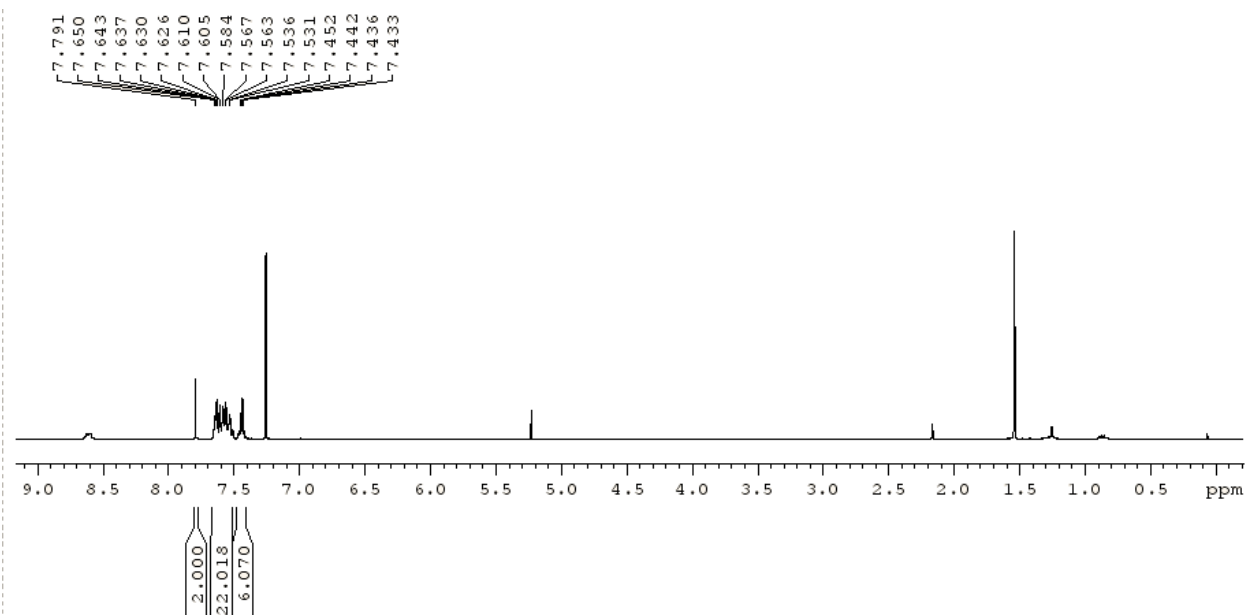


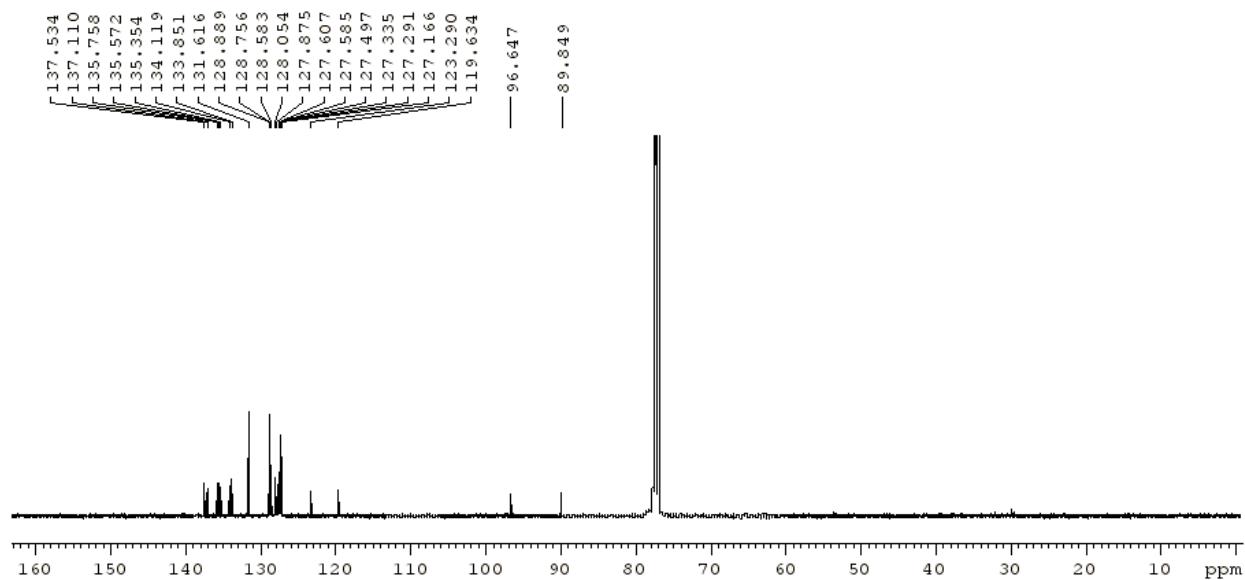
2',5'-bis(thiophen-2-ylethynyl)-1,1':4',1''-terphenyl (T-Th)



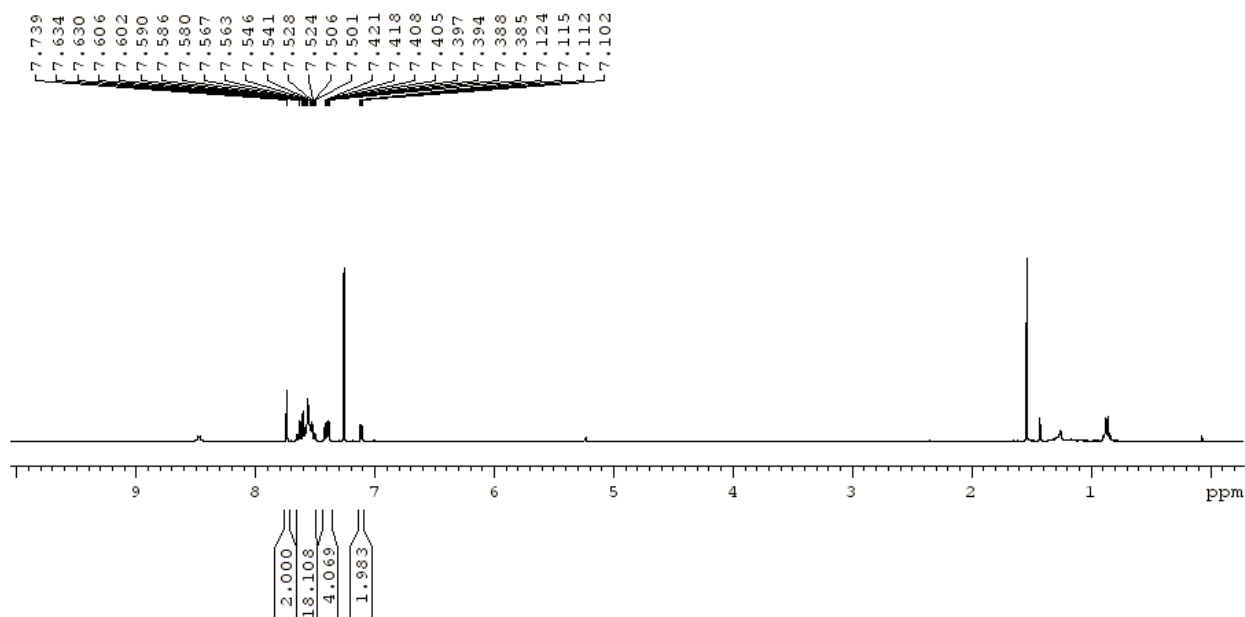


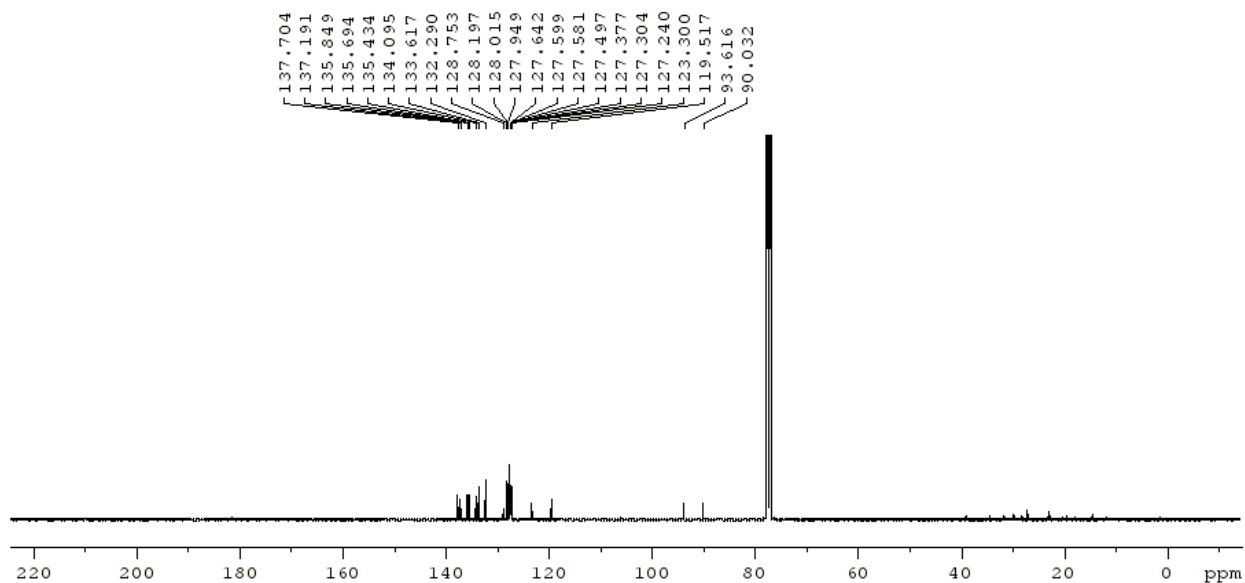
[6]-Ph



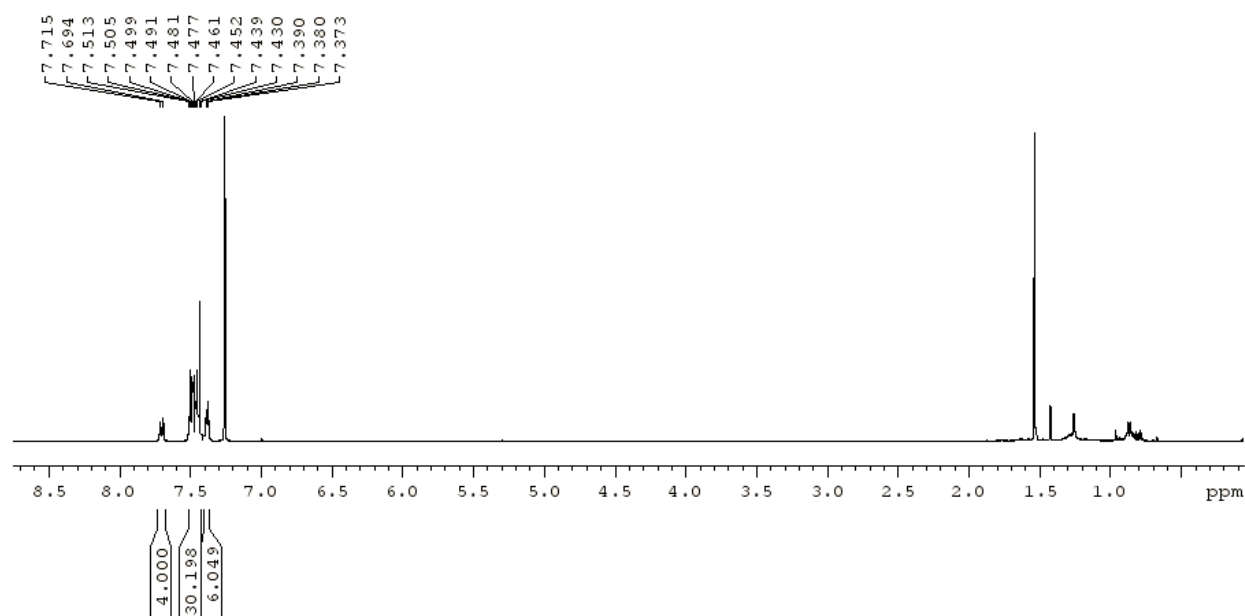


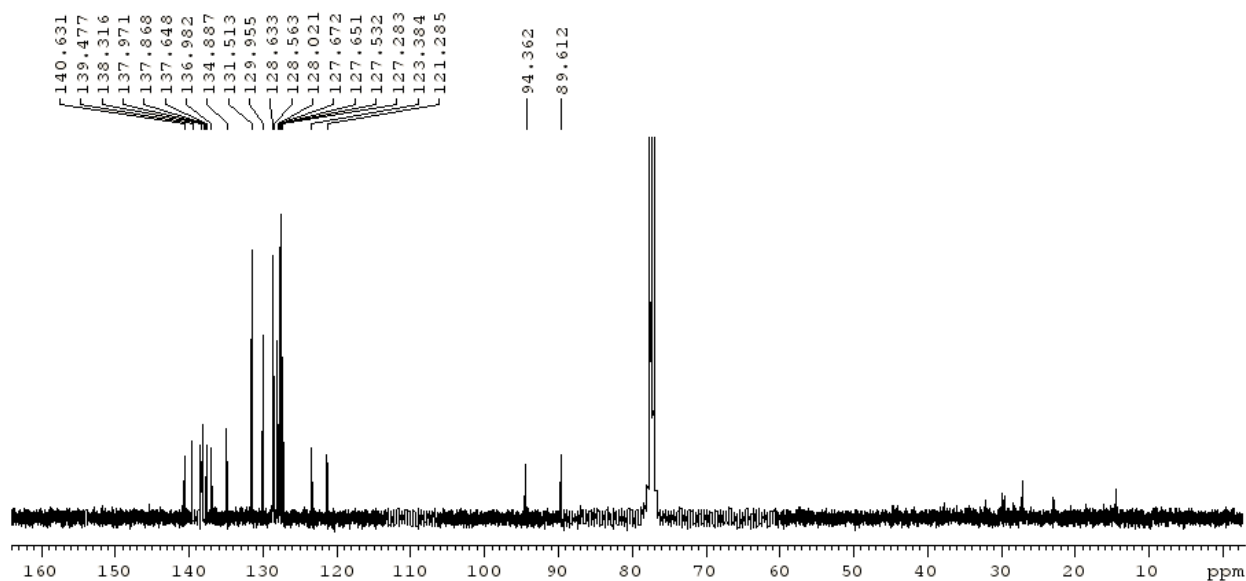
[6]-Th



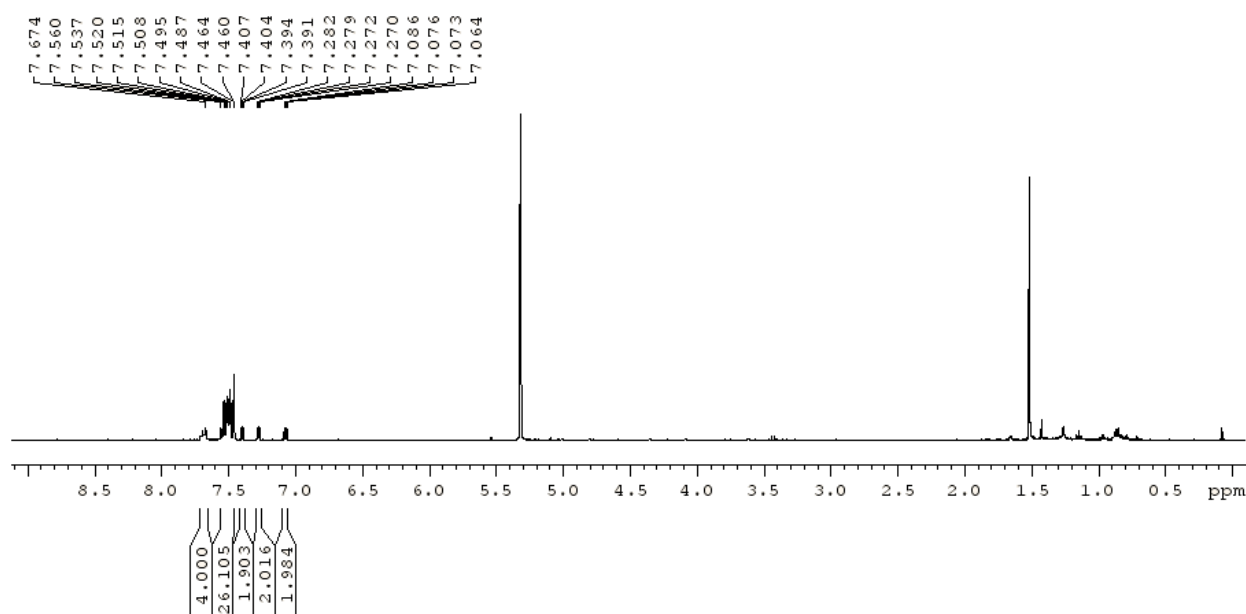


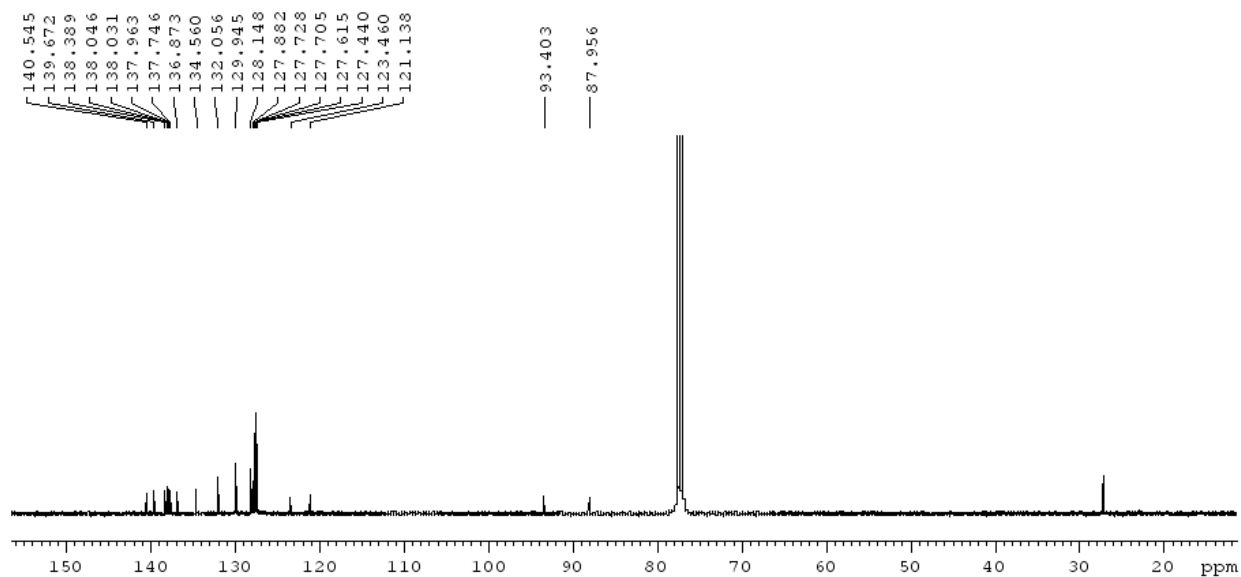
[8]-Ph



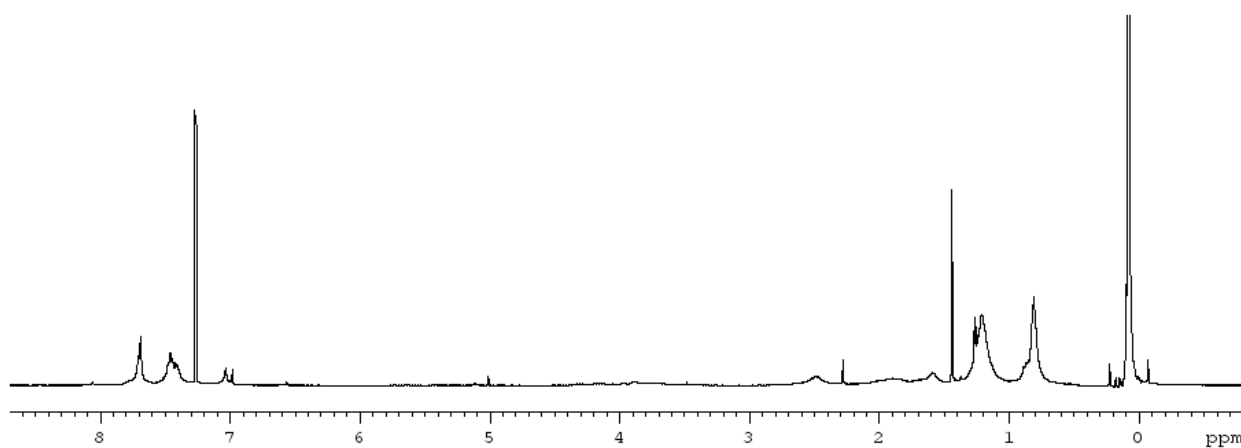


P[8]-Th

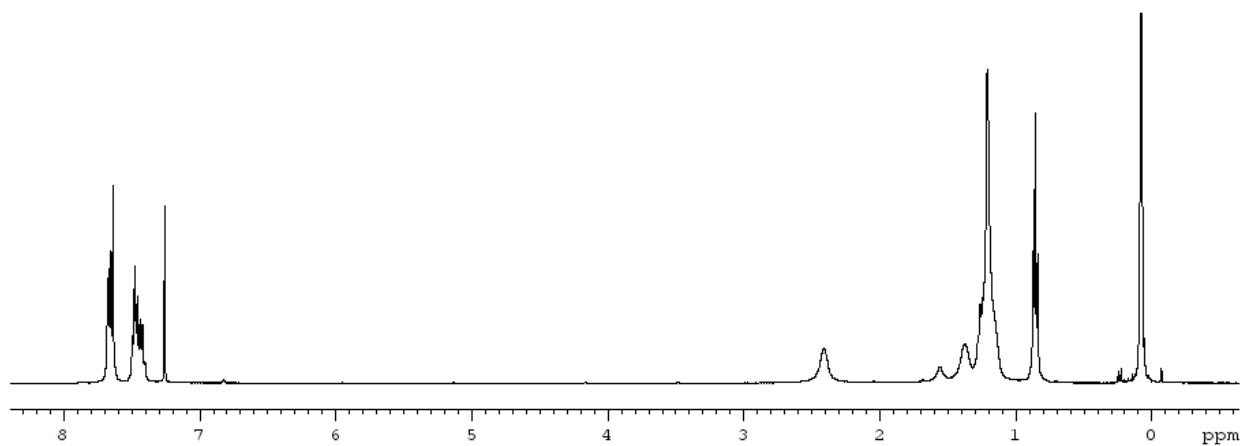




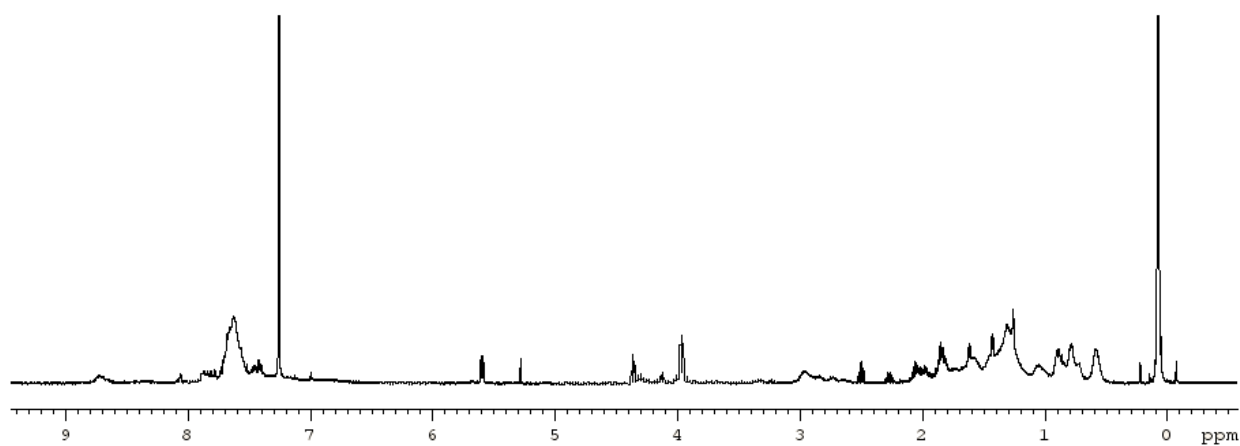
PT-Ph



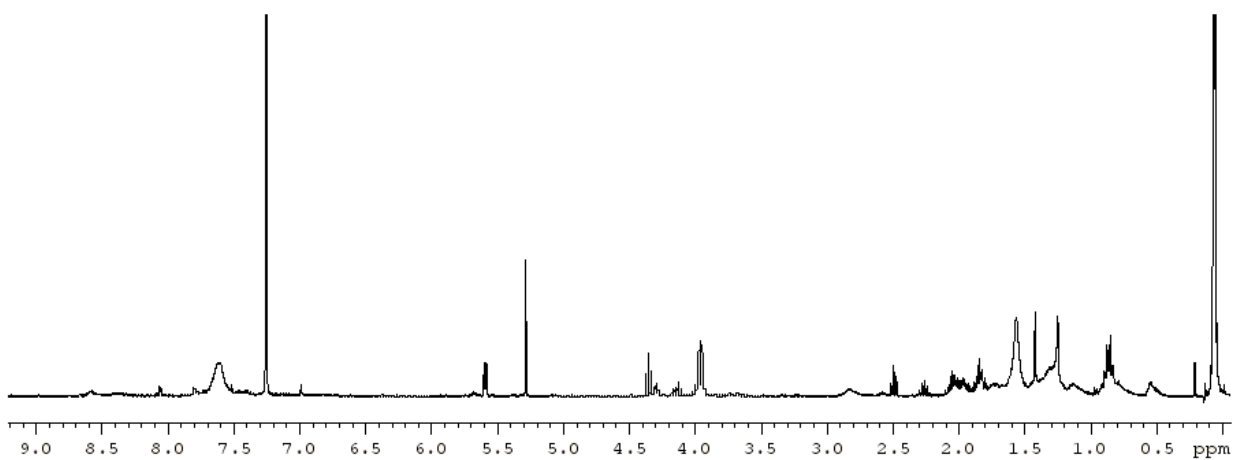
PT-Th



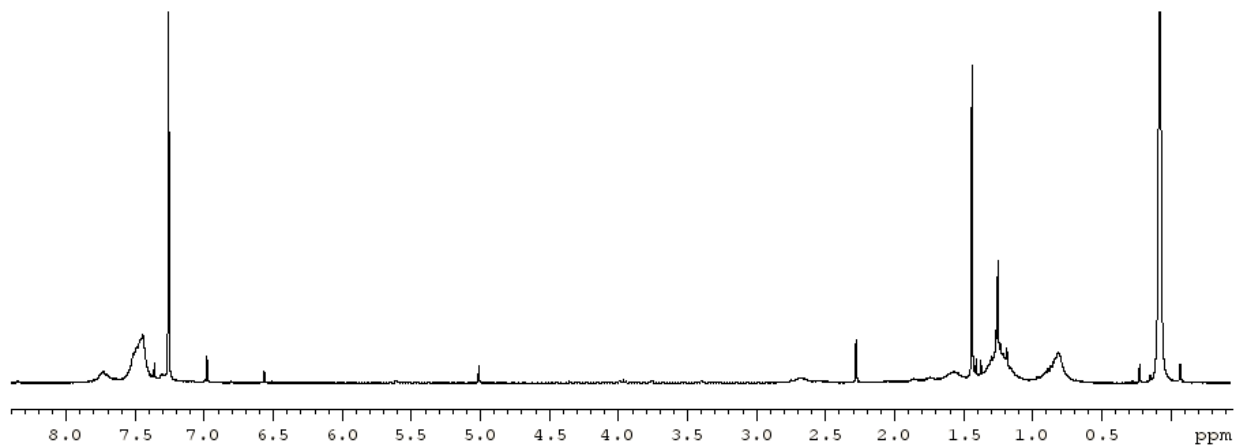
P[6]-Ph



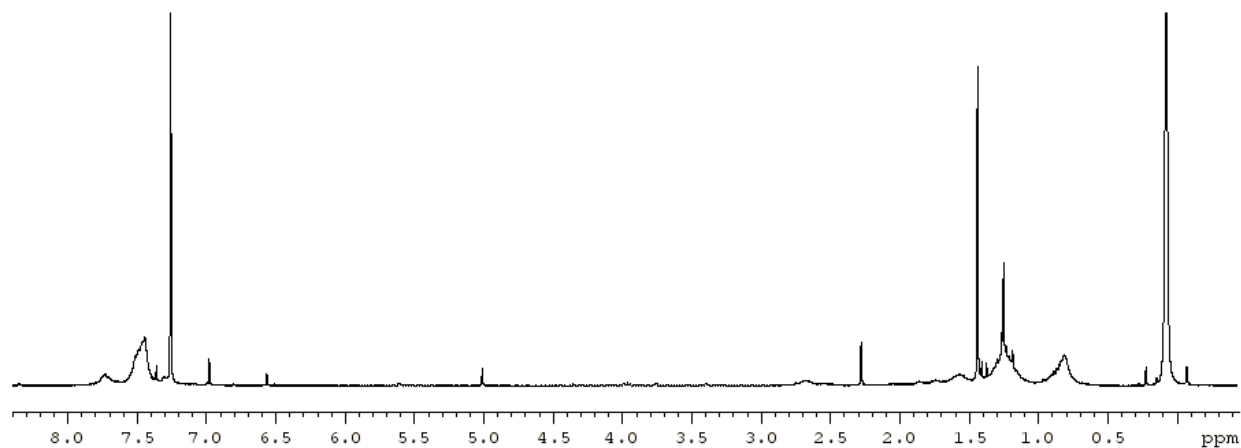
P[6]-Th



P[8]-Ph



P[8]-Th



Garvin Mihdi Peters

5426 N. Mascher St. Philadelphia, PA 19120

267-269-1895 • garvinmpeters@gmail.com • linkedin.com/in/garvinpeters

Summary

- Highly autonomous, efficient, and creative in performing laboratory research on multiple projects, requiring minimal direction from supervisor.
- Collaborative experience working with several groups drawing on multiple skillsets to accomplish a unified goal.
- Scientific mentorship experience in training three undergraduate students in three vastly different projects.
- Extensive experience in designing, synthesizing, and characterizing novel complex organic molecules, with a synthetic, technical, and theoretical toolkit applicable to polymeric materials, pharmaceuticals, and biochemistry.
- Trained to handle air-sensitive (glovebox and Schlenk line), moisture-sensitive, and flammable/toxic chemicals.
- Proficiency in: ^1H NMR, ^{13}C NMR, UV-Vis, IR, Fluorimetry, Electrochemistry, GPC, HPLC, thin-film processes.
- Fluency in: Gaussian 09 computational software, Spartan 04, Word, Excel, PowerPoint.

Experience

Graduate Research Assistant (Johns Hopkins University) **2014-2019**

- Synthesis and characterization of light-responsive aromatic molecules for switchable conductive polymers.
- Designed polymeric materials containing curved aromatic macrocycles (cycloparaphenylenes).

Research Assistant (Temple University) **2012-2014**

- Inorganic synthesis of cobalt complexes for carbon monoxide reduction to small organic molecules.
- Porphyrin-like macrocycle ligand synthesis and transition metal complexation for catalysis.

MARC Scholar Research Assistant (University of Illinois Urbana-Champaign) **2012**

- Investigated the antifreeze activity in the blood serum of fish species *Theragra chalcogramma*.
- Biochemical techniques to determine proteins responsible for thermal hysteresis.

Publications

- Peters, G. M.; Tovar, J. D. "Pendant Photochromic Conjugated Polymers Incorporating a Highly Functionalizable Thieno[3,4-*b*]thiophene Switching Motif" *J. Am. Chem. Soc.* **2019**. *Accepted*. DOI: 10.1021/jacs.8b12617.
- Young, D.; Honick, C. R.; Zhou, J.; Pitts, C. R.; Ghorbani, F.; Peters, G. M.; Tovar, J. D.; Lectka, T.; Bragg, A. E. "Energy- and Conformer-dependent Excited-State Relaxation of an E/Z Photoswitchable Thienyl-Ethene". *Phys. Chem. Chem. Phys.* **2019**. *Accepted*. DOI: 10.1039/c9cp01226e.
- Peters, G. M.; Winegrad, J. B.; Gau, M. R.; Imler, G. H.; Wayland, B. B.; Zdilla, M. J. "Synthesis and Structure of 2,5-bis[N-(2,6-mesityl)iminomethyl]pyrrolylcobalt(II): Evidence for One-electron-oxidized, Redox-non-innocent Ligand Behavior" *Inorg. Chem.* **2017**, 56 (6), 3377-3385.
- Imler, G. H.; Peters, G. M.; Zdilla, M. J.; Wayland, B. B. "Heterobimetallic Complexes of Rhodium Dibenzo-tetramethylaza[14]annulene: Formation, Structures, and Bond Dissociation Energetics" *Inorg. Chem.* **2015**, 54 (1), 273-279.

Awards and Scholarships

- Sarah and Adolph Roseman Achievement Award – Outstanding Research Accomplishments in Chemistry (2019)
- Ernest M. Marks Award – in recognition of Teaching Excellence (2016)
- NIH-NIGMS MARC Student Training in Academic Research Scholar 2-year scholarship (2012-2014 academic years)
- ACS Undergraduate Excellence in Chemistry Award (2014)

Presentations

- 2nd From Carbon-Rich Molecules to Carbon-Based Materials Conference Nassau, Bahamas **2018**
Rational Design of Pendant Photochromic Heteroacenes and their Application in Switchable Conjugated Polymers
- 17th International Symposium on Novel Aromatics (ISNA 17) Stony Brook, NY **2017**
Synthesis of Pendant Photochromic Monomers for Switchable Conductive Polymers
- 248th American Chemical Society National Meeting San Francisco, CA **2014**
Synthesis and Late Transition Metal Complexes of Electronically Flexible Pyrrole Ligands
- Annual Biomedical Research Conference for Minority Students Nashville, TN **2013**

Education

Johns Hopkins University Baltimore, MD **2014-2019**

- PhD in Chemistry (September 2019)
- M.A. in Chemistry (August 2016)
- Relevant coursework: Advanced Organic Synthesis I & II, Chemistry of Materials Synthesis, Advanced Mechanistic Organic Chemistry I & II, Physical Properties of Materials, Advanced Inorganic & Organometallic Reaction Mechanisms.

Temple University (Main Campus) Philadelphia, PA **2009-2014**

- B.S. in Chemistry (Chemistry GPA: 3.7 Overall GPA: 3.5)
- Relevant Coursework: Organic Structure and Mechanisms, Advanced Organic Preparations, Organic Synthesis Methodology, Heterocyclic Chemistry, Organic Reaction Mechanisms.

Teaching

Johns Hopkins University

Head Teaching Assistant Organic Chemistry I **2015-2017**

- Occasionally conducted primary course lectures in the absence of the Primary Lecturer.
- Worked alongside the instructor in designing exam questions.
- Developed weekly assignments for TA's / students relevant to current coursework.
- Taught a conference section weekly, consisting of approximately 90 students.
- Assigned responsibilities to TA's for exam grading, review sessions, and material to be covered in each conference.
- Led review sessions centered on test-taking strategies based on the current coursework.

Head Teaching Assistant Physical Organic Chemistry I **Spring 2016**

- Worked with graduate students to aid in deciphering complex mechanistic processes.

Teaching Assistant General Chemistry Lab / Lecture **2014-2015**

- Guided students through introductory organic and inorganic synthetic experiments.

Temple University

- Met with MARC U*Star scholars regularly to assist with their concerns across a broad range of chemical topics.

Miscellaneous

- U.S. Citizen